

[Theses and Dissertations](#)

[Theses and Dissertations](#)

12-11-2015

Synthesis and Catalytic Activity of -NHC Group 9 Metal Pincer Complexes

Sean William Reilly

Follow this and additional works at: <https://scholarsjunction.msstate.edu/td>

Recommended Citation

Reilly, Sean William, "Synthesis and Catalytic Activity of -NHC Group 9 Metal Pincer Complexes" (2015).
Theses and Dissertations. 4180.
<https://scholarsjunction.msstate.edu/td/4180>

This Dissertation - Open Access is brought to you for free and open access by the Theses and Dissertations at Scholars Junction. It has been accepted for inclusion in Theses and Dissertations by an authorized administrator of Scholars Junction. For more information, please contact scholcomm@msstate.libanswers.com.

Synthesis and catalytic activity of CCC-NHC group 9 metal pincer complexes

By

Sean William Reilly

A Dissertation
Submitted to the Faculty of
Mississippi State University
in Partial Fulfillment of the Requirements
for the Degree of Doctor of Philosophy
in Chemistry
in the Department of Chemistry

Mississippi State, Mississippi

December 2015

Copyright by

Sean William Reilly

2015

Synthesis and catalytic activity of CCC-NHC group 9 metal pincer complexes

By

Sean William Reilly

Approved:

Keith T. Mead
(Major Professor)

Andrzej Sygula
(Committee Member)

Joseph P. Emerson
(Committee Member)

Edwin A. Lewis
(Committee Member)

Stephen C. Foster
(Committee Member/Graduate Coordinator)

R. Gregory Dunaway
Dean
College of Arts & Sciences

Name: Sean William Reilly

Date of Degree: December 11, 2015

Institution: Mississippi State University

Major Field: Chemistry

Major Professor: Keith T. Mead, Ph.D.

Title of Study: Synthesis and catalytic activity of CCC-NHC group 9 metal pincer complexes

Pages in Study 244

Candidate for Degree of Doctor of Philosophy

N-Heterocyclic carbenes (NHCs) are one of the few ligand systems that can finely tune transition metal catalysts via sterics and electronics. The strong sigma-donating properties of these ancillary ligands allow the development of robust tridentate NHC pincer framework, which has emerged as an alternative to the phosphine pincer ligands. The combination of NHC and pincer systems has resulted in a new generation of catalytically active organometallic complexes reported throughout the literature.

CCC-NHC Rh pincer complexes were found to be catalytically active in C-C and C-B bond formation via 1,4-addition reactions. In addition, the *in-situ* generated CCC-NHC Ir(H) pincer complex demonstrated catalytic activity in borylation of arene C-H bonds. Preliminary results are comparable to the C-H borylation results published by Hartwig and co-workers. The CCC-NHC Ir(H) pincer complex may also prove to be a suitable catalyst for alkane dehydrogenation, due to framework similarities of the highly active and durable PCP and POCOP pincer hydride systems.

Expansion of group 9 metal sources for transmetalation of the CCC-NHC Zr pincer complex afforded the development of CCC-NHC Rh(CO) and CCC-NHC Co

complexes. Group 9 metal carbonyl complexes have been reported as active catalysts in photocatalytic C-H activation of small molecules. Testing of Co sources for transmetalation afforded three rare Co pincer complexes, and the first examples of CCC-NHC Co pincer complexes to date. Development of CCC-NHC pincer complexes with base metals provide cost-effect alternatives to pincer systems with precious metal centers, and is reported herein.

DEDICATION

This dissertation is dedicated to my mom and dad who have been supportive and encouraging throughout my time in graduate school.

ACKNOWLEDGEMENTS

I would like to thank all the Hollis Lab group members I was fortunate to have worked with during my time in the Ph.D. program: Hannah Box, Tyler Howell, Wesley Clark, Griffin Burk, Henry Valle, Chris Cain, Ginger Tyson, Gopalakrishna Akurathi, Amarraj Chakraborty, Dr. Ted Helgert, and Dr. Xiaofei Zhang.

Finally, I would like to thank my advisor Dr. Mead and my committee members, Dr. Emerson, Dr. Lewis, Dr. Foster, and Dr. Sygula, for your patience and guidance during my time at Mississippi State University.

TABLE OF CONTENTS

DEDICATION.....	ii
ACKNOWLEDGEMENTS.....	iii
LIST OF TABLES.....	vi
LIST OF FIGURES	ix
LIST OF SCHEMES.....	xvi
CHAPTER	
I. INTRODUCTION.....	1
1.1 <i>N</i> -Heterocyclic Carbenes (NHCs)	1
1.2 Pincer Ligands	4
1.3 CCC-NHC Pincer Ligands	5
II. SYNTHESIS OF AIR-STABLE CCC-NHC PINCER COBALT COMPLEXES	9
2.1 Introduction	9
2.2 Results and Discussion	11
2.3 Conclusion.....	17
2.4 Experimental.....	17
2.4.1 General Considerations	17
2.4.2 Synthesis of CCC-NHC Pincer Cobalt Complex 4	18
2.4.3 Synthesis of CCC-NHC Pincer Cobalt Complex 6	18
2.4.4 Synthesis of CCC-NHC Pincer Cobalt Complex 7	19
III. 1,4-ADDITION OF ARYL BORONIC ACIDS TO α,β -UNSATURATED KETONES CATALYZED BY A CCC-NHC PINCER RHODIUM COMPLEX	21
3.1 Introduction	21
3.2 Results and Discussion	22
3.3 Conclusion.....	29
3.4 Experimental.....	30
3.4.1 General Consideration	30

3.4.2	General Procedure for Catalytic Trials.....	30
3.4.3	Synthesis of 3-(1H-pyrazol-4-yl)cyclohexan-1-one	30
3.4.4	Product Characterization	31
IV.	ROOM TEMPERATURE β-BORATION OF α,β-UNSATURATED CARBONYL COMPOUNDS CATALYZED BY CCC-NHC PINCER RHODIUM COMPLEXES	35
4.1	Introduction	35
4.2	Results and Discussion	37
4.3	Conclusion.....	46
4.4	Experimental.....	47
4.4.1	General Consideration.....	47
4.4.2	Synthesis of CCC-NHC Pincer Rhodium Complexes 10.....	48
4.4.3	General Procedure for Catalytic Trials.....	49
4.4.4	Product Characterization	50
V.	DEVELOPMENT OF CCC-NHC Ir AND Rh PINCER COMPLEXES FOR BORYLATION OF ARENE AND ALKANE C–H BONDS	53
5.1	Introduction	53
5.2	Results and Discussion	54
5.3	Conclusions	62
5.4	Experimental.....	63
5.4.1	General Considerations	63
5.4.2	Synthesis of CCC-NHC Iridium Pincer Complex 12	64
5.4.3	Synthesis of CCC-NHC Rhodium Pincer Complex 13	64
5.4.4	Synthesis of CCC-NHC Rhodium Pincer Complex 14	65
5.4.5	General Procedure for Catalytic Trials.....	65
REFERENCES	66
APPENDIX		
A.	SPECTROSCOPIC DATA	83
A.1	Chapter II Compounds	84
A.1.1	Crystal Summary for 4	100
A.1.2	Crystal Summary for 7	111
A.2	Chapter III Compounds	112
A.3	Chapter IV Compounds	136
A.3.1	Crystal Summary for 9	205
A.4	Chapter V Compounds	207
A.4.1	Crystal Summary for 12	222
A.4.2	Crystal Summary for 13	232
A.4.3	Crystal Summary for 14	244

LIST OF TABLES

2.1	Selected Bond Lengths (Å) and Angles (°) for 4	13
2.2	Selected Bond Lengths (Å) and Angles (°) for 7	17
3.1	Optimization of 8 with Cyclohexenone and PhB(OH) ₂	24
3.2	Scope of Michael Acceptors with PhB(OH) ₂ ^a	25
3.3	Scope of Cyclohexenone with ArB(OH) ₂ ^a	27
3.4	Scope of Cyclohexenone with Heterocycle Boronic Acids ^a	29
4.1	Optimization of β-Boration Reaction Conditions ^a	38
4.2	Scope of Acyclic Substrate Reactivity in the β-Boration with B ₂ pin ₂ ^a	40
4.3	Scope of Cyclic Substrate Reactivity in the β-Boration with B ₂ pin ₂ ^a	42
4.4	Selected Bond Lengths (Å) and Angles (°) for 9	46
4.5	GC-MS Method for β-Boration Catalysis	48
5.1	Benzene C–H Borylation Optimization ^a	55
5.2	Arenes Substrates for C–H Borylation ^a	56
5.3	Selected Bond Lengths (Å) and Angles (°) for 12	58
5.4	Selected Bond Lengths (Å) and Angles (°) for 13	61
5.5	Selected Bond Lengths (Å) and Angles (°) for 14	62
5.6	GC-MS Method for C–H Borylation Catalysis	64
A.1	Crystal Data and Structure Refinement for 4	92
A.2	Atomic Coordinates and Equivalent Isotropic Displacement Parameters (Å ²) for 4	93
A.3	Anisotropic Displacement Parameters (Å ²) for 4	95

A.4	Bond Lengths [\AA] for 4	96
A.5	Bond Angles [°] for 4	97
A.6	Torsion Angles [°] for 4	99
A.7	Crystal Data and Structure Refinement for 7	102
A.8	Atomic Coordinates and Equivalent Isotropic Displacement Parameters (\AA^2) for 7	103
A.9	Anisotropic Displacement Parameters (\AA^2) for 7	105
A.10	Bond Lengths [\AA] for 7	106
A.11	Bond Angles [°] for 7	107
A.12	Torsion Angles [°] for 7	110
A.13	Crystal Data and Structure Refinement for 9	197
A.14	Atomic Coordinates and Equivalent Isotropic Displacement Parameters (\AA^2) for 9	198
A.15	Anisotropic Displacement Parameters (\AA^2) for 9	200
A.16	Bond Lengths [\AA] for 9	201
A.17	Bond Angles [°] for 9	202
A.18	Torsion Angles [°] for 9	204
A.19	Hydrogen Bonds for 9	205
A.20	Crystal Data and Structure Refinement for 12	215
A.21	Atomic Coordinates and Equivalent Isotropic Displacement Parameters (\AA^2) for 12	216
A.22	Anisotropic Displacement Parameters (\AA^2) for 12	218
A.23	Bond Lengths [\AA] for 12	219
A.24	Bond Angles [°] for 12	220
A.25	Torsion Angles [°] for 12	221
A.26	Crystal Data and Structure Refinement for 13	224

A.27	Atomic Coordinates and Equivalent Isotropic Displacement Parameters (\AA^2) for 13	225
A.28	Anisotropic Displacement Parameters (\AA^2) for 13	227
A.29	Bond Lengths [\AA] for 13	228
A.30	Bond Angles [°] for 13	229
A.31	Torsion Angles [°] for 13	231
A.32	Crystal Data and Structure Refinement 14	234
A.33	Atomic Coordinates and Equivalent Isotropic Displacement Parameters (\AA^2) for 14	235
A.34	Anisotropic Displacement Parameters (\AA^2) for 14	238
A.35	Bond Lengths [\AA] for 14	239
A.36	Bond Angles [°] for 14	240
A.37	Torsion Angles [°] for 14	243

LIST OF FIGURES

1.1	Triplet carbenes vs. singlet carbenes	1
1.2	Triplet vs singlet carbene energy diagram.....	2
1.3	Electronic stabilization of NHC in imidazole-2-ylidene scaffold	3
1.4	Applications of NHC complexes.....	4
1.5	Generic pincer ligand design.....	4
1.6	Type of NHC pincer framework.....	6
1.7	Type C , PCP, and POCOP pincer framework.....	7
1.8	General synthesis of CCC-NHC ligand precursors	7
1.9	General synthesis of CCC-NHC Ir and Rh pincer complexes	8
2.1	CCC-NHC pincer Zr complexes as transmetalating reagents	11
2.2	X-ray molecular structure of 4	13
2.3	X-ray molecular structure of 7	16
4.1	CCC-NHC Rh amine adduct (9) and crude isolate (10).....	37
4.2	Diastereotopic methylene peaks of 10 observed in ^1H NMR spectrum	43
4.3	Rh–C _{aromatic} and Rh–C _{carbene} doublets of 10 observed in ^{13}C spectrum.....	44
4.4	X-ray molecular structure of 9	46
5.1	X-ray structure of 12	58
5.2	Coordinatively unsaturated CCC-NHC Rh(CO) pincer complex	59
5.3	X-ray structure of 13	60
5.4	X-ray structure of 14	62

A.1	^1H NMR (600 MHz, CDCl_3) spectrum of reaction mixture (Scheme 2.1).....	84
A.2	^1H NMR (600 MHz, CDCl_3) spectrum of 6	85
A.3	^{13}C NMR (150 MHz, CDCl_3) spectrum of 6	86
A.4	HRMS spectrum of 6	87
A.5	^1H NMR (600 MHz, CDCl_3) spectrum of 7	88
A.6	^{13}C NMR (150 MHz, CDCl_3) spectrum of 7	89
A.7	HRMS spectrum of 7	90
A.8	X-ray molecular structure of 4	91
A.9	X-ray molecular structure of 7	101
A.10	^1H NMR (600 MHz, CDCl_3) spectrum of isolated product (Table 3.2, Entry 1).....	112
A.11	^1H NMR (300 MHz, CDCl_3) spectrum of isolated product (Table 3.2, Entry 2).....	113
A.12	^1H NMR (300 MHz, CDCl_3) spectrum of isolated product (Table 3.2, Entry 3).....	114
A.13	^1H NMR (600 MHz, CDCl_3) spectrum of isolated product (Table 3.2, Entry 4).....	115
A.14	^1H NMR (600 MHz, CDCl_3) spectrum of isolated product (Table 3.2, Entry 5).....	116
A.15	^1H NMR (300 MHz, CDCl_3) spectrum of isolated product (Table 3.2, Entry 6).....	117
A.16	^1H NMR (300 MHz, CDCl_3) spectrum of isolated product (Table 3.2, Entry 7).....	118
A.17	^1H NMR (600 MHz, CDCl_3) spectrum of isolated product (Table 3.2, Entry 8).....	119
A.18	^1H NMR (300 MHz, CDCl_3) spectrum of isolated product (Table 3.3, Entry 1).....	120
A.19	^1H NMR (300 MHz, CDCl_3) spectrum of isolated product (Table 3.3, Entry 2).....	121

A.20	^1H NMR (600 MHz, CDCl_3) spectrum of isolated product (Table 3.3, Entry 3).....	122
A.21	^1H NMR (600 MHz, CDCl_3) spectrum of isolated product (Table 3.3, Entry 4).....	123
A.22	^1H NMR (600 MHz, CDCl_3) spectrum of isolated product (Table 3.3, Entry 5).....	124
A.23	^1H NMR (600 MHz, CDCl_3) spectrum of isolated product (Table 3.3, Entry 6).....	125
A.24	^1H NMR (600 MHz, CDCl_3) spectrum of isolated product (Table 3.3, Entry 8).....	126
A.25	^1H NMR (600 MHz, CDCl_3) spectrum of isolated product (Table 3.3, Entry 9).....	127
A.26	^1H NMR (300 MHz, CDCl_3) spectrum of isolated product (Table 3.3, Entry 10).....	128
A.27	^1H NMR (300 MHz, CDCl_3) spectrum of isolated product (Table 3.4, Entry 1).....	129
A.28	^1H NMR (300 MHz, CDCl_3) spectrum of isolated product (Table 3.4, Entry 2).....	130
A.29	^1H NMR (300 MHz, CDCl_3) spectrum of isolated product (Table 3.4, Entry 5).....	131
A.30	^1H NMR (300 MHz, CDCl_3) spectrum of isolated product (Table 3.4, Entry 4).....	132
A.31	^{13}C NMR (150 MHz, CDCl_3) spectrum of isolated product (Table 3.4, Entry 4).....	133
A.32	HRMS of isolated product (Table 3.4, Entry 4)	134
A.33	IR spectrum of isolated product (Table 3.4, Entry 4).....	135
A.34	^1H NMR (600 MHz, CDCl_3) spectrum of 10	136
A.35	^{13}C NMR (150 MHz, CDCl_3) spectrum of 10	137
A.36	^{13}C DEPT 135 NMR (150 MHz, CDCl_3) spectrum of 10	138
A.37	HRMS of 10	139

A.38	GC-MS chromatogram spectrum of catalytic trial (Table 4.1, Entry 2)	140
A.39	¹ H NMR spectrum (600 MHz, CDCl ₃) of isolated product (Table 4.1, Entry 2).....	141
A.40	¹³ C NMR (150 MHz, CDCl ₃) spectrum of isolated product (Table 4.1, Entry 2).....	142
A.41	HRMS of product (Table 4.1, Entry 2).....	143
A.42	GC-MS chromatogram spectrum of catalytic trial (Table 4.2, Entry 1)	144
A.43	¹ H NMR (600 MHz, CDCl ₃) spectrum of isolated product (Table 4.2, Entry 1).....	145
A.44	¹³ C NMR (150 MHz, CDCl ₃) spectrum of isolated product (Table 4.2, Entry 1).....	146
A.45	HRMS of product (Table 4.2, Entry 1).....	147
A.46	GC-MS chromatogram spectrum of catalytic trial (Table 4.2, Entry 2)	148
A.47	¹ H NMR (600 MHz, CDCl ₃) spectrum of isolated product (Table 4.2, Entry 2).....	149
A.48	¹³ C NMR (150 MHz, CDCl ₃) spectrum of isolated product (Table 4.2, Entry 2).....	150
A.49	HRMS of product (Table 4.2, Entry 2).....	151
A.50	GC-MS chromatogram spectrum of catalytic trial (Table 4.2, Entry 3)	152
A.51	¹ H NMR (600 MHz, CDCl ₃) spectrum of isolated product (Table 4.2, Entry 3).....	153
A.52	¹³ C NMR (150 MHz, CDCl ₃) spectrum of isolated product (Table 4.2, Entry 3).....	154
A.53	HRMS of product (Table 4.2, Entry 3).....	155
A.54	GC-MS chromatogram spectrum of catalytic trial (Table 4.2, Entry 4)	156
A.55	¹ H NMR (600 MHz, CDCl ₃) spectrum of isolated product (Table 4.2, Entry 4).....	157
A.56	¹³ C NMR (150 MHz, CDCl ₃) spectrum of isolated product (Table 4.2, Entry 4).....	158

A.57	HRMS of product (Table 4.2, Entry 4).....	159
A.58	GC-MS chromatogram spectrum of catalytic trial (Table 4.2, Entry 7)	160
A.59	¹ H NMR (600 MHz, CDCl ₃) spectrum of isolated product (Table 4.2, Entry 7).....	161
A.60	¹³ C NMR (150 MHz, CDCl ₃) of isolated product (Table 4.2, Entry 7).....	162
A.61	HRMS of product (Table 4.2, Entry 7).....	163
A.62	GC-MS chromatogram spectrum of catalytic trial (Table 4.2, Entry 8)	164
A.63	¹ H NMR (600 MHz, CDCl ₃) spectrum of isolated product (Table 4.2, Entry 8).....	165
A.64	¹³ C NMR (150 MHz, CDCl ₃) spectrum of isolated product (Table 4.2, Entry 8).....	166
A.65	HRMS of product (Table 4.2, Entry 8).....	167
A.66	GC-MS chromatogram spectrum of catalytic trial (Table 4.2, Entry 9)	168
A.67	¹ H NMR (600 MHz, CDCl ₃) spectrum of isolated product (Table 4.2, Entry 10).....	169
A.68	¹³ C NMR (150 MHz, CDCl ₃) spectrum of isolated product (Table 4.2, Entry 10).....	170
A.69	HRMS of product (Table 4.2, Entry 10).....	171
A.70	GC-MS chromatogram spectrum of catalytic trial (Table 4.3, Entry 1)	172
A.71	¹ H NMR (600 MHz, CDCl ₃) spectrum of isolated product (Table 4.3, Entry 1).....	173
A.72	¹³ C NMR (150 MHz, CDCl ₃) spectrum of isolated product (Table 4.3, Entry 1).....	174
A.73	HRMS of product (Table 4.3, Entry 1).....	175
A.74	GC-MS chromatogram spectrum of catalytic trial (Table 4.3, Entry 2)	176
A.75	¹ H NMR (600 MHz, CDCl ₃) spectrum of isolated product (Table 4.3, Entry 2).....	177

A.76	^{13}C NMR (150 MHz, CDCl_3) spectrum of isolated product (Table 4.3, Entry 2).....	178
A.77	HRMS of product (Table 4.3, Entry 2).....	179
A.78	GC-MS chromatogram spectrum of catalytic trial (Table 4.3, Entry 3)	180
A.79	^1H NMR (600 MHz, CDCl_3) spectrum of isolated product (Table 4.3, Entry 3).....	181
A.80	^{13}C NMR (150 MHz, CDCl_3) spectrum of isolated product (Table 4.3, Entry 3).....	182
A.81	HRMS of product (Table 4.3, Entry 3).....	183
A.82	GC-MS chromatogram spectrum of catalytic trial (Table 4.3, Entry 4)	184
A.83	^1H NMR (600 MHz, CDCl_3) spectrum of isolated product (Table 4.3, Entry 4).....	185
A.84	^{13}C NMR (150 MHz, CDCl_3) spectrum of isolated product (Table 4.3, Entry 4).....	186
A.85	HRMS of product (Table 4.3, Entry 4).....	187
A.86	GC-MS chromatogram spectrum of catalytic trial (Table 4.3, Entry 5)	188
A.87	^1H NMR (600 MHz, CDCl_3) spectrum of isolated product (Table 4.3, Entry 5).....	189
A.88	^{13}C NMR (150 MHz, CDCl_3) spectrum of isolated product (Table 4.3, Entry 5).....	190
A.89	HRMS of product (Table 4.3, Entry 5).....	191
A.90	GC-MS chromatogram spectrum of catalytic trial (Table 4.3, Entry 6)	192
A.91	^1H NMR (600 MHz, CDCl_3) spectrum of isolated product (Table 4.3, Entry 6).....	193
A.92	^{13}C NMR (150 MHz, CDCl_3) spectrum of isolated product (Table 4.3, Entry 6).....	194
A.93	HRMS of product (Table 4.3, Entry 6).....	195
A.94	X-ray molecular structure of 9	196
A.95	GC-MS chromatogram spectrum of catalytic trial (Table 5.1, Entry 4)	207

A.96	GC-MS chromatogram spectrum of catalytic trial (Table 5.2, Entry 1)	208
A.97	GC-MS chromatogram spectrum of catalytic trial (Table 5.2, Entry 2)	209
A.98	GC-MS chromatogram spectrum of catalytic trial (Table 5.2, Entry 3)	210
A.99	^1H NMR (600 MHz, CDCl_3) spectrum of 13	211
A.100	^{13}C NMR (150 MHz, CDCl_3) spectrum of 13	212
A.101	^{13}C DEPT 135 NMR (150 MHz, CDCl_3) spectrum of 13	213
A.102	X-ray molecular structure of 12	214
A.103	X-ray molecular structure of 13	223
A.104	X-ray molecular structure of 14	233

LIST OF SCHEMES

2.1	Synthesis of 4	12
2.2	Synthesis of 6	14
2.3	Synthesis of 7	15
3.1	Equilibrium of CCC-NHC Rh iodo-bridged dimer (8) and amine adduct (9).....	23
5.1	Synthesis of 11	54
5.2	Synthesis of 12	57
5.3	Synthesis of 13	60
5.4	Synthesis of 14	61

CHAPTER I

INTRODUCTION

1.1 **N-Heterocyclic Carbenes (NHCs)**

Carbenes are a widely researched class of neutral compounds containing a divalent carbon atom with six electrons in their valence shells.^{1,2} Singlet carbenes (Figure 1.1) contain a lone pair of electrons in the sp^2 hybridized orbital of the carbon atom resulting in a vacant p orbital. This electron occupancy differs from the triplet carbene, in which each two electron resides in an individual in a degenerate p orbital.

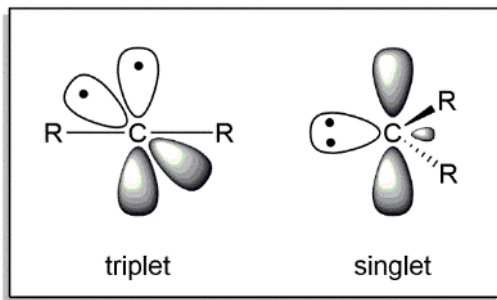


Figure 1.1 Triplet carbenes vs. singlet carbenes

Figure adapted from ref. 3

The competing electronic states of these two carbene classes is driven by the singlet-triplet σ - p_{π} gap (Figure 1.2). The linear geometry of the triplet carbene results in two nonbonding degenerate p orbitals (p_x and p_y) on the divalent carbon, commonly regarded as a diradical system. The singlet carbene, however, contains a bent geometry

resulting in a sp^2 hybridization thereby breaking the degeneracy of the p_x and p_y orbitals. This change in geometry fosters two new inequivalent p_π and σ orbitals, resulting from the former p_y (remains mostly unchanged), and the p_x (acquires s character), respectively.² The σ - p_π gap in the singlet ground-state is heavily favored with σ -electron withdrawing substituents on the carbene carbon thereby stabilizing the non-bonding σ orbital. In contrast, σ -electron donating groups decrease the σ - p_π energy gap, favoring the carbene in the singlet ground state.^{3,4}

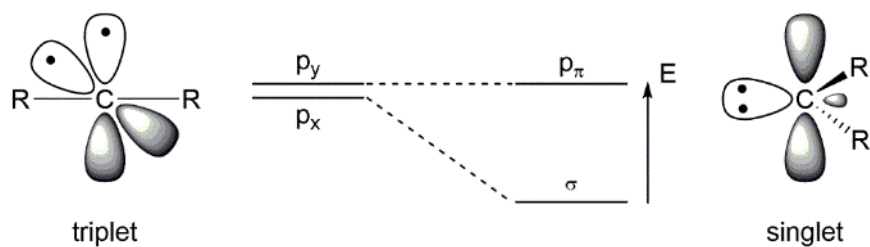


Figure 1.2 Triplet vs singlet carbene energy diagram

Figure adapted from ref. 2

NHCs are a specific class of carbenes which include increased electronic stability due to the nitrogen atoms.⁵ The inductive σ -electron withdrawing and π -electron donating ability of the nitrogen atom decreases the electron density on the carbene carbon thereby inducing stabilization of the NHC (Figure 1.3).⁶ Furthermore, N -substituents allow for manipulation of carbene stabilization from steric bulk through kinetic stability and electronic stabilization by incorporation of electron withdrawing and/or donating groups.⁶

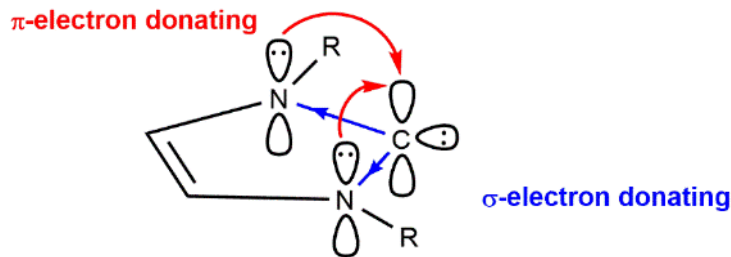


Figure 1.3 Electronic stabilization of NHC in imidazole-2-ylidene scaffold

Figure adapted from ref. 6

The increased stabilization and electronic tuning abilities of the NHC ligands have led to a substantial increase of reports demonstrating their catalytic applications with transition metals, rivaling the phosphine and cyclopentadienyl ligands.^{7,8} While NHCs and the phosphine congeners both bind to metal centers via dative coordination by their respective lone pairs, the strong σ donating capabilities make NHC ligands more attractive than their phosphine counterparts in many applications. The increased electron-donating properties of NHC ligands leads to thermodynamically stronger C–M bonds in NHC complexes represented by greater bond disassociation energies along with decreased bond lengths compared to the metal–ligand binding in phosphine complexes.⁹ This durability has allowed NHC complexes to be pertinent in many other chemical applications as well (Figure 1.4).^{5,10-15}

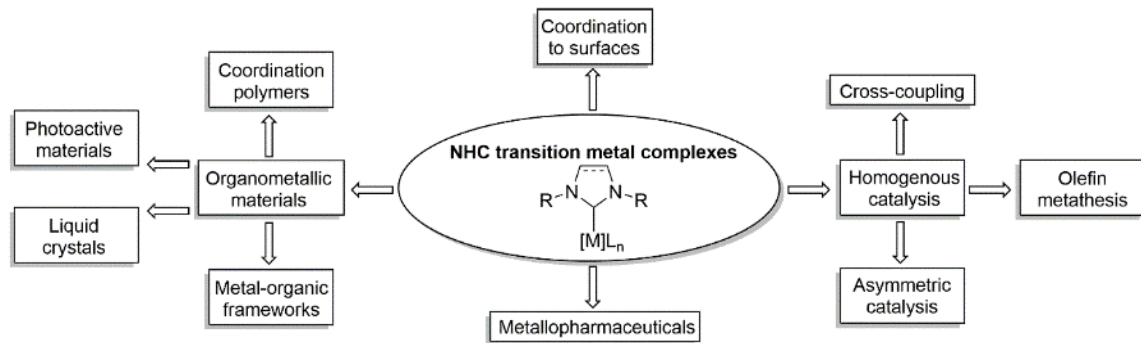


Figure 1.4 Applications of NHC complexes

Figure adapted from ref. 6

1.2 Pincer Ligands

Pincer ligands are tridentate chelators which coordinate in a meridional tridentate fashion thereby increasing the stability of organometallic complexes.¹⁶ This ligand architecture allows Shaw and co-workers were the first to introduce pincer-ligated transition metal complexes in the 1970's.¹⁷⁻¹⁹ Since then, there has been an enormous amount of development due to the variation that is allowed in pincer architectures (Figure 1.5).²⁰⁻²⁵

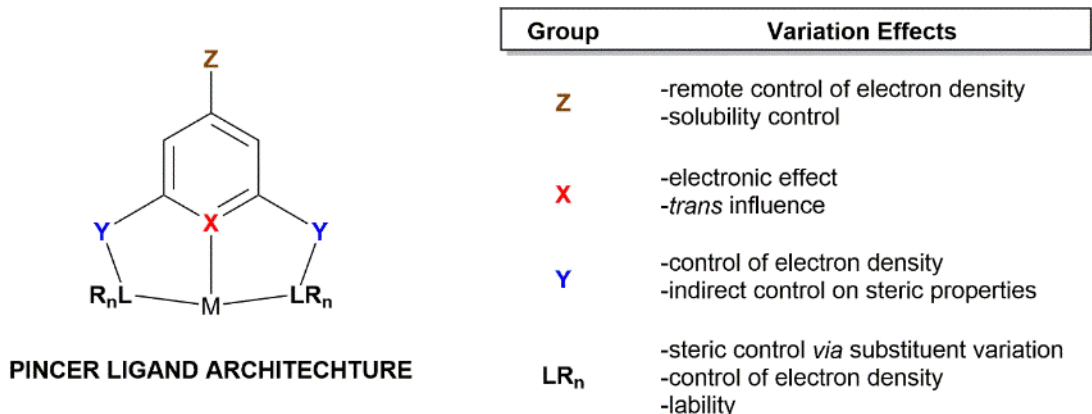


Figure 1.5 Generic pincer ligand design

Figure adapted from ref. 20

Pincer ligand architecture has led to high or unparalleled catalytic activity in many application including small molecule activation.^{16,26-28} In fact, the first report demonstrating the activation of an unstrained C–C bond in solution was catalyzed with a PCP pincer Rh complex.²⁹ The tridentate coordination of the pincer ligand to the metal center allows for increased kinetic stability in ligand–metal chelation. This robust and rigid ligand framework results in thermal stabilization of pincer complexes. Thus, pincer systems are suitable catalysts for endothermic reactions requiring high temperatures such as C–H bond functionalization, most notably alkane dehydrogenation.^{20,30-36}

1.3 CCC-NHC Pincer Ligands

Incorporation of NHCs into pincer architecture has been demonstrated in four different types of ligand design (Figure 1.6). (The common pincer nomenclature is based on the ligand coordinating atoms to the metal center; thus Type **A** and **C** are CNC and CCC, respectively.) Carbon and nitrogen are the two prevalent central atom donors to the metal centers, flanked with or without methylene spacers between the aryl and lateral NHC ligands (methylene spacer represented with a “^”). Since the seminal report of Type **C** CCC-NHC pincer complex,³⁷ groups worldwide have continued develop and expand on this class of ligand system.^{16,38-48}

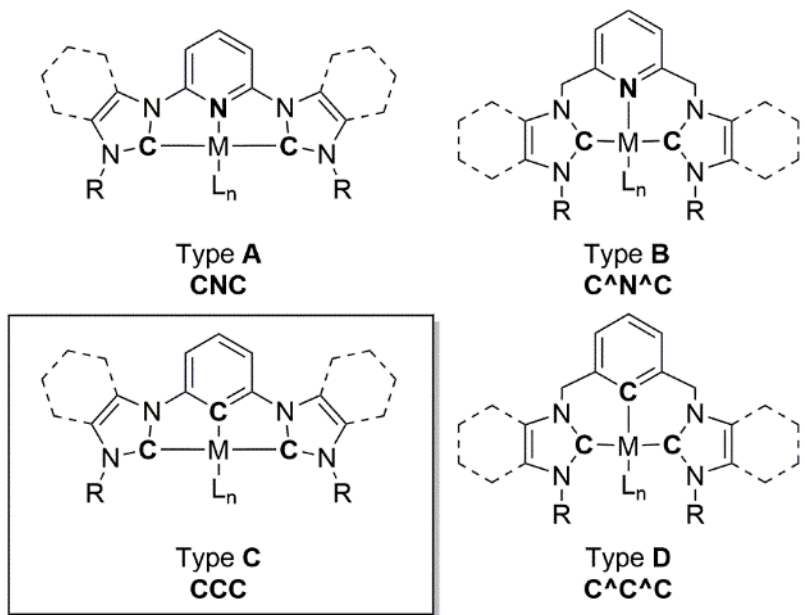


Figure 1.6 Type of NHC pincer framework

Type **C** framework was developed with the intention of being applicable for endothermic reactions, such as dehydrogenation of alkanes, due to the inherent thermal stability of the NHC pincer ligand architecture. Dehydrogenation reactions are favorable for Ir pincer framework due to the three-coordinate chelation, with two LR_2 (see Figure 1.5) groups (NHC for Type **C**) linked to the central coordinating group, leaving the *trans* site to the central group vacant.²⁰ This lack of congestion and three-coordinate d^8 Ir metal center allows for C–H oxidative addition and subsequent β -hydride elimination of the hydrocarbon substrate. With greater C–M bond strengths in NHC ligands, compared to the phosphine analogues, the CCC-NHC Ir pincer complex could offer increased stability at higher reaction temperatures compared to the active PCP and POCOP pincer reported by Jensen³⁵ and Brookhart,^{32,49} respectively (Figure 1.7).

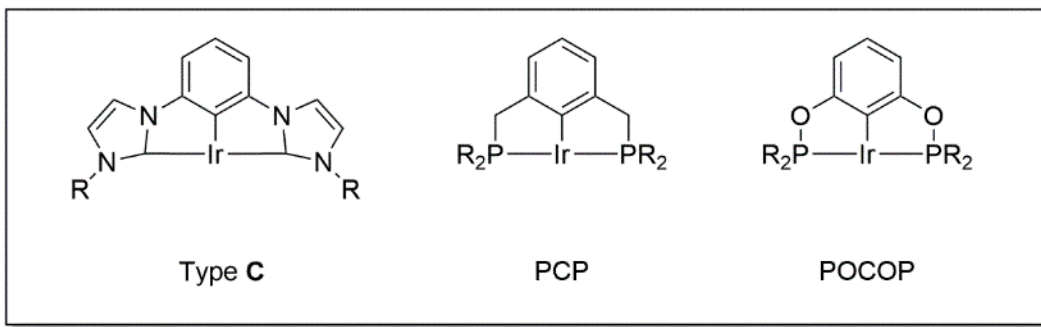


Figure 1.7 Type C, PCP, and POCOP pincer framework

The synthesis of CCC-NHC (Type C) ligand precursors begins with a Cu-catalyzed coupling of the desired heterocycle and 1,3-dibromobenzene, followed by alkylation affording the salt precursors for generation of CCC-NHC pincer complexes.^{50,51}

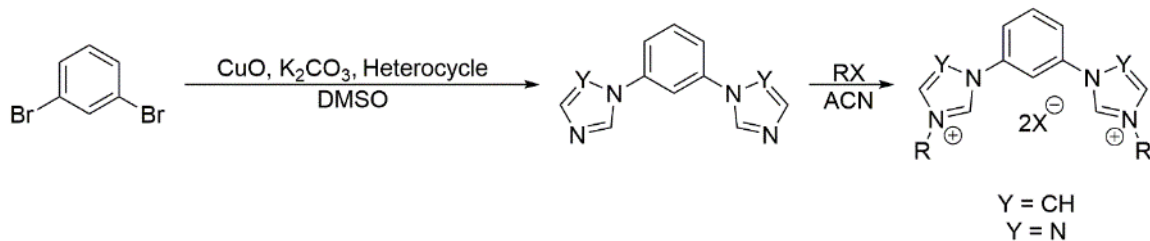


Figure 1.8 General synthesis of CCC-NHC ligand precursors

In preparation of CCC-NHC Rh and Ir pincer complexes, the Hollis group reported transmetalation of a CCC-NHC Zr pincer complex with Rh and Ir sources (Figure 1.9).^{37,52} Zr(NMe₂)₄ serves the two-fold purpose of acting as a base to generate the NHC's, and activating the aryl C–H bond via the electrophilic Zr center.

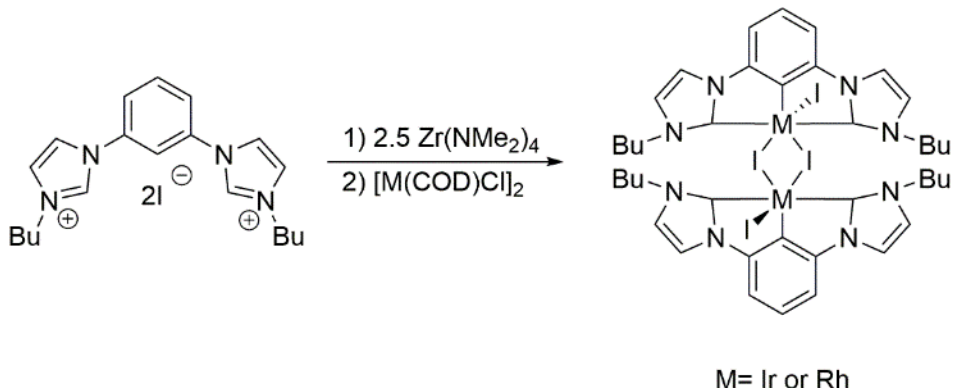


Figure 1.9 General synthesis of CCC-NHC Ir and Rh pincer complexes

Aside from screening the CCC-NHC Rh and Ir pincer complex for catalytic activity in intramolecular hydroamination/cyclization,⁵² studies of these pincer complexes have been limited. The work herein discusses the applicability of the CCC-NHC Rh pincer complex in synthetically useful C–C and C–B bond forming reactions, including room temperature β -boration catalysis. Preliminary studies show catalytic activity of the CCC-NHC Ir pincer complex activating aryl C–H bonds. Furthermore, the development of CCC-NHC pincer complexes with Co was explored, resulting in the first CCC-NHC Co pincer complexes to date. Finally, synthesis for CCC-NHC Rh(CO) complexes will also be reviewed, along with their potential role as a catalyst for photocatalytic C–H bond functionalization.

CHAPTER II

SYNTHESIS OF AIR-STABLE CCC-NHC PINCER COBALT COMPLEXES

2.1 Introduction

Pincer ligands have played a significant role in the development of homogenous catalysis ever since their introduction in the 1970's.^{26,53-55} The tridentate meridional architecture of the pincer ligand is a durable framework for various transition metal catalysis, most notably C–C bond formation,^{31,56-61} C–H bond activation,^{20,31,36,56,57,62-66} as well as small molecule activation^{66,67} including NH₃,^{67,68} CO₂,^{31,57,69-71} H₂O,^{56,72} and N₂ fixation.^{73,74} *N*-Heterocyclic carbenes (NHCs) increase the durability of these resilient ligand systems due to their strong σ-electron-donating properties, resulting in pincer scaffolds with profound metal–NHC bond strengths.^{5,12,16,55,75} As a result, these σ donors have become an attractive ligand to implement into catalytic systems with base metal centers such as Fe, Ni, and Co.⁷⁶⁻⁸⁴

Numerous NHC base metal pincer complexes have been reported with a CNC-NHC framework (refer to Figure 1.6).⁸⁵⁻⁹⁵ Danopoulos et al. reported some of the first examples of CNC-NHC pincers with low valent Fe and Co centers.^{85,86} Chirik and co-workers have illustrated several examples of catalytically active CNC-NHC Fe and Co complexes in hydrogenation^{96,97} and hydroboration.⁹⁸ More specifically, Co pincer complexes have shown to be effective in various catalysis such as alkene⁹⁹⁻¹⁰¹ and

nitrile^{102,103} hydrogenation, alcohol dehydrogenation,¹⁰⁴ CO₂ activation,^{71,105} alkene hydroboration^{106,107} and silylation,¹⁰⁸ and C–H borylation.⁶⁵

Despite the increasing reported examples of base metal pincer complexes, the CCC-NHC variants are exceedingly rare. In fact, the only reported CCC-NHC late transition base metal complexes to date are the bis(diisopropylphenylimidazol-2-ylidene)phenyl (^{DIPPO}CCC)Ni complexes recently reported by Fout and co-workers.¹⁰⁹ Prior to that report, the only other late transition metal monoanionic tridentate pincers in the literature are the bis(arylimidazol-2-ylidene)pyridine (^{iPr}CNC)Co complexes, published by Chirik and co-workers in 2013.⁹⁶ In order to promote metalation of the CCC imidazolium salt pre-cursor, activation of both the aryl C–H bond and the NHC protons of the CCC-NHC pro-ligand are required. The need for an electrophile to activate the aryl C–H bond, compounded with the inherently weak nature of M–C bonds of first row metals, has hindered the advance in CCC-NHC base metal complexes. However, use of early transition-metal amido starting materials have been effective in activating ligand pre-cursors in order to access multidentate complexes.¹¹⁰⁻¹¹⁴ The electrophilic nature of the d⁰ metal center along with the basicity of the amidos serves the two fold purpose needed to synthesize CCC-NHC pincer complexes. This also allows a synthetic route to late transition metal CCC-NHC pincer complexes through transmetalation. In 2005 and 2008, the Hollis group utilized this methodology to generate CCC-NHC Rh³⁷ and Ir⁵² pincer complexes, respectively. Herein, we extend this methodology to Co and discuss the synthesis of the first reported CCC-NHC Co pincer complexes.

2.2 Results and Discussion

The Hollis group has reported the synthesis of CCC-NHC Rh³⁷ and Ir⁵² pincer complexes via transmetalation of a CCC-NHC Zr complex with [Rh(COD)Cl]₂ and [Ir(COD)Cl]₂, respectively. Due to the successful formation of these group 9 pincer complexes, several Co transmetalating sources were screened with CCC-NHC Zr pincer complexes **1** and **2** (Figure 2.1) in order to access CCC-NHC Co complexes.

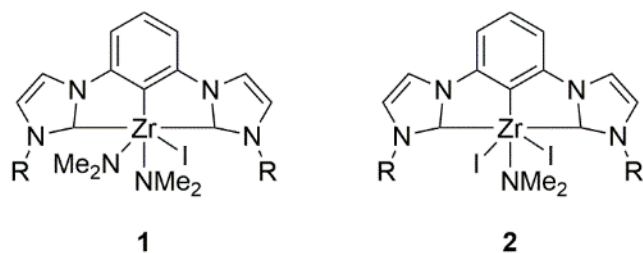
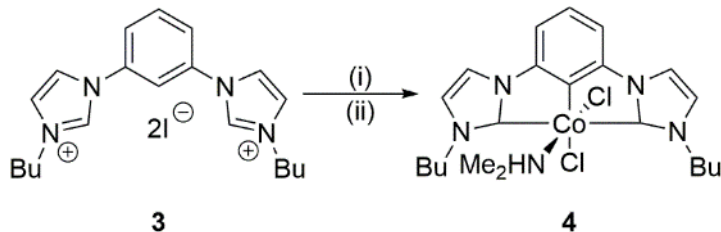


Figure 2.1 CCC-NHC pincer Zr complexes as transmetalating reagents

Initially, Co(acac)₃ was examined as a viable Co source for transmetalation. Investigation began with addition of 2.5 equiv of Zr(NMe₂)₄ to the (1,3-bis(3-butylimidazol-1-yl)benzene diiodide ligand precursor (**3**) to generate the Zr diamido complex (**1**) *in-situ* in dichloromethane, followed by addition of Co(acac)₃ (Scheme 2.1). The ¹H NMR spectrum indicated an absence of imidazolium proton signals at δ 11.27, however, various indistinguishable chemical species also appeared in the ¹H NMR spectrum (see Figure A. 1). A single red crystal was retrieved from the reaction mixture, which also included several blue and clear crystals, and identified as **4** from X-ray analysis.



Scheme 2.1 Synthesis of **4**

Conditions: (i) 2.5 equiv $\text{Zr}(\text{NMe}_2)_4$, CH_2Cl_2 , rt, 1h; (ii) 1.1 equiv $\text{Co}(\text{acac})_3$, CH_2Cl_2 , 12 h

An ORTEP plot of **4** is presented in Figure 2.2 with selected metric data in Table 2.1. Due to the meridional coordination and rigidity of the CCC-NHC tridentate ligand, Co complex **4** contains a distorted-octahedral center resulting in a $(\text{C}_{\text{NHC}})\text{--Co--}(\text{C}_{\text{NHC}})$ bond angle of 145.6° . The $(\text{C}_{\text{NHC}})\text{--Co}$ bonds length is 2.175 \AA , which is 0.213 \AA longer than the $(\text{C}_{\text{NHC}})\text{--Co}$ bond length of the $\text{Co}(\text{CNC})\text{Br}_3$ pincer reported by Danopoulos in 2004.⁸⁵ This trend of $(\text{C}_{\text{NHC}})\text{--Co}$ increased bond length is also observed when compared to Chirik's $(4\text{-CPh}_2\text{CH}_3\text{-}^{\text{iPr}}\text{CNC})\text{-CoN}_2$ pincer complex.⁹⁶ Although imidazolium pro-ligand **3** contained iodide halogens, complex **4** contained two coordinated chloride atoms, signifying halide exchange with dichloromethane.

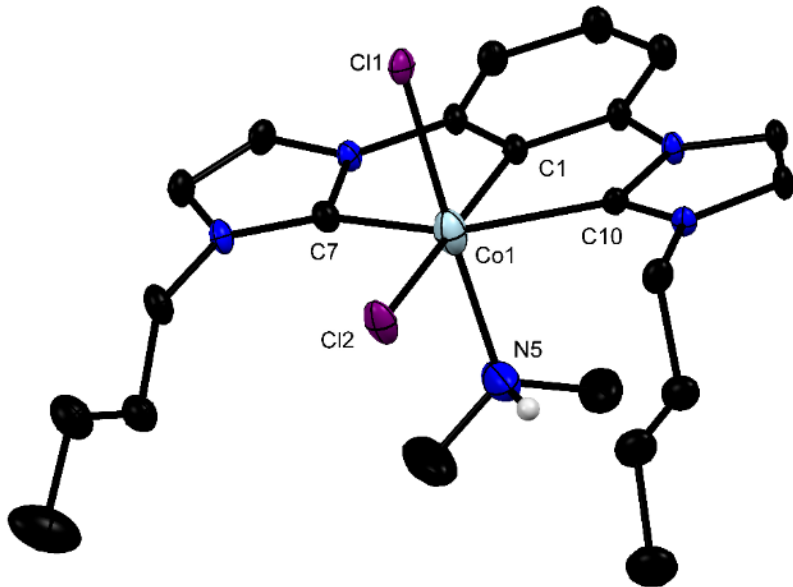


Figure 2.2 X-ray molecular structure of 4

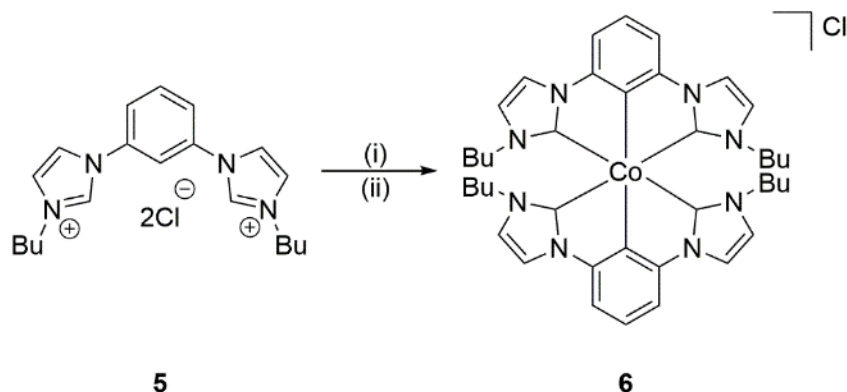
All but amine hydrogen are omitted for clarity. Thermal ellipsoids are shown at 50% probability.

Table 2.1 Selected Bond Lengths (\AA) and Angles ($^\circ$) for 4

	length (\AA)		angle ($^\circ$)
Co(1)–Cl(1)	2.411(1)	C(1)–Co(1)–C(7)	72.7(2)
Co(1)–Cl(2)	2.360(1)	C(1)–Co(1)–C(10)	73.0(2)
Co(1)–N(5)	2.135(5)	C(7)–Co(1)–C(10)	145.6(2)
Co(1)–C(1)	2.107(4)	Cl(2)–Co(1)–Cl(1)	90.06(4)
Co(1)–C(7)	2.202(4)	N(5)–Co(1)–Cl(2)	87.63(13)
Co(1)–C(10)	2.175(4)	C(10)–Co(1)–Cl(2)	106.04(10)

With many recent Co pincer reports exhibiting a chloride coordinated to the Co center,^{103,106,115-117} it was hypothesized the chloride imidazolium pro-ligand would be a more appropriate ligand pre-cursor in order to synthesize the desired Co complex 4 in high yield. In addition, CoCl_2 was examined as a Co source in hopes of further favoring the formation of 4. However, the reaction outlined in Scheme 2.2 resulted in the

formation of a single product, a presumed bis-coordination of two CCC-NHC ligands to the Co center (**6**).



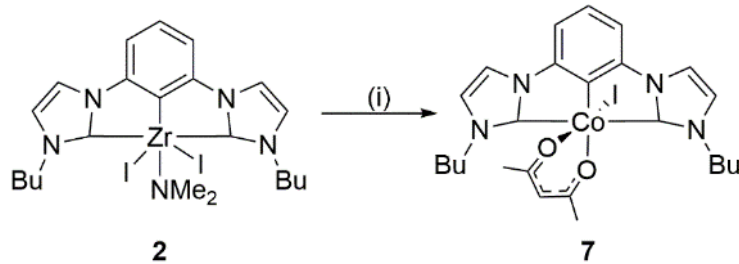
Scheme 2.2 Synthesis of **6**

Conditions: (i) 2.5 equiv $\text{Zr}(\text{NMe}_2)_4$, CH_2Cl_2 , rt, 1h; (ii) 1.1 equiv CoCl_2 , CH_2Cl_2 , 12 h

Accurate mass measurements of **6** contained the correct isotopic distribution pattern at $m/z = 701.3463$ to match the formulation of $\text{M} = \text{C}_{40}\text{H}_{50}\text{CoN}_8\text{Cl}$ ($[\text{M}-\text{Cl}]^+$) as the major product (see Figure A.2-4). Further evidence of **6** was observed in the ^1H NMR spectrum with a single methylene peak shifted upfield at $\delta = 2.80$, dissimilar to the diastereotopic methylene peaks shift of around $\delta = 4.5\text{-}5.5$ commonly observed in our previously reported mono-ligated CCC-NHC pincer complexes.¹¹⁸⁻¹²⁰ In addition, the butyl chain peaks of **6** overlapped and were also shifted upfield at $\delta = 0.66\text{-}0.73$. The C_{NHC} and the $\text{Co}-\text{C}_{\text{aryl}}$ peak were observed in the ^{13}C NMR spectrum at $\delta = 183.9$ and $\delta = 176.0$, respectively, verifying metalation to the Co center. It should also be noted this hexacoordination has also been reported with several CNC and scorpionato type Fe NHC complexes.⁷⁶ While further studies continue on air-stable **6**, investigation was continued

to into developing a facile methodology that would allow access to a single, mono-coordinated CCC-NHC Co complex.

Despite numerous experimental designs to directly access a single mono-coordinated CCC-NHC Co pincer complex, incomplete metalation or product mixtures continuously occurred. It was then surmised that the *in-situ* formed Zr diamido species **1** could be correlated to these experimental shortcomings. Zr diiodo complex **2** was then considered as a transmetalating reagent in hopes of accessing the desired mono-coordinated product in high yield. Ultimately, Zr diiodo complex **2** was found to be a competent transmetalating reagent resulting in the formation of a single product (**7**) (Scheme 2.3). Due to the lower solubility of complex **2**, compared to that of **1**, increased reaction temperatures were required to carry out the reaction in Scheme 2.3.



Scheme 2.3 Synthesis of **7**

Conditions: (i) 1.1 equiv Co(acac)₃, toluene, 90 °C, 12 h

¹H NMR spectrum of **7** reveals the diastereotopic methylene signals indicating the octahedral geometry that is also observed in our reported CCC-NHC Rh and Ir pincer complexes. The unique Co-acac six-membered chelate ring is easily identifiable in the ¹H NMR spectrum with two distinct singlets at δ 2.29 and δ 1.19 representing the methyl groups of the bidentate acac ligand. The carbene and Co–C_{aryl} signals at δ 183.9 and

□ 175.9, respectively, in the ^{13}C spectrum were also consistent with successful metalation.

X-ray quality crystals were grown by recrystallization using a DCM/hexane solvent system. The chelation of the acac ligand was further confirmed through X-ray analysis along with a coordinated iodide atom to the Co metal center. An ORTEP plot of Co complex **7** is displayed in Figure 2.3 along with selected metric data in Table 2.2. Compared to **4**, Co complex **7** adopts a less distorted octahedral geometry due to the chelation of the bidentate acac. The (C_{aryl})–Co bond length in **7** was measured at 1.874 Å (Table 2.2), noticeably shorter to the analogous bond distance in **4**.

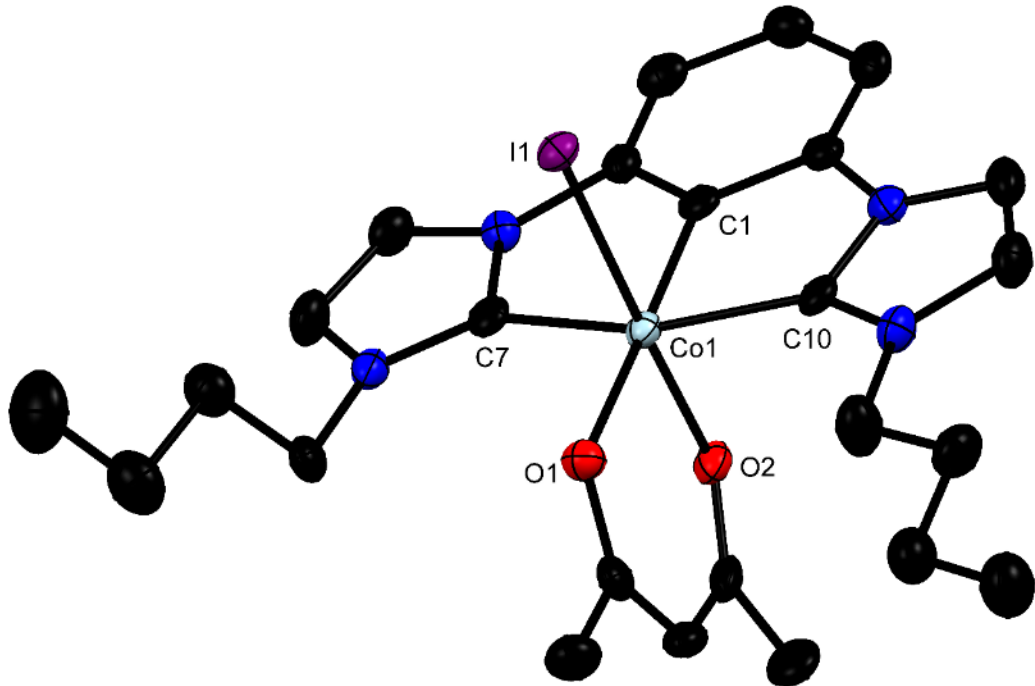


Figure 2.3 X-ray molecular structure of **7**

The hydrogens and one dichloromethane molecule were omitted for clarity. Thermal ellipsoids are shown at 50% probability.

Table 2.2 Selected Bond Lengths (Å) and Angles (°) for **7**

length (Å)	angle (°)
Co(1)–C(1)	1.874(5)
Co(1)–O(2)	1.941(3)
Co(1)–C(10)	1.965(4)
Co(1)–C(7)	1.971(4)
Co(1)–O(1)	2.002(3)
Co(1)–I(1)	2.5685(6)
C(1)–Co(1)–C(10)	80.09(19)
C(1)–Co(1)–C(7)	79.84(19)
C(10)–Co(1)–C(7))	159.9(2)
O(2)–Co(1)–O(1)	92.81(13)
C(1)–Co(1)–O(2)	89.48(16)
C(1)–Co(1)–I(1)	89.73(12)

2.3 Conclusion

In conclusion, air stable CCC-NHC Co pincer complexes have been synthesized via transmetalation of CCC-NHC Zr pincer complexes **1** and **2**. Furthermore, this facile methodology could potentially allow access to more economic catalyst development, an attractive alternative to costly precious metals systems. This synthetic route resulted in complexes **4**, **6**, and **7**, the first monoanionic CCC Co pincer complexes reported to date. Due to previous reports of Co(III) complexes being active catalysts in C–H activation,^{121–124} studies are currently ongoing in identifying the reactivity of Co complexes **4**, **6**, and **7**, as well as employing this methodology to access various oxidation states of the Co metal center.

2.4 Experimental

2.4.1 General Considerations

All NMR spectra were taken on a Bruker Advance III 600 MHz. High-resolution mass spectrometer (HRMS) data was acquired using ESI on a Bruker UHPLC-Micro-Q/T OF-MS/MS. Standard inert-atmosphere techniques were used unless otherwise noted. Synthesis of **1**, **2**, **3**, and **5** were prepared from previously reported literature procedures.^{37,51,125} Solvents were dried using molecular sieves and the SP-1 Solvent

System from LC Technology Solutions Inc. All commercial reagents were used as received. Chemical shifts (δ) in the NMR spectra (^1H and ^{13}C) were referenced by assigning the residual solvent peaks.

2.4.2 Synthesis of CCC-NHC Pincer Cobalt Complex 4

1,3-Bis(3-butylimidazol-1-yl)benzene diiodide (**3**) (0.200 g, 0.350 mmol), $\text{Zr}(\text{NMe}_2)_4$ (0.230 g, 0.870 mmol), and CH_2Cl_2 (15.0 mL) were combined in a 50 mL flask and stirred at room temperature (22 °C) for 1 h or until a light yellow homogenous solution appeared. Upon reaction mixture homogeneity, $\text{Co}(\text{acac})_3$ (0.137 g, 0.385 mmol) was added to the flask to afford an instantaneous dark blue homogenous solution, and stirring continued at room temperature for 12 h. Deionized water (1 mL) was added, and it was stirred vigorously for 10 minutes providing a white precipitate and a dark red supernatant. The red supernatant was filtered and the solvent was removed under reduced pressure affording a light brown solid. The solid was washed with hexanes (25 mL) and ether (25 mL) yielding a red/brown solid. The red/brown solid was dissolved in CH_2Cl_2 and hexanes was diffused into the saturated solution resulting in several red crystals (**4**).

2.4.3 Synthesis of CCC-NHC Pincer Cobalt Complex 6

1,3-Bis(3-butylimidazol-1-yl)benzene diichloride (**5**) (0.275 g, 0.698 mmol), $\text{Zr}(\text{NMe}_2)_4$ (0.190 g, 0.712 mmol), and CH_2Cl_2 (15.0 mL) were combined in a 50 mL flask and stirred at room temperature (22 °C) for 1 h or until a light yellow homogenous solution appeared. Upon reaction mixture homogeneity, $\text{Co}(\text{Cl})_2$ (0.099 g, 0.767 mmol) was added to the flask to afford an instantaneous dark blue homogenous solution, and stirring continued at room temperature for 6 h. Deionized water (1 mL) was added, and it

was stirred vigorously for 10 minutes providing a white precipitate and a dark red supernatant. The red supernatant was filtered and the solvent was removed under reduced pressure yielding a red/brown solid. The solid was washed with hexanes (25 mL) and (10 mL) of deionized water to remove unreacted **5** and Co(Cl)₂. The resulting brown/red supernatant was decanted resulting in an opaque green solid (0.180 g, 57%).) ¹H NMR (600 MHz, CDCl₃): δ 7.64 (s, 4H), 7.44-7.43 (t, *J* = 7.50 Hz, 2H), 7.34-7.33 (d, *J* = 7.50, 4H), 6.79 (s, 4H), 2.81-2.79 (m, 8H), 0.73-0.69 (m, 16H), 0.67-0.66 (m, 9H). ¹³C (150 MHz, CDCl₃): δ 183.9, 175.9, 148.1, 124.8, 123.2, 115.0, 107.3, 48.9, 33.7, 19.6, 13.9 HRMS-ESI (m/z): [M-Cl]⁺ calcd for C₄₀H₅₀CoN₈, 701.3485; found, 701.3463.

2.4.4 Synthesis of CCC-NHC Pincer Cobalt Complex **7**

2-(1,3-Bis(30-butyl-imidazol-20-ylidene)phenylene)(dimethylamido)diiodo zirconium (IV) (**2**) (0.100 g, 0.141 mmol), Co(acac)₃ (0.063 g, 0.1555 mmol) and toluene (15.0 mL) were combined in a 50 mL sealed vessel and stirred at 90 °C for 12 h. After cooling to room temperature, unreacted **2** conveniently precipitated out of the dark blue solution. The reaction mixture was then filtered, followed by solvent removal under reduced pressure. The resulting dark blue solid was heated under vacuum at 100 °C, to remove impurities, resulting in a black solid (0.070 g, 82%). X-ray quality crystals of **7** were grown by vapor diffusion of hexane into a saturated solution of CH₂Cl₂. ¹H NMR (600 MHz, CDCl₃): δ 7.69-7.68 (d, *J* = 1.50 Hz, 2H), 7.16-7.14 (t, *J* = 7.8 Hz, 1H), 7.09-7.08 (d, *J* = 7.50 Hz, 2H), 7.05-7.04 (d, *J* = 1.50 Hz, 2H), 5.17 (s, 1H), 4.73-4.68 (m, 2H), 4.52-4.47 (m, 2H), 2.29 (s, 1H), 2.20-1.97 (m, 4H), 1.92 (s, 1H), 1.00-0.98 (t, *J* = 7.52 Hz, 6H). ¹³C (150 MHz, CDCl₃): δ 188.6, 188.04, 187.6, 160.6, 149.7, 124.3, 121.6,

116.2, 107.7, 97.5, 49.5, 33.4, 28.4, 27.3, 20.3, 13.4. HRMS-ESI (m/z): [M-I]⁺ calcd for C₂₅H₃₂CoN₄O₂, 479.1852; found, 479.1836.

CHAPTER III

1,4-ADDITION OF ARYL BORONIC ACIDS TO α,β -UNSATURATED KETONES CATALYZED BY A CCC-NHC PINCER RHODIUM COMPLEX

3.1 Introduction

Catalytic formation of C–C bonds has been a major focus in organic synthesis for decades.¹²⁶⁻¹³⁰ A wide range of transition metals have been reported to induce C–C bond-forming reactions.¹³¹⁻¹³⁸ Two traditional metals used in C–C bond formations are Cu^{128,139-142} and Pd.^{131,143-150} Many cross coupling reactions are catalyzed by Pd, such as couplings with carbonyl groups at site-specific β -positions and desulfitative conjugate addition of aryl sulfonic acids.¹⁵¹ In 1997, Miyaura reported an innovative method for C–C bond formation utilizing Rh in a catalytic 1,4-addition of aryl boronic acids to electron deficient olefins,¹⁵² which produced C–C bonds, chiral centers, and biologically-active structural motifs.¹⁵³⁻¹⁶⁰ Due to air- and water-stability and wider substrate scope in 1,4-addition reactions with aryl boronic acids, Rh catalysts provided an attractive alternative to Cu and diorganozinc.^{136,155,161-167} Most reports of Rh catalyzed 1,4-addition have employed the use of phosphine ligands,^{152,153,155,158,159,160,162,164,168-185} which have exhibited broad applicability to a variety of Michael acceptors including enantioselective variants.^{158,176-178,184,186-189} However, reports using alternative ligands are sparse.^{157,163,167,189,190} Many of these methods used co-solvents that are less environmentally-friendly such as DME, toluene, THF, and dioxane.^{155,163,164,175,191-194}

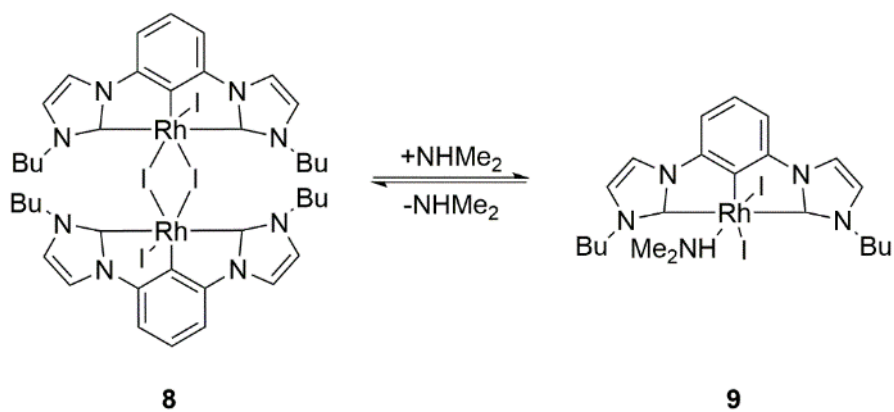
The Hollis group reported an air- and water- stable CCC–NHC pincer Rh complex that catalyzed the hydroamination/cyclization of unactivated alkene amines to produce five- and six-membered nitrogen heterocycles in high yields (>98%) while utilizing environmentally-friendly aqueous solvent.⁵² While excellent yields were obtained for cyclization, intermolecular hydroamination trials gave no reaction. The lack of reactivity was attributed to poor binding of the electron rich alkene to the electron rich metal center, therefore, reactivity with electron deficient alkenes was sought. With the goal of catalyzing an intermolecular reaction and extending the applicability of these complexes to other important catalytic reactions, 1,4-addition of aryl boronic acids to enones was examined. We report herein the coupling of α,β -unsaturated enones with aryl boronic acids catalyzed by a CCC–NHC pincer Rh complex in environmentally-friendly alcohol/water solvents.

3.2 Results and Discussion

Initial catalytic trials using freshly isolated **9** (Scheme 3.1) for the coupling of 2-cyclohexenone with 1.2 equiv of PhB(OH)₂ at 50 °C in MeOH/H₂O produced >99% yield in 1 h (Table 3.1, entry 2). In time the catalytic activity of **9** was observed to decline, since **9** was believed to dimerize³⁷ and lose NHMe₂, which could be detected over the isolated complex. Addition of NHMe₂ to the reactions was found to consistently generate a catalytically active species (Table 3.1, entries 2-4). The mol% of added NHMe₂ was varied and 3 mol% was found to be a good compromise that gave excellent yields and reproducibility. In the absence of the Rh complex, no product was formed (entry 5). A variety of protic and aprotic solvents were also screened. The reaction proceeded in a variety of “green” protic solvents.¹⁹⁵ Limited conversion was observed in

purely aprotic solvents such as benzene or methylene chloride (entries 17 and 18).

Conveniently, a 1:1 MeOH/H₂O mixture (entry 10) was found to give high yields comparable with 10:1 solvent mixtures, and was, therefore, chosen for further catalytic trials. It should be noted, with extended reaction times, biphenyl was observed in the GC-MS spectra in minor amounts (<3%, entries 12-16).



Scheme 3.1 Equilibrium of CCC-NHC Rh iodo-bridged dimer (**8**) and amine adduct (**9**)

Table 3.1 Optimization of **8** with Cyclohexenone and PhB(OH)₂

entry	solvent	cat.	mol % NHMe ₂	time	yield ^a
1	10:1 MeOH/H ₂ O	8	--	1h	0
2	10:1 MeOH/H ₂ O	8	0.6	1h	>98
3	10:1 MeOH/H ₂ O	8	3.0	1h	>98
4	10:1 MeOH/H ₂ O	8	11.0	1h	>98
5	10:1 MeOH/H ₂ O	--	12.0	1h	0
6	H ₂ O	8	3.0	1h	>98
7	MeOH	8	3.0	1h	>98
8	EtOH	8	3.0	1h	>98
9	10:1 EtOH/H ₂ O	8	3.0	1h	>98
10	1:1 MeOH/H ₂ O	8	3.0	1h	>98
11	10:1 Dioxane/H ₂ O	8	3.0	1h	>98
12	10:1 Dioxane/H ₂ O	--	--	48h	0
13	H ₂ O	--	--	20h	0
14	10:1 EtOH/H ₂ O	[Rh(COD)Cl] ₂	--	20h	51
15	10:1 EtOH/H ₂ O	--	3.0	20h	0
16	10:1 EtOH/H ₂ O	8	--	16h	0
17	CH ₂ Cl ₂	8	3.0	1h	0
18	Benzene	8	3.0	1h	10

^aYields were determined by ¹H NMR and identified by GC-MS

Once the reaction conditions were optimized, the catalyst loading was lowered to 1 and 0.1 mol% (Table 3.2, entry 1). Even at the reduced loading, moderate conversion was seen within 1 h, although not at the level seen with 2 mol%. Therefore, all remaining reactions were carried out with 2 mol% of the catalyst. While good to moderate yields ($\geq 77\%$) were obtained at 50 °C (entries 5 and 7) and even room temperature (entry 1), low yields were observed for several substrates at these temperatures (entries 4 and 6). Therefore a higher temperature of 80 °C was evaluated and found to produce consistently higher yields. The screening of cyclic enones also included 2-cyclopentenone to examine 5-membered rings, (entry 2) which also produced a high yield with PhB(OH)₂. 3-Methylcyclohexenone (entry 3) reacted much slower, which was attributed to the methyl group at the β -position creating steric hindrance. All acyclic Michael acceptors screened

in Table 3.2 demonstrated excellent yields with PhB(OH)₂ including the enal cinnamaldehyde (entry 6). High yields were also obtained with chalcone (entry 8), a Michael acceptor with medicinal significance due to its cytotoxic, anticancer, and other therapeutic characteristics.¹⁹⁶ Since consistently high yields were obtained at 80 °C with α,β-unsaturated enones and enals, this temperature was adopted for further studies.

Table 3.2 Scope of Michael Acceptors with PhB(OH)₂^a

entry	product	yield ^b (mol%, time, temp.)	entry	product	yield ^b (mol%, time, temp.)
1		92(2,1h,80 °C) ^c 99(2,24h,rt) 99(2,1h,50 °C) 86(1,1h,50 °C) 69(0.1,1h,50 °C)	5		68(2,1h,80 °C) ^c 86(2,1h,50 °C) 96(2,1h,80 °C)
2		78(2,1h,80 °C) ^c 99(2,1h, 80 °C)	6		40(2,1h,80 °C) ^c 20(2,1h,50 °C) 99(2,1h,80 °C)
3		21(2,72h,80 °C) ^c 57(2,72h,80 °C)	7		91(2,1h,80 °C) ^c 77(2,1h,50 °C) 99(2,1h,80 °C)
4		94(2,1h,80 °C) ^c 15(2,1h,50 °C) 99(2,1h,80 °C)	8		93(2,1h,80 °C) ^c 99(2,1h,80 °C)

^aSubstrate (0.0735 mmol), PhB(OH)₂ (0.0880 mmol), NHMe₂ (0.002 mmol), **8** (0.00150 mmol), and 0.700 mL of solvent were heated at 80 °C. ^b% yield determined by ¹H NMR spectrum and product ion peaks were observed by GC-MS. ^cIsolated yield.

The scope of reaction with aryl boronic acids was examined (Table 3.3). Utilizing previously optimized conditions of 1.2 equiv of PhB(OH)₂, initial catalytic trials with substituted-aryl boronic acids with 2-cyclohexenone produced low yields (entries 6 and

8). Upon careful observation of the ^1H NMR spectra and GC-MS data, deborylated aryl compounds could be observed, indicating deborylation of the boronic acid. This observation is consistent with previously reported literature, stating hydrolysis of boronic acids occurs as a competing side reaction under basic conditions and/or elevated temperatures.¹⁹⁷ Previous reports had overcome this loss of boronic acid due by increasing the boronic acid equivalents, which resulted in higher yields of product.¹⁹⁸ Therefore, 2.5 equiv of all aryl boronic acids were evaluated and found to produce excellent yields. Many of the boronic acids with electron rich substituents generated yields >97% in 1 h (entries 1, 2, and 4). A high yield was obtained using naphthalene boronic acid (entry 5), which is noteworthy due to naphthalene's importance in the production of plastic, dyes, and insecticides.^{199,200} It has been reported that aryl boronic acids with *ortho*-substituents drastically slow the rate of 1,4-addition,¹⁵² which held true for 2,4,6-trimethylphenyl boronic acid (entry 3). However, 2-methylphenyl and 2-methoxyphenyl boronic acid (entries 2 and 9) resulted in high yields in just 1 h. While longer reaction times were required to obtain high yields with boronic acids containing strong electron withdrawing substituents (entries 6 and 8), no yield was obtained when using 1,3-dibromophenyl boronic acid (entry 7). Boronic acids containing moderate electron withdrawing groups, (entries 9 and 10), produced yields of >99% in just 1 h.

Table 3.3 Scope of Cyclohexenone with ArB(OH)₂^a

entry	yield ^b (mol%, time, temp.)	entry	yield ^b (mol%, time, temp.)		
1		77(2,1h,80°C) ^c 97(2,1h, 80°C)	6		64(2,1h, 80°C) ^c 62(2,72h,80°C) ^d 99(2,7h,80°C)
2		70 (2,1h, 80°C) ^c 99(2,1h, 80°C)	7		NR(2,63h,80°C)
3		76(2,1h, 80°C) ^c 99(2,24h,80°C)	8		34(2,1h, 80°C) ^c 22(2,72h,80°C) ^d 46(2,72h,80°C)
4		81(2,1h, 80°C) ^c 98(2,1h, 80°C)	9		92(2,1h, 80°C) ^c 99(2,1h, 80°C)
5		80 (2,1h,80°C) ^c 99(2,1h,80°C)	10		92(2,1h,80°C) ^c 99(2,1h,80°C)

^aSubstrate (0.0735 mmol), PhB(OH)₂ (0.0880 mmol), NHMe₂ (0.002 mmol), **8** (0.00150 mmol), and 0.700 mL of solvent were heated at 80 °C. ^b% yield determined by ¹H NMR spectrum and product ion peaks were observed by GC-MS. ^cIsolated yield. ^d% yield when using 1.2 equiv (0.088 mmol) of ArB(OH)₂.

Nitrogen heterocycles such as pyrazole and pyridine are some of the most common heterocycles in biologically- and medicinally-active compounds.²⁰¹⁻²⁰³ Pyrimidine is an important pharmacophore and plays a vital role in the synthesis of nucleic acids and the HIV drug zidovudine.²⁰⁴ 5-Fluorouracil (5-FU) is an important chemotherapy agent and has shown inhibitory effects on human gastric carcinoma cell

growth.²⁰⁵ Sulfur heterocycles such as thiophenes, can be coupled to produce polythiophenes electron acceptors which have attracted considerable attention due to their outstanding electrical, optical, and magnetic properties.^{206,207} Polysubstituted furans are also important building block throughout synthetic chemistry, and widely seen throughout pharmaceutical and natural products.²⁰⁸ The scope of reaction with heterocyclic boronic acids was examined with 2-cyclohexenone as the Michael acceptor (Table 3.4).

Deborylation products were also observed in the early screenings of heterocyclic boronic acid, therefore 2.5 equiv of boronic acid were employed. With this increase, higher yields were obtained for many 1,4-addition products. It was found longer reaction times were required compared to many of the aryl boronic acids to produce moderate to high yields for most of the heterocycles screened in Table 3.4. With extended reaction times, a yield of 77% was obtained with furan-3-boronic acid (entry 1). Thiophene-3-boronic acid (entry 2) produced moderate conversion, while no conversion was observed when using uracil-5-boronic acid (entry 3). Nitrogen heterocycles, 3-pyrazole boronic acid and 4-pyridine boronic acid, were successfully coupled to 2-cyclohexenone in high yields (entries 4 and 5). Pyrimidine boronic acid showed no conversion despite the increase in equivalents and extended reaction times (entry 6).

Table 3.4 Scope of Cyclohexenone with Heterocycle Boronic Acids^a

entry	yield ^b (mol%, time, temp.)	entry	yield ^b (mol%, time, temp.)
1 	26(2,72h,80°C) ^c 77(2,72h,80°C)	4 	87(2,7h,80°C) ^c 99(2,7h,80°C)
2 	46(2,72h,80°C) ^c 69(2,72h,80°C)	5 	36(2,72h,80°C) ^c 83(2,7h,80°C)
3 	NR(72h)	6 	NR(72h)

^a2-Cyclohexenone (0.0735 mmol), heterocycle boronic acid (0.184 mmol), NHMe₂ (0.002 mmol), **8** (0.00150 mmol), and 0.700 mL of solvent were heated at 80 °C. ^b% yield determined by ¹H NMR and the product was observed by GC-MS. ^cIsolated yield.

3.3 Conclusion

A CCC–NHC pincer Rh complex has been reported to catalyze the coupling of aryl and heterocyclic boronic acids to cyclic and acyclic α,β -unsaturated enones and enals in high yields without the exclusion of air and water. Promising results were observed in the 1,4-addition of nitrogen heterocycles, which are commonly seen in medicinal- and biologically-active compounds.²⁰¹⁻²⁰³ Additionally, high yields were observed while utilizing solely environmentally “green” alcohol/water solvents. Further development of the scope and limitations of this methodology is underway.

3.4 Experimental

3.4.1 General Consideration

Gas chromatography mass spectrometer (GC-MS) data was collected on a Shimadzu GCMS-QP2010 plus. All NMR spectra were taken on a Bruker Avance III 300 or 600 MHz. High-resolution mass spectrometer (HRMS) were acquired using ESI technique on a Bruker UHPLC-Micro-Q/T of MS/MS. IR spectrum was collected using Thermo Scientific Nicolet iS 5 FT-IR.

3.4.2 General Procedure for Catalytic Trials

On a bench top, a NMR tube was charged with enone (0.0735 mmol), boronic acid (0.1836 mmol), catalyst **8** (0.00150 mmol), 2M NHMe₂ (0.002 mmol), H₂O (0.350 mL), and MeOH (0.350 mL). The NMR tube was closed and heated to 80 °C. The reaction was monitored by ¹H NMR spectroscopy. The crude reaction mixture was then filtered through a plug of celite to remove any insolubles. Volatiles from the filtered reaction mixture were then removed under reduced pressure resulting in an oil. 5 mL of CHCl₃ was added to the oil and the resultant mixture was passed through a second plug of celite. The solvent was removed under reduced pressure to afford the crude product.

3.4.3 Synthesis of 3-(1*H*-pyrazol-4-yl)cyclohexan-1-one

*3-(1*H*-pyrazol-4-yl)cyclohexan-1-one* (Table 3.4, entry 4): The title compound was prepared according to the general procedure using H₂O and MeOH. Volatiles were removed under reduced pressure resulting in a yellow oil, which was passed through a short plug of silica with 1×25 mL CH₂Cl₂ and concentrated again. Purification by column chromatography (silica gel) eluting with CH₂Cl₂, (5 mL), CH₂Cl₂:iPrOH (10 mL,

20:1), and CH₂Cl₂:iPrOH (15 mL, 10:1) gave a yellow solid (10.9 mg, 87%). Due to volatility trace solvents remained observable in the ¹H NMR spectrum. ¹H NMR (300 MHz, CDCl₃) δ 7.51 (d, *J* = 1.63 Hz, 1H), 7.39 (d, *J* = 2.31 Hz, 1H), 6.22 (t, *J* = 2.12 Hz, 1H), 4.52 (m, 1H), 3.00 (dd, *J*₁ = 10.16 Hz, *J*₂ = 10.26 Hz, 1H), 2.82 (dd, *J*₁ = 5.13 Hz, *J*₂ = 4.96 Hz, 1H), 2.41 (m, 1H), 2.2 (m, 2H), 2.04 (m, 1H), 1.71 (m, 1H); ¹³C NMR (600 MHz, CDCl₃) δ 208.02, 139.55, 139.49, 127.56, 105.42, 59.80, 47.40, 31.85, 21.81; HRMS (ESI) C₉H₁₃N₂O⁺ [M+H]⁺ calculated m/z = 165.1022, found 165.1022.

3.4.4 Product Characterization

For Michael Addition products known from previous literature (Table 3.2, Entries 1-8), (Table 3.3, Entries 1-6,8-10), and (Table 3.4, Entries 1-3,5), ¹H NMR spectra are provided. Full characterization data are provided for (Table 3.4, Entry 4).

3-phenylcyclohexan-1-one (Table 3.2, Entry 1):¹⁵¹ ¹H NMR (600 MHz, CDCl₃) δ 7.33 (m, 2H), 7.23 (m, 3H), 3.01 (t, *J* = 11.7 Hz, 1H), 2.61 (m, 1H), 2.59 (m, 1H), 2.45 (m, 1H), 2.39 (m, 1H), 2.16 (m, 1H), 2.10 (m, 1H), 1.83 (m, 2H).

3-phenylcyclopentan-1-one (Table 3.2, Entry 2):²⁰⁹ ¹H NMR (300 MHz, CDCl₃) δ 7.30 (m, 2H), 7.25 (m, 3H), 3.33 (m, 1H), 2.65 (m, 1H), 2.43 (m, 4H), 1.95 (m, 1H)

3-methyl-3-phenylcyclohexan-1-one (Table 3.2, Entry 3):²¹⁰ ¹H NMR (300 MHz, CDCl₃) δ 7.31 (m, 5H), 2.91 (d, *J* = 14.22 Hz, 1H), 2.32 (t, *J* = 7.24 Hz, 2H), 2.19 (m, 1H), 1.89 (m, 2H), 1.71 (m, 1H).

3-phenylcycloheptan-1-one (Table 3.2, Entry 4):²¹¹ ¹H NMR (600 MHz, CDCl₃) δ 7.30 (m, 2H), 7.18 (m, 3H), 2.91 (m, 2H), 2.66 (d, *J* = 11.1 Hz, 1H), 2.58 (m, 2H), 2.10 (m, 2H), 2.02 (m, 1H), 1.73 (m, 2H), 1.51 (m, 1H).

4-phenylnonan-2-one (Table 3.2, Entry 5):²⁰⁹ ^1H NMR (600 MHz, CDCl_3) δ 7.29 (m, 2H), 7.17 (m, 3H), 3.10 (m, 1H), 2.71 (m, 2H), 2.01 (s, 3H), 1.58 (m, 2H), 1.21 (m, 6H), 0.82 (t, $J = 6.68$ Hz, 1H).

3,3-diphenylpropanal (Table 3.2, Entry 6):²¹² ^1H NMR (300 MHz, CDCl_3) δ 9.77 (t, $J = 1.89$ Hz, 1H), 7.31 (m, 10H), 4.66 (m, 1H), 3.22 (dd, $J_1 = 1.90$ Hz, $J_2 = 1.88$ Hz, 2H).

4,4-diphenylbutan-2-one (Table 3.2, Entry 7):²¹³ ^1H NMR (300 MHz, CDCl_3) δ 7.25 (m, 10H), 4.59 (t, $J = 7.51$ Hz, 1H), 3.18 (d, $J = 7.61$ Hz, 3H).

1,3,3-triphenylpropan-1-one (Table 3.2, entry 8):²¹⁴ ^1H NMR (600 MHz, CDCl_3) δ 7.93 (d, $J = 6.83$ Hz, 2H), 7.53 (t, $J = 7.21$ Hz, 1H), 7.43 (t, $J = 7.67$ Hz, 2H), 7.27 (m, 8H), 4.83 (t, $J = 7.29$ Hz, 1H), 3.74 (d, $J = 7.35$ Hz, 2H).

3-(p-tolyl)cyclohexan-1-one (Table 3.3, Entry 1):¹⁵¹ ^1H NMR (300 MHz, CDCl_3) δ 7.11 (m, 4H), 2.98 (m, 1H), 2.57 (m, 2H), 2.48 (m, 2H), 2.36 (s, 3H), 2.15 (m, 2H), 1.82 (m, 2H).

3-(o-tolyl)cyclohexan-1-one (Table 3.3, Entry 2):¹⁵¹ ^1H NMR (300 MHz, CDCl_3) δ 7.24 (m, 2H), 7.16 (m, 2H), 3.21 (m, 1H), 2.53 (m, 2H), 2.46 (m, 1H), 2.32 (s, 3H), 2.19 (m, 1H), 2.00 (m, 1H), 1.81 (m, 2H).

3-mesitylcyclohexan-1-one (Table 3.3, Entry 3):¹⁷⁹ ^1H NMR (600 MHz, CDCl_3) δ 6.84 (s, 2H), 3.40 (m, 1H), 2.94 (t, $J = 14.05$ Hz, 1H), 2.32 (m, 14H), 1.88 (m, 1H), 1.75 (m, 1H).

3-(4-(tert-butyl)phenyl)cyclohexan-1-one (Table 3.3, Entry 4):²⁰⁹ ^1H NMR (300 MHz, CDCl_3) δ 7.36 (m, 2H), 7.16 (m, 2H), 2.99 (m, 1H), 2.50 (m, 4H), 2.16 (m, 2H), 2.14 (m, 2H), 1.32 (s, 9H).

3-(naphthalen-1-yl)cyclohexan-1-one (Table 3.3, Entry 5):¹⁵¹ ¹H NMR (600 MHz, CDCl₃) δ 8.05 (d, *J* = 8.75 Hz, 1H), 7.89 (d, *J* = 7.90 Hz, 1H), 7.75 (d, *J* = 8.40 Hz, 1H), 7.50 (m, 1H), 7.55 (m, 1H), 7.53 (m, 2H), 7.41 (m, 1H), 3.86 (m, 1H), 2.76 (m, 1H), 2.67 (t, *J* = 12.52 Hz, 1H), 2.57 (m, 1H), 2.50 (m, 1H), 2.25 (m, 2H), 2.03 (m, 1H), 1.96 (m, 1H).

3-(3-bromophenyl)cyclohexan-1-one (Table 3.3, Entry 6):²¹⁵ ¹H NMR (600 MHz, CDCl₃) δ 7.37 (d, *J* = 7.02 Hz, 2H), 7.21 (t, *J* = 7.40 Hz, 1H), 7.14 (d, *J* = 7.09 Hz, 1H), 2.98 (m, 1H), 2.59 (m, 1H), 2.51 (m, 2H), 2.39 (m, 1H), 2.16 (m, 1H), 2.06 (m, 1H), 1.76 (m, 2H).

3-(4-nitrophenyl)cyclohexan-1-one (Table 3.3, Entry 8):¹⁵¹ ¹H NMR (600 MHz, CDCl₃) δ 8.21 (d, *J* = 8.32 Hz, 2H), 7.40 (d, *J* = 8.37 Hz, 2H), 3.14 (m, 1H), 2.63 (m, 1H), 2.53 (m, 2H), 2.41 (m, 1H), 2.20 (m, 1H), 2.11 (m, 1H), 1.86 (m, 2H).

3-(2-methoxyphenyl)cyclohexan-1-one (Table 3.3, Entry 9):¹⁵¹ ¹H NMR (600 MHz, CDCl₃) δ 7.22 (m, 2H), 7.19 (t, *J* = 7.78 Hz, 1H), 6.88 (d, *J* = 7.66 Hz, 1H), 3.82 (s, 3H), 3.43 (m, 1H), 2.59 (m, 1H), 2.53 (m, 1H), 2.45 (m, 1H), 2.35 (m, 1H), 2.11 (m, 1H), 2.01 (m, 1H), 1.82 (m, 2H).

methyl 4-(3-oxocyclohexyl)benzoate (Table 3.3, Entry 10):¹⁵¹ ¹H NMR (300 MHz, CDCl₃) δ 8.02 (m, 2H), 7.32 (m, 2H), 3.93 (s, 3H), 3.10 (m, 1H), 2.58 (m, 4H), 2.19 (m, 2H), 1.79 (m, 2H).

3-(furan-3-yl)cyclohexan-1-one (Table 3.4, Entry 1):²¹⁶ ¹H NMR (300 MHz, CDCl₃) δ 7.37 (m, 1H), 7.23 (m, 1H), 6.30 (m, 1H), 3.00 (m, 1H), 2.62 (m, 1H), 2.42 (m, 3H), 2.30 (m, 2H), 1.75 (m, 2H).

3-(thiophen-3-yl)cyclohexan-1-one (Table 3.4, Entry 2):¹⁶⁶ ^1H NMR (300 MHz, CDCl₃) δ 7.29 (m, 1H), 6.98 (m, 2H), 3.16 (m, 1H), 2.72 (m, 1H), 2.66 (m, 3H), 2.16 (m, 2H), 1.78 (m, 2H),

3-(pyridin-4-yl)cyclohexan-1-one (Table 3.4, Entry 5):²¹⁷ ^1H NMR (300 MHz, CDCl₃) δ 8.56 (m, 2H), 7.14 (m, 2H), 3.03 (m, 1H), 2.58 (m, 4H), 2.16 (m, 2H), 1.84 (m, 2H).

CHAPTER IV

ROOM TEMPERATURE β -BORATION OF α,β -UNSATURATED CARBONYL
COMPOUNDS CATALYZED BY CCC-NHC PINCER
RHODIUM COMPLEXES

4.1 Introduction

Organoborane compounds are highly sought after intermediates in organic synthesis. The facile transformation of the C–B bond into other functional groups such as alcohols, amines, and alkenes allows direct access to a wide range of organic molecules.²¹⁸⁻²²⁰ In 1997, a Pt catalyst was utilized in the first report of β -boration of α,β -unsaturated carbonyl compounds using a diboron reagent.²²¹ To date, the boration of α,β -unsaturated carbonyl compounds has been catalyzed with Pt,²²¹⁻²²⁴ Pd,^{225,226} Rh,^{173,188,227,228} Cu,²²⁹⁻²⁵⁴ Ni,^{226,255,256} Fe,²⁵⁷ metal-free phosphines,²⁵⁸⁻²⁶⁰ and NHCs.²⁶¹⁻²⁶³ Subsequently, β -boration of α,β -unsaturated carbonyl compounds has become very useful due to the additional carbonyl contained in the product.^{222,227,231-236,255,257} Oxidation of the product provides access to β -hydroxy compounds as an alternative to the aldol reaction or reduction of β -keto carbonyl compounds. β -Hydroxy carbonyl compounds are found widely in natural products and pharmaceuticals.^{264,265} Additionally, β -boro-carbonyl compounds have been reported as being effective therapeutic agents in cancer treatment.^{266,267}

Cu systems have been the most commonly applied catalysts for β -boration of α,β -unsaturated carbonyl compounds. Noteworthy examples have been reported using strictly protic solvents such as MeOH²⁴⁰ and H₂O.^{250,251,268-271} In 2009, Santos reported the synthesis of an innovative sp²–sp³ diboron reagent and demonstrated its application in a Cu catalyzed β -boration of acyclic substrates.²⁴⁶ In 2008, the first asymmetric catalysis for β -boration of acyclic compounds was reported using a chiral Cu phosphine complex,²²⁹ opening the path for innovative work such as asymmetric β -borations conducted in water.^{251,268-270} Subsequently, other examples of asymmetric catalysis have been reported with Ni,²²⁶ Pd,²²⁶ Rh,^{188,227,228} and Cu.^{232,235,236,241-244,247-249,253,254,271-273} Metal free-catalysis has also been developed, including asymmetric variants,^{260,262} such as a chiral NHC salt reported by Hoveyda.^{262,263} Surprisingly, only a few examples in the literature have utilized Rh. In 2002, Kabalka¹⁷³ reported the first Rh catalyzed β -boration of α,β -unsaturated electron deficient olefins. Then in 2009 several enantioselective Rh catalyzed examples were reported using Rh(Phebox).²²⁸ Despite many reports utilizing various transition metals, base additives or high temperatures have been required for efficient rates, and limitations to acyclic α,β -unsaturated carbonyl substrates have been noted. In addition, very few cyclic products with boron-substituted quaternary carbon centers have been reported.²⁶¹ A catalyst that provides cyclic β -boro-carbonyl compounds containing quarternary carbon centers and can operate at room temperature will be an advance in the formation of C–B bonds as well as β -hydroxy carbonyl compound derived thereof.

Previously, we had reported a mixture of the CCC-NHC pincer Rh complexes **8/9** (refer to Scheme 3.1) that efficiently catalyzed 1,4-addition of aryl boronic acids to

electron-deficient alkenes.²⁷⁴ CCC-NHC pincer Rh complexes **8/9** with added NHMe₂, produced excellent yields (>90%) with various Michael acceptors and arylboronic acids in protic solvents.²⁷⁴ Upon further attempts to optimize the synthesis of **9**, a crude isolate (**10**) that was orange in color was obtained reproducibly (Figure 4.1). We report herein the results of screening material **10** in the β -boration of cyclic and acyclic α,β -unsaturated, electron-deficient alkenes and a partial characterization of the mixture **10**. To our knowledge, this is the first report of a CCC-NHC pincer Rh complex catalyzing 1,4-addition reactions at room temperature.

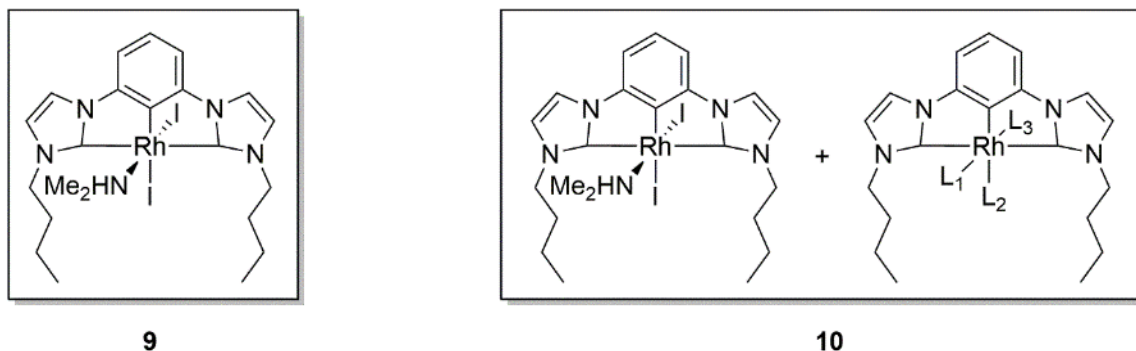


Figure 4.1 CCC-NHC Rh amine adduct (**9**) and crude isolate (**10**)

4.2 Results and Discussion

Because high yields were observed previously for Michael addition products in a H₂O/MeOH solvent mixture,²⁷⁴ pre-catalyst loading optimization of **10** in β -boration reactions was conducted in MeOH with *trans*-3-nonen-2-one and B₂pin₂ (Table 4.1). Although the material **10** is a mixture, 2 mg (~4 mol %) were typically used in a catalytic

trial. The molecular weight of amine adduct **9** (722.98 g/mol) was used as a surrogate for the entire sample to calculate pre-catalyst loading (mol %) for comparative purposes.

Table 4.1 Optimization of β -Boration Reaction Conditions^a

entry	solvent	cat. (mol %)	B ₂ pin ₂ (equiv)	time	conv % ^b
1	MeOH	10 (4)	1.5	1 h	34
2	MeOH	10 (4)	2.5	1 h	>99
3	MeOH	-----	2.5	1 h	0
4	MeOH	[Rh(COD)Cl] ₂ (4)	2.5	1 h	9
5	MeOH	NHMe ₂ (4)	2.5	1 h	<3
6	MeOH	10 (2)	2.5	1.5 h	>99
7	MeOH	10 (4)	2.5	1 h	60 ^c
8	EtOH	10 (4)	2.5	1 h	93
9	H ₂ O	10 (4)	2.5	1 h	>99

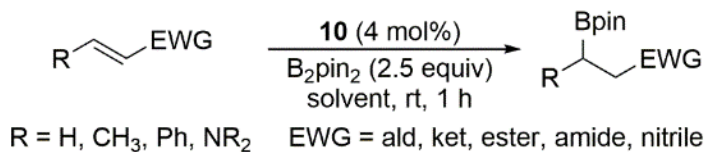
^atrans-3-nonen-2-one (0.0735 mmol), B₂pin₂, cat **10** (2.00 mg, ~2.94 μ mol), and solvent (0.700 mL) were added to a 1 dram vial with a magnetic stir bar, sonicated for 1 min and stirred for 1 h at rt. ^bConversion was determined by GC-MS analysis. ^cReaction was conducted at 0 °C.

Initially, 1.5 equiv of B₂pin₂ were used with trans-3-nonen-2-one, and a 34% conversion to the borated product was observed (entry 1). Previously, using 2.5 equiv of aryl boronic acids with α,β -unsaturated carbonyl compounds in 1,4-additions gave higher conversion. Therefore, the B₂pin₂ concentration was increased to 2.5 equiv, and as expected, conversion to the borated trans-3-nonen-2-one of >99% was observed in 1 h (entry 2). A control experiment without added **10** (entry 3) resulted in no reaction. Evaluating 4 mol % [Rh(COD)Cl]₂ dimer as a potential catalyst (entry 4) provided only 1 turnover (8-atom mol % Rh and 9% yield) in 1 h, thus eliminating extraneous starting material as the active catalyst. To demonstrate that the amine base was not the active catalyst, 4 mol % of NHMe₂ only produced <3% conversion (entry 5). The catalyst

loading was lowered to examine the efficiency of **10** (entries 6 vs. 7). At 2 mol % (1 mg) pre-catalyst loading (entry 6), >99% conversion was observed in 1.5 h. The reaction was also conducted at 0 °C to determine the efficiency of the catalyst below rt (entry 7), which resulted in a respectable 60% conversion in only one hour. High conversion was also observed using eco-friendly solvents, H₂O (>99%) and EtOH (>93%) (entries 8 and 9). These results are consistent with previous work of Yun and co-workers²⁴⁰ and Fernández and co-workers,²⁵⁹ in which both demonstrated an enhanced rate of β-boration of α,β-unsaturated carbonyl compounds with the use of alcohol additives such as MeOH. Moreover, Santos clearly demonstrated, through detailed mechanistic studies, the ability of the amine base to activate a nucleophilic water molecule generating the sp²–sp³ diboryl adduct that participates in transmetalation.²⁵⁰ Protic solvents MeOH and EtOH were used throughout the screening of activated acyclic and cyclic alkenes to evaluate the effect on the rate of conversion. Because >99% conversion was observed in 1 h with 4 mol % of **10** (entry 2, Table 4.1), the scope and limitations studies were conducted under these optimized conditions.

Utilizing the optimized reaction conditions, activated acyclic alkenes were examined (Table 4.2). Excellent conversions (>99%) of the aldehyde substrates (crotonaldehyde and cinnamaldehyde, entries 1 and 2) were observed in both MeOH and EtOH. *trans*-4-Phenyl-3-buten-2-one (entry 3) and chalcone (entry 4) had the least conversion in 1 h.

Table 4.2 Scope of Acyclic Substrate Reactivity in the β -Boration with $B_2pin_2^a$



entry	product	MeOH conv% ^b (yield%) ^c	EtOH	entry	product	MeOH conv% ^b (yield%) ^c	EtOH
1		>99 (86)	>99 (81)	6		0 ^d	0 ^d
2		>99 (86)	>99 (84)	7		>99 (90)	>99 (94)
3		96 (82)	84 (61)	8		>99 (93)	>99 (96)
4		81 (66)	49 (22)	9		0 ^d	0 ^d
5		0 ^d	0 ^d	10		>99 (84)	>99 (83)

^aAcyclic α,β -unsaturated compound (0.0735 mmol), bis(pinacolato)diboron (0.184 mmol), **10** (2.00 mg, ~2.94 μ mol), and 0.700 mL of MeOH were added to a 1 dram vial with a magnetic stir bar, and stirred for 1h at rt. ^bConversion was determined by GC-MS analysis. ^cIsolated yield. ^dAfter 24 h reaction time.

Due to lack of reported borated products containing nitro functionalities, *trans*- β -nitro styrene (entry 5) and 1-(dimethylamino)-2-nitroethylene (entry 6) were both screened. No product was observed for any of the nitro-containing substrates despite extended reaction time of 24 h. Ethyl acrylate (entry 7) exhibited excellent conversion (>99%) in both MeOH and EtOH. Methyl vinyl ketone (entry 8) was another acyclic substrate to show high conversion in MeOH and EtOH. Acrylonitrile (entry 9) was evaluated but no product was observed. Boration of *N,N*-dimethylacrylamide (entry 10) was successful (>99% conversion) in both MeOH and EtOH.

Previously, little success has been reported in borating cyclic enones with Rh catalysts. Reports include Rh(Phebox)²²⁷ with 0% conversion of cyclohexenone and Wilkinson's catalyst with extended reactions times (12-13 h) and elevated temperature (80 °C) for the boration of cyclohexenone (78%) and cycloheptenone (75%) in good yields.¹⁷³ Thus, cyclic enones were evaluated under the optimized conditions with 4 mol % (2.00 mg) of **10**, and the results are presented in Table 4.3. Conversions of >99% in just 1 h were observed for all three non-substituted cyclic substrates (entries 1-3) in MeOH and EtOH. This rate of conversion of cyclohexenone is comparable to catalytic reports with Cu (99%, 1 h)²⁵⁰ and an NHC (91%, 1 h)²⁶¹ catalysts. The rate of product formation with cyloheptenone (entry 3, >93%), in all solvents, is also comparable or faster than the best previous reports.^{173,261} Only modest conversions were observed for the α -substituted, 2-methylcyclopent-2-en-1-one (entry 4) in 1h, but upon extended reaction times improved conversions to the borated product were obtained. No significant diastereoselectivity was observed in the reactions with 2-methylcyclopent-2-en-1-one (entry 4). Excellent conversions have been reported for sterically hindered β -substituted cyclic enones in 1 h reaction times with Cu or NHC catalysts.^{250,261,262} However, extended reaction times were required when pre-catalyst **10** was employed for both 2-methyl cyclopentenone (entry 5) and 2-methyl cyclohexenone (entry 6) in ethanol and methanol, resulting in only fair to good conversions. After 1 h, moderate conversion (70%) was observed when using MeOH as a solvent for 3-methyl-2-cyclopentenone (entry 6), while less was observed in EtOH (57%). A drastic reduction in conversion rate was observed for 3-methyl-2-cyclohexenone (entry 6). This observation is consistent with

Nishiyama²²⁷ and co-workers' proposed catalytic cycle, which suggests that the steric congestion due to the methyl group hinders the boryl-insertion at the β -position.

Table 4.3 Scope of Cyclic Substrate Reactivity in the β -Boration with $B_2\text{pin}_2^a$

$n = 0, 1, 2$
 $R, R' = H, \text{CH}_3$

entry	product	MeOH conv% ^b	EtOH conv% ^b	(yield%) ^c	entry	product	MeOH conv% ^b	EtOH conv% ^b	(yield%) ^c
1		>99 (90)	1 h	>99 (70)	4		75, 1 h (dr = 1.1:1)	70, 1 h (dr = 1.7:1)	
2		>99 (88)	1 h	>99 (84)	5		70, 1 h 86 (51), 24 h	57, 1 h 63 (40), 24 h	
3		>99 (91)	1 h	94 (90)	6		40, 1 h 51 (40), 24 h	26, 1 h 38 (25), 24 h	

^aCyclic α,β -unsaturated compound (0.0735 mmol), bis(pinacolato)diboron (0.184 mmol), **10** (2.00 mg, ~2.94 μmol), and 0.700 mL of MeOH were added to a 1 dram vial with a magnetic stir bar, stirred for 1 or 24 h at rt. ^bConversion was determined by GC-MS analysis. ^cIsolated yield.

It was noted that if isolate **10** was “aged” (i.e. was stored for several months) there was an impact on its catalytic efficiency. Thus, using a five month old sample of **10** for the boration of cyclohexenone only an 83% conversion was found in 1 h, compared to Table 4.3, entry 2, which was quantitatively converted in 1 h with freshly prepared **10**. While 83% conversion is still very good, freshly isolated pre-catalyst **10** is best for optimum catalytic activity.

Spectroscopic data indicated that orange mixture **10** consisted of primarily two CCC-NHC pincer Rh complexes. However, many peaks in the ^1H NMR spectrum overlapped (see Figure A. 34). While full characterization is currently ongoing, partial characterization can be presented. Fortunately, several sets of signals in the spectroscopic data have led to partial characterization, thus indicating similarities between the two complexes. Two sets of diastereotopic methylene peaks indicating a mixture of CCC-NHC pincer Rh complexes. **x** and **x'** indicate signals due to CCC-NHC pincer Rh amine adduct **9** (Figure 4.2).

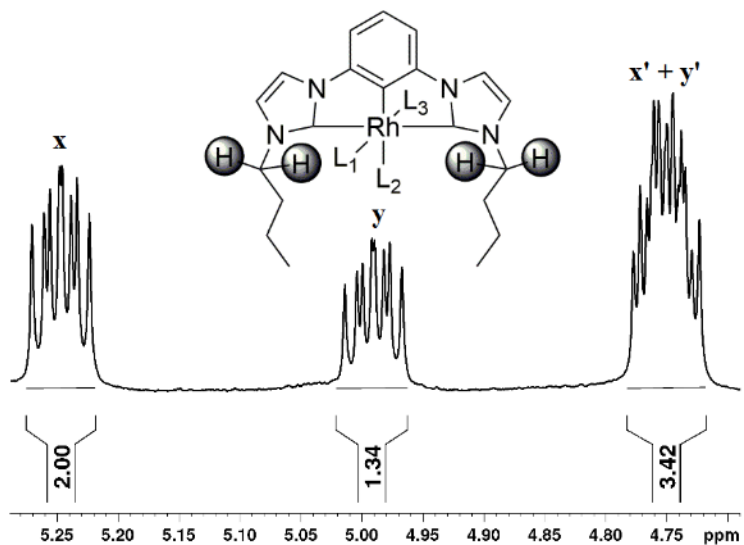


Figure 4.2 Diastereotopic methylene peaks of **10** observed in ^1H NMR spectrum
Two sets of diastereotopic methylene peaks indicating a mixture of CCC-NHC pincer Rh complexes. **x** and **x'** indicate signals due to CCC-NHC pincer Rh amine adduct **9**.

For example, an integration value of 2 was set for the multiplet at 5.20 ppm (Figure 4.2, **x**), a signal observed for diastereotopic methylene peaks, yet an integration value of 3.42 is observed for the other corresponding diastereotopic methylene signal at

4.75 ppm. This integral intensity is due to overlapping diastereotopic methylene peaks (\mathbf{x}', \mathbf{y}' , see Figure 4.2) at 4.75 ppm, while the other diastereotopic peak (\mathbf{y}) corresponding to the minor complex is slightly downfield at 4.95 ppm. Two doublets of doublets were observed at 1.59 and 1.64 ppm with identical coupling values (dd, ${}^3J_{\text{H-H}} = 1.2$ Hz, ${}^3J_{\text{Rh-H}} = 6.3$ Hz) in the ${}^1\text{H}$ NMR spectrum (see Figure A. 34) due to the unique heteronuclear coupling of NMR active ${}^{103}\text{Rh}$ to coordinated NHMe_2 .

Two Rh–C_{aromatic} and Rh–C_{carbene} doublets (Figure 4.3) observed in the ${}^{13}\text{C}$ NMR spectrum further advances our assignment of structural similarities between the two species. Identical coupling values are observed for the Rh–C_{carbene} and the Rh–C_{aromatic} doublets (${}^1J = 39$ Hz and $J = 29$ Hz, respectively).

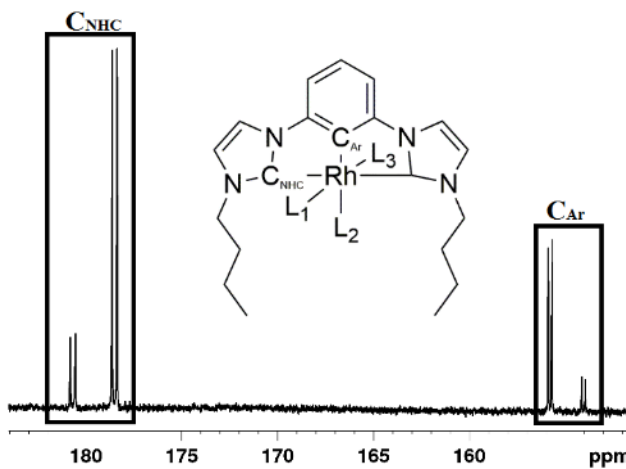


Figure 4.3 Rh–C_{aromatic} and Rh–C_{carbene} doublets of **10** observed in ${}^{13}\text{C}$ spectrum

Partial chromatographic separation of **10** was accomplished using silica gel. The main component isolated was a dark orange solid in 26% yield. Analysis of the spectroscopic data of this component leads to the assignment of axial amine adduct **9** as

the structure,³⁷ which has NMR peaks coincident with the major component of mixture **9**. Additionally, orange X-ray quality crystals were grown by vapor diffusion (toluene/DCM) from mixture **9**. X-ray crystal structure analysis determined molecular structure **9** (Figure 4.4) was indeed the axial isomer.²⁷⁵ The equatorial isomer of **9** may be ruled out as the other component of the mixture because it would not be expected to give rise to diastereotopic signals as observed for **y** (Figure 4.2). The molecular structure was observed to be a distorted octahedral geometry with the amine ligand in an axial position. The metric data (bond distances and angles) are normal for this ligand system (Table 4.4). A catalytic trial was performed under optimized reaction conditions using 2 mg of **9** with cyclohexenone. However, only a 72% conversion to the borated product was observed in 1 h (compared to >99% in Table 3, entry 2), indicating that **8** alone was not as catalytically active as the mixture **10**.

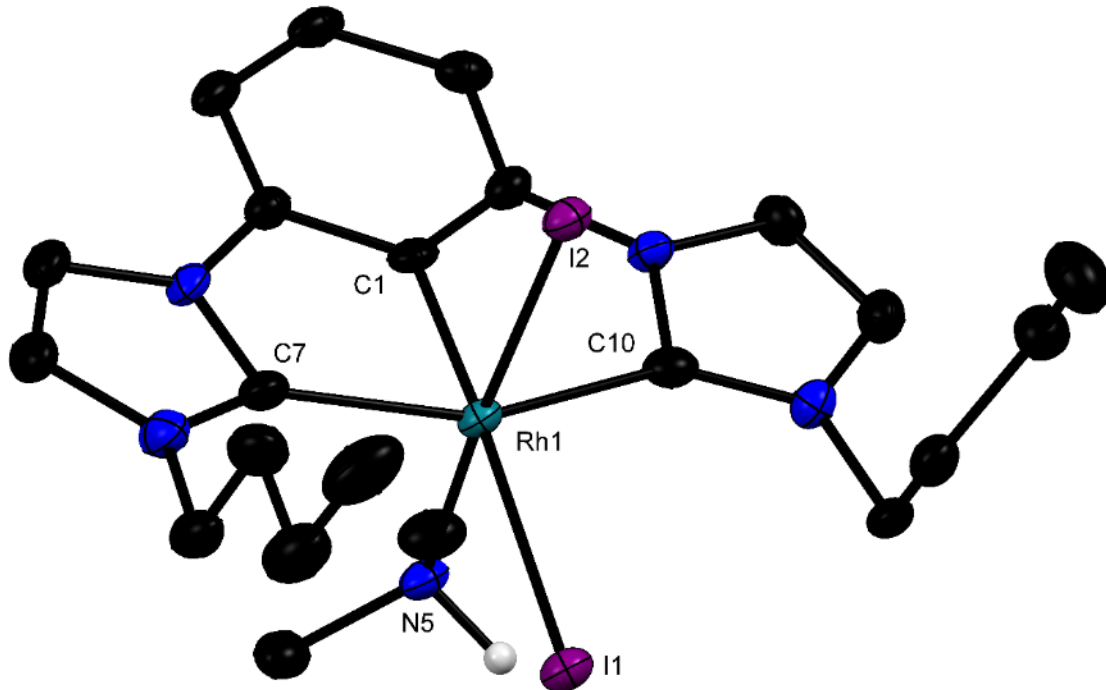


Figure 4.4 X-ray molecular structure of **9**

All but amine hydrogens are omitted for clarity. Thermal ellipsoids are shown at 50% probability.

Table 4.4 Selected Bond Lengths (\AA) and Angles ($^\circ$) for **9**

length (\AA)	angle ($^\circ$)
Rh(1)–C(1)	C(1)–Rh(1)–C(10)
Rh(1)–C(7)	C(1)–Rh(1)–C(7)
Rh(1)–N(5)	C(10)–Rh(1)–C(7))
Rh(1)–I(1)	N(5)–Rh(1)–I(1)

4.3 Conclusion

In conclusion, the CCC-NHC pincer Rh complex mixture **10** catalyzed the β -boration of α,β -unsaturated activated alkenes at room temperature in quantitative yield, typically in only 1 h, producing tertiary and quaternary carbon centers. The reported method does not require the exclusion of air or H_2O due to the stability of pre-catalyst **10**.

To our knowledge, this is the first report of β -boration using a CCC pincer complex catalyst to produce tertiary and quaternary β -substituted carbon centers using MeOH and EtOH as the solvent. The rates obtained with **9** for β -boration are comparable to the best reported.^{250,261} Separating and identifying the remaining component of pre-catalyst **10**, its reactivity and synergy with **9**, and identifying the precipitate observed during the catalytic trials and the catalytically active species will be the subject of future work.

4.4 Experimental

4.4.1 General Consideration

All NMR spectra were taken on a Bruker Advance III 300 or 600 MHz. High-resolution mass spectrometer (HRMS) data was acquired using ESI technique on a Bruker UHPLC-Micro-Q/T OF-MS/MS. Gas chromatography mass spectrometer (GC-MS) data was collected on a Shimadzu GCMS-QP2010 plus. A Zebron capillary GC column was used with the following dimensions: length - 30 m; I.D. - 0.25 mm; film thickness - 0.25 μ m. The following method, Table 4.5, was employed on the GC-MS for all catalysis trials:

Table 4.5 GC-MS Method for β -Boration Catalysis

Column Oven Temp.	50.0 °C
Injection Temp.	250.0 °C
Injection Mode	Split
Flow Control Mode	Linear Velocity
Pressure	53.6 kPa
Total Flow	102.0 mL/min
Column FLow	1.00 mL/min
Linear Velocity	36.3 cm/sec
Purge Flow	1.0 mL/min
Split Ratio	100.0
High Pressure Injection	OFF
Carrier Gas Saver	ON
Carrier Gas Saver Split Ratio	5.0
Carrier Gas Saver Time	1.00 min
Splitter Hold	OFF
Oven Temp. Program	
<u>Rate</u>	<u>Temperature (°C) : Hold Time (min)</u>
--	50.0 : 0
10.00	250.0 : 5.00

4.4.2 Synthesis of CCC-NHC Pincer Rhodium Complexes 10

1, 3-bis (1-butylimidazolium-3-yl) benzene iodide (**3**) (0.150 g, 0.260 mmol), and tetrakis(dimethylamido)zirconium (0.173 g, 0.650 mmol) were weighed in under inert atmosphere and dry THF (15 ml) was added into a 50 mL flask. The mixture was stirred at room temperature for approximately 1 hour or until a light yellow homogenous solution was obtained. Once the solution became homogeneous, $[\text{Rh}(\text{COD})\text{Cl}]_2$ (0.128 g, 0.260 mmol) was added to the flask and stirring continued at room temperature for another 12 hours. Deionized water (1 mL) was added, and it was stirred vigorously for 10 minutes providing a white precipitate and a bright orange supernatant. The orange supernatant was filtered and the solvent was removed under reduced pressure yielding a dark orange solid. The solid was washed with hexanes (25 mL) and ether (25 mL) and

dried to obtain dark orange/red solid (0.128 g, 68 %). Orange X-ray quality crystals of **9** were grown by vapor diffusion (toluene/DCM). Catalyst **10** mixture (Two components: ratio ~1.6:1) ¹H NMR (600 MHz, CDCl₃): δ 7.61-7.60 (m, 3H), 7.27-7.13 (m, 5.1H), 7.11-7.07 (m, 3.1H), 5.25-5.21 (m, 2H), 4.97-4.94 (m, 1.2H), 4.79-4.74 (m, 3.2H), 3.72 (m, 1H), 3.69 (m, 0.6H), 2.05-1.99 (m, 6.4H), 1.65-1.63 (dd, ³J H–H = 1.2 Hz, ³J Rh–H = 6.3 Hz, 3.3H), 1.60-1.59 (dd, ³J H–H = 1.2 Hz, ³J Rh–H = 6.3 Hz, 5.8H), 1.57-1.51 (m, 6.5H), 1.02-0.99 (m, 9.4H). ¹³C (150 MHz, CDCl₃): δ 180.6 (d, J = 39 Hz, Rh–C_{carbene}), 178.4 (d, J = 39 Hz, Rh–C_{carbene}), 155.7 (d, J = 29 Hz, Rh–C_{aromatic}), 153.9 (d, J = 29 Hz, Rh–C_{aromatic}), 145.8, 145.5, 124.0, 123.7, 121.6, 121.1, 115.8, 115.5, 108.6, 108.5, 51.7, 49.8, 44.6, 44.5, 33.6, 33.2, 20.1, 19.9, 14.1, 14.0. HRMS-ESI (m/z): [M-I]⁺ calcd for C₂₂H₃₂IN₅Rh, 596.0752; found, 596.0740; [M-I-NHMe₂]⁺ calcd for C₂₀H₂₅IN₄Rh, 551.0173; found, 551.0163.

4.4.3 General Procedure for Catalytic Trials

A 1 dram vial with a magnetic stir bar was charged with α,β -unsaturated compound (0.0735 mmol), bis(pinacolato)diboron (0.184 mmol), pre-catalyst **10** (2.00 mg, 2.94 μ mol), and solvent (0.700 mL). The vial was closed and stirred vigorously for 1 h at rt during which time a dark precipitate was observed to form. After 1 h, a 10 μ L aliquot was passed through a short plug of celite and a 0.45 μ m PTFE filter and was injected into the GC-MS to determine conversion. The crude reaction mixture was then filtered through a plug of celite to remove insolubles. Volatiles from the filtered reaction mixture were then removed under reduced pressure resulting in an oil. ¹H NMR and HRMS was then taken of the crude product to confirm the borylated product. The crude product was then purified by silica gel chromatography to determine an isolated yield.

4.4.4 Product Characterization

Borated Products: Table 4.1, Entry 2; Table 4.2, Entries 1-5,7; and Table 4.3, Entries 1-7.

4-(4,4,5,5-tetramethyl-1,3,2-dioxaborolan-2-yl)nonan-2-one (Table 4.1, Entry 2): Colorless oil, eluted with 1:10 / EtOAc:Hexanes, R_f 0.25. ¹H and ¹³C NMR match previously reported literature.²⁵⁰ HRMS-ESI (*m/z*): [M+H]⁺ calcd for C₁₅H₃₀BO₃, 269.2285; found 269.2297.

3-(4,4,5,5-tetramethyl-1,3,2-dioxaborolan-2-yl)butanal (Table 4.2, Entry 1): Colorless oil, eluted with 1:10 / Et₂O:Hexanes, R_f 0.27. ¹H and ¹³C NMR match previously reported literature.²³⁴ HRMS-ESI (*m/z*): [M+H]⁺ calcd for C₁₀H₁₉BO₃, 199.1502; found, 199.1506; [M+Na]⁺ calcd for C₁₀H₁₉BO₃Na, 221.1321; found 221.1318.

3-phenyl-3-(4,4,5,5-tetramethyl-1,3,2-dioxaborolan-2-yl)propanal (Table 4.2, Entry 2): Colorless oil, eluted with 1:15 / EtOAc:Hexanes, R_f 0.24. ¹H and ¹³C NMR match previously reported literature.²³⁴ HRMS-ESI (*m/z*): [M-OH]⁺ calcd for C₁₅H₂₀BO₂, 243.1554; found 243.1559; [M+Na]⁺ calcd for C₁₅H₂₁BO₃Na, 283.1479; found 283.1483.

4-phenyl-4-(4,4,5,5-tetramethyl-1,3,2-dioxaborolan-2-yl)butan-2-one (Table 4.2, Entry 3): Colorless oil, eluted with 1:10 / EtOAc:Hexanes, R_f 0.25. ¹H and ¹³C NMR match previously reported literature.²³⁴ HRMS-ESI (*m/z*): [M+H]⁺ calcd for C₁₆H₂₄BO₃, 275.1816; found 275.1812; [M+Na]⁺ calcd for C₁₆H₂₃BO₃Na 297.1635; found 297.1632.

1,3-diphenyl-3-(4,4,5,5-tetramethyl-1,3,2-dioxaborolan-2-yl)propan-1-one (Table 4.2, Entry 4): Colorless oil, eluted with 1:15 / EtOAc:Hexanes, R_f 0.29. ¹H and ¹³C NMR

match previously reported literature.²³⁴ HRMS-ESI (*m/z*): [M+H]⁺ calcd for C₂₅H₂₆BO₃, 337.1970; found 337.1973; [M+Na]⁺ calcd for C₂₁H₂₅BO₃Na, 359.1793; found 359.1789.

ethyl 3-(4,4,5,5-tetramethyl-1,3,2-dioxaborolan-2-yl)propanoate (Table 4.2, Entry 7): Colorless oil, eluted with 1:10 / EtOAc:Hexanes, R_f 0.32. ¹H and ¹³C NMR match previously reported literature.²⁴⁶ HRMS-ESI (*m/z*): [M+H]⁺ calcd for C₁₁H₂₂BO₄, 229.1608; found 229.1597; [M+Na]⁺ calcd for C₁₁H₂₁BO₄Na, 251.1425; found 251.1427.

4-(4,4,5,5-tetramethyl-1,3,2-dioxaborolan-2-yl)butan-2-one (Table 4.2, Entry 8): Colorless oil, eluted with 1:10 / EtOAc:Hexanes, R_f 0.36. ¹H and ¹³C NMR match previously reported literature.²³⁴ HRMS-ESI (*m/z*): [M+H]⁺ calcd for C₁₀H₂₀BO₃, 199.1502; found 199.1502; [M+Na]⁺ C₁₀H₁₉BO₃Na, 221.1321; found 221.1324

N,N-dimethyl-3-(4,4,5,5-tetramethyl-1,3,2-dioxaborolan-2-yl)propanamide (Table 4.2, Entry 10): Yellow oil, eluted with 1:10 / Hexanes:EtOAc, R_f 0.10. ¹H and ¹³C NMR match previously reported literature.²⁴⁶ HRMS-ESI (*m/z*): [M+H]⁺ calcd for C₁₁H₂₃BNO₃, 228.1768; found 228.1767; [M+Na]⁺ calcd for C₁₁H₂₂BNO₃Na, 250.1587; found 250.1587.

3-(4,4,5,5-tetramethyl-1,3,2-dioxaborolan-2-yl)cyclopentan-1-one (Table 4.3, Entry 1): Colorless oil, eluted with 1:10 / EtOAc:Hexanes, R_f 0.33. ¹H and ¹³C NMR match previously reported literature.²⁶¹ HRMS-ESI (*m/z*): [M+H]⁺ calcd for C₁₁H₂₀BO₃, 211.1502; found 211.1503.

3-(4,4,5,5-tetramethyl-1,3,2-dioxaborolan-2-yl)cyclohexan-1-one (Table 4.3, Entry 2): Colorless oil, eluted with 1:15 / EtOAc:Hexanes, R_f 0.23. ¹H and ¹³C NMR match previously reported literature.¹⁷³ HRMS-ESI (*m/z*): [M+H]⁺ calcd for C₁₂H₂₂BO₃, 225.1659; found 225.1653.

3-(4,4,5,5-tetramethyl-1,3,2-dioxaborolan-2-yl)cycloheptan-1-one (Table 4.3, Entry 3): Colorless oil, eluted with 1:15 / EtOAc:Hexanes, R_f 0.27. ¹H and ¹³C NMR match previously reported literature.²⁷⁶ HRMS-ESI (*m/z*): [M+H]⁺ calcd for C₃₂H₂₃BO₃, 239.1815; found 239.1820; [M+Na]⁺ calcd for C₃₂H₂₃BO₃Na, 261.1635; found 261.1641.

2-methyl-3-(4,4,5,5-tetramethyl-1,3,2-dioxaborolan-2-yl)cyclopentan-1-one (Table 4.3, Entry 4): Colorless oil, eluted with 1:15 / EtOAc:Hexanes, R_f 0.32. ¹H and ¹³C NMR match previously reported literature.²⁶¹ HRMS-ESI (*m/z*): [M+H]⁺ calcd for C₁₂H₂₂BO₃, 225.1659; found 225.1655.

3-methyl-3-(4,4,5,5-tetramethyl-1,3,2-dioxaborolan-2-yl)cyclopentan-1-one (Table 4.3, Entry 5): Colorless oil, eluted with 1:15 / EtOAc:Hexanes, R_f 0.33. ¹H and ¹³C NMR match previously reported literature.²⁶¹ HRMS-ESI (*m/z*): [M+H]⁺ calcd for C₁₂H₂₂BO₃, 225.1659; found 225.1658.

3-methyl-3-(4,4,5,5-tetramethyl-1,3,2-dioxaborolan-2-yl)cyclohexan-1-one (Table 4.3, Entry 6): Colorless oil, eluted with 1:15 / EtOAc:Hexanes, R_f 0.26. ¹H and ¹³C NMR match previously reported literature.²⁶¹ HRMS-ESI (*m/z*): [M+H]⁺ calcd for C₁₃H₂₄BO₃, 39.1815; found 239.1810.

CHAPTER V

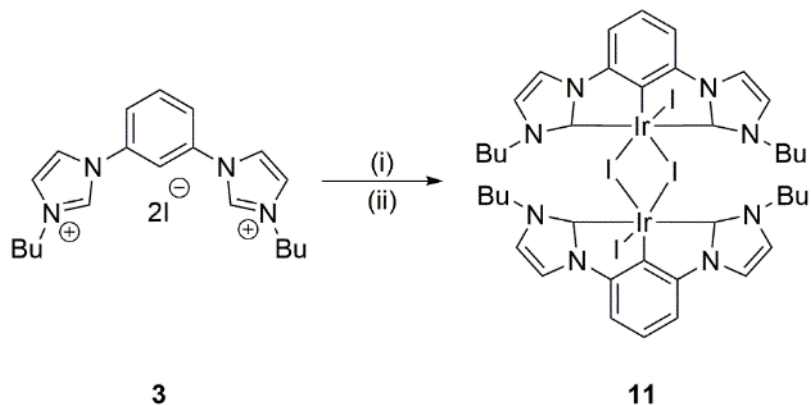
DEVELOPMENT OF CCC-NHC Ir AND Rh PINCER COMPLEXES FOR BORYLATION OF ARENE AND ALKANE C–H BONDS

5.1 Introduction

Organoboron compounds are valuable synthetic intermediates for development of many pharmaceuticals, agrochemicals, and materials science products.^{218,220,277,278} In addition, aryl organoborates are essential building blocks for synthesis of C–C bonds in the Suzuki Coupling reaction.^{145,146} Direct access to these versatile aryl boronate esters were reported by Miyaura demonstrating Pd catalyzed borylation of aryl halides.²⁷⁹ In 1995, Hartwig and co-workers reported the first borylation of arenes and alkenes with well-defined metal–boryl catalysts, producing free boronate ester products in high yield.²⁸⁰ This direct borylation methodology does not require the use of aryl halides or pseudohalides, in contrast to Miyaura’s report, allowing for a more facile synthetic pathway with fewer steps.

Ir catalyzed C–H borylation has been the most efficient method in the formation of arylboronate compounds using bis(pinacolato)diboron ($B_2\text{pin}_2$) and pinacolborane (HBpin) reagents.^{277,278,281–283} Recently, high turnovers have also been reported in Ir catalyzed borylation of heteroarene substrates.^{284–287} Furthermore, mono- and bidentate Ir-NHC complexes have shown to be applicable in the synthesis of boronic acid esters *via* C–H functionalization with diboryl agents.^{41,288,289} Inspired by these reports, we

investigated CCC-NHC Ir pincer complex **11** (Scheme 5.1) as a potential catalyst in C–H borylation reactions.⁵²



Scheme 5.1 Synthesis of **11**

Conditions: (i) 2.5 equiv Zr(NMe₂)₄, THF, rt, 1h; (ii) 1 equiv [Ir(COD)Cl]₂, THF, 6 h

5.2 Results and Discussion

Following the optimization conditions for borylation of arenes reported by Hartwig and co-workers,²⁹⁰ complex **11** was tested for activity in functionalization of benzylic C–H bonds outlined in Table 5.1. Initially, complex **11** was evaluated with B₂pin₂ in benzene resulting in minimal conversion (entry 1). It was then surmised a possible hydride source could advance the sluggish results due to Smith and co-workers report outlining an active Ir^{III}(H) intermediate in their proposed catalytic cycle of arene borylation.²⁹¹ Indeed, upon addition of excess NaH (entry 2), the boryl source was completely consumed in 6 h giving the benzene ester product. This result is competitive with Hartwig and Miyaura's 2002 publication, in which they reported a 96% yield at 80 °C, with similar catalyst loading at 16 h.²⁹⁰ Conversions held steady when lowering the NaH loading from 50% to 15% in catalytic trials 3 and 4. However, when limiting the

amount of added NaH (entries 5 and 6) conversions dropped drastically, indicating **11** acts as a pre-catalyst to a hypothesized CCC-NHC Ir(H) adduct. $[\text{Ir}(\text{COD})\text{Cl}]_2$, a common catalyst precursor in many arene borylation reports,²⁷⁷ was also screened resulting in minimal conversion (entry 8). Lower conversions were also observed in shorter time periods (entries 9 and 10), although a respectable 92% conversion was still obtained at 4 h (entry 9).

Table 5.1 Benzene C–H Borylation Optimization^a

entry	11 mol% ^a	NaH mol% ^b	time (h)	conv (%)
1	1.5	-	6	4
2	1.5	50	6	>99
3	1.5	30	6	>99
4	1.5	15	6	>99
5	1.5	8	6	53
6	1.5	4	6	5
7	-	15	6	0
8	- ^c	15	6	9
9	1.5	15	4	92
10	1.5	15	2	64

^amol % of **11** and NaH calculated from mmol of B_2Pin_2 (0.187 mmol). ^b% conv based on boron atom in B_2Pin_2 determined by GC-MS. ^c1.5 mol% of $[\text{Ir}(\text{COD})\text{Cl}]_2$ used as catalyst.

Hartwig and Miyaura illustrated through kinetic and computational studies how electron rich arenes formed stable η^2 -arene Ir intermediate complexes that precede oxidative addition, thereby resulting in lower conversions compared to electron poor aryl derivatives.²⁹² Therefore, *o*-xylene and chlorobenzene were screened (Table 5.2) to observe if the *in-situ* generated active catalyst followed this reported trend.

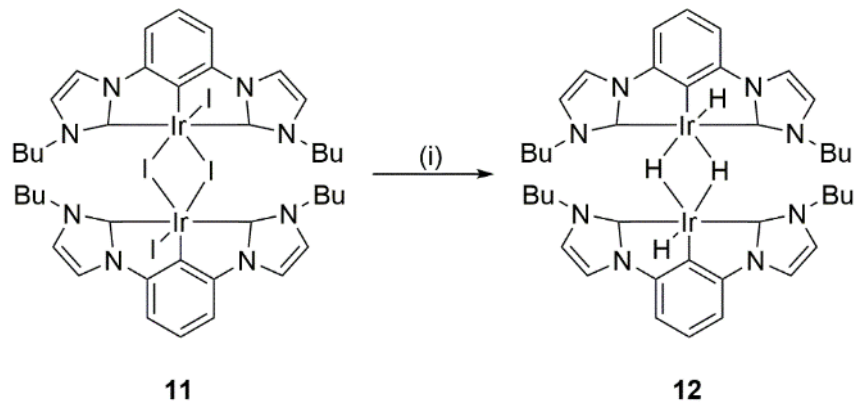
Table 5.2 Arenes Substrates for C–H Borylation^a

entry	product	time (h)	conv (%) ^b	isomer ratio ^c
1		2	18	60:40
		4	46	
		7	53	
		15	76	
2		2	83	75:25
		4	94	
3		2	41	60:40

^aAll reactions were conducted in a 1 dram vial with B₂Pin₂ (1.0 equiv), arene (60 equiv), **11** (1.5 mol %), and NaH (15 mol %) neat. ^bConversion was determined by GC-MS analysis. ^cIsomer ratio determined by GC-MS.

Indeed, lower conversion was observed with *o*-xylene (entry 1) compared to the electron poor chlorobenzene (entry 2). Borylation of heteroarenes could allow development in new synthetic pathways to important pharmaceutical and natural products. While the scope is still limited in the application of heteroarene borylation, a recent report by Hartwig and co-workers, revealing mechanistic studies and regioselectivity of C–H functionalization of heteroarenes, may help in furthering the development of synthetically useful heteroaryl boronate esters.²⁸⁴ Pyridine (entry 3) was examined and observed a 41% conversion observed in 2 h. While this result, along with results of entries 1 and 2, are preliminary, they are nevertheless encouraging, as the basicity of the non-bonding electrons on nitrogen in many heterocycles have been reported to poison many catalytic systems in C–H functionalization of heteroarenes.²⁸⁴

Intrigued by the results discussed in Tables 5.1 and 5.2, investigation was turned to determining the identity of the active catalyst in the borylation reactions. Following the conditions outlined in Scheme 5.2, 50 equiv of NaH was added to **11** in THF at room temperature, resulting in a brown heterogeneous mixture that was left standing for 12 h. Afterwards, a single opaque X-ray quality crystal was retrieved from the reaction mixture and was identified as a H–Ir(μ -H)₂Ir–H bridged dimer (**12**) upon X-ray analysis. An ORTEP plot of **12** is displayed in Figure 5.1 along with selected metric data in Table 5.3. While further studies are currently ongoing, complex **12** is believed to be the active species in Tables 5.1 and 5.2. Furthermore, complex **12** is presently being evaluated for activity in alkane dehydrogenation studies due to the similar framework of the active PCP hydride pincer catalysts reported,²⁰ most notably by Jensen^{34,35} and Goldman.^{33,293}



Scheme 5.2 Synthesis of **12**

Conditions: (i) 50 equiv of NaH, THF, rt, 12 h;

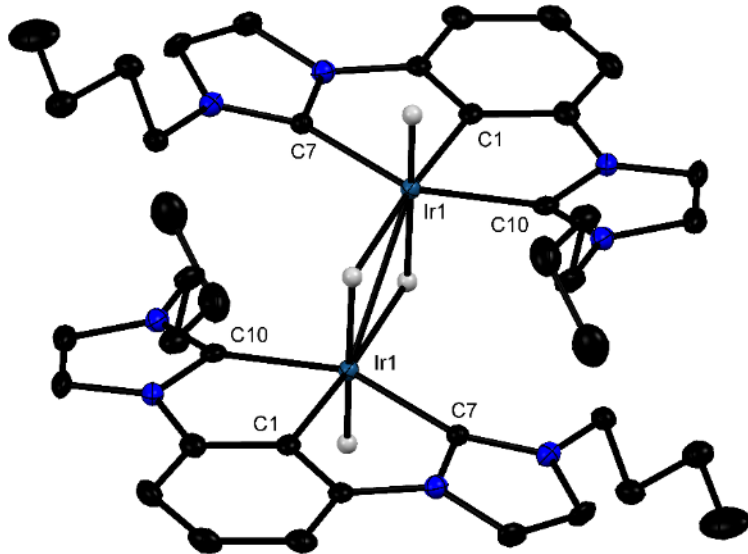


Figure 5.1 X-ray structure of **12**

Excluding Ir–H's, hydrogens are omitted for clarity. Thermal ellipsoids are shown at 50% probability.

Table 5.3 Selected Bond Lengths (\AA) and Angles ($^\circ$) for **12**

length (\AA)	angle ($^\circ$)
Ir(1)–C(1)	1.967(3)
Ir(1)–C(10)	2.035(3)
Ir(1)–C(7)	2.035(3)
Ir(1)–Ir'(1)	2.7837(2)
C(1)–Ir(1)–C(10)	77.99(12)
C(1)–Ir(1)–C(7)	78.10(12)
C(10)–Ir(1)–C(7))	154.55(12)
C(2)–C(1)–Ir(1)	120.8(2)

With promising preliminary results obtained in C–H borylation of arenes utilizing presumed catalyst **12**, a potentially more reactive second row CCC-NHC Rh pincer variant was pursued for possible activation of alkyl C–H bonds. Hartwig and co-workers pioneered the first selective catalytic C–H functionalization of alkanes at the terminal position with $\text{Cp}^*\text{Rh}(\text{R})_x$ (Cp^* $\text{C}_5\text{Me}_5\text{H}$, Me = CH₃) complexes.²⁹⁴ Harris and Bergman developed $\text{Tp}^*\text{Rh}(\text{CO})_2$ (Tp^* 5 HB–Pz3*, Pz* = 3,5-dimethylpyrazolyl) photocatalytic catalysts which activated alkyl C–H bonds at room temperature.^{295,296} It was reasoned a

CCC-NHC Rh pincer complex with a CO ligand could provide access to an unsaturated CCC-NHC Rh species by simple halide abstraction, generating a 16 e⁻ square planar species with a d⁸ metal center (Figure 5.2). This resulting complex would provide a pathway to a further coordinatively unsaturated 14 e⁻ d⁸ metal complex *via* photolysis of the CO ligand. These systems have been reported as active intermediates in C-H activation, and can be stabilized by NHC ligand systems.^{297,298}

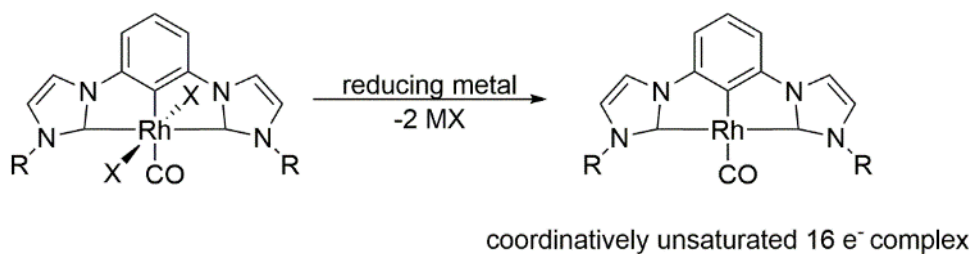
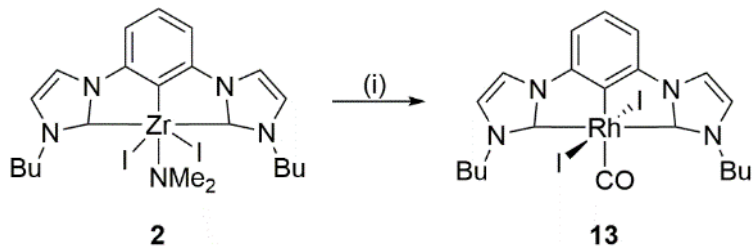


Figure 5.2 Coordinatively unsaturated CCC-NHC Rh(CO) pincer complex

CCC-NHC Zr pincer complex **2** was explored as a transmetalating reagent in order to access a single CCC-NHC Rh(CO) variant due to the successful formation of complex CCC-NHC Co pincer complex **7** in high yield, using the Zr diiodo species (refer to Scheme 2.3). Fortunately, upon addition of 1.2 equiv of [Rh(CO)₂Cl]₂ to Zr complex **2** (Scheme 5.3), complex **13** was formed and confirmed by ¹H and ¹³C NMR along with DEPT 135 (see Figure A.99-101).



Scheme 5.3 Synthesis of **13**

Conditions: 1.2 equiv $[\text{Rh}(\text{CO})_2\text{Cl}]_2$, CH_2Cl_2 , rt, 12 h

Orange crystals suitable for single crystal X-ray diffraction of **13** were grown by vapor diffusion of hexane into a saturated solution CH_2Cl_2 and further confirmed through X-ray analysis. An ORTEP plot of **13** is displayed in Figure 5.2 along with selected metric data in Table 5.4. Complex **13** will provide access to the desired $16e^-$ square planar CCC-NHC $\text{Rh}(\text{I})(\text{CO})$ species, outlined in Figure 5.2, to generate the coordinatively unsaturated $14 e^- \text{d}^8$ metal complex via photolysis of the CO ligand.

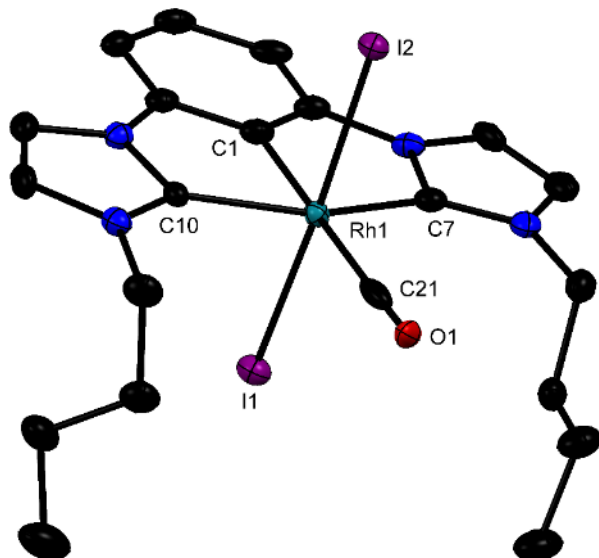


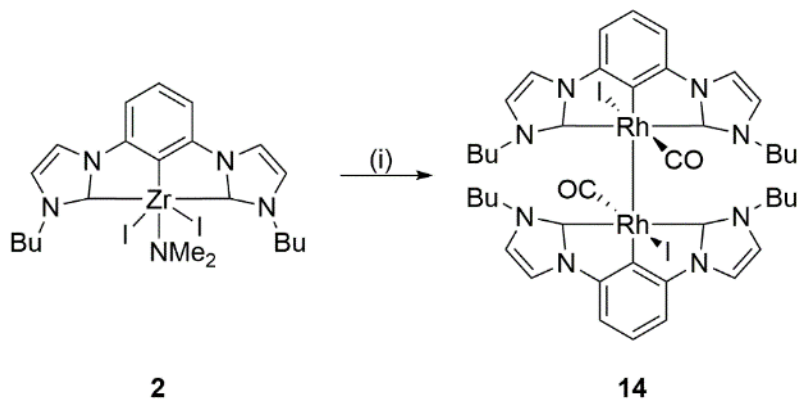
Figure 5.3 X-ray structure of **13**

Hydrogens are omitted for clarity. Thermal ellipsoids are shown at 50% probability.

Table 5.4 Selected Bond Lengths (\AA) and Angles ($^\circ$) for **13**

length (\AA)	angle ($^\circ$)
I(1)–Rh(1)	2.6685(3)
Rh(1)–C(10)	2.061(3)
Rh(1)–C(7)	2.057(3)
Rh(1)–C(21)	1.999(4)
C(1)–Rh(1)–I(1)	87.12(9)
C(1)–Rh(1)–C(21)	178.53(13)
O(1)–C(21)–Rh(1)	178.6(3)
N(2)–C(1O)–Rh(1)	140.9(2)

With the successful formation of complex **13**, a CCC-NHC Rh(CO) hydride variant was then sought due extensive reports of Rh(H)(CO) complexes active in catalytic carbonylation of olefins.²⁹⁹ Moreover, Marder and co-workers reported catalytic C–H bond activation occurring directly from Rh–H complexes.^{300–302} Following similar reaction conditions outlined in Scheme 5.3, attempts to synthesize a CCC-NHC Rh(CO) hydride species with various hydride sources were pursued. However, no product formation was observed for the desired Rh–H complex. Therefore, Rh(CO)₂(acac) was examined as an alternative Rh transmetalating reagent, along with LiAlH₄ as a hydride source, resulting in the unexpected formation of **14**, demonstrated in Scheme 5.4.



Scheme 5.4 Synthesis of **14**

Conditions: 1.2 equiv Rh(CO)₂(acac), 5.0 equiv LiAlH₄, CH₂Cl₂, rt, 12 h

Several crystals precipitated from the reaction mixture and were solved by X-ray analysis, characterizing complex **14** as a bimetallic Rh(II)(CO)–Rh(II)(CO) complex (Figure 5.4). Selected bond lengths and angles for **14** are given in Table 5.5.

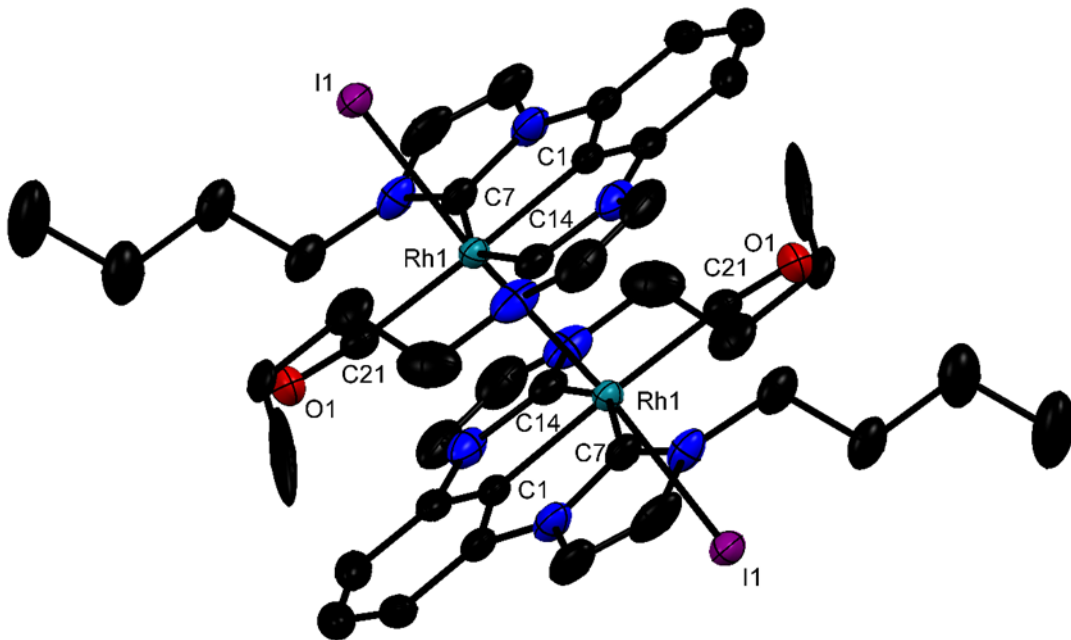


Figure 5.4 X-ray structure of **14**

Hydrogens are omitted for clarity. Thermal ellipsoids are shown at 50% probability.

Table 5.5 Selected Bond Lengths (\AA) and Angles ($^\circ$) for **14**

length (\AA)		angle ($^\circ$)	
Rh(1)–Rh(1)	2.8102(5)	C(1)–Rh(1)–I(1)	89.77(10)
Rh(1)–C(1)	1.984(4)	C(1)–Rh(1)–C(21)	177.91(14)
Rh(1)–C(21)	1.949(4)	O(1)–C(21)–Rh(1)	173.1(3)
C(21)–O(1)	1.136(5)	C(21)–Rh(1)–Rh(1)	96.60(11)

5.3 Conclusions

The formation of a CCC-NHC Ir(H) pincer complex (**12**) has been successfully demonstrated, the surmised active catalyst in our preliminary trials in C–H borylation of

arenes. Furthermore, we present a direct synthetic pathway in developing CCC-NHC Rh(III)(CO) and CCC-NHC Rh(II)(CO) pincer complexes, potential pre-catalysts for photocatalytic C–H bond activation of alkyl derivatives. Further studies are ongoing in expanding the scope of our studies outlined in Table 5.2, along with providing full spectroscopic characterization of CCC-NHC pincer complexes **12-14**.

5.4 Experimental

5.4.1 General Considerations

All NMR spectra were taken on a Bruker Advance III 600 MHz. High-resolution mass spectrometer (HRMS) data was acquired using ESI technique on a Bruker UHPLC-Micro-Q/T OF-MS/MS. Standard inert-atmosphere techniques were used unless otherwise noted. Synthesis of **2** and **11** were prepared from previously reported literature procedures.^{37,51,125} CH₂Cl₂, THF, and toluene were dried by using molecular sieves and the SP-1 Solvent System from LC Technology Solutions Inc. All commercial reagents were used as received. Chemical shifts (δ) in the NMR spectra (¹H and ¹³C) were referenced by assigning the residual solvent peaks. Gas chromatography mass spectrometer (GC-MS) data was collected on a Shimadzu GCMS-QP2010 plus. A Zebron capillary GC column was used with the following dimensions: length - 30 m: I.D. - 0.25 mm: film thickness - 0.25 μm. The following method, Table 5.2, was employed on the GC-MS for all catalysis trials:

Table 5.6 GC-MS Method for C–H Borylation Catalysis

Column Oven Temp.	50.0 °C
Injection Temp.	250.0 °C
Injection Mode	Split
Flow Control Mode	Linear Velocity
Pressure	53.6 kPa
Total Flow	102.0 mL/min
Column FLow	1.00 mL/min
Linear Velocity	36.3 cm/sec
Purge Flow	1.0 mL/min
Split Ratio	100.0
High Pressure Injection	OFF
Carrier Gas Saver	ON
Carrier Gas Saver Split Ratio	5.0
Carrier Gas Saver Time	1.00 min
Splitter Hold	OFF
Oven Temp. Program	
<u>Rate</u>	<u>Temperature (°C) : Hold Time (min)</u>
--	50.0 : 0
10.00	250.0 : 5.00

5.4.2 Synthesis of CCC-NHC Iridium Pincer Complex 12

1, 3-bis(imidazolene-3-yl)benzene tetra(iodo)-di(iridium)(III) complex (**11**) (0.020 g, 0.016 mmol), sodium hydride (NaH) (0.019 g, 0.780 mmol) and THF (0.50 mL) were combined in a one dram vial at room temperature (22 °C). Reaction mixture became a brown heterogeneous mixture and allowed to sit at room temperature for 12 h. A single opaque x-ray quality crystal of **12** was retrieved out of the reaction mixture.

5.4.3 Synthesis of CCC-NHC Rhodium Pincer Complex 13

2-(1,3-Bis(30-butyl-imidazol-20-ylidene)phenylene)(dimethylamido)diiodo zirconium(IV) complex (**2**) (0.025 g, 0.035 mmol), [Rh(CO)₂Cl]₂ (0.017 g, 0.043 mmol) and CH₂Cl₂ (0.50 mL) were combined in a one dram vial at room temperature (22 °C). Reaction mixture immediately became a red homogeneous mixture and was allowed to sit

at room temperature for 12 h. Orange x-ray quality crystals of **13** were grown by vapor diffusion of hexane into a saturated solution of CH₂Cl₂. ¹H NMR (600 MHz, CDCl₃): δ 7.61-7.60 (d, *J* = 1.83 Hz, 2H), 7.19 (s, 3H), 7.04-7.03 (d, *J* = 1.83 Hz, 2H), 4.32-4.29 (t, *J* = 7.96 Hz, 4H), 1.55-1.49 (m, 4H), 1.52-1.50 (m, 4H), 1.05-0.99 (t, *J* = 7.28 Hz, 6H). ¹³C (150 MHz, CDCl₃): δ 188.6 (d, *J* = 42 Hz, Rh-C_{NHC}), 180.1 (d, *J* = 69 Hz, Rh-C_{co}), 180.1 (d, *J* = 35 Hz, Rh-C_{aryl}), 145.3, 125.4, 121.2, 116.4, 109.0, 51.8, 32.8, 20.0, 13.7.

5.4.4 Synthesis of CCC-NHC Rhodium Pincer Complex **14**

2-(1,3-Bis(30-butyl-imidazol-20-ylidene)phenylene)(dimethylamido)diodo zirconium(IV) complex (**2**) (0.025 g, 0.035 mmol), lithium aluminum hydride (LAH) (0.007 g, 0.176 mmol) (acetylacetonato)dicarbonylrhodium(I) (0.011 g, 0.043 mmol) and CH₂Cl₂ (0.50 mL) were combined in a one dram vial at room temperature (22 °C). Reaction mixture immediately became a dark red homogenous mixture and was allowed to sit at room temperature for 12 h. Orange x-ray quality crystals of **14** were grown by vapor diffusion of hexane into a saturated solution of CH₂Cl₂.

5.4.5 General Procedure for Catalytic Trials

A 1 dram vial with a magnetic stir bar was charged with arene (1.0 mL), bis(pinacolato)diboron (60 equiv), **11** (1.5 mol%), NaH (15 mol %) and was conducted neat. The vial was closed and stirred vigorously for at 80 °C. After 6 h, a 10 µL aliquot was passed through a short plug of celite and a 0.45 um PTFE filter and was injected into the GC-MS to determine conversion.

REFERENCES

- (1) Soleilhavoup, M.; Bertrand, G. *Acc. Chem. Res.* **2015**, *48*, 256-266.
- (2) Bourissou, D.; Guerret, O.; Gabbaï, F. P.; Bertrand, G. *Chem. Rev.* **2000**, *100*, 39-92.
- (3) Harrison, J. F.; Liedtke, R. C.; Liebman, J. F. *J. Am. Chem. Soc.* **1979**, *101*, 7162-7168.
- (4) Harrison, J. F. *J. Am. Chem. Soc.* **1971**, *93*, 4112-4119.
- (5) Nelson, D. J.; Nolan, S. P.: *N-Heterocyclic Carbenes. In N-Heterocyclic Carbenes Effective Tools for Organometallic Synthesis*; Nolan, S. P., Ed.; Wiley-VCH: Weinheim, Germany, 2015; pp 1-22.
- (6) Hopkinson, M. N.; Richter, C.; Schedler, M.; Glorius, F. *Nature* **2014**, *510*, 485-496.
- (7) Nelson, D. J.; Nolan, S. P. *Chem. Soc. Rev.* **2013**, *42*, 6723-6753.
- (8) Hahn, F. E.; Jahnke, M. C. *Angew. Chem., Int. Ed.* **2008**, *47*, 3122-3172.
- (9) Díez-González, S.; Nolan, S. P. *Coord. Chem. Rev.* **2007**, *251*, 874-883.
- (10) Gaillard, S.; Cazin, C. S. J.; Nolan, S. P. *Acc. Chem. Res.* **2012**, *45*, 778-787.
- (11) Fortman, G. C.; Nolan, S. P. *Chem. Soc. Rev.* **2011**, *40*, 5151-5169.
- (12) Díez-González, S.; Marion, N.; Nolan, S. P. *Chem. Rev.* **2009**, *109*, 3612-3676.
- (13) Marion, N.; Nolan, S. P. *Acc. Chem. Res.* **2008**, *41*, 1440-1449.
- (14) Marion, N.; Díez-González, S.; Nolan, S. P. *Angew. Chem., Int. Ed.* **2007**, *46*, 2988-3000.
- (15) Vougioukalakis, G. C.; Grubbs, R. H. *Chem. Rev.* **2010**, *110*, 1746-1787.
- (16) Peris, E.; H. Crabtree, R.: ‘Pincer’-Carbene Complexes. In *The Chemistry of Pincer Compounds*; Jensen, C. M., Morales-Morales, D., Eds.; Elsevier Science B.V.: Amsterdam, 2007; pp 107-124.

- (17) Crocker, C.; Errington, R. J.; Markham, R.; Moulton, C. J.; Shaw, B. L. *Journal of the Chemical Society, Dalton Transactions* **1982**, 387-395.
- (18) Al-Salem, N. A.; Empsall, H. D.; Markham, R.; Shaw, B. L.; Weeks, B. *Journal of the Chemical Society, Dalton Transactions* **1979**, 1972-1982.
- (19) Moulton, C. J.; Shaw, B. L. *Journal of the Chemical Society, Dalton Transactions* **1976**, 1020-1024.
- (20) Choi, J.; MacArthur, A. H. R.; Brookhart, M.; Goldman, A. S. *Chem. Rev.* **2011**, *111*, 1761-1779.
- (21) O'Reilly, M. E.; Veige, A. S. *Chem. Soc. Rev.* **2014**, *43*, 6325-6369.
- (22) Li, H.; Hall, M. B. *ACS Catalysis* **2015**, *5*, 1895-1913.
- (23) van Koten, G. *J. Organomet. Chem.* **2013**, *730*, 156-164.
- (24) Deng, Q.-H.; Melen, R. L.; Gade, L. H. *Acc. Chem. Res.* **2014**, *47*, 3162-3173.
- (25) Gelman, D.; Musa, S. *ACS Catalysis* **2012**, *2*, 2456-2466.
- (26) Dupont, J.; S. Consorti, C.; Spencer, J.: Organometallic Pincer-Type Complexes: Recent Applications in Synthesis and Catalysis. In *The Chemistry of Pincer Compounds*; Jensen, C. M., Morales-Morales, D., Eds.; Elsevier Science B.V.: Amsterdam, 2007; pp 1-24.
- (27) Chakraborty, S.; Bhattacharya, P.; Dai, H.; Guan, H. *Acc. Chem. Res.* **2015**, *48*, 1995-2003.
- (28) Younus, H. A.; Su, W.; Ahmad, N.; Chen, S.; Verpoort, F. *Adv. Synth. Catal.* **2015**, *357*, 283-330.
- (29) Gozin, M.; Weisman, A.; Ben-David, Y.; Milstein, D. *Nature* **1993**, *364*, 699-701.
- (30) Zell, T.; Milstein, D. *Acc. Chem. Res.* **2015**, *48*, 1979-1994.
- (31) van der Boom, M. E.; Milstein, D. *Chem. Rev.* **2003**, *103*, 1759-1792.
- (32) Göttker-Schnetmann, I.; Brookhart, M. *J. Am. Chem. Soc.* **2004**, *126*, 9330-9338.
- (33) Liu, F.; Pak, E. B.; Singh, B.; Jensen, C. M.; Goldman, A. S. *J. Am. Chem. Soc.* **1999**, *121*, 4086-4087.
- (34) Lee, D. W.; Kaska, W. C.; Jensen, C. M. *Organometallics* **1998**, *17*, 1-3.
- (35) Gupta, M.; Hagen, C.; Flesher, R. J.; Kaska, W. C.; Jensen, C. M. *Chem. Commun.* **1996**, 2083-2084.

- (36) Goldman, A. S.; Roy, A. H.; Huang, Z.; Ahuja, R.; Schinski, W.; Brookhart, M. *Science* **2006**, *312*, 257-261.
- (37) Rubio, R. J.; Andavan, G. T. S.; Bauer, E. B.; Hollis, T. K.; Cho, J.; Tham, F. S.; Donnadieu, B. *J. Organomet. Chem.* **2005**, *690*, 5353-5364.
- (38) Zhang, D.; Zi, G. *Chem. Soc. Rev.* **2015**, *44*, 1898-1921.
- (39) Zhang, X.; Wright, A. M.; DeYonker, N. J.; Hollis, T. K.; Hammer, N. I.; Webster, C. E.; Valente, E. J. *Organometallics* **2012**, *31*, 1664-1672.
- (40) Chianese, A. R.; Drance, M. J.; Jensen, K. H.; McCollom, S. P.; Yusufova, N.; Shaner, S. E.; Shopov, D. Y.; Tendler, J. A. *Organometallics* **2014**, *33*, 457-464.
- (41) Chianese, A. R.; Mo, A.; Lampland, N. L.; Swartz, R. L.; Bremer, P. T. *Organometallics* **2010**, *29*, 3019-3026.
- (42) Chianese, A. R.; Shaner, S. E.; Tendler, J. A.; Pudalov, D. M.; Shopov, D. Y.; Kim, D.; Rogers, S. L.; Mo, A. *Organometallics* **2012**, *31*, 7359-7367.
- (43) Zhang, Y.-M.; Shao, J.-Y.; Yao, C.-J.; Zhong, Y.-W. *Dalton Trans.* **2012**, *41*, 9280-9282.
- (44) Raynal, M.; Pattacini, R.; Cazin, C. S. J.; Vallée, C.; Olivier-Bourbigou, H.; Braunstein, P. *Organometallics* **2009**, *28*, 4028-4047.
- (45) Raynal, M.; Cazin, C. S. J.; Vallee, C.; Olivier-Bourbigou, H.; Braunstein, P. *Chem. Commun.* **2008**, 3983-3985.
- (46) Zuo, W.; Braunstein, P. *Organometallics* **2012**, *31*, 2606-2615.
- (47) Zuo, W.; Braunstein, P. *Dalton Trans.* **2012**, *41*, 636-643.
- (48) Lin, W.-J.; Naziruddin, A. R.; Chen, Y.-H.; Sun, B.-J.; Chang, A. H. H.; Wang, W.-J.; Hwang, W.-S. *Chem.-Asian J.* **2015**, *10*, 728-739.
- (49) Göttker-Schnetmann, I.; White, P.; Brookhart, M. *J. Am. Chem. Soc.* **2004**, *126*, 1804-1811.
- (50) Clark, W. D.; Tyson, G. E.; Hollis, T. K.; Valle, H. U.; Valente, E. J.; Oliver, A. G.; Dukes, M. P. *Dalton Trans.* **2013**, *42*, 7338-7344.
- (51) Vargas, V. C.; Rubio, R. J.; Hollis, T. K.; Salcido, M. E. *Org. Lett.* **2003**, *5*, 4847-4849.
- (52) Bauer, E. B.; Andavan, G. T. S.; Hollis, T. K.; Rubio, R. J.; Cho, J.; Kuchenbeiser, G. R.; Helgert, T. R.; Letko, C. S.; Tham, F. S. *Org. Lett.* **2008**, *10*, 1175-1178.

- (53) Albrecht, M.; van Koten, G. *Angew. Chem., Int. Ed.* **2001**, *40*, 3750-3781.
- (54) Crabtree, R. H.: *The Organometallic Chemistry of the Transition Metals*, 4th Edition; 4th ed.; John Wiley & Sons, Inc.: Hoboken, New Jersey, 2005.
- (55) Pugh, D.; Danopoulos, A. A. *Coord. Chem. Rev.* **2007**, *251*, 610-641.
- (56) Gunanathan, C.; Milstein, D. *Chem. Rev.* **2014**, *114*, 12024-12087.
- (57) Selander, N.; J. Szabó, K. *Chem. Rev.* **2010**, *111*, 2048-2076.
- (58) Benito-Garagorri, D.; Kirchner, K. *Acc. Chem. Res.* **2008**, *41*, 201-213.
- (59) Tu, T.; Assenmacher, W.; Peterlik, H.; Weisbarth, R.; Nieger, M.; Dötz, K. H. *Angew. Chem., Int. Ed.* **2007**, *46*, 6368-6371.
- (60) Hahn, F. E.; Jahnke, M. C.; Pape, T. *Organometallics* **2006**, *26*, 150-154.
- (61) Eberhard, M. R. *Org. Lett.* **2004**, *6*, 2125-2128.
- (62) Peris, E.; Crabtree, R. H. *Coord. Chem. Rev.* **2004**, *248*, 2239-2246.
- (63) Crabtree, R. H. *J. Organomet. Chem.* **2004**, *689*, 4083-4091.
- (64) Rybtchinski, B.; Milstein, D.: Pincer Systems as Models for the Activation of Strong Bonds: Scope and Mechanism. In *The Chemistry of Pincer Compounds*; Jensen, C. M., Morales-Morales, D., Eds.; Elsevier Science B.V.: Amsterdam, 2007; pp 87-105.
- (65) Obligacion, J. V.; Semproni, S. P.; Chirik, P. J. *J. Am. Chem. Soc.* **2014**, *136*, 4133-4136.
- (66) Hojilla Atienza, C. C.; Bowman, A. C.; Lobkovsky, E.; Chirik, P. J. *J. Am. Chem. Soc.* **2010**, *132*, 16343-16345.
- (67) Balaraman, E.; Gnanaprakasam, B.; Shimon, L. J. W.; Milstein, D. *J. Am. Chem. Soc.* **2010**, *132*, 16756-16758.
- (68) Gunanathan, C.; Milstein, D. *Angew. Chem., Int. Ed.* **2008**, *47*, 8661-8664.
- (69) Balaraman, E.; Gunanathan, C.; Zhang, J.; Shimon, L. J. W.; Milstein, D. *Nat Chem* **2011**, *3*, 609-614.
- (70) Takaya, J.; Iwasawa, N. *J. Am. Chem. Soc.* **2008**, *130*, 15254-15255.
- (71) Scheuermann, M. L.; Semproni, S. P.; Pappas, I.; Chirik, P. J. *Inorg. Chem.* **2014**, *53*, 9463-9465.

- (72) Gutsulyak, D. V.; Piers, W. E.; Borau-Garcia, J.; Parvez, M. *J. Am. Chem. Soc.* **2013**, *135*, 11776-11779.
- (73) Arashiba, K.; Miyake, Y.; Nishibayashi, Y. *Nat Chem* **2011**, *3*, 120-125.
- (74) Tanaka, H.; Arashiba, K.; Kuriyama, S.; Sasada, A.; Nakajima, K.; Yoshizawa, K.; Nishibayashi, Y. *Nat Commun* **2014**, *5*.
- (75) Herrmann, W. A. *Angew. Chem., Int. Ed.* **2002**, *41*, 1290-1309.
- (76) Riener, K.; Haslinger, S.; Raba, A.; Högerl, M. P.; Cokoja, M.; Herrmann, W. A.; Kühn, F. E. *Chem. Rev.* **2014**, *114*, 5215-5272.
- (77) Bauer, I.; Knölker, H.-J. *Chem. Rev.* **2015**.
- (78) Pellissier, H.; Clavier, H. *Chem. Rev.* **2014**, *114*, 2775-2823.
- (79) Gao, K.; Yoshikai, N. *Acc. Chem. Res.* **2014**, *47*, 1208-1219.
- (80) Tasker, S. Z.; Standley, E. A.; Jamison, T. F. *Nature* **2014**, *509*, 299-309.
- (81) Cahiez, G.; Moyeux, A. *Chem. Rev.* **2010**, *110*, 1435-1462.
- (82) Käß, M.; Hohenberger, J.; Adelhardt, M.; Zolnhofer, E. M.; Mossin, S.; Heinemann, F. W.; Sutter, J.; Meyer, K. *Inorg. Chem.* **2014**, *53*, 2460-2470.
- (83) Kropp, H.; King, A. E.; Khusniyarov, M. M.; Heinemann, F. W.; Lancaster, K. M.; DeBeer, S.; Bill, E.; Meyer, K. *J. Am. Chem. Soc.* **2012**, *134*, 15538-15544.
- (84) Vogel, C.; Heinemann, F. W.; Sutter, J.; Anthon, C.; Meyer, K. *Angew. Chem., Int. Ed.* **2008**, *47*, 2681-2684.
- (85) Danopoulos, A. A.; Wright, J. A.; Motherwell, W. B.; Ellwood, S. *Organometallics* **2004**, *23*, 4807-4810.
- (86) Danopoulos, A. A.; Tsoureas, N.; Wright, J. A.; Light, M. E. *Organometallics* **2004**, *23*, 166-168.
- (87) McGuinness, D. S.; Gibson, V. C.; Steed, J. W. *Organometallics* **2004**, *23*, 6288-6292.
- (88) McGuinness, D. S.; Gibson, V. C.; Wass, D. F.; Steed, J. W. *J. Am. Chem. Soc.* **2003**, *125*, 12716-12717.
- (89) Yoshida, K.; Horiuchi, S.; Takeichi, T.; Shida, H.; Imamoto, T.; Yanagisawa, A. *Org. Lett.* **2010**, *12*, 1764-1767.

- (90) Danopoulos, A. A.; Pugh, D.; Smith, H.; Saßmannshausen, J. *Chem.-Eur. J.* **2009**, *15*, 5491-5502.
- (91) Inamoto, K.; Kuroda, J.-i.; Hiroya, K.; Noda, Y.; Watanabe, M.; Sakamoto, T. *Organometallics* **2006**, *25*, 3095-3098.
- (92) Mrutu, A.; Goldberg, K. I.; Kemp, R. A. *Inorg. Chim. Acta* **2010**, *364*, 115-119.
- (93) Danopoulos, A. A.; Wright, J. A.; Motherwell, W. B. *Chem. Commun.* **2005**, 784-786.
- (94) Pugh, D.; Wells, N. J.; Evans, D. J.; Danopoulos, A. A. *Dalton Trans.* **2009**, 7189-7195.
- (95) Inamoto, K.; Kuroda, J.-i.; Kwon, E.; Hiroya, K.; Doi, T. *J. Organomet. Chem.* **2009**, *694*, 389-396.
- (96) Yu, R. P.; Darmon, J. M.; Milsmann, C.; Margulieux, G. W.; Stieber, S. C. E.; DeBeer, S.; Chirik, P. J. *J. Am. Chem. Soc.* **2013**, *135*, 13168-13184.
- (97) Yu, R. P.; Darmon, J. M.; Hoyt, J. M.; Margulieux, G. W.; Turner, Z. R.; Chirik, P. J. *ACS Catalysis* **2012**, *2*, 1760-1764.
- (98) Obligacion, J. V.; Chirik, P. J. *Org. Lett.* **2013**, *15*, 2680-2683.
- (99) Lin, T.-P.; Peters, J. C. *J. Am. Chem. Soc.* **2014**, *136*, 13672-13683.
- (100) Zhang, G.; Vasudevan, K. V.; Scott, B. L.; Hanson, S. K. *J. Am. Chem. Soc.* **2013**, *135*, 8668-8681.
- (101) Monfette, S.; Turner, Z. R.; Semproni, S. P.; Chirik, P. J. *J. Am. Chem. Soc.* **2012**, *134*, 4561-4564.
- (102) Zhang, G.; Scott, B. L.; Hanson, S. K. *Angew. Chem., Int. Ed.* **2012**, *51*, 12102-12106.
- (103) Mukherjee, A.; Srimani, D.; Chakraborty, S.; Ben-David, Y.; Milstein, D. *J. Am. Chem. Soc.* **2015**, *137*, 8888-8891.
- (104) Zhang, G.; Hanson, S. K. *Org. Lett.* **2013**, *15*, 650-653.
- (105) Chan, S. L.-F.; Lam, T. L.; Yang, C.; Yan, S.-C.; Cheng, N. M. *Chem. Commun.* **2015**.
- (106) Zhang, L.; Zuo, Z.; Leng, X.; Huang, Z. *Angew. Chem., Int. Ed.* **2014**, *53*, 2696-2700.

- (107) Obligacion, J. V.; Neely, J. M.; Yazdani, A. N.; Pappas, I.; Chirik, P. J. *J. Am. Chem. Soc.* **2015**, *137*, 5855-5858.
- (108) Atienza, C. C. H.; Diao, T.; Weller, K. J.; Nye, S. A.; Lewis, K. M.; Delis, J. G. P.; Boyer, J. L.; Roy, A. K.; Chirik, P. J. *J. Am. Chem. Soc.* **2014**, *136*, 12108-12118.
- (109) Matson, E. M.; Espinosa Martinez, G.; Ibrahim, A. D.; Jackson, B. J.; Bertke, J. A.; Fout, A. R. *Organometallics* **2014**, *34*, 399-407.
- (110) Spencer, L. P.; Winston, S.; Fryzuk, M. D. *Organometallics* **2004**, *23*, 3372-3374.
- (111) Diamond, G. M.; Jordan, R. F.; Petersen, J. L. *Organometallics* **1996**, *15*, 4045-4053.
- (112) Diamond, G. M.; Jordan, R. F.; Petersen, J. L. *Organometallics* **1996**, *15*, 4030-4037.
- (113) Diamond, G. M.; Rodewald, S.; Jordan, R. F. *Organometallics* **1995**, *14*, 5-7.
- (114) Liddle, S. T.; Edworthy, I. S.; Arnold, P. L. *Chem. Soc. Rev.* **2007**, *36*, 1732-1744.
- (115) Schaefer, B. A.; Margulieux, G. W.; Small, B. L.; Chirik, P. J. *Organometallics* **2015**, *34*, 1307-1320.
- (116) Semproni, S. P.; Milsmann, C.; Chirik, P. J. *J. Am. Chem. Soc.* **2014**, *136*, 9211-9224.
- (117) Murugesan, S.; Stöger, B.; Weil, M.; Veiros, L. F.; Kirchner, K. *Organometallics* **2015**, *34*, 1364-1372.
- (118) Helgert, T. R.; Hollis, T. K.; Oliver, A. G.; Valle, H. U.; Wu, Y.; Webster, C. E. *Organometallics* **2014**, *33*, 952-958.
- (119) Helgert, T. R.; Hollis, T. K.; Valente, E. J. *Organometallics* **2012**, *31*, 3002-3009.
- (120) Clark, W. D.; Cho, J.; Valle, H. U.; Hollis, T. K.; Valente, E. J. *J. Organomet. Chem.* **2014**, *751*, 534-540.
- (121) Yu, D.-G.; Gensch, T.; de Azambuja, F.; Vásquez-Céspedes, S.; Glorius, F. *J. Am. Chem. Soc.* **2014**, *136*, 17722-17725.
- (122) Hummel, J. R.; Ellman, J. A. *J. Am. Chem. Soc.* **2015**, *137*, 490-498.
- (123) Ikemoto, H.; Yoshino, T.; Sakata, K.; Matsunaga, S.; Kanai, M. *J. Am. Chem. Soc.* **2014**, *136*, 5424-5431.
- (124) Yoshino, T.; Ikemoto, H.; Matsunaga, S.; Kanai, M. *Angew. Chem., Int. Ed.* **2013**, *52*, 2207-2211.

- (125) Cho, J.; Hollis, T. K.; Helgert, T. R.; Valente, E. *J. Chem. Commun.* **2008**, 5001-5003.
- (126) Li, C. *J. Chem. Rev.* **1993**, 93, 2023-2035.
- (127) Li, C.-J. *Chem. Rev.* **2005**, 105, 3095-3166.
- (128) Posner, G. H. *Organic Reactions* **1972**, 19, 3-113.
- (129) Mukaiyama, T. *Organic Reactions* **1982**, 28, 203-331.
- (130) Farina, V.; Krishnamurthy, V.; Scott, W. *Organic Reactions* **1997**, 50, 1-652.
- (131) Ritleng, V.; Sirlin, C.; Pfeffer, M. *Chem. Rev.* **2002**, 102, 1731-1770.
- (132) Negishi, E. *Acc. Chem. Res.* **1982**, 15, 340-348.
- (133) Iqbal, J.; Bhatia, B.; Nayyar, N. K. *Chem. Rev.* **1994**, 94, 519-564.
- (134) Ramulu, B. V.; Mahendar, L.; Krishna, J.; Reddy, A. G. K.; Suchand, B.; Satyanarayana, G. *Tetrahedron* **2013**, 69, 8305-8315.
- (135) Mitchell, T. N. *Metal-Catalyzed Cross-Coupling Reactions* **2004**, 1, 125-155.
- (136) Fagnou, K.; Lautens, M. *Chem. Rev.* **2002**, 103, 169-196.
- (137) Colby, D. A.; Bergman, R. G.; Ellman, J. A. *Chem. Rev.* **2009**, 110, 624-655.
- (138) Knochel, P.; Calaza, M.; Hupe, P. *Metal-Catalyzed Cross-Coupling Reactions* **2004**, 2, 619-670.
- (139) Gujadhur, R. K.; Bates, C. G.; Venkataraman, D. *Org. Lett.* **2001**, 3, 4315-4317.
- (140) Li, Z.; Bohle, D. S.; Li, C.-J. *Proc. Natl. Acad. Sci. USA* **2006**, 103, 8928-8933.
- (141) Deutsch, C.; Krause, N.; Lipshutz, B. H. *Chem. Rev.* **2008**, 108, 2916-2927.
- (142) Shibasaki, M.; Kanai, M. *Chem. Rev.* **2008**, 108, 2853-2873.
- (143) Beletskaya, I. P.; Cheprakov, A. V. *Chem. Rev.* **2000**, 100, 3009-3066.
- (144) Cabri, W.; Candiani, I. *Acc. Chem. Res.* **1995**, 28, 2-7.
- (145) Miyaura, N.; Suzuki, A. *Chem. Rev.* **1995**, 95, 2457-2483.
- (146) Suzuki, A. *J. Organomet. Chem.* **1999**, 576, 147-168.
- (147) Balanta, A.; Godard, C.; Claver, C. *Chem. Soc. Rev.* **2011**, 40, 4973-4985.

- (148) Brown, J. M.; Cooley, N. A. *Chem. Rev.* **1988**, *88*, 1031-1046.
- (149) Negishi, E.; Zeng, X.; Tan, Z.; Qian, M.; Hu, Q.; Huang, Z. *Metal-Catalyzed Cross-Coupling Reactions* **2004**, *2*, 815-889.
- (150) Firouzabadi, H.; Iranpoor, N.; Gholinejad, M.; Akbari, S.; Jeddi, N. *RSC Adv.* **2014**, *4*, 17060-17070.
- (151) Huang, Z.; Dong, G. *J. Am. Chem. Soc.* **2013**, *135*, 17747-17750.
- (152) Sakai, M.; Hayashi, H.; Miyaura, N. *Organometallics* **1997**, *16*, 4229-4231.
- (153) Yu, Y.-N.; Xu, M.-H. *J. Org. Chem.* **2013**, *78*, 2736-2741.
- (154) Wang, Z.; Zhao, K.; Fu, J.; Zhang, J.; Yin, W.; Tang, Y. *Org. Biomol. Chem.* **2013**, *11*, 2093-2097.
- (155) Korenaga, T.; Ko, A.; Shimada, K. *J. Org. Chem.* **2013**, *78*, 9975-9980.
- (156) Fei, X.-D.; Zhou, Z.; Li, W.; Zhu, Y.-M.; Shen, J.-K. *Eur. J. Org. Chem.* **2012**, *2012*, 3001-3008.
- (157) Chen, G.; Gui, J.; Cao, P.; Liao, J. *Tetrahedron* **2012**, *68*, 3220-3224.
- (158) Nishimura, T.; Wang, J.; Nagaosa, M.; Okamoto, K.; Shintani, R.; Kwong, F.-y.; Yu, W.-y.; Chan, A. S. C.; Hayashi, T. *J. Am. Chem. Soc.* **2009**, *132*, 464-465.
- (159) Shintani, R.; Duan, W.-L.; Nagano, T.; Okada, A.; Hayashi, T. *Angew. Chem., Int. Ed.* **2005**, *44*, 4611-4614.
- (160) Shintani, R.; Duan, W.-L.; Hayashi, T. *J. Am. Chem. Soc.* **2006**, *128*, 5628-5629.
- (161) Knochel, P.; Calaza, M.; P., H. *Metal-Catalyzed Cross-Coupling Reactions* **2004**, *2*, 619-667.
- (162) Hayashi, T.; Takahashi, M.; Takaya, Y.; Ogasawara, M. *J. Am. Chem. Soc.* **2002**, *124*, 5052-5058.
- (163) Trenkle, W. C.; Barkin, J. L.; Son, S. U.; Sweigart, D. A. *Organometallics* **2006**, *25*, 3548-3551.
- (164) Kuriyama, M.; Nagai, K.; Yamada, K.-i.; Miwa, Y.; Taga, T.; Tomioka, K. *J. Am. Chem. Soc.* **2002**, *124*, 8932-8939.
- (165) Takaya, Y.; Ogasawara, M.; Hayashi, T. *Chirality* **2000**, *12*, 469-471.
- (166) Batey, R. A.; Thadani, A. N.; Smil, D. V. *Org. Lett.* **1999**, *1*, 1683-1686.

- (167) Shao, C.; Yu, H.-J.; Feng, C.-G.; Wang, R.; Lin, G.-Q. *Tetrahedron Lett.* **2012**, *53*, 2733-2735.
- (168) Chen, G.; Xing, J.; Cao, P.; Liao, J. *Tetrahedron* **2012**, *68*, 5908-5911.
- (169) Takaya, Y.; Ogasawara, M.; Hayashi, T. *Tetrahedron Lett.* **1998**, *39*, 8479-8482.
- (170) Takaya, Y.; Ogasawara, M.; Hayashi, T.; Sakai, M.; Miyaura, N. *J. Am. Chem. Soc.* **1998**, *120*, 5579-5580.
- (171) Takaya, Y.; Ogasawara, M.; Hayashi, T. *Tetrahedron Lett.* **1999**, *40*, 6957-6961.
- (172) Takaya, Y.; Senda, T.; Kurushima, H.; Ogasawara, M.; Hayashi, T. *Tetrahedron: Asymmetry* **1999**, *10*, 4047-4056.
- (173) Kabalka, G. W.; Das, B. C.; Das, S. *Tetrahedron Lett.* **2002**, *43*, 2323-2325.
- (174) Iguchi, Y.; Itooka, R.; Miyaura, N. *Synlett* **2003**, *2003*, 1040-1042.
- (175) Itooka, R.; Iguchi, Y.; Miyaura, N. *J. Org. Chem.* **2003**, *68*, 6000-6004.
- (176) Tokunaga, N.; Yoshida, K.; Hayashi, T. *Proc. Natl. Acad. Sci. U.S.A.* **2004**, *101*, 5445-5449.
- (177) Duan, W.-L.; Iwamura, H.; Shintani, R.; Hayashi, T. *J. Am. Chem. Soc.* **2007**, *129*, 2130-2138.
- (178) Duan, W.-L.; Imazaki, Y.; Shintani, R.; Hayashi, T. *Tetrahedron* **2007**, *63*, 8529-8536.
- (179) Nakao, Y.; Chen, J.; Imanaka, H.; Hiyama, T.; Ichikawa, Y.; Duan, W.-L.; Shintani, R.; Hayashi, T. *J. Am. Chem. Soc.* **2007**, *129*, 9137-9143.
- (180) Morgan, B. P.; Smith, R. C. *J. Organomet. Chem.* **2008**, *693*, 11-16.
- (181) Gendrineau, T.; Genet, J.-P.; Darses, S. *Org. Lett.* **2009**, *11*, 3486-3489.
- (182) Berhal, F.; Wu, Z.; Genet, J.-P.; Ayad, T.; Ratovelomanana-Vidal, V. *J. Org. Chem.* **2011**, *76*, 6320-6326.
- (183) Le Boucher d'Herouville, F.; Millet, A.; Scalone, M.; Michelet, V. r. *J. Org. Chem.* **2011**, *76*, 6925-6930.
- (184) Yamamoto, Y.; Kurihara, K.; Takahashi, Y.; Miyaura, N. *Mol.* **2012**, *18*, 14-26.
- (185) Morigaki, A.; Tanaka, T.; Miyabe, T.; Ishihara, T.; Konno, T. *Org. Biomol. Chem.* **2013**, *11*, 586-595.

- (186) Yu, X.-Q.; Shirai, T.; Yamamoto, Y.; Miyaura, N. *Chem.-Asian J.* **2011**, *6*, 932-937.
- (187) Miyaura, N. *Bull. Chem. Soc. Jpn.* **2008**, *81*, 1535-1553.
- (188) Sasaki, K.; Hayashi, T. *Angew. Chem., Int. Ed.* **2010**, *49*, 8145-8147.
- (189) Sasaki, K.; Nishimura, T.; Shintani, R.; Kantchev, E. A. B.; Hayashi, T. *Chem. Sci.* **2012**, *3*, 1278-1283.
- (190) Helbig, S.; Axenov, K. V.; Tussetschläger, S.; Frey, W.; Laschat, S. *Tetrahedron Lett.* **2012**, *53*, 3506-3509.
- (191) Boiteau, J.-G.; Minnaard, A. J.; Feringa, B. L. *J. Org. Chem.* **2003**, *68*, 9481-9484.
- (192) Ma, Y.; Song, C.; Ma, C.; Sun, Z.; Chai, Q.; Andrus, M. B. *Angew. Chem., Int. Ed.* **2003**, *42*, 5871-5874.
- (193) Imamoto, T.; Sugita, K.; Yoshida, K. *J. Am. Chem. Soc.* **2005**, *127*, 11934-11935.
- (194) Peñafiel, I.; Pastor, I. M.; Yus, M.; Esteruelas, M. A.; Oliván, M. *Organometallics* **2012**, *31*, 6154-6161.
- (195) Shaughnessy, K. H. *Chem. Rev.* **2009**, *109*, 643-710.
- (196) Dimmock, J. R.; Elias, D. W.; Beazely, M. A.; Kandepu, N. M. *Curr. Med. Chem* **1999**, *6*, 1125-1149.
- (197) Hall, D. G.: Structure, Properties, and Preparation of Boronic Acid Derivatives. In *Boronic Acids*; Wiley-VCH Verlag GmbH & Co. KGaA, 2011; pp 14.
- (198) Hayashi, T.; Yamasaki, K. *Chem. Rev.* **2003**, *103*, 2829-2844.
- (199) Daisy, B. H.; Strobel, G. A.; Castillo, U.; Ezra, D.; Sears, J.; Weaver, D. K.; Runyon, J. B. *Microbiology* **2002**, *148*, 3737-3741.
- (200) Collin, G.; Höke, H.; Greim, H.: Naphthalene and Hydronaphthalenes. In *Ullmann's Encyclopedia of Industrial Chemistry*; Wiley-VCH Verlag GmbH & Co. KGaA, 2000.
- (201) Primas, N.; Bouillon, A.; Rault, S. *Tetrahedron* **2010**, *66*, 8121-8136.
- (202) Cui, J. J.; Shen, H.; Tran-Dubé, M.; Nambu, M.; McTigue, M.; Grodsky, N.; Ryan, K.; Yamazaki, S.; Aguirre, S.; Parker, M.; Li, Q.; Zou, H.; Christensen, J. *J. Med. Chem.* **2013**, *56*, 6651-6665.

- (203) Aghazadeh Tabrizi, M.; Baraldi, P. G.; Saponaro, G.; Moorman, A. R.; Romagnoli, R.; Preti, D.; Baraldi, S.; Ruggiero, E.; Tintori, C.; Tuccinardi, T.; Vincenzi, F.; Borea, P. A.; Varani, K. *J. Med. Chem.* **2013**, *56*, 4482-4496.
- (204) Lagoja, I. M. *Chemistry & Biodiversity* **2005**, *2*, 1-50.
- (205) Wang, J.; Liu, W.; Zhao, Q.; Qi, Q.; Lu, N.; Yang, Y.; Nei, F.-F.; Rong, J.-J.; You, Q.-D.; Guo, Q.-L. *Toxicology* **2009**, *256*, 135-140.
- (206) Mohammadizadeh, M.; Pourabbas, B.; Mahmoodian, M.; Foroutani, K.; Fallahian, M. *Mater. Sci. Semi. Proc.* **2014**, *20*, 74-83.
- (207) Wei, S.; Xia, J.; Dell, E. J.; Jiang, Y.; Song, R.; Lee, H.; Rodenbough, P.; Briseno, A. L.; Campos, L. M. *Angew. Chem., Int. Ed.* **2014**, *53*, 1832-1836.
- (208) Hou, X. L.; Cheung, H. Y.; Hon, T. Y.; Kwan, P. L.; Lo, T. H.; Tong, S. Y.; Wong, H. N. C. *Tetrahedron* **1998**, *54*, 1955-2020.
- (209) Yasukawa, T.; Miyamura, H.; Kobayashi, S. *J. Am. Chem. Soc.* **2012**, *134*, 16963-16966.
- (210) Lin, S.; Lu, X. *Org. Lett.* **2010**, *12*, 2536-2539.
- (211) Jana, R.; Tunge, J. A. *J. Org. Chem.* **2011**, *76*, 8376-8385.
- (212) Kelly, C. B.; Mercadante, M. A.; Wiles, R. J.; Leadbeater, N. E. *Org. Lett.* **2013**, *15*, 2222-2225.
- (213) Wang, H.; Li, Y.; Zhang, R.; Jin, K.; Zhao, D.; Duan, C. *J. Org. Chem.* **2012**, *77*, 4849-4853.
- (214) He, P.; Lu, Y.; Dong, C.-G.; Hu, Q.-S. *Org. Lett.* **2006**, *9*, 343-346.
- (215) Marumoto, S. N., Toyoki; Ebisawa, Masayuki; Asoh, Yusuke; Fukushima Yasuo; Kato, Mikio Preparation of N-((1R)-1-arylethyl)-N-(aryl)cycloalkyl)amine derivatives as agonists of calcium sensing receptor (CaSR). Japan Patent WO2010021351, February 25, 2010.
- (216) Lerebours, R.; Wolf, C. *Org. Lett.* **2007**, *9*, 2737-2740.
- (217) Bernardi, R.; Caronna, T.; Coggiola, D. *Tetrahedron Lett.* **1983**, *24*, 5019-5022.
- (218) Brown, H. C.: *Organic Syntheses Via Boranes*; John Wiley & Sons: New York, 1975.
- (219) Miyaura, N.: Rhodium-Catalyzed Addition Reactions of Organoboronic Acids. In *Organoboranes for Syntheses*; Ramachandra, P. V., Brown, H. C., Eds.; Oxford University Press: Washington DC, 2001; pp 94-107.

- (220) Ramachandran, P. V.; Brown, H. C.: Recent Advances in Borane Chemistry. In *Organoboranes for Syntheses*; Ramachandran, P. V., Brown, H. C., Eds.; Oxford University Press: Washington DC, 2001; pp 1-15.
- (221) Lawson, Y. G.; Gerald Lesley, M. J.; Norman, N. C.; Rice, C. R.; Lawson, Y. G.; Marder, T. B. *Chem. Commun.* **1997**, 2051-2052.
- (222) Liu, B.; Gao, M.; Dang, L.; Zhao, H.; Marder, T. B.; Lin, Z. *Organometallics* **2012**, *31*, 3410-3425.
- (223) Bell, N. J.; Cox, A. J.; Cameron, N. R.; Evans, J. S. O.; Marder, T. B.; Duin, M. A.; Elsevier, C. J.; Baucherel, X.; Tulloch, A. A. D.; Tooze, R. P. *Chem. Commun.* **2004**, 1854-1855.
- (224) Abu Ali, H.; Goldberg, I.; Srebnik, M. *Organometallics* **2001**, *20*, 3962-3965.
- (225) Bonet, A.; Gulyás, H.; Koshevoy, I. O.; Estevan, F.; Sanaú, M.; Úbeda, M. A.; Fernández, E. *Chem.-Eur. J.* **2010**, *16*, 6382-6390.
- (226) Lillo, V.; Geier, M. J.; Westcott, S. A.; Fernandez, E. *Org. Biomol. Chem.* **2009**, *7*, 4674-4676.
- (227) Toribatake, K.; Zhou, L.; Tsuruta, A.; Nishiyama, H. *Tetrahedron* **2013**, *69*, 3551-3560.
- (228) Shiomi, T.; Adachi, T.; Toribatake, K.; Zhou, L.; Nishiyama, H. *Chem. Commun.* **2009**, 5987-5989.
- (229) Lee, J.-E.; Yun, J. *Angew. Chem., Int. Ed.* **2008**, *47*, 145-147.
- (230) Lee, J.-E.; Kwon, J.; Yun, J. *Chem. Commun.* **2008**, 733-734.
- (231) Calow, A. D. J.; Solé, C.; Whiting, A.; Fernández, E. *ChemCatChem* **2013**, *5*, 2233-2239.
- (232) Zhao, L.; Ma, Y.; Duan, W.; He, F.; Chen, J.; Song, C. *Org. Lett.* **2012**, *14*, 5780-5783.
- (233) Molander, G. A.; McKee, S. A. *Org. Lett.* **2011**, *13*, 4684-4687.
- (234) Gao, M.; Thorpe, S. B.; Kleeberg, C.; Slebodnick, C.; Marder, T. B.; Santos, W. L. *J. Org. Chem.* **2011**, *76*, 3997-4007.
- (235) Mantilli, L.; Mazet, C. *ChemCatChem* **2010**, *2*, 501-504.
- (236) Sim, H.-S.; Feng, X.; Yun, J. *Chem.-Eur. J.* **2009**, *15*, 1939-1943.

- (237) Ito, H.; Yamanaka, H.; Tateiwa, J.-i.; Hosomi, A. *Tetrahedron Lett.* **2000**, *41*, 6821-6825.
- (238) Takahashi, K.; Ishiyama, T.; Miyaura, N. *Chem. Lett.* **2000**, *29*, 982-983.
- (239) Takahashi, K.; Ishiyama, T.; Miyaura, N. *J. Organomet. Chem.* **2001**, *625*, 47-53.
- (240) Mun, S.; Lee, J.-E.; Yun, J. *Org. Lett.* **2006**, *8*, 4887-4889.
- (241) Chea, H.; Sim, H.-S.; Yun, J. *Adv. Synth. Catal.* **2009**, *351*, 855-858.
- (242) Lillo, V.; Prieto, A.; Bonet, A.; Díaz-Requejo, M. M.; Ramírez, J.; Pérez, P. J.; Fernández, E. *Organometallics* **2008**, *28*, 659-662.
- (243) Lillo, V.; Bonet, A.; Fernandez, E. *Dalton Trans.* **2009**, 2899-2908.
- (244) Fleming, W. J.; Muller-Bunz, H.; Lillo, V.; Fernandez, E.; Guiry, P. J. *Org. Biomol. Chem.* **2009**, *7*, 2520-2524.
- (245) Bonet, A.; Lillo, V.; Ramirez, J.; Diaz-Requejo, M. M.; Fernandez, E. *Org. Biomol. Chem.* **2009**, *7*, 1533-1535.
- (246) Gao, M.; Thorpe, S. B.; Santos, W. L. *Org. Lett.* **2009**, *11*, 3478-3481.
- (247) Schiffner, J. A.; Müther, K.; Oestreich, M. *Angew. Chem., Int. Ed.* **2010**, *49*, 1194-1196.
- (248) Feng, X.; Yun, J. *Chem. Commun.* **2009**, 6577-6579.
- (249) Thorpe, S. B.; Guo, X.; Santos, W. L. *Chem. Commun.* **2011**, *47*, 424-426.
- (250) Thorpe, S. B.; Calderone, J. A.; Santos, W. L. *Org. Lett.* **2012**, *14*, 1918-1921.
- (251) Kobayashi, S.; Xu, P.; Endo, T.; Ueno, M.; Kitanosono, T. *Angew. Chem., Int. Ed.* **2012**, *51*, 12763-12766.
- (252) Sole, C.; Bonet, A.; de Vries, A. H. M.; de Vries, J. G.; Lefort, L.; Gulyás, H.; Fernández, E. *Organometallics* **2012**, *31*, 7855-7861.
- (253) Ibrahim, I.; Breistein, P.; Córdova, A. *Angew. Chem., Int. Ed.* **2011**, *50*, 12036-12041.
- (254) Chen, I. H.; Yin, L.; Itano, W.; Kanai, M.; Shibasaki, M. *J. Am. Chem. Soc.* **2009**, *131*, 11664-11665.
- (255) Hirano, K.; Yorimitsu, H.; Oshima, K. *Org. Lett.* **2007**, *9*, 5031-5033.
- (256) Cho, H. Y.; Morken, J. P. *J. Am. Chem. Soc.* **2008**, *130*, 16140-16141.

- (257) Bonet, A.; Sole, C.; Gulyás, H.; Fernández, E. *Chem.-Asian J.* **2011**, *6*, 1011-1014.
- (258) Pubill-Ulldemolins, C.; Bonet, A.; Gulyas, H.; Bo, C.; Fernandez, E. *Org. Biomol. Chem.* **2012**, *10*, 9677-9682.
- (259) Pubill-Ulldemolins , C.; Bonet, A.; Bo, C.; Gulyás, H.; Fernández, E. *Chem. Eur. J.* **2012**, *18*, 1121-1126.
- (260) Bonet, A.; Gulyás, H.; Fernández, E. *Angew. Chem., Int. Ed.* **2010**, *49*, 5130-5134.
- (261) Lee, K.-s.; Zhugralin, A. R.; Hoveyda, A. H. *J. Am. Chem. Soc.* **2009**, *131*, 7253-7255.
- (262) Radomkit, S.; Hoveyda, A. H. *Angew. Chem., Int. Ed.* **2014**, *53*, 3387-3391.
- (263) Wu, H.; Radomkit, S.; O'Brien, J. M.; Hoveyda, A. H. *J. Am. Chem. Soc.* **2012**, *134*, 8277-8285.
- (264) Hartmann, E.; Vyas, D. J.; Oestreich, M. *Chem. Commun.* **2011**, *47*, 7917-7932.
- (265) Hagemann, B.; Junge, K.; Enthaler, S.; Michalik, M.; Riermeier, T.; Monsees, A.; Beller, M. *Adv. Synth. Catal.* **2005**, *347*, 1978-1986.
- (266) Kabalka, G. W.; Das, B. C.; Das, S. *Tetrahedron Lett.* **2001**, *42*, 7145-7146.
- (267) Kabalka, G. W.; Yao, M.-L. *J. Organomet. Chem.* **2009**, *694*, 1638-1641.
- (268) Kitanosono, T.; Xu, P.; Isshiki, S.; Zhu, L.; Kobayashi, S. *Chem. Commun.* **2014**, *50*, 9336-9339.
- (269) Kitanosono, T.; Xu, P.; Kobayashi, S. *Chem.-Asian J.* **2014**, *9*, 179-188.
- (270) Kitanosono, T.; Xu, P.; Kobayashi, S. *Chem. Commun.* **2013**, *49*, 8184-8186.
- (271) Stavber, G.; Časar, Z. *Appl. Organomet. Chem.* **2013**, *27*, 159-165.
- (272) Molander, G. A.; Wisniewski, S. R.; Hosseini-Sarvari, M. *Adv. Synth. Catal.* **2013**, *355*, 3037-3057.
- (273) Niu, Z.; Chen, J.; Chen, Z.; Ma, M.; Song, C.; Ma, Y. *J. Org. Chem.* **2015**, *80*, 602-608.
- (274) Reilly, S. W.; Box, H. K.; Kuchenbeiser, G. R.; Rubio, R. J.; Letko, C. S.; Cousineau, K. D.; Hollis, T. K. *Tetrahedron Lett.* **2014**, *55*, 6738-6742.

- (275) The Crystal structure of 2-(1,3-bis(N-butylimidazol-2-ylidene)phenylene)(dimethylammido)bis(iodo) rhodium(III) (1) has been deposited at the Cambridge Crystallographic Data Centre. The crystal structure (CCDC 1059458) can be viewed at <http://www.ccdc.cam.ac.uk/pages/Home.aspx>.
- (276) Ishiyama, T.; Miyaura, N. *J. Organomet. Chem.* **2000**, *611*, 392-402.
- (277) Mkhald, I. A. I.; Barnard, J. H.; Marder, T. B.; Murphy, J. M.; Hartwig, J. F. *Chem. Rev.* **2009**, *110*, 890-931.
- (278) Hartwig, J. F. *Acc. Chem. Res.* **2011**, *45*, 864-873.
- (279) Ishiyama, T.; Murata, M.; Miyaura, N. *J. Org. Chem.* **1995**, *60*, 7508-7510.
- (280) Waltz, K. M.; He, X.; Muhoro, C.; Hartwig, J. F. *J. Am. Chem. Soc.* **1995**, *117*, 11357-11358.
- (281) Hartwig, J. F. *Chem. Soc. Rev.* **2011**, *40*, 1992-2002.
- (282) Larsen, M. A.; Wilson, C. V.; Hartwig, J. F. *J. Am. Chem. Soc.* **2015**, *137*, 8633-8643.
- (283) Partridge, B. M.; Hartwig, J. F. *Org. Lett.* **2012**, *15*, 140-143.
- (284) Larsen, M. A.; Hartwig, J. F. *J. Am. Chem. Soc.* **2014**, *136*, 4287-4299.
- (285) Sadler, S. A.; Tajuddin, H.; Mkhald, I. A. I.; Batsanov, A. S.; Albesa-Jove, D.; Cheung, M. S.; Maxwell, A. C.; Shukla, L.; Roberts, B.; Blakemore, D. C.; Lin, Z.; Marder, T. B.; Steel, P. G. *Org. Biomol. Chem.* **2014**, *12*, 7318-7327.
- (286) Wang, G.; Xu, L.; Li, P. *J. Am. Chem. Soc.* **2015**, *137*, 8058-8061.
- (287) Green, A. G.; Liu, P.; Merlic, C. A.; Houk, K. N. *J. Am. Chem. Soc.* **2014**, *136*, 4575-4583.
- (288) Rentzsch, C. F.; Tosh, E.; Herrmann, W. A.; Kuhn, F. E. *Green Chemistry* **2009**, *11*, 1610-1617.
- (289) Frey, G. D.; Rentzsch, C. F.; von Preysing, D.; Scherg, T.; Mühlhofer, M.; Herdtweck, E.; Herrmann, W. A. *J. Organomet. Chem.* **2006**, *691*, 5725-5738.
- (290) Ishiyama, T.; Takagi, J.; Ishida, K.; Miyaura, N.; Anastasi, N. R.; Hartwig, J. F. *J. Am. Chem. Soc.* **2001**, *124*, 390-391.
- (291) Cho, J.-Y.; Tse, M. K.; Holmes, D.; Maleczka, R. E.; Smith, M. R. *Science* **2002**, *295*, 305-308.

- (292) Boller, T. M.; Murphy, J. M.; Hapke, M.; Ishiyama, T.; Miyaura, N.; Hartwig, J. F. *J. Am. Chem. Soc.* **2005**, *127*, 14263-14278.
- (293) Kanzelberger, M.; Singh, B.; Czerw, M.; Krogh-Jespersen, K.; Goldman, A. S. *J. Am. Chem. Soc.* **2000**, *122*, 11017-11018.
- (294) Chen, H.; Schlecht, S.; Semple, T. C.; Hartwig, J. F. *Science* **2000**, *287*, 1995-1997.
- (295) Bromberg, S. E.; Yang, H.; Asplund, M. C.; Lian, T.; McNamara, B. K.; Kotz, K. T.; Yeston, J. S.; Wilkens, M.; Frei, H.; Bergman, R. G.; Harris, C. B. *Science* **1997**, *278*, 260-263.
- (296) Lian, T.; Bromberg, S. E.; Yang, H.; Proulx, G.; Bergman, R. G.; Harris, C. B. *J. Am. Chem. Soc.* **1996**, *118*, 3769-3770.
- (297) Scott, N. M.; Dorta, R.; Stevens, E. D.; Correa, A.; Cavallo, L.; Nolan, S. P. *J. Am. Chem. Soc.* **2005**, *127*, 3516-3526.
- (298) Dorta, R.; Stevens, E. D.; Nolan, S. P. *J. Am. Chem. Soc.* **2004**, *126*, 5054-5055.
- (299) Hartwig, J.; Casey, C. R.: Catalytic Carbonylation. In *Organotransition Metal Chemistry: From Bonding to Catalysis*; University Science Books, 2010; Vol. 2; pp 745-774.
- (300) Shimada, S.; Batsanov, A. S.; Howard, J. A. K.; Marder, T. B. *Angew. Chem., Int. Ed.* **2001**, *40*, 2168-2171.
- (301) Lam, W. H.; Lam, K. C.; Lin, Z.; Shimada, S.; Perutz, R. N.; Marder, T. B. *Dalton Trans.* **2004**, 1556-1562.
- (302) Lam, W. H.; Shimada, S.; Batsanov, A. S.; Lin, Z.; Marder, T. B.; Cowan, J. A.; Howard, J. A. K.; Mason, S. A.; McIntyre, G. J. *Organometallics* **2003**, *22*, 4557-4568.
- (303) AXS, B.: APEX-2. Bruker-Nonius AXS: Madison, Wisconsin, USA, 2008.
- (304) Sheldrick, G. M. *Acta Crystallographica Section A* **2008**, *64*, 112-122.
- (305) Bruker: APEX2, SAINT and SADABS. Bruker AXS Inc.: Madison, Wisconsin, USA, 2013.
- (306) Sheldrick, G. M. *Acta Crystallographica Section A* **2015**, *71*, 3-8.
- (307) Sheldrick, G. *Acta Crystallographica Section C* **2015**, *71*, 3-8.
- (308) Dolomanov, O. V.; Bourhis, L. J.; Gildea, R. J.; Howard, J. A. K.; Puschmann, H. *Journal of Applied Crystallography* **2009**, *42*, 339-341.

APPENDIX A
SPECTROSCOPIC DATA

A.1 Chapter II Compounds

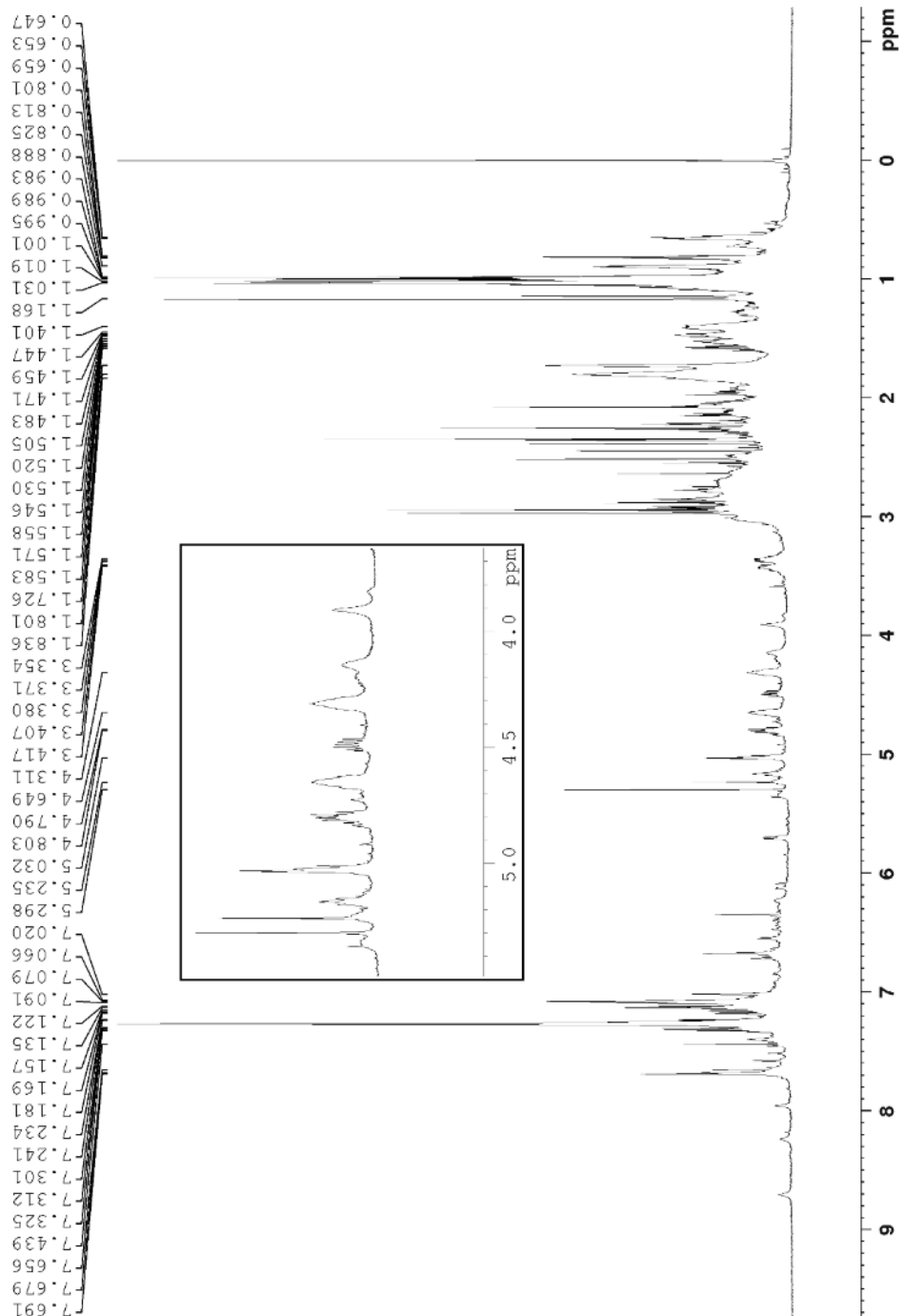


Figure A.1 ¹H NMR (600 MHz, CDCl₃) spectrum of reaction mixture (Scheme 2.1)

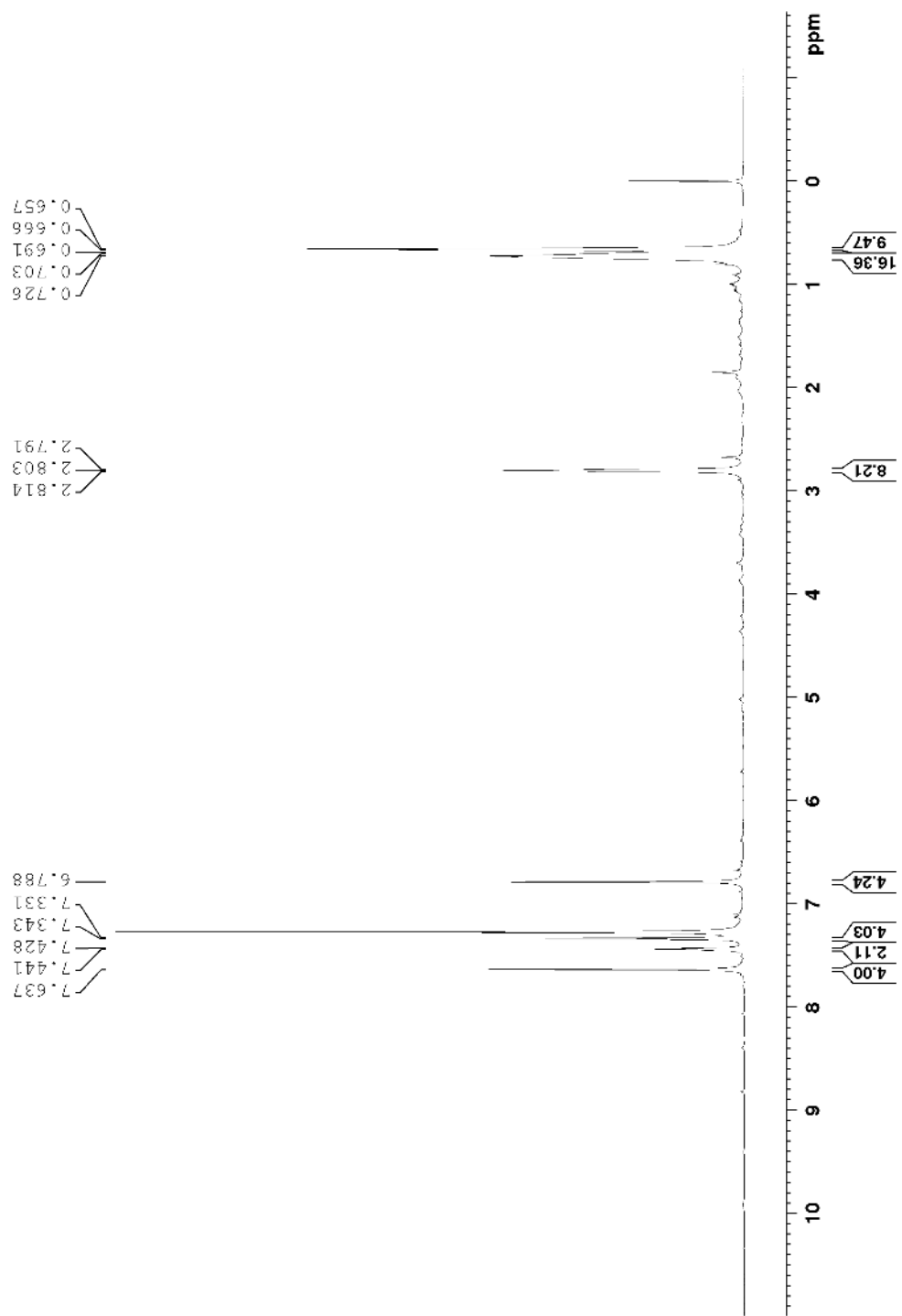


Figure A.2 ^1H NMR (600 MHz, CDCl_3) spectrum of **6**

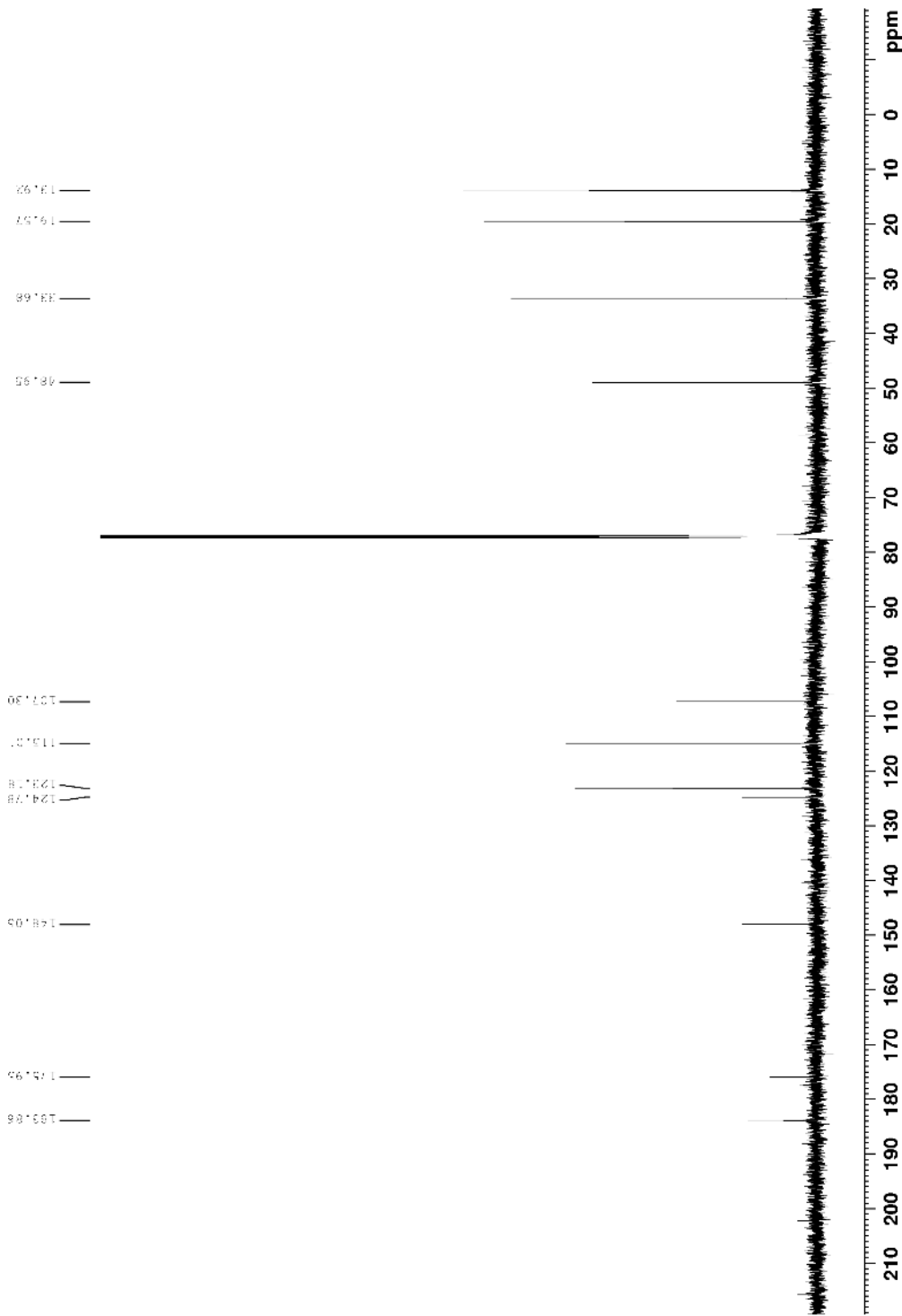


Figure A.3 ^{13}C NMR (150 MHz, CDCl_3) spectrum of **6**

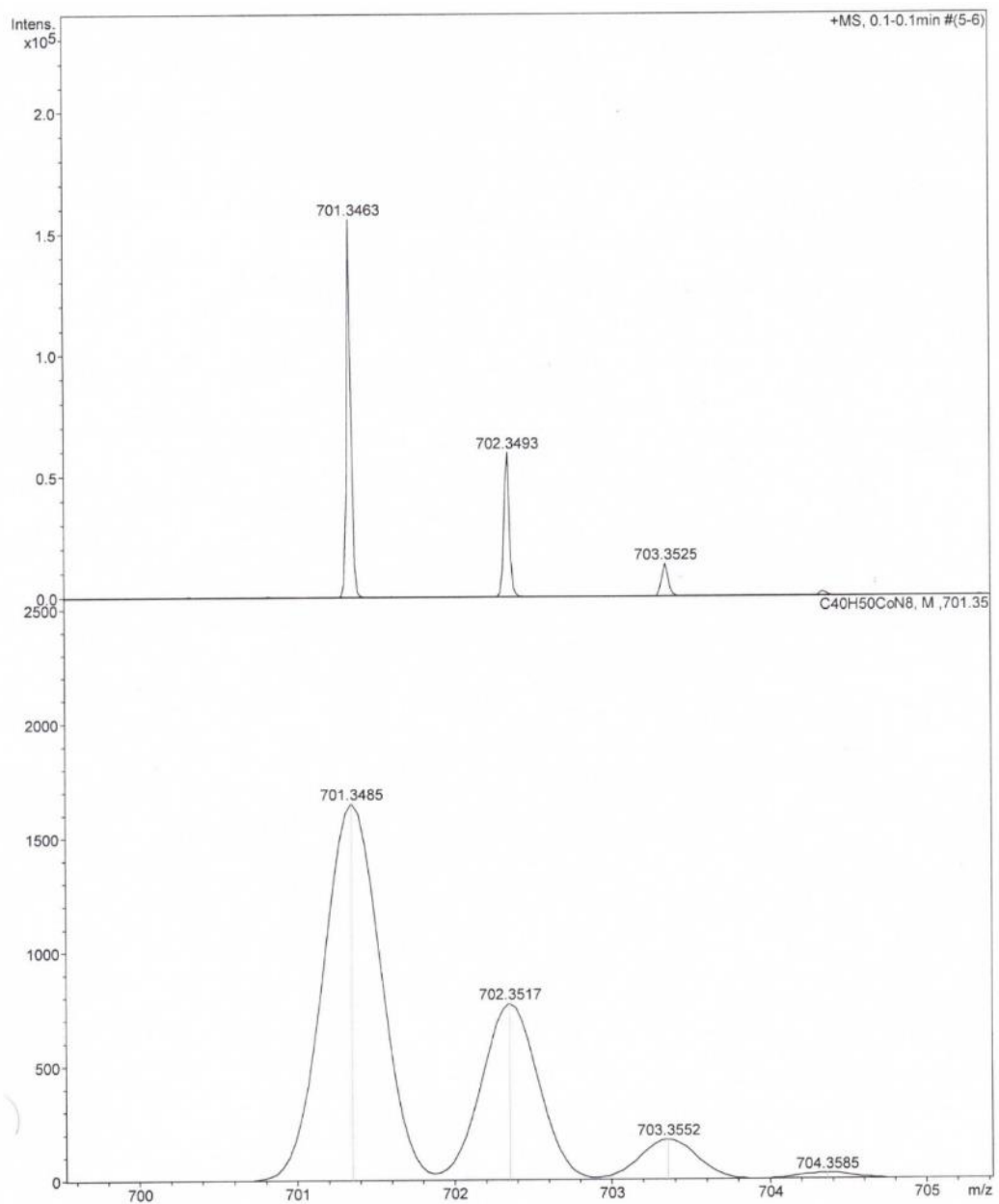


Figure A.4 HRMS spectrum of **6**

HRMS-ESI (m/z): [M-Cl]⁺ calcd (bottom) for C₄₀H₅₀CoN₈, 701.3485; found (top), 701.3463

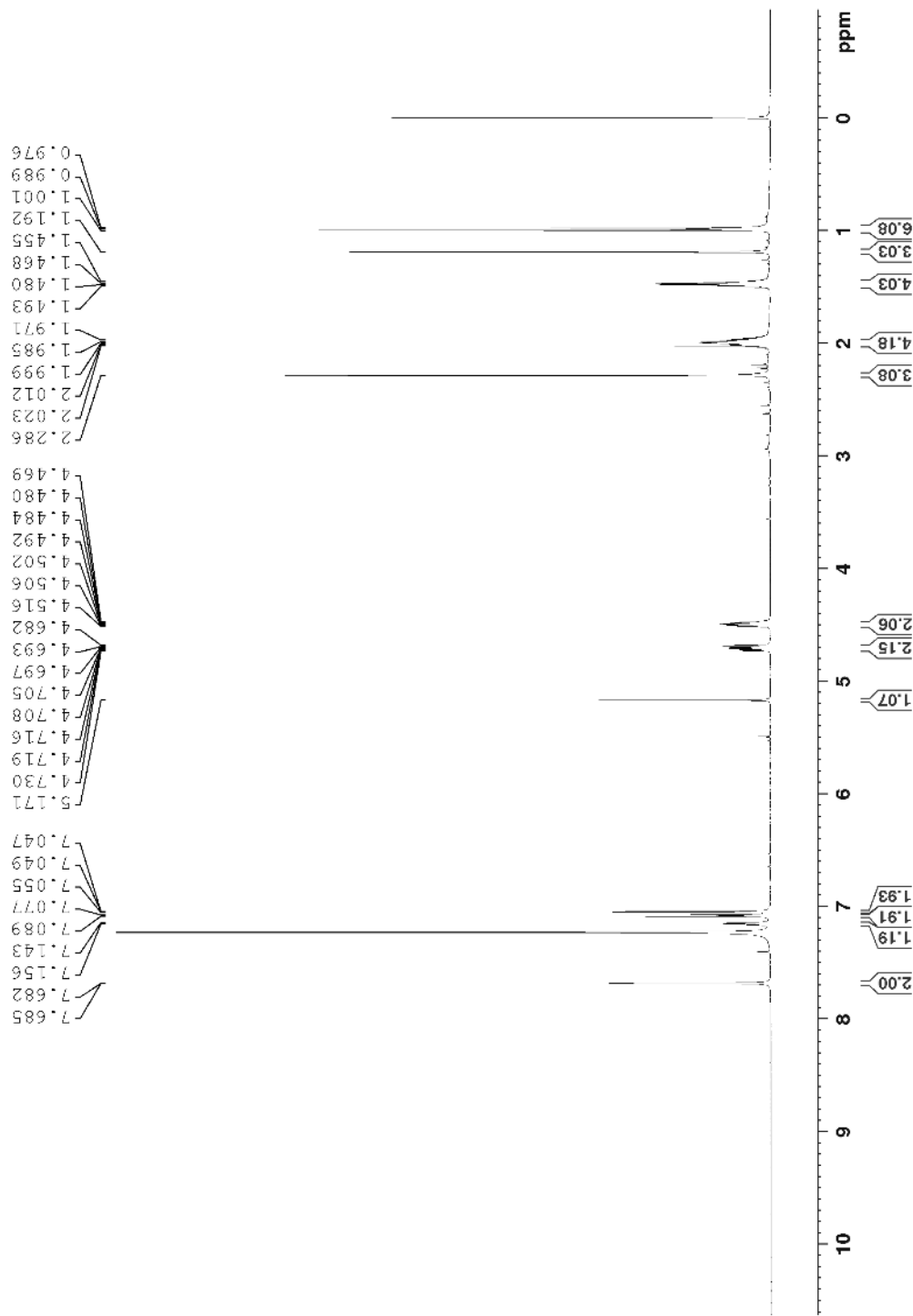


Figure A.5 ^1H NMR (600 MHz, CDCl_3) spectrum of 7

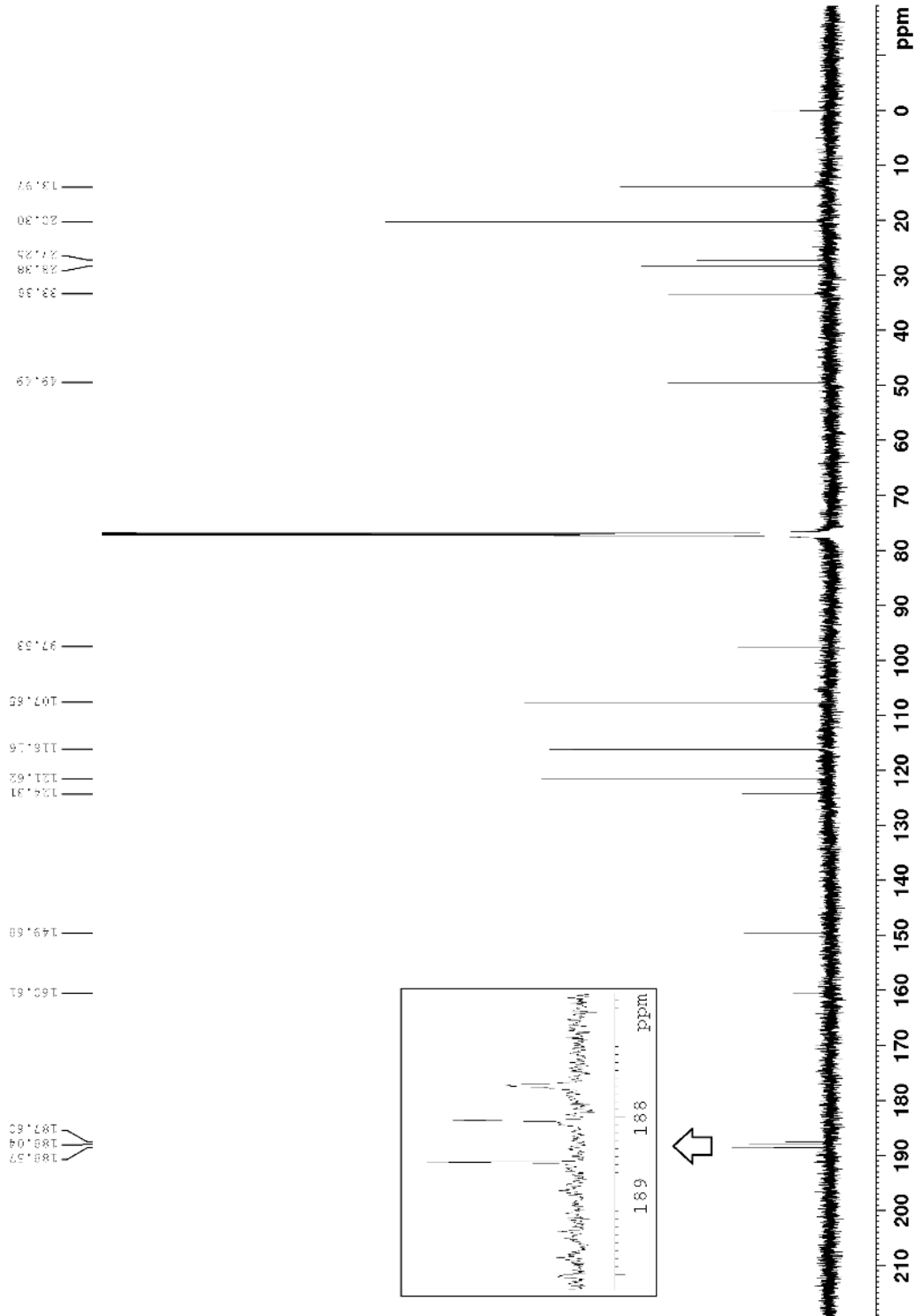


Figure A.6 ^{13}C NMR (150 MHz, CDCl_3) spectrum of 7

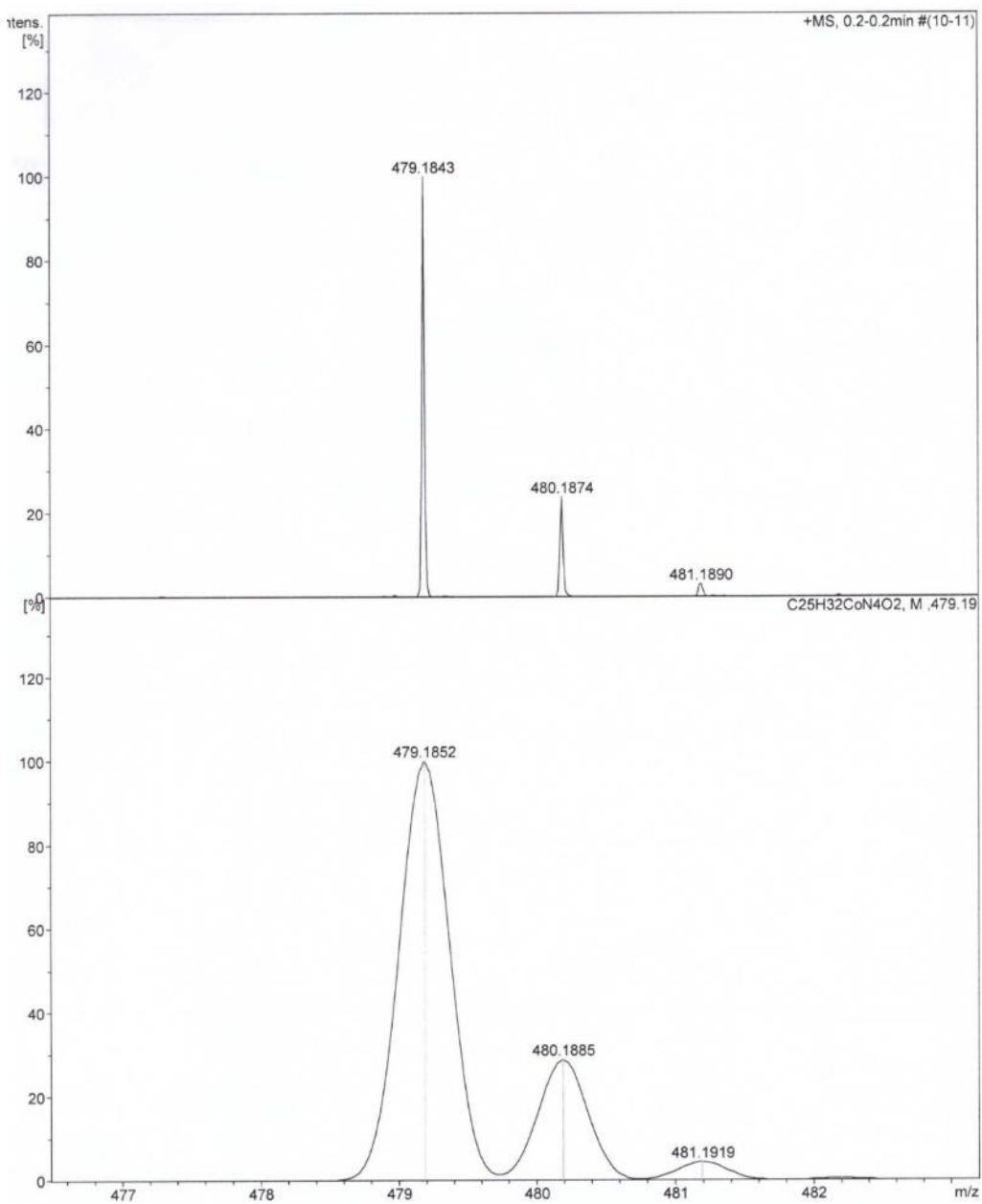


Figure A.7 HRMS spectrum of 7

HRMS-ESI (m/z): [M-I]⁺ calcd (bottom) for C₂₅H₃₂CoN₄O₂, 479.1852; found (top), 479.1836

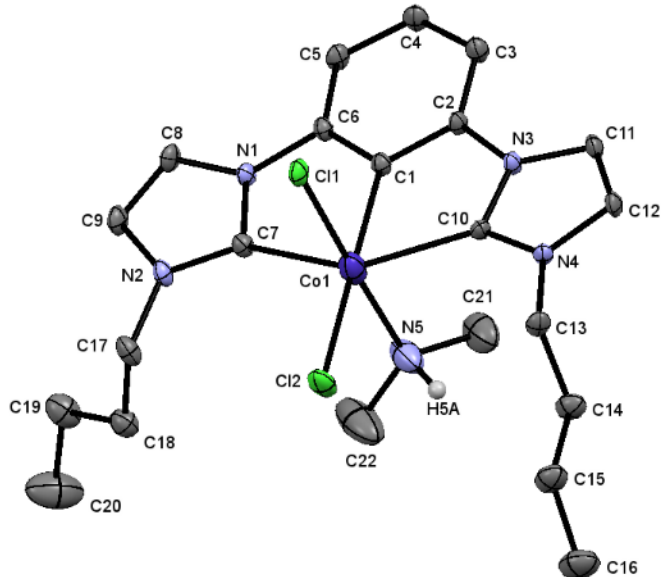


Figure A.8 X-ray molecular structure of 4

Table A.1 Crystal Data and Structure Refinement for 4

Empirical formula	C ₂₂ H ₃₂ Cl ₂ CoN ₅		
Formula weight	496.35		
Temperature	100(2) K		
Wavelength	0.71073 Å		
Crystal system	Monoclinic		
Space group	P2 ₁ /n		
Unit cell dimensions	<i>a</i> = 12.0081(2) Å	α = 90°	
	<i>b</i> = 13.2257(2) Å	β = 94.0720(10)°	
	<i>c</i> = 15.1254(2) Å	γ = 90°	
Volume	2396.08(6) Å ³		
Z	4		
Density (calculated)	1.376 g.cm ⁻³		
Absorption coefficient (μ)	0.958 mm ⁻¹		
F(000)	1040		
Crystal color, habit	Colorless, Plates		
Crystal size	0.35 × 0.065 × 0.042 mm ³		
θ range for data collection	2.048 to 27.884°		
Index ranges	-14 ≤ <i>h</i> ≤ 15, -17 ≤ <i>k</i> ≤ 17, -19 ≤ <i>l</i> ≤ 17		
Reflections collected	17925		
Independent reflections	5607 [R _{int} = 0.0316]		
Completeness to θ = 26.000°	99.7 %		
Refinement method	Full-matrix least-squares on F ²		
Data / restraints / parameters	5607 / 0 / 275		
Goodness-of-fit on F ²	1.076		
Final R indices [I>2σ(I)]	R ₁ = 0.0670, wR ₂ = 0.2089		
R indices (all data)	R ₁ = 0.0811, wR ₂ = 0.2205		
Extinction coefficient	n/a		
Largest diff. peak and hole	1.006 and -1.863 e ⁻ .Å ⁻³		

Table A.2 Atomic Coordinates and Equivalent Isotropic Displacement Parameters (\AA^2) for **4**

	x	y	z	U(eq)
Co(1)	0.26871(5)	0.35802(5)	0.60172(4)	0.026(1)
Cl(1)	0.12381(7)	0.36043(6)	0.70418(6)	0.016(1)
Cl(2)	0.14811(9)	0.27212(8)	0.49708(7)	0.024(1)
N(1)	0.3052(3)	0.5838(2)	0.6397(2)	0.013(1)
N(2)	0.1863(3)	0.5865(2)	0.5272(2)	0.015(1)
N(3)	0.4311(2)	0.2723(2)	0.7469(2)	0.013(1)
N(4)	0.3622(2)	0.1396(2)	0.6835(2)	0.012(1)
N(5)	0.3958(4)	0.3440(4)	0.5107(3)	0.037(1)
C(1)	0.3755(3)	0.4323(3)	0.6974(2)	0.013(1)
C(2)	0.4410(3)	0.3784(3)	0.7603(2)	0.013(1)
C(3)	0.5055(3)	0.4240(3)	0.8292(3)	0.017(1)
C(4)	0.5048(3)	0.5298(3)	0.8333(3)	0.018(1)
C(5)	0.4414(3)	0.5880(3)	0.7715(3)	0.015(1)
C(6)	0.3778(3)	0.5363(3)	0.7056(2)	0.013(1)
C(7)	0.2498(3)	0.5217(3)	0.5784(2)	0.014(1)
C(8)	0.2753(3)	0.6845(3)	0.6278(3)	0.016(1)
C(9)	0.2002(3)	0.6858(3)	0.5568(3)	0.017(1)
C(10)	0.3564(3)	0.2414(3)	0.6805(2)	0.013(1)
C(11)	0.4828(3)	0.1912(3)	0.7900(2)	0.015(1)
C(12)	0.4395(3)	0.1077(3)	0.7501(2)	0.014(1)
C(13)	0.2946(3)	0.0711(3)	0.6251(3)	0.015(1)
C(14)	0.3534(3)	0.0385(3)	0.5443(3)	0.021(1)
C(15)	0.2737(4)	-0.0180(4)	0.4793(3)	0.025(1)
C(16)	0.3252(4)	-0.0500(4)	0.3948(3)	0.035(1)
C(17)	0.1152(3)	0.5583(3)	0.4480(3)	0.018(1)
C(18)	0.1677(3)	0.5817(3)	0.3619(3)	0.023(1)
C(19)	0.1845(4)	0.6940(4)	0.3428(3)	0.029(1)
C(20)	0.2222(6)	0.7106(5)	0.2503(4)	0.055(2)
C(21)	0.5141(4)	0.3295(5)	0.5432(4)	0.043(1)
C(22)	0.3829(6)	0.3847(7)	0.4259(4)	0.067(2)
H(5A)	0.3805	0.2736	0.4939	0.044
H(3)	0.5475	0.3857	0.8710	0.020

Table A.2 (Continued)

H(4)	0.5477	0.5621	0.8784	0.021
H(5)	0.4417	0.6583	0.7742	0.018
H(8)	0.3014	0.7394	0.6615	0.019
H(9)	0.1644	0.7427	0.5322	0.021
H(11)	0.5368	0.1937	0.8371	0.018
H(12)	0.4579	0.0412	0.7645	0.017
H(13A)	0.2253	0.1046	0.6057	0.018
H(13B)	0.2761	0.0115	0.6585	0.018
H(14A)	0.4160	-0.0049	0.5626	0.025
H(14B)	0.3822	0.0975	0.5155	0.025
H(15A)	0.2097	0.0248	0.4638	0.031
H(15B)	0.2469	-0.0778	0.5083	0.031
H(16A)	0.2681	-0.0767	0.3536	0.052
H(16B)	0.3806	-0.1011	0.4084	0.052
H(16C)	0.3594	0.0074	0.3689	0.052
H(17A)	0.0448	0.5942	0.4486	0.022
H(17B)	0.0993	0.4865	0.4503	0.022
H(18A)	0.1210	0.5528	0.3134	0.027
H(18B)	0.2396	0.5482	0.3631	0.027
H(19A)	0.1149	0.7298	0.3487	0.035
H(19B)	0.2399	0.7215	0.3859	0.035
H(20A)	0.1658	0.6864	0.2074	0.082
H(20B)	0.2905	0.6744	0.2440	0.082
H(20C)	0.2342	0.7814	0.2411	0.082
H(21A)	0.5439	0.3922	0.5665	0.064
H(21B)	0.5563	0.3078	0.4951	0.064
H(21C)	0.5186	0.2792	0.5890	0.064
H(22A)	0.3049	0.3888	0.4074	0.100
H(22B)	0.4199	0.3423	0.3856	0.100
H(22C)	0.4150	0.4512	0.4261	0.100

U(eq) is defined as one third of the trace of the orthogonalized U_{ij} tensor.

Table A.3 Anisotropic Displacement Parameters (\AA^2) for 4

	\mathbf{U}_{11}	\mathbf{U}_{22}	\mathbf{U}_{33}	\mathbf{U}_{23}	\mathbf{U}_{13}	\mathbf{U}_{12}
Co(1)	0.0307(4)	0.0184(3)	0.0281(4)	0.0003(2)	-0.0083(3)	0.0008(2)
Cl(1)	0.0187(4)	0.0091(4)	0.0204(5)	0.0018(3)	-0.0012(3)	0.0021(3)
Cl(2)	0.0310(5)	0.0180(5)	0.0217(5)	-0.0030(4)	-0.0128(4)	-0.0015(4)
N(1)	0.0165(14)	0.0076(14)	0.0137(14)	0.0013(11)	-0.0009(11)	0.0002(11)
N(2)	0.0159(14)	0.0111(15)	0.0165(15)	0.0043(12)	-0.0022(11)	-0.0001(12)
N(3)	0.0145(14)	0.0082(14)	0.0144(15)	0.0000(11)	-0.0036(11)	0.0007(11)
N(4)	0.0126(14)	0.0097(15)	0.0133(14)	-0.0021(11)	-0.0032(11)	0.0000(11)
N(5)	0.030(2)	0.056(3)	0.024(2)	0.0080(19)	0.0000(16)	0.0083(19)
C(1)	0.0129(15)	0.0107(17)	0.0140(17)	0.0009(13)	-0.0008(12)	-0.0002(13)
C(2)	0.0139(16)	0.0082(16)	0.0153(17)	0.0000(13)	-0.0025(13)	0.0000(12)
C(3)	0.0178(17)	0.0129(18)	0.0191(18)	-0.0002(14)	-0.0045(14)	-0.0001(14)
C(4)	0.0175(17)	0.0146(19)	0.0205(19)	-0.0031(15)	-0.0054(14)	-0.0011(14)
C(5)	0.0172(16)	0.0087(16)	0.0195(18)	-0.0008(14)	-0.0013(14)	-0.0025(13)
C(6)	0.0125(15)	0.0104(17)	0.0143(17)	0.0021(13)	-0.0007(12)	0.0000(12)
C(7)	0.0145(16)	0.0116(17)	0.0140(17)	0.0014(13)	-0.0015(13)	-0.0021(13)
C(8)	0.0197(17)	0.0068(17)	0.0211(19)	0.0016(14)	0.0015(14)	0.0008(13)
C(9)	0.0208(18)	0.0093(17)	0.0218(19)	0.0038(14)	-0.0002(14)	0.0019(14)
C(10)	0.0143(16)	0.0105(17)	0.0126(17)	-0.0025(13)	-0.0014(13)	0.0018(13)
C(11)	0.0156(16)	0.0134(18)	0.0157(18)	0.0027(14)	-0.0039(13)	0.0036(13)
C(12)	0.0160(16)	0.0096(17)	0.0171(18)	0.0030(14)	-0.0031(13)	0.0031(13)
C(13)	0.0141(16)	0.0105(17)	0.0205(18)	-0.0040(14)	-0.0027(13)	-0.0023(13)
C(14)	0.0173(18)	0.023(2)	0.022(2)	-0.0069(16)	-0.0015(15)	-0.0034(15)
C(15)	0.023(2)	0.025(2)	0.027(2)	-0.0105(18)	-0.0023(16)	-0.0025(17)
C(16)	0.036(2)	0.039(3)	0.030(2)	-0.014(2)	-0.0013(19)	-0.005(2)
C(17)	0.0171(17)	0.0165(19)	0.0193(18)	0.0056(15)	-0.0054(14)	-0.0033(14)
C(18)	0.0230(19)	0.024(2)	0.020(2)	0.0003(16)	-0.0022(15)	-0.0014(16)
C(19)	0.032(2)	0.027(2)	0.027(2)	0.0049(19)	-0.0025(18)	-0.0082(18)
C(20)	0.087(5)	0.044(4)	0.035(3)	0.001(3)	0.012(3)	-0.028(3)
C(21)	0.024(2)	0.068(4)	0.037(3)	0.006(3)	0.005(2)	0.008(2)
C(22)	0.042(3)	0.124(7)	0.035(3)	0.025(4)	0.009(3)	0.014(4)

$$2\pi^2[h^2a^*{}^2U_{11} + \dots + 2hka^*b^*U_{12}] \quad (\text{A.1})$$

Table A.4 Bond Lengths [\AA] for **4**

atom-atom	distance	atom-atom	distance
Co(1)-C(1)	2.107(4)	Co(1)-N(5)	2.134(4)
Co(1)-C(10)	2.174(4)	Co(1)-C(7)	2.203(4)
Co(1)-Cl(2)	2.3596(11)	Co(1)-Cl(1)	2.4111(11)
N(1)-C(7)	1.374(5)	N(1)-C(8)	1.388(5)
N(1)-C(6)	1.423(5)	N(2)-C(7)	1.354(5)
N(2)-C(9)	1.394(5)	N(2)-C(17)	1.469(5)
N(3)-C(10)	1.361(5)	N(3)-C(11)	1.380(5)
N(3)-C(2)	1.423(5)	N(4)-C(10)	1.349(5)
N(4)-C(12)	1.386(5)	N(4)-C(13)	1.469(5)
N(5)-C(22)	1.390(7)	N(5)-C(21)	1.482(6)
N(5)-H(5A)	0.9800	C(1)-C(6)	1.381(5)
C(1)-C(2)	1.388(5)	C(2)-C(3)	1.391(5)
C(3)-C(4)	1.401(5)	C(3)-H(3)	0.9300
C(4)-C(5)	1.394(5)	C(4)-H(4)	0.9300
C(5)-C(6)	1.392(5)	C(5)-H(5)	0.9300
C(8)-C(9)	1.352(5)	C(8)-H(8)	0.9300
C(9)-H(9)	0.9300	C(11)-C(12)	1.345(5)
C(11)-H(11)	0.9300	C(12)-H(12)	0.9300
C(13)-C(14)	1.518(5)	C(13)-H(13A)	0.9700
C(13)-H(13B)	0.9700	C(14)-C(15)	1.519(5)
C(14)-H(14A)	0.9700	C(14)-H(14B)	0.9700
C(15)-C(16)	1.519(6)	C(15)-H(15A)	0.9700
C(15)-H(15B)	0.9700	C(16)-H(16A)	0.9600
C(16)-H(16B)	0.9600	C(16)-H(16C)	0.9600
C(17)-C(18)	1.518(6)	C(17)-H(17A)	0.9700
C(17)-H(17B)	0.9700	C(18)-C(19)	1.530(6)
C(18)-H(18A)	0.9700	C(18)-H(18B)	0.9700
C(19)-C(20)	1.516(7)	C(19)-H(19A)	0.9700
C(19)-H(19B)	0.9700	C(20)-H(20A)	0.9600
C(20)-H(20B)	0.9600	C(20)-H(20C)	0.9600
C(21)-H(21A)	0.9600	C(21)-H(21B)	0.9600
C(21)-H(21C)	0.9600	C(22)-H(22A)	0.9600
C(22)-H(22B)	0.9600	C(22)-H(22C)	0.9600

Symmetry transformations used to generate equivalent atoms.

Table A.5 Bond Angles [°] for 4

atom-atom-atom	angle	atom-atom-atom	angle
C(1)-Co(1)-N(5)	93.18(16)	C(1)-Co(1)-C(10)	72.95(14)
N(5)-Co(1)-C(10)	87.22(15)	C(1)-Co(1)-C(7)	72.70(14)
N(5)-Co(1)-C(7)	92.99(17)	C(10)-Co(1)-C(7)	145.61(14)
C(1)-Co(1)-Cl(2)	178.66(11)	N(5)-Co(1)-Cl(2)	87.63(13)
C(10)-Co(1)-Cl(2)	106.04(10)	C(7)-Co(1)-Cl(2)	108.33(10)
C(1)-Co(1)-Cl(1)	89.07(10)	N(5)-Co(1)-Cl(1)	175.78(15)
C(10)-Co(1)-Cl(1)	90.02(10)	C(7)-Co(1)-Cl(1)	91.09(10)
Cl(2)-Co(1)-Cl(1)	90.06(4)	C(7)-N(1)-C(8)	112.1(3)
C(7)-N(1)-C(6)	116.9(3)	C(8)-N(1)-C(6)	130.9(3)
C(7)-N(2)-C(9)	111.3(3)	C(7)-N(2)-C(17)	125.3(3)
C(9)-N(2)-C(17)	123.4(3)	C(10)-N(3)-C(11)	111.5(3)
C(10)-N(3)-C(2)	116.4(3)	C(11)-N(3)-C(2)	132.0(3)
C(10)-N(4)-C(12)	111.0(3)	C(10)-N(4)-C(13)	124.8(3)
C(12)-N(4)-C(13)	124.2(3)	C(22)-N(5)-C(21)	113.4(5)
C(22)-N(5)-Co(1)	121.6(4)	C(21)-N(5)-Co(1)	120.7(3)
C(22)-N(5)-H(5A)	96.9	C(21)-N(5)-H(5A)	96.9
Co(1)-N(5)-H(5A)	96.9	C(6)-C(1)-C(2)	116.3(3)
C(6)-C(1)-Co(1)	122.2(3)	C(2)-C(1)-Co(1)	121.3(3)
C(1)-C(2)-C(3)	123.4(3)	C(1)-C(2)-N(3)	111.8(3)
C(3)-C(2)-N(3)	124.8(3)	C(2)-C(3)-C(4)	117.4(4)
C(2)-C(3)-H(3)	121.3	C(4)-C(3)-H(3)	121.3
C(5)-C(4)-C(3)	121.8(4)	C(5)-C(4)-H(4)	119.1
C(3)-C(4)-H(4)	119.1	C(6)-C(5)-C(4)	117.0(3)
C(6)-C(5)-H(5)	121.5	C(4)-C(5)-H(5)	121.5
C(1)-C(6)-C(5)	124.1(3)	C(1)-C(6)-N(1)	111.7(3)
C(5)-C(6)-N(1)	124.2(3)	N(2)-C(7)-N(1)	103.6(3)
N(2)-C(7)-Co(1)	139.6(3)	N(1)-C(7)-Co(1)	116.1(2)
C(9)-C(8)-N(1)	105.6(3)	C(9)-C(8)-H(8)	127.2
N(1)-C(8)-H(8)	127.2	C(8)-C(9)-N(2)	107.5(3)
C(8)-C(9)-H(9)	126.3	N(2)-C(9)-H(9)	126.3
N(4)-C(10)-N(3)	104.2(3)	N(4)-C(10)-Co(1)	138.4(3)
N(3)-C(10)-Co(1)	117.4(3)	C(12)-C(11)-N(3)	106.2(3)

Table A.5 (Continued)

C(12)-C(11)-H(11)	126.9	N(3)-C(11)-H(11)	126.9
C(11)-C(12)-N(4)	107.1(3)	C(11)-C(12)-H(12)	126.4
N(4)-C(12)-H(12)	126.4	N(4)-C(13)-C(14)	113.0(3)
N(4)-C(13)-H(13A)	109.0	C(14)-C(13)-H(13A)	109.0
N(4)-C(13)-H(13B)	109.0	C(14)-C(13)-H(13B)	109.0
H(13A)-C(13)-H(13B)	107.8	C(13)-C(14)-C(15)	110.7(3)
C(13)-C(14)-H(14A)	109.5	C(15)-C(14)-H(14A)	109.5
C(13)-C(14)-H(14B)	109.5	C(15)-C(14)-H(14B)	109.5
H(14A)-C(14)-H(14B)	108.1	C(14)-C(15)-C(16)	113.9(4)
C(14)-C(15)-H(15A)	108.8	C(16)-C(15)-H(15A)	108.8
C(14)-C(15)-H(15B)	108.8	C(16)-C(15)-H(15B)	108.8
H(15A)-C(15)-H(15B)	107.7	C(15)-C(16)-H(16A)	109.5
C(15)-C(16)-H(16B)	109.5	H(16A)-C(16)-H(16B)	109.5
C(15)-C(16)-H(16C)	109.5	H(16A)-C(16)-H(16C)	109.5
H(16B)-C(16)-H(16C)	109.5	N(2)-C(17)-C(18)	113.3(3)
N(2)-C(17)-H(17A)	108.9	C(18)-C(17)-H(17A)	108.9
N(2)-C(17)-H(17B)	108.9	C(18)-C(17)-H(17B)	108.9
H(17A)-C(17)-H(17B)	107.7	C(17)-C(18)-C(19)	115.4(4)
C(17)-C(18)-H(18A)	108.4	C(19)-C(18)-H(18A)	108.4
C(17)-C(18)-H(18B)	108.4	C(19)-C(18)-H(18B)	108.4
H(18A)-C(18)-H(18B)	107.5	C(20)-C(19)-C(18)	111.6(4)
C(20)-C(19)-H(19A)	109.3	C(18)-C(19)-H(19A)	109.3
C(20)-C(19)-H(19B)	109.3	C(18)-C(19)-H(19B)	109.3
H(19A)-C(19)-H(19B)	108.0	C(19)-C(20)-H(20A)	109.5
C(19)-C(20)-H(20B)	109.5	H(20A)-C(20)-H(20B)	109.5
C(19)-C(20)-H(20C)	109.5	H(20A)-C(20)-H(20C)	109.5
H(20B)-C(20)-H(20C)	109.5	N(5)-C(21)-H(21A)	109.5
N(5)-C(21)-H(21B)	109.5	H(21A)-C(21)-H(21B)	109.5
N(5)-C(21)-H(21C)	109.5	H(21A)-C(21)-H(21C)	109.5
H(21B)-C(21)-H(21C)	109.5	N(5)-C(22)-H(22A)	109.5
N(5)-C(22)-H(22B)	109.5	H(22A)-C(22)-H(22B)	109.5
N(5)-C(22)-H(22C)	109.5	H(22A)-C(22)-H(22C)	109.5
H(22B)-C(22)-H(22C)	109.5		

Symmetry transformations used to generate equivalent atoms.

Table A.6 Torsion Angles [°] for **4**

atom-atom-atom-atom	angle	atom-atom-atom-atom	angle
C(6)-C(1)-C(2)-C(3)	0.7(5)	Co(1)-C(1)-C(2)-C(3)	-174.4(3)
C(6)-C(1)-C(2)-N(3)	178.9(3)	Co(1)-C(1)-C(2)-N(3)	3.8(4)
C(10)-N(3)-C(2)-C(1)	-3.9(5)	C(11)-N(3)-C(2)-C(1)	177.1(4)
C(10)-N(3)-C(2)-C(3)	174.3(3)	C(11)-N(3)-C(2)-C(3)	-4.7(6)
C(1)-C(2)-C(3)-C(4)	-1.3(6)	N(3)-C(2)-C(3)-C(4)	-179.2(4)
C(2)-C(3)-C(4)-C(5)	0.6(6)	C(3)-C(4)-C(5)-C(6)	0.5(6)
C(2)-C(1)-C(6)-C(5)	0.5(5)	Co(1)-C(1)-C(6)-C(5)	175.6(3)
C(2)-C(1)-C(6)-N(1)	-178.2(3)	Co(1)-C(1)-C(6)-N(1)	-3.1(4)
C(4)-C(5)-C(6)-C(1)	-1.1(6)	C(4)-C(5)-C(6)-N(1)	177.4(3)
C(7)-N(1)-C(6)-C(1)	-2.5(4)	C(8)-N(1)-C(6)-C(1)	174.2(3)
C(7)-N(1)-C(6)-C(5)	178.8(3)	C(8)-N(1)-C(6)-C(5)	-4.5(6)
C(9)-N(2)-C(7)-N(1)	-1.0(4)	C(17)-N(2)-C(7)-N(1)	176.3(3)
C(9)-N(2)-C(7)-Co(1)	167.5(3)	C(17)-N(2)-C(7)-Co(1)	-15.1(6)
C(8)-N(1)-C(7)-N(2)	1.0(4)	C(6)-N(1)-C(7)-N(2)	178.3(3)
C(8)-N(1)-C(7)-Co(1)	-170.7(2)	C(6)-N(1)-C(7)-Co(1)	6.6(4)
C(7)-N(1)-C(8)-C(9)	-0.6(4)	C(6)-N(1)-C(8)-C(9)	-177.4(4)
N(1)-C(8)-C(9)-N(2)	0.0(4)	C(7)-N(2)-C(9)-C(8)	0.7(4)
C(17)-N(2)-C(9)-C(8)	-176.7(3)	C(12)-N(4)-C(10)-N(3)	-0.3(4)
C(13)-N(4)-C(10)-N(3)	178.7(3)	C(12)-N(4)-C(10)-Co(1)	177.9(3)
C(13)-N(4)-C(10)-Co(1)	-3.0(6)	C(11)-N(3)-C(10)-N(4)	0.3(4)
C(2)-N(3)-C(10)-N(4)	-178.8(3)	C(11)-N(3)-C(10)-Co(1)	-178.4(2)
C(2)-N(3)-C(10)-Co(1)	2.5(4)	C(10)-N(3)-C(11)-C(12)	-0.2(4)
C(2)-N(3)-C(11)-C(12)	178.8(4)	N(3)-C(11)-C(12)-N(4)	0.0(4)
C(10)-N(4)-C(12)-C(11)	0.2(4)	C(13)-N(4)-C(12)-C(11)	-178.9(3)
C(10)-N(4)-C(13)-C(14)	94.6(4)	C(12)-N(4)-C(13)-C(14)	-86.5(4)
N(4)-C(13)-C(14)-C(15)	-170.9(3)	C(13)-C(14)-C(15)-C(16)	177.9(4)
C(7)-N(2)-C(17)-C(18)	-100.7(4)	C(9)-N(2)-C(17)-C(18)	76.3(5)
N(2)-C(17)-C(18)-C(19)	-66.0(5)	C(17)-C(18)-C(19)-C(20)	-172.2(4)

Symmetry transformations used to generate equivalent atoms.

A.1.1 Crystal Summary for 4

Crystal data for C₂₂H₃₂Cl₂CoN₅; M_r = 496.35; Monoclinic; space group P2₁/n; *a* = 12.0081(2) Å; *b* = 13.2257(2) Å; *c* = 15.1254(2) Å; α = 90°; β = 94.0720(10)°; γ = 90°; V = 2396.08(6) Å³; Z = 4; T = 100(2) K; λ (Mo-Kα) = 0.71073 Å; μ (Mo-Kα) = 0.958 mm⁻¹; d_{calc} = 1.376 g.cm⁻³; 17925 reflections collected; 5607 unique ($R_{\text{int}} = 0.0316$); giving $R_1 = 0.0670$, $wR_2 = 0.2089$ for 4540 data with [$I > 2\sigma(I)$] and $R_1 = 0.0811$, $wR_2 = 0.2205$ for all 5607 data. Residual electron density (e⁻.Å⁻³) max/min: 1.006/-1.863.

An arbitrary sphere of data were collected on a Colorless Plates-like crystal, having approximate dimensions of 0.35 × 0.065 × 0.042 mm, on a Bruker APEX-II diffractometer using a combination of ω - and φ -scans of 0.5°.³⁰³ Data were corrected for absorption and polarization effects and analyzed for space group determination. The structure was solved by vecmap methods and expanded routinely.³⁰⁴ The model was refined by full-matrix least-squares analysis of F² against all reflections. All non-hydrogen atoms were refined with anisotropic thermal displacement parameters. Unless otherwise noted, hydrogen atoms were included in calculated positions. Thermal parameters for the hydrogens were tied to the isotropic thermal parameter of the atom to which they are bonded (1.5 × for methyl, 1.2 × for all others).

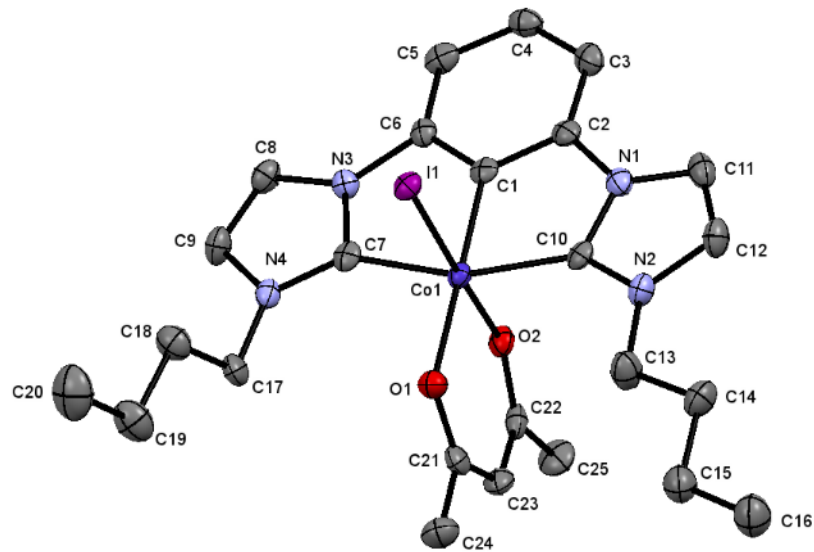


Figure A.9 X-ray molecular structure of 7

Table A.7 Crystal Data and Structure Refinement for 7

Empirical formula	C ₂₆ H ₃₃ Cl ₃ CoIN ₄ O ₂		
Formula weight	725.74		
Temperature	100(2) K		
Wavelength	0.71073 Å		
Crystal system	Triclinic		
Space group	P-1		
Unit cell dimensions	<i>a</i> = 8.4464(3) Å	<i>α</i> = 94.144(2)°	
	<i>b</i> = 10.4389(4) Å	<i>β</i> = 99.879(2)°	
	<i>c</i> = 18.6009(7) Å	<i>γ</i> = 110.932(2)°	
Volume	1493.13(10) Å ³		
Z	2		
Density (calculated)	1.614 g.cm ⁻³		
Absorption coefficient (μ)	1.907 mm ⁻¹		
F(000)	728		
Crystal color, habit	?, Tablet		
Crystal size	0.347 × 0.194 × 0.060 mm ³		
θ range for data collection	2.111 to 26.036°		
Index ranges	-10 ≤ <i>h</i> ≤ 10, -12 ≤ <i>k</i> ≤ 8, -18 ≤ <i>l</i> ≤ 22		
Reflections collected	8785		
Independent reflections	5318 [R _{int} = 0.0273]		
Completeness to θ = 25.242°	92.3 %		
Absorption correction	Semi-empirical from equivalents		
Max. and min. transmission	0.9635 and 0.7253		
Refinement method	Full-matrix least-squares on F ²		
Data / restraints / parameters	5318 / 0 / 334		
Goodness-of-fit on F ²	1.042		
Final R indices [I>2σ(I)]	R ₁ = 0.0393, wR ₂ = 0.0907		
R indices (all data)	R ₁ = 0.0474, wR ₂ = 0.0962		
Extinction coefficient	n/a		
Largest diff. peak and hole	0.645 and -1.174 e ⁻ .Å ⁻³		

Table A.8 Atomic Coordinates and Equivalent Isotropic Displacement Parameters (\AA^2) for **7**

	x	y	z	U(eq)
Co(1)	1.21787(7)	0.67590(6)	0.83772(3)	0.015(1)
Cl(1)	-0.3209(2)	0.11226(17)	0.44437(9)	0.048(1)
Cl(2)	0.03891(19)	0.20982(17)	0.43630(9)	0.052(1)
Cl(3)	-0.1920(2)	-0.06629(15)	0.36796(9)	0.051(1)
I(1)	1.17610(4)	0.90212(3)	0.81356(2)	0.019(1)
O(1)	1.2237(4)	0.6427(3)	0.73104(17)	0.021(1)
O(2)	1.2439(4)	0.5034(3)	0.85687(18)	0.021(1)
N(1)	0.9141(5)	0.5965(4)	0.8956(2)	0.020(1)
N(2)	0.8163(5)	0.5248(4)	0.7796(2)	0.022(1)
N(3)	1.5036(4)	0.8159(4)	0.9557(2)	0.018(1)
N(4)	1.6227(4)	0.8200(4)	0.8627(2)	0.019(1)
C(1)	1.2085(6)	0.7126(4)	0.9367(2)	0.017(1)
C(2)	1.0512(6)	0.6640(4)	0.9582(3)	0.020(1)
C(3)	1.0400(6)	0.6804(5)	1.0312(3)	0.025(1)
C(4)	1.1934(6)	0.7504(5)	1.0830(3)	0.024(1)
C(5)	1.3549(6)	0.8014(5)	1.0637(3)	0.023(1)
C(6)	1.3576(5)	0.7797(4)	0.9902(3)	0.018(1)
C(7)	1.4662(6)	0.7781(4)	0.8810(3)	0.019(1)
C(8)	1.6815(6)	0.8811(5)	0.9837(3)	0.023(1)
C(9)	1.7549(6)	0.8829(5)	0.9249(3)	0.025(1)
C(10)	0.9664(6)	0.5895(4)	0.8305(3)	0.018(1)
C(11)	0.7372(6)	0.5395(5)	0.8857(3)	0.026(1)
C(12)	0.6752(6)	0.4938(5)	0.8136(3)	0.026(1)
C(13)	0.8123(6)	0.4956(6)	0.7009(3)	0.031(1)
C(14)	0.6365(6)	0.4245(5)	0.6527(3)	0.031(1)
C(15)	0.6463(7)	0.3932(6)	0.5733(3)	0.034(1)
C(16)	0.4723(7)	0.3217(6)	0.5221(3)	0.040(1)
C(17)	1.6517(6)	0.8119(5)	0.7880(3)	0.023(1)
C(18)	1.6904(7)	0.9512(5)	0.7600(3)	0.030(1)
C(19)	1.7342(7)	0.9488(6)	0.6847(3)	0.038(1)
C(20)	1.7703(8)	1.0890(7)	0.6567(4)	0.051(2)
C(21)	1.2130(6)	0.5291(5)	0.6984(3)	0.022(1)

Table A.8 (Continued)

C(22)	1.2321(5)	0.4100(5)	0.8085(3)	0.021(1)
C(23)	1.2135(6)	0.4137(5)	0.7324(3)	0.023(1)
C(24)	1.1981(7)	0.5197(5)	0.6156(3)	0.030(1)
C(25)	1.2414(7)	0.2789(5)	0.8361(3)	0.032(1)
C(26)	-0.1721(7)	0.1068(5)	0.3897(3)	0.033(1)
H(3A)	0.9316	0.6451	1.0455	0.030
H(4A)	1.1880	0.7641	1.1335	0.029
H(5A)	1.4584	0.8491	1.0999	0.027
H(8A)	1.7387	0.9167	1.0337	0.027
H(9A)	1.8756	0.9205	0.9256	0.030
H(11A)	0.6713	0.5336	0.9228	0.031
H(12A)	0.5565	0.4484	0.7899	0.032
H(13A)	0.8809	0.4374	0.6951	0.038
H(13B)	0.8704	0.5843	0.6833	0.038
H(14A)	0.5686	0.4842	0.6556	0.037
H(14B)	0.5754	0.3369	0.6706	0.037
H(15A)	0.7087	0.4812	0.5560	0.041
H(15B)	0.7149	0.3340	0.5710	0.041
H(16A)	0.4884	0.3047	0.4719	0.060
H(16B)	0.4107	0.2333	0.5380	0.060
H(16C)	0.4045	0.3806	0.5231	0.060
H(17A)	1.5474	0.7416	0.7549	0.028
H(17B)	1.7503	0.7822	0.7870	0.028
H(18A)	1.5881	0.9773	0.7577	0.036
H(18B)	1.7889	1.0228	0.7953	0.036
H(19A)	1.6364	0.8764	0.6493	0.045
H(19B)	1.8376	0.9241	0.6870	0.045
H(20A)	1.7981	1.0832	0.6078	0.076
H(20B)	1.6674	1.1129	0.6534	0.076
H(20C)	1.8685	1.1606	0.6910	0.076
H(23A)	1.2003	0.3322	0.7017	0.027
H(24A)	1.1905	0.4277	0.5957	0.045
H(24B)	1.0937	0.5346	0.5929	0.045

Table A.8 (Continued)

H(24C)	1.3005	0.5907	0.6049	0.045
H(25A)	1.2310	0.2117	0.7942	0.047
H(25B)	1.3527	0.3014	0.8704	0.047
H(25C)	1.1465	0.2390	0.8616	0.047
H(26A)	-0.1994	0.1435	0.3429	0.040

U(eq) is defined as one third of the trace of the orthogonalized U_{ij} tensor.

Table A.9 Anisotropic Displacement Parameters (\AA^2) for 7

	U₁₁	U₂₂	U₃₃	U₂₃	U₁₃	U₁₂
Co(1)	0.0160(3)	0.0117(3)	0.0176(3)	0.0028(2)	0.0034(2)	0.0047(2)
Cl(1)	0.0473(8)	0.0577(10)	0.0471(9)	0.0090(8)	0.0184(7)	0.0251(8)
Cl(2)	0.0355(8)	0.0519(9)	0.0544(10)	0.0011(8)	-0.0022(7)	0.0075(7)
Cl(3)	0.0772(11)	0.0288(7)	0.0505(10)	0.0096(7)	0.0288(8)	0.0173(7)
I(1)	0.0217(2)	0.0143(2)	0.0203(2)	0.0042(1)	0.0027(1)	0.0073(1)
O(1)	0.0235(16)	0.0202(17)	0.0197(17)	0.0025(14)	0.0053(13)	0.0091(13)
O(2)	0.0204(16)	0.0145(16)	0.0274(19)	0.0062(15)	0.0070(13)	0.0052(13)
N(1)	0.0207(19)	0.0160(19)	0.025(2)	0.0047(17)	0.0072(16)	0.0073(16)
N(2)	0.0172(19)	0.020(2)	0.024(2)	0.0026(17)	0.0015(16)	0.0035(16)
N(3)	0.0169(18)	0.0182(19)	0.018(2)	0.0056(16)	0.0035(15)	0.0074(15)
N(4)	0.0157(18)	0.0154(19)	0.026(2)	0.0033(17)	0.0037(16)	0.0054(15)
C(1)	0.024(2)	0.010(2)	0.019(2)	0.0054(18)	0.0054(18)	0.0083(18)
C(2)	0.026(2)	0.013(2)	0.024(3)	0.0040(19)	0.0087(19)	0.0086(18)
C(3)	0.030(3)	0.019(2)	0.028(3)	0.010(2)	0.012(2)	0.009(2)
C(4)	0.033(3)	0.022(2)	0.021(3)	0.005(2)	0.009(2)	0.013(2)
C(5)	0.032(3)	0.018(2)	0.019(3)	0.006(2)	0.0022(19)	0.011(2)
C(6)	0.018(2)	0.014(2)	0.023(3)	0.0057(19)	0.0052(18)	0.0073(17)
C(7)	0.022(2)	0.012(2)	0.023(3)	0.0071(19)	0.0041(18)	0.0081(18)
C(8)	0.020(2)	0.021(2)	0.023(3)	0.003(2)	-0.0023(19)	0.0067(19)
C(9)	0.018(2)	0.024(3)	0.029(3)	0.006(2)	0.0003(19)	0.0025(19)
C(10)	0.021(2)	0.010(2)	0.022(3)	0.0043(19)	0.0028(18)	0.0050(17)
C(11)	0.022(2)	0.022(2)	0.038(3)	0.011(2)	0.013(2)	0.008(2)
C(12)	0.016(2)	0.027(3)	0.033(3)	0.008(2)	0.002(2)	0.005(2)

Table A.9 (Continued)

C(13)	0.024(3)	0.039(3)	0.025(3)	0.005(2)	0.003(2)	0.005(2)
C(14)	0.026(3)	0.027(3)	0.032(3)	0.000(2)	0.000(2)	0.005(2)
C(15)	0.028(3)	0.032(3)	0.038(3)	0.005(3)	0.009(2)	0.008(2)
C(16)	0.034(3)	0.044(3)	0.038(3)	0.007(3)	0.007(2)	0.009(3)
C(17)	0.016(2)	0.026(3)	0.028(3)	0.003(2)	0.0084(19)	0.0066(19)
C(18)	0.033(3)	0.033(3)	0.026(3)	0.009(2)	0.009(2)	0.014(2)
C(19)	0.039(3)	0.050(4)	0.030(3)	0.015(3)	0.011(2)	0.020(3)
C(20)	0.050(4)	0.054(4)	0.047(4)	0.028(3)	0.011(3)	0.013(3)
C(21)	0.014(2)	0.025(3)	0.027(3)	0.003(2)	0.0074(18)	0.0074(19)
C(22)	0.014(2)	0.014(2)	0.036(3)	0.009(2)	0.0063(19)	0.0041(17)
C(23)	0.024(2)	0.015(2)	0.030(3)	0.000(2)	0.007(2)	0.0081(19)
C(24)	0.035(3)	0.029(3)	0.024(3)	-0.001(2)	0.004(2)	0.012(2)
C(25)	0.041(3)	0.017(2)	0.042(3)	0.010(2)	0.012(2)	0.014(2)
C(26)	0.042(3)	0.030(3)	0.029(3)	0.004(2)	0.007(2)	0.015(2)

$$-2\pi^2[h^2a^{*2}U_{11} + \dots + 2hka^*b^*U_{12}] \quad (\text{A.2})$$

Table A.10 Bond Lengths [Å] for 7

atom-atom	distance	atom-atom	distance
Co(1)-C(1)	1.874(5)	Co(1)-O(2)	1.941(3)
Co(1)-C(10)	1.965(4)	Co(1)-C(7)	1.971(4)
Co(1)-O(1)	2.002(3)	Co(1)-I(1)	2.5685(6)
Cl(1)-C(26)	1.760(6)	Cl(2)-C(26)	1.746(6)
Cl(3)-C(26)	1.764(5)	O(1)-C(21)	1.258(6)
O(2)-C(22)	1.243(6)	N(1)-C(10)	1.364(6)
N(1)-C(11)	1.370(6)	N(1)-C(2)	1.424(6)
N(2)-C(10)	1.359(6)	N(2)-C(12)	1.392(6)
N(2)-C(13)	1.465(6)	N(3)-C(7)	1.368(6)
N(3)-C(8)	1.393(6)	N(3)-C(6)	1.430(6)
N(4)-C(7)	1.348(6)	N(4)-C(9)	1.393(6)
N(4)-C(17)	1.453(6)	C(1)-C(6)	1.380(6)
C(1)-C(2)	1.383(6)	C(2)-C(3)	1.380(7)

Table A.10 (Continued)

C(3)-C(4)	1.391(7)	C(3)-H(3A)	0.9500
C(4)-C(5)	1.396(7)	C(4)-H(4A)	0.9500
C(5)-C(6)	1.377(7)	C(5)-H(5A)	0.9500
C(8)-C(9)	1.345(7)	C(8)-H(8A)	0.9500
C(9)-H(9A)	0.9500	C(11)-C(12)	1.337(7)
C(11)-H(11A)	0.9500	C(12)-H(12A)	0.9500
C(13)-C(14)	1.490(7)	C(13)-H(13A)	0.9900
C(13)-H(13B)	0.9900	C(14)-C(15)	1.512(8)
C(14)-H(14A)	0.9900	C(14)-H(14B)	0.9900
C(15)-C(16)	1.502(7)	C(15)-H(15A)	0.9900
C(15)-H(15B)	0.9900	C(16)-H(16A)	0.9800
C(16)-H(16B)	0.9800	C(16)-H(16C)	0.9800
C(17)-C(18)	1.523(6)	C(17)-H(17A)	0.9900
C(17)-H(17B)	0.9900	C(18)-C(19)	1.509(7)
C(18)-H(18A)	0.9900	C(18)-H(18B)	0.9900
C(19)-C(20)	1.534(8)	C(19)-H(19A)	0.9900
C(19)-H(19B)	0.9900	C(20)-H(20A)	0.9800
C(20)-H(20B)	0.9800	C(20)-H(20C)	0.9800
C(21)-C(23)	1.402(6)	C(21)-C(24)	1.516(7)
C(22)-C(23)	1.401(7)	C(22)-C(25)	1.520(6)
C(23)-H(23A)	0.9500	C(24)-H(24A)	0.9800
C(24)-H(24B)	0.9800	C(24)-H(24C)	0.9800
C(25)-H(25A)	0.9800	C(25)-H(25B)	0.9800
C(25)-H(25C)	0.9800	C(26)-H(26A)	1.0000

Symmetry transformations used to generate equivalent atoms

Table A.11 Bond Angles [°] for 7

atom-atom-atom	angle	atom-atom-atom	angle
C(1)-Co(1)-O(2)	89.48(16)	C(1)-Co(1)-C(10)	80.09(19)
O(2)-Co(1)-C(10)	90.68(15)	C(1)-Co(1)-C(7)	79.84(19)
O(2)-Co(1)-C(7)	89.85(15)	C(10)-Co(1)-C(7)	159.9(2)
C(1)-Co(1)-O(1)	177.62(15)	O(2)-Co(1)-O(1)	92.81(13)
C(10)-Co(1)-O(1)	99.20(16)	C(7)-Co(1)-O(1)	100.83(16)

Table A.11 (Continued)

C(1)-Co(1)-I(1)	89.73(12)	O(2)-Co(1)-I(1)	178.52(9)
C(10)-Co(1)-I(1)	87.96(12)	C(7)-Co(1)-I(1)	91.23(12)
O(1)-Co(1)-I(1)	87.98(9)	C(21)-O(1)-Co(1)	124.1(3)
C(22)-O(2)-Co(1)	124.7(3)	C(10)-N(1)-C(11)	111.6(4)
C(10)-N(1)-C(2)	114.6(4)	C(11)-N(1)-C(2)	133.7(4)
C(10)-N(2)-C(12)	110.0(4)	C(10)-N(2)-C(13)	122.6(4)
C(12)-N(2)-C(13)	127.4(4)	C(7)-N(3)-C(8)	111.8(4)
C(7)-N(3)-C(6)	115.7(4)	C(8)-N(3)-C(6)	132.5(4)
C(7)-N(4)-C(9)	110.8(4)	C(7)-N(4)-C(17)	125.3(4)
C(9)-N(4)-C(17)	123.7(4)	C(6)-C(1)-C(2)	118.6(4)
C(6)-C(1)-Co(1)	121.2(3)	C(2)-C(1)-Co(1)	120.0(3)
C(3)-C(2)-C(1)	121.8(4)	C(3)-C(2)-N(1)	128.0(4)
C(1)-C(2)-N(1)	110.2(4)	C(2)-C(3)-C(4)	117.5(4)
C(2)-C(3)-H(3A)	121.2	C(4)-C(3)-H(3A)	121.2
C(3)-C(4)-C(5)	122.5(5)	C(3)-C(4)-H(4A)	118.8
C(5)-C(4)-H(4A)	118.8	C(6)-C(5)-C(4)	117.1(4)
C(6)-C(5)-H(5A)	121.4	C(4)-C(5)-H(5A)	121.4
C(5)-C(6)-C(1)	122.4(4)	C(5)-C(6)-N(3)	128.8(4)
C(1)-C(6)-N(3)	108.8(4)	N(4)-C(7)-N(3)	104.1(4)
N(4)-C(7)-Co(1)	141.4(4)	N(3)-C(7)-Co(1)	114.4(3)
C(9)-C(8)-N(3)	105.3(4)	C(9)-C(8)-H(8A)	127.4
N(3)-C(8)-H(8A)	127.4	C(8)-C(9)-N(4)	107.9(4)
C(8)-C(9)-H(9A)	126.0	N(4)-C(9)-H(9A)	126.0
N(2)-C(10)-N(1)	104.2(4)	N(2)-C(10)-Co(1)	140.7(4)
N(1)-C(10)-Co(1)	115.0(3)	C(12)-C(11)-N(1)	106.6(4)
C(12)-C(11)-H(11A)	126.7	N(1)-C(11)-H(11A)	126.7
C(11)-C(12)-N(2)	107.6(4)	C(11)-C(12)-H(12A)	126.2
N(2)-C(12)-H(12A)	126.2	N(2)-C(13)-C(14)	115.5(4)
N(2)-C(13)-H(13A)	108.4	C(14)-C(13)-H(13A)	108.4
N(2)-C(13)-H(13B)	108.4	C(14)-C(13)-H(13B)	108.4
H(13A)-C(13)-H(13B)	107.5	C(13)-C(14)-C(15)	111.6(4)
C(13)-C(14)-H(14A)	109.3	C(15)-C(14)-H(14A)	109.3
C(13)-C(14)-H(14B)	109.3	C(15)-C(14)-H(14B)	109.3

Table A.11 (Continued)

H(14A)-C(14)-H(14B)	108.0	C(16)-C(15)-C(14)	113.8(5)
C(16)-C(15)-H(15A)	108.8	C(14)-C(15)-H(15A)	108.8
C(16)-C(15)-H(15B)	108.8	C(14)-C(15)-H(15B)	108.8
H(15A)-C(15)-H(15B)	107.7	C(15)-C(16)-H(16A)	109.5
C(15)-C(16)-H(16B)	109.5	H(16A)-C(16)-H(16B)	109.5
C(15)-C(16)-H(16C)	109.5	H(16A)-C(16)-H(16C)	109.5
H(16B)-C(16)-H(16C)	109.5	N(4)-C(17)-C(18)	111.4(4)
N(4)-C(17)-H(17A)	109.3	C(18)-C(17)-H(17A)	109.3
N(4)-C(17)-H(17B)	109.3	C(18)-C(17)-H(17B)	109.3
H(17A)-C(17)-H(17B)	108.0	C(19)-C(18)-C(17)	112.6(4)
C(19)-C(18)-H(18A)	109.1	C(17)-C(18)-H(18A)	109.1
C(19)-C(18)-H(18B)	109.1	C(17)-C(18)-H(18B)	109.1
H(18A)-C(18)-H(18B)	107.8	C(18)-C(19)-C(20)	112.0(5)
C(18)-C(19)-H(19A)	109.2	C(20)-C(19)-H(19A)	109.2
C(18)-C(19)-H(19B)	109.2	C(20)-C(19)-H(19B)	109.2
H(19A)-C(19)-H(19B)	107.9	C(19)-C(20)-H(20A)	109.5
C(19)-C(20)-H(20B)	109.5	H(20A)-C(20)-H(20B)	109.5
C(19)-C(20)-H(20C)	109.5	H(20A)-C(20)-H(20C)	109.5
H(20B)-C(20)-H(20C)	109.5	O(1)-C(21)-C(23)	125.3(4)
O(1)-C(21)-C(24)	115.9(4)	C(23)-C(21)-C(24)	118.8(4)
O(2)-C(22)-C(23)	127.2(4)	O(2)-C(22)-C(25)	115.4(4)
C(23)-C(22)-C(25)	117.4(4)	C(22)-C(23)-C(21)	124.6(4)
C(22)-C(23)-H(23A)	117.7	C(21)-C(23)-H(23A)	117.7
C(21)-C(24)-H(24A)	109.5	C(21)-C(24)-H(24B)	109.5
H(24A)-C(24)-H(24B)	109.5	C(21)-C(24)-H(24C)	109.5
H(24A)-C(24)-H(24C)	109.5	H(24B)-C(24)-H(24C)	109.5
C(22)-C(25)-H(25A)	109.5	C(22)-C(25)-H(25B)	109.5
H(25A)-C(25)-H(25B)	109.5	C(22)-C(25)-H(25C)	109.5
H(25A)-C(25)-H(25C)	109.5	H(25B)-C(25)-H(25C)	109.5
Cl(2)-C(26)-Cl(1)	110.1(3)	Cl(2)-C(26)-Cl(3)	110.6(3)
Cl(1)-C(26)-Cl(3)	109.4(3)	Cl(2)-C(26)-H(26A)	108.9
Cl(1)-C(26)-H(26A)	108.9	Cl(3)-C(26)-H(26A)	108.9

Symmetry transformations used to generate equivalent atoms

Table A.12 Torsion Angles [°] for 7

atom-atom-atom-atom	angle	atom-atom-atom-atom	angle
O(2)-Co(1)-C(1)-C(6)	87.3(3)	C(10)-Co(1)-C(1)-C(6)	178.1(4)
C(7)-Co(1)-C(1)-C(6)	-2.7(3)	I(1)-Co(1)-C(1)-C(6)	-94.0(3)
O(2)-Co(1)-C(1)-C(2)	-88.3(3)	C(10)-Co(1)-C(1)-C(2)	2.5(3)
C(7)-Co(1)-C(1)-C(2)	-178.3(4)	I(1)-Co(1)-C(1)-C(2)	90.4(3)
C(6)-C(1)-C(2)-C(3)	-0.3(6)	Co(1)-C(1)-C(2)-C(3)	175.4(3)
C(6)-C(1)-C(2)-N(1)	-179.1(4)	Co(1)-C(1)-C(2)-N(1)	-3.4(5)
C(10)-N(1)-C(2)-C(3)	-176.3(4)	C(11)-N(1)-C(2)-C(3)	6.2(8)
C(10)-N(1)-C(2)-C(1)	2.5(5)	C(11)-N(1)-C(2)-C(1)	-175.0(4)
C(1)-C(2)-C(3)-C(4)	1.2(6)	N(1)-C(2)-C(3)-C(4)	179.8(4)
C(2)-C(3)-C(4)-C(5)	-1.1(7)	C(3)-C(4)-C(5)-C(6)	0.0(7)
C(4)-C(5)-C(6)-C(1)	1.0(6)	C(4)-C(5)-C(6)-N(3)	-177.5(4)
C(2)-C(1)-C(6)-C(5)	-0.9(6)	Co(1)-C(1)-C(6)-C(5)	-176.5(3)
C(2)-C(1)-C(6)-N(3)	177.9(4)	Co(1)-C(1)-C(6)-N(3)	2.3(5)
C(7)-N(3)-C(6)-C(5)	178.7(4)	C(8)-N(3)-C(6)-C(5)	0.2(8)
C(7)-N(3)-C(6)-C(1)	0.0(5)	C(8)-N(3)-C(6)-C(1)	-178.5(4)
C(9)-N(4)-C(7)-N(3)	-0.1(5)	C(17)-N(4)-C(7)-N(3)	-175.4(4)
C(9)-N(4)-C(7)-Co(1)	-175.1(4)	C(17)-N(4)-C(7)-Co(1)	9.7(7)
C(8)-N(3)-C(7)-N(4)	0.2(5)	C(6)-N(3)-C(7)-N(4)	-178.5(3)
C(8)-N(3)-C(7)-Co(1)	176.8(3)	C(6)-N(3)-C(7)-Co(1)	-2.0(5)
C(7)-N(3)-C(8)-C(9)	-0.2(5)	C(6)-N(3)-C(8)-C(9)	178.2(4)
N(3)-C(8)-C(9)-N(4)	0.1(5)	C(7)-N(4)-C(9)-C(8)	0.0(5)
C(17)-N(4)-C(9)-C(8)	175.3(4)	C(12)-N(2)-C(10)-N(1)	0.3(5)
C(13)-N(2)-C(10)-N(1)	180.0(4)	C(12)-N(2)-C(10)-Co(1)	-176.9(4)
C(13)-N(2)-C(10)-Co(1)	2.7(7)	C(11)-N(1)-C(10)-N(2)	-0.7(5)
C(2)-N(1)-C(10)-N(2)	-178.8(3)	C(11)-N(1)-C(10)-Co(1)	177.4(3)
C(2)-N(1)-C(10)-Co(1)	-0.7(5)	C(10)-N(1)-C(11)-C(12)	0.8(5)
C(2)-N(1)-C(11)-C(12)	178.4(4)	N(1)-C(11)-C(12)-N(2)	-0.6(5)
C(10)-N(2)-C(12)-C(11)	0.2(5)	C(13)-N(2)-C(12)-C(11)	-179.4(4)
C(10)-N(2)-C(13)-C(14)	-179.7(4)	C(12)-N(2)-C(13)-C(14)	-0.1(7)
N(2)-C(13)-C(14)-C(15)	-177.4(4)	C(13)-C(14)-C(15)-C(16)	-179.9(5)
C(7)-N(4)-C(17)-C(18)	99.7(5)	C(9)-N(4)-C(17)-C(18)	-74.9(5)
N(4)-C(17)-C(18)-C(19)	175.8(4)	C(17)-C(18)-C(19)-C(20)	179.2(5)

Table A.12 (Continued)

Co(1)-O(1)-C(21)-C(23)	-7.0(6)	Co(1)-O(1)-C(21)-C(24)	172.9(3)
Co(1)-O(2)-C(22)-C(23)	6.0(6)	Co(1)-O(2)-C(22)-C(25)	-174.8(3)
O(2)-C(22)-C(23)-C(21)	3.1(8)	C(25)-C(22)-C(23)-C(21)	-176.1(4)
O(1)-C(21)-C(23)-C(22)	-2.3(7)	C(24)-C(21)-C(23)-C(22)	177.8(4)

Symmetry transformations used to generate equivalent atoms.

A.1.2 Crystal Summary for 7

Crystal data for $C_{26}H_{33}Cl_3CoIN_4O_2$; $M_r = 725.74$; Triclinic; space group P-1; $a = 8.4464(3)$ Å; $b = 10.4389(4)$ Å; $c = 18.6009(7)$ Å; $\alpha = 94.144(2)^\circ$; $\beta = 99.879(2)^\circ$; $\gamma = 110.932(2)^\circ$; $V = 1493.13(10)$ Å³; $Z = 2$; $T = 100(2)$ K; $\lambda(\text{Mo-K}\alpha) = 0.71073$ Å; $\mu(\text{Mo-K}\alpha) = 1.907$ mm⁻¹; $d_{\text{calc}} = 1.614$ g.cm⁻³; 8785 reflections collected; 5318 unique ($R_{\text{int}} = 0.0273$); giving $R_1 = 0.0393$, $wR_2 = 0.0907$ for 4578 data with [$I > 2\sigma(I)$] and $R_1 = 0.0474$, $wR_2 = 0.0962$ for all 5318 data. Residual electron density (e⁻.Å⁻³) max/min: 0.645/-1.174.

An arbitrary sphere of data were collected on a Tablet-like crystal, having approximate dimensions of $0.347 \times 0.194 \times 0.060$ mm, on a Bruker APEX-II diffractometer using a combination of ω - and φ -scans of 0.5° ³⁰³ Data were corrected for absorption and polarization effects and analyzed for space group determination. The structure was solved by vecmap methods and expanded routinely.³⁰⁴ The model was refined by full-matrix least-squares analysis of F^2 against all reflections. All non-hydrogen atoms were refined with anisotropic thermal displacement parameters. Unless otherwise noted, hydrogen atoms were included in calculated positions. Thermal parameters for the hydrogens were tied to the isotropic thermal parameter of the atom to which they are bonded (1.5 × for methyl, 1.2 × for all others).

A.2 Chapter III Compounds

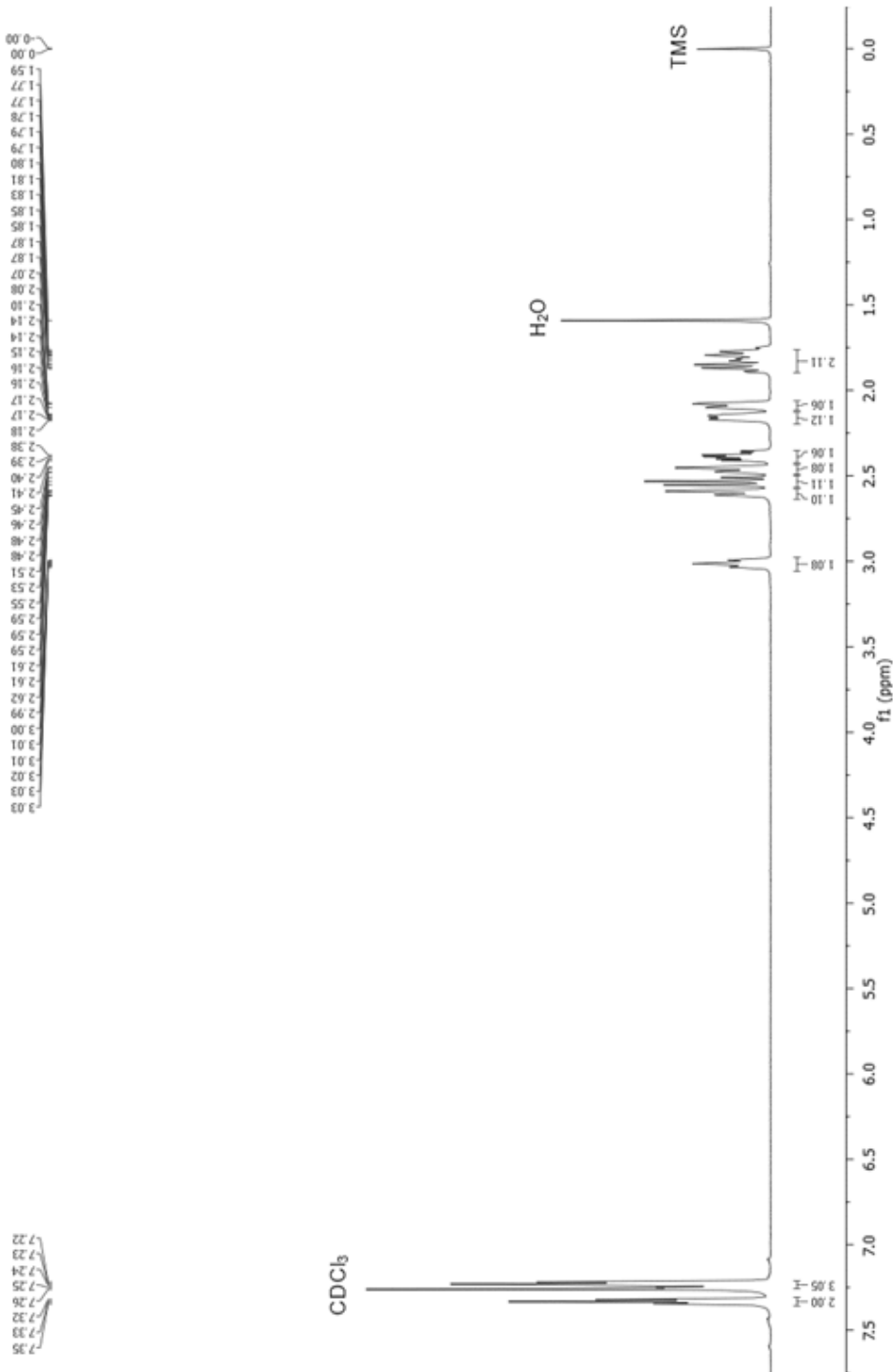


Figure A.10 ${}^1\text{H}$ NMR (600 MHz, CDCl_3) spectrum of isolated product (Table 3.2, Entry 1)

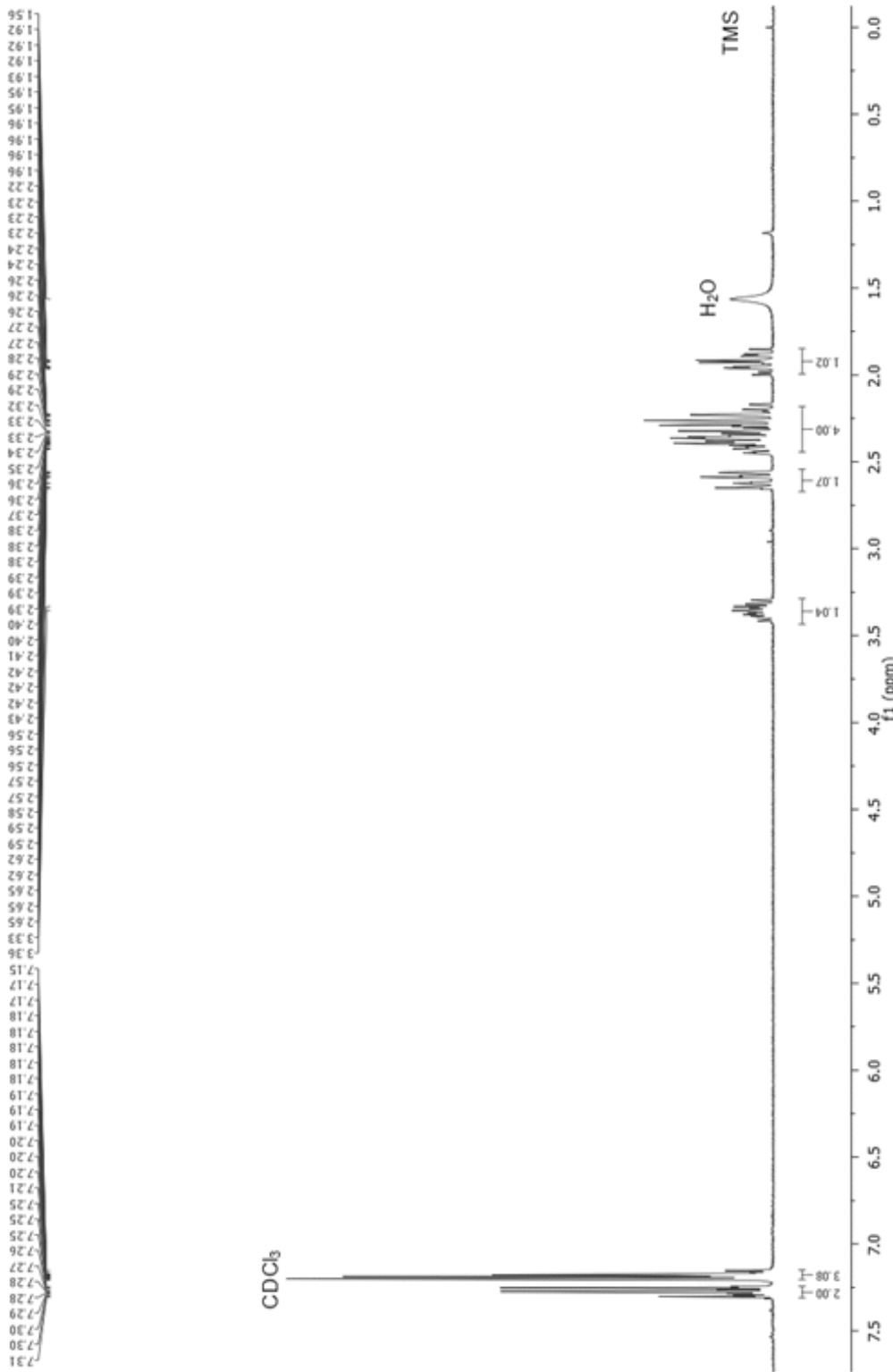


Figure A.11 ^1H NMR (300 MHz, CDCl_3) spectrum of isolated product (Table 3.2, Entry 2)

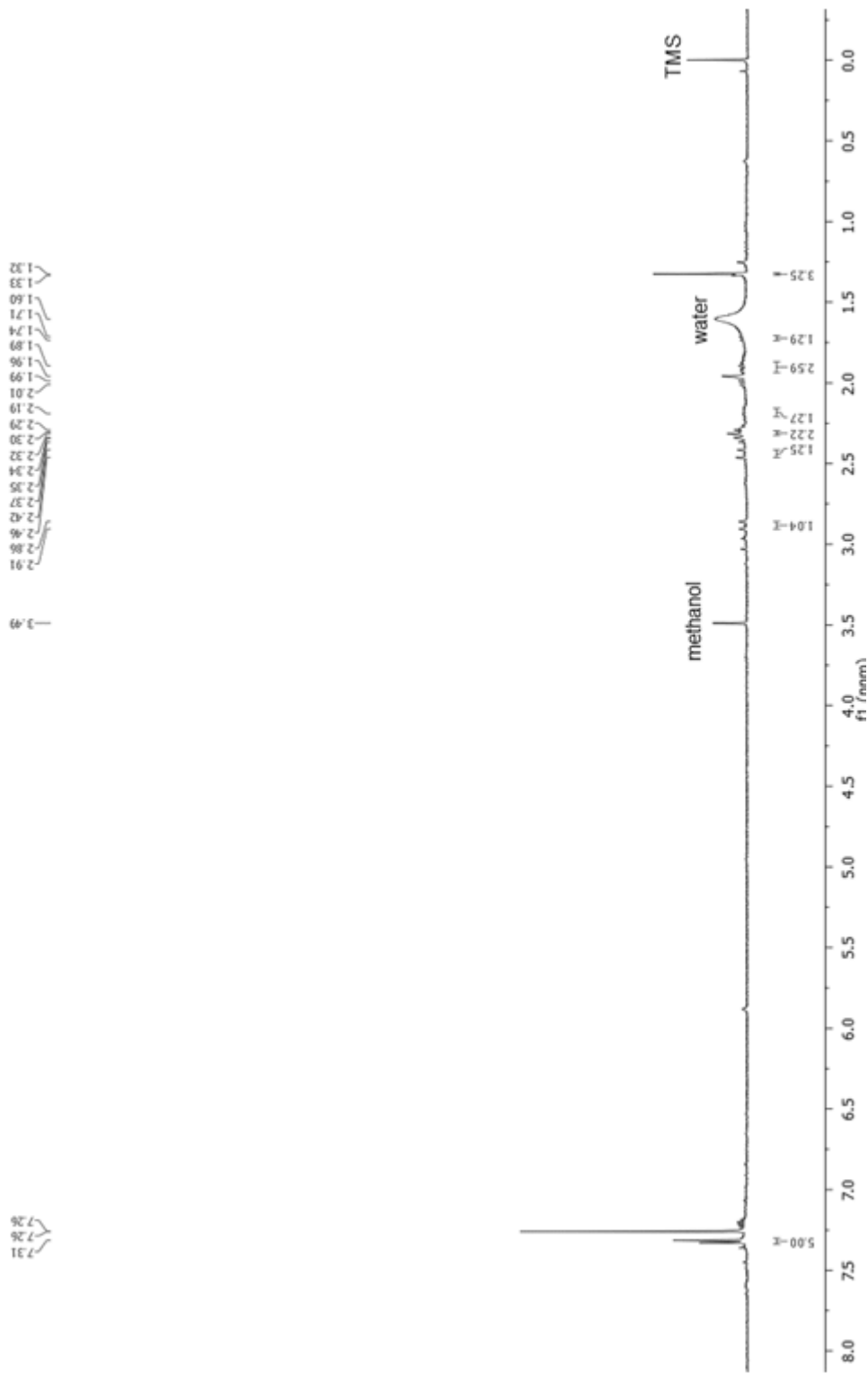


Figure A.12 ${}^1\text{H}$ NMR (300 MHz, CDCl_3) spectrum of isolated product (Table 3.2, Entry 3)

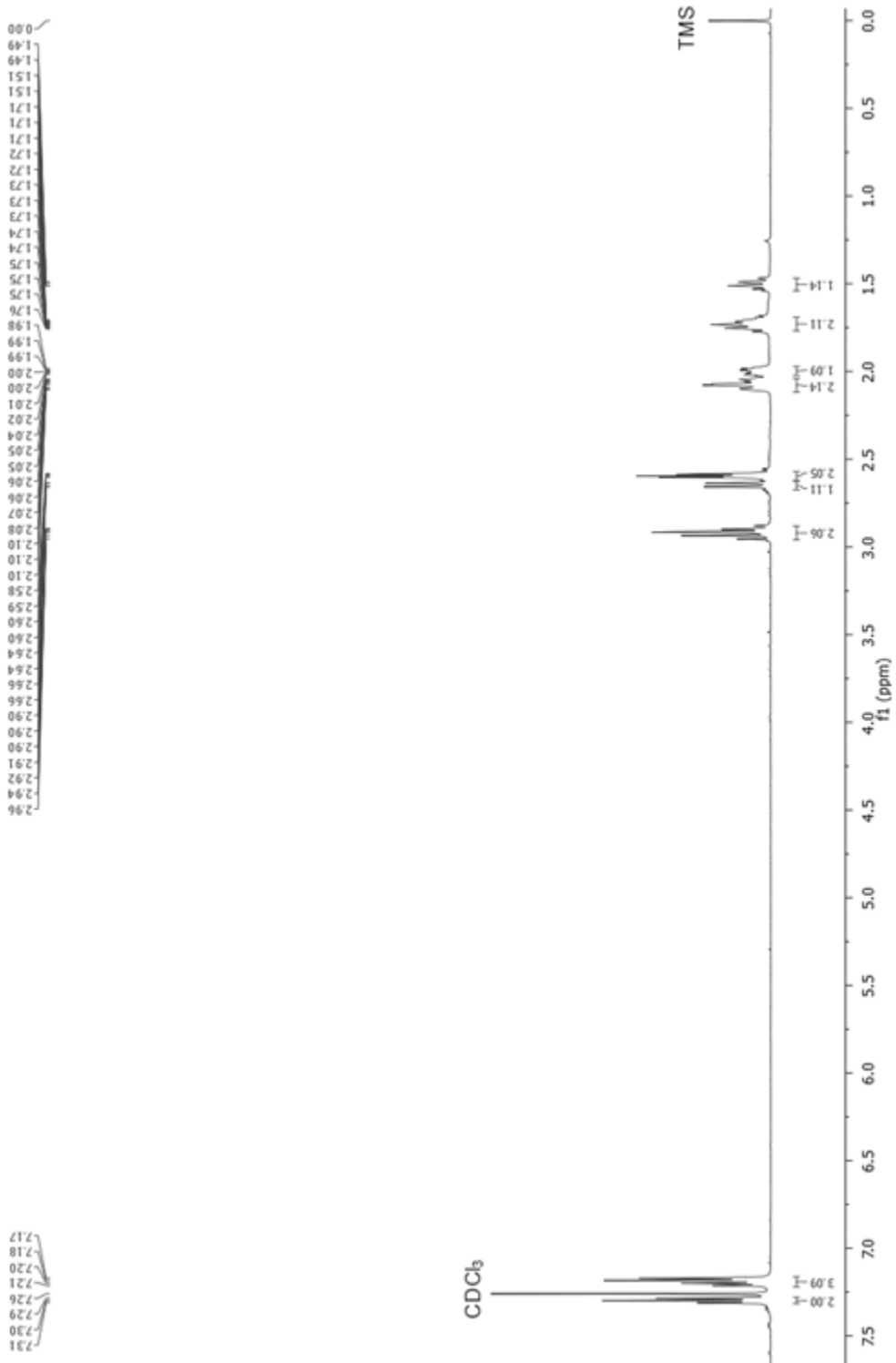


Figure A.13 ${}^1\text{H}$ NMR (600 MHz, CDCl₃) spectrum of isolated product (Table 3.2, Entry 4)

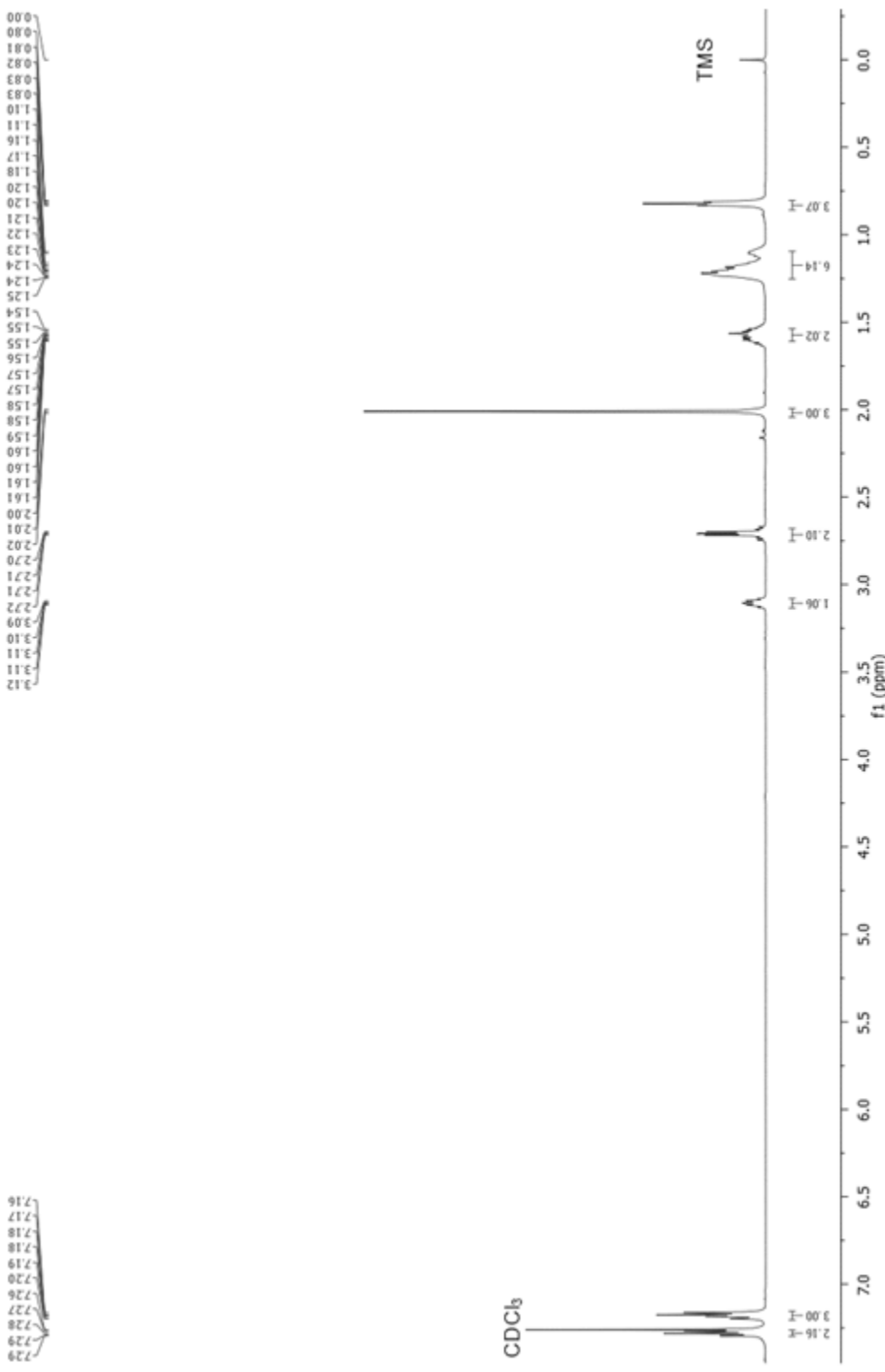


Figure A.14 ^1H NMR (600 MHz, CDCl_3) spectrum of isolated product (Table 3.2, Entry 5)

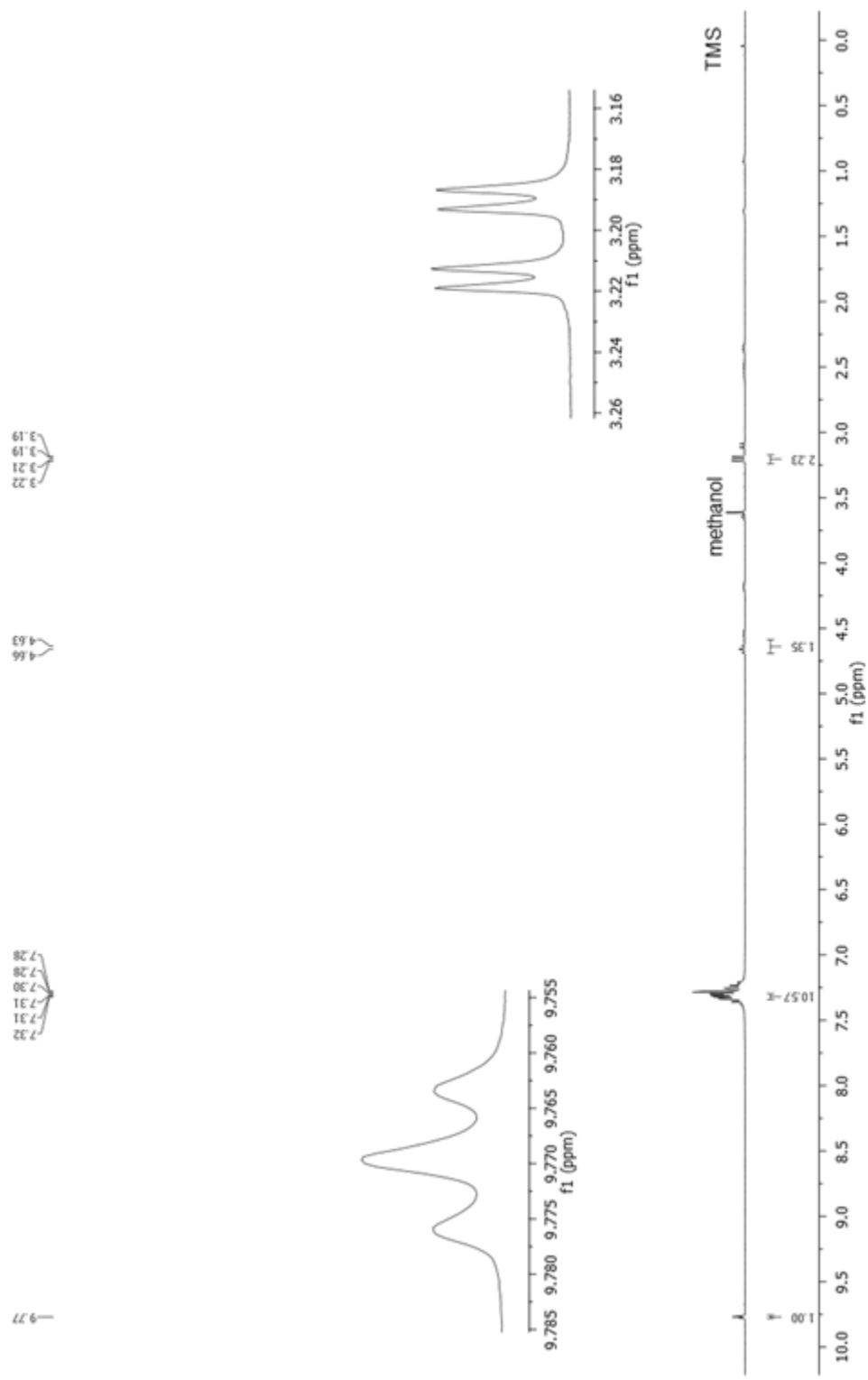


Figure A.15 ${}^1\text{H}$ NMR (300 MHz, CDCl_3) spectrum of isolated product (Table 3.2, Entry 6)

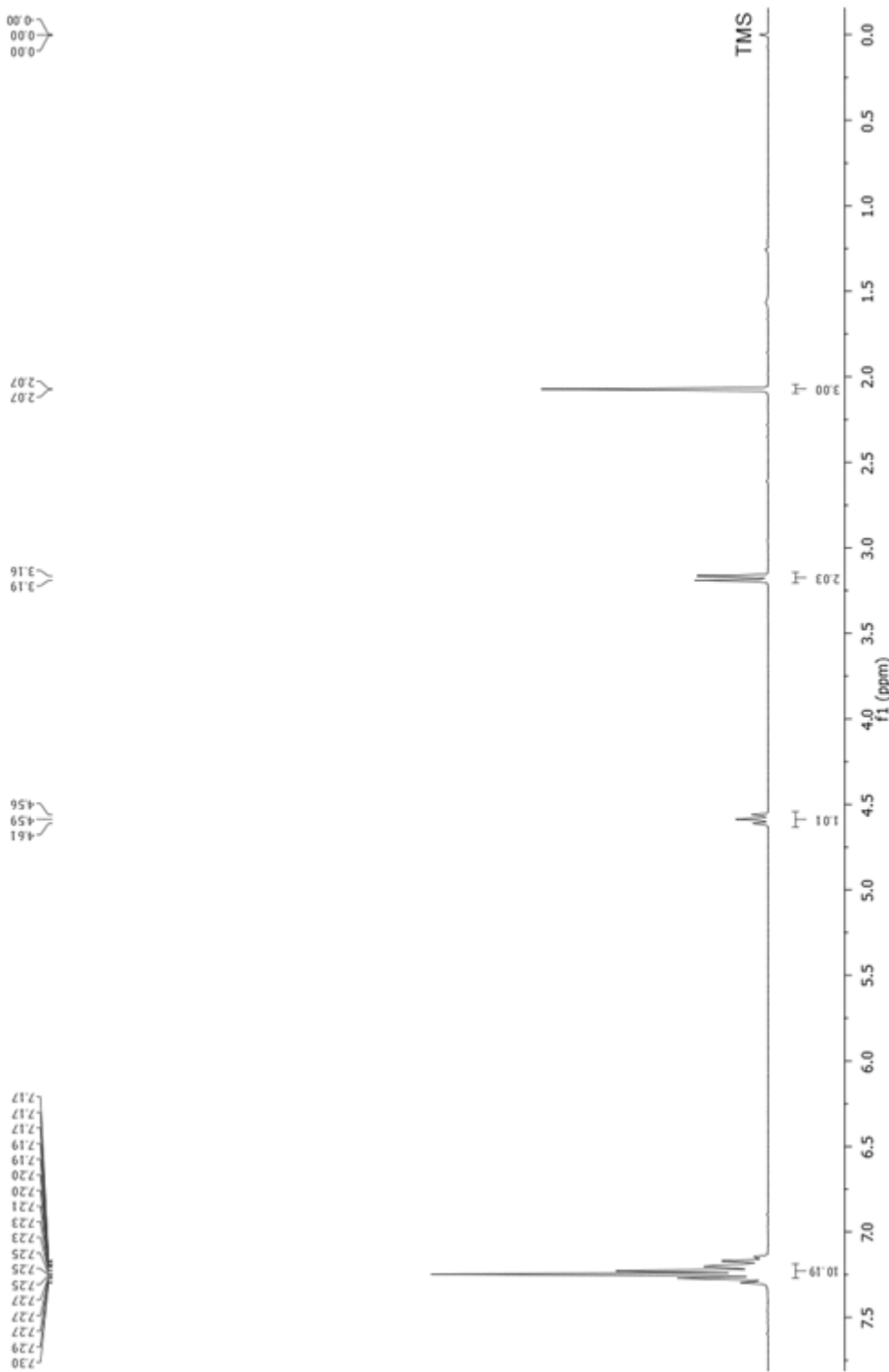


Figure A.16 ^1H NMR (300 MHz, CDCl_3) spectrum of isolated product (Table 3.2, Entry 7)

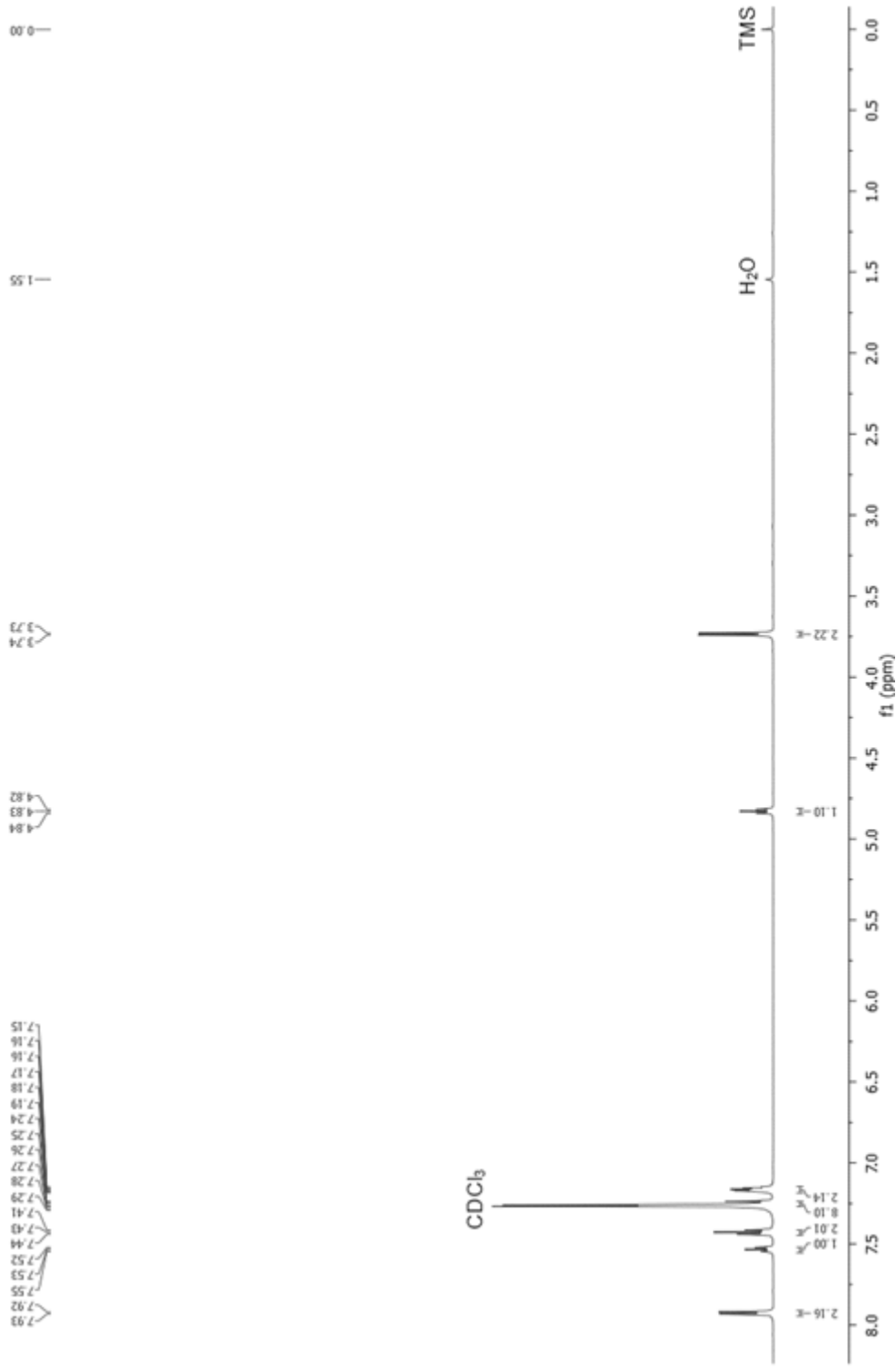


Figure A.17 ^1H NMR (600 MHz, CDCl_3) spectrum of isolated product (Table 3.2, Entry 8)

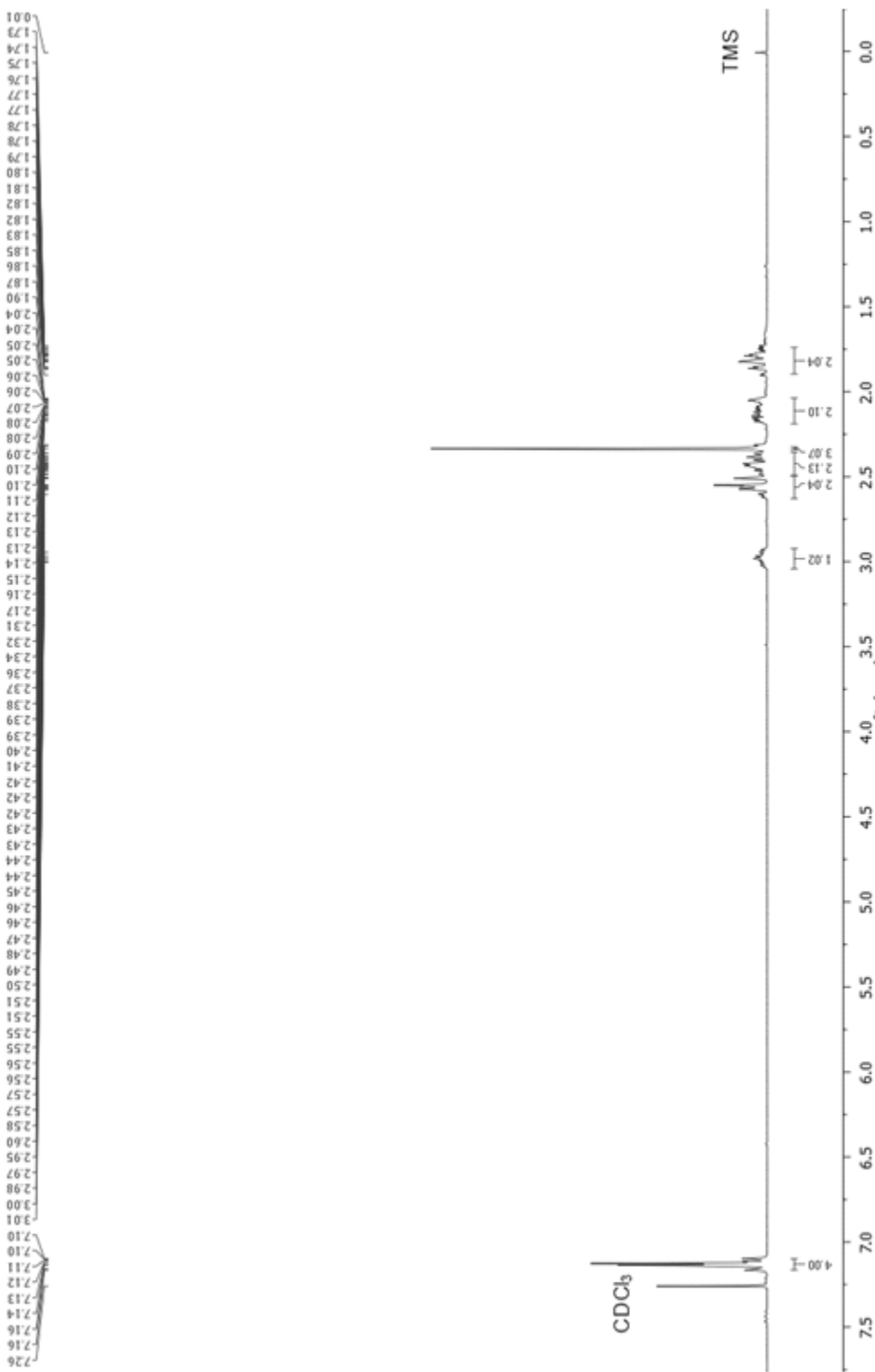


Figure A.18 ^1H NMR (300 MHz, CDCl_3) spectrum of isolated product (Table 3.3, Entry 1)

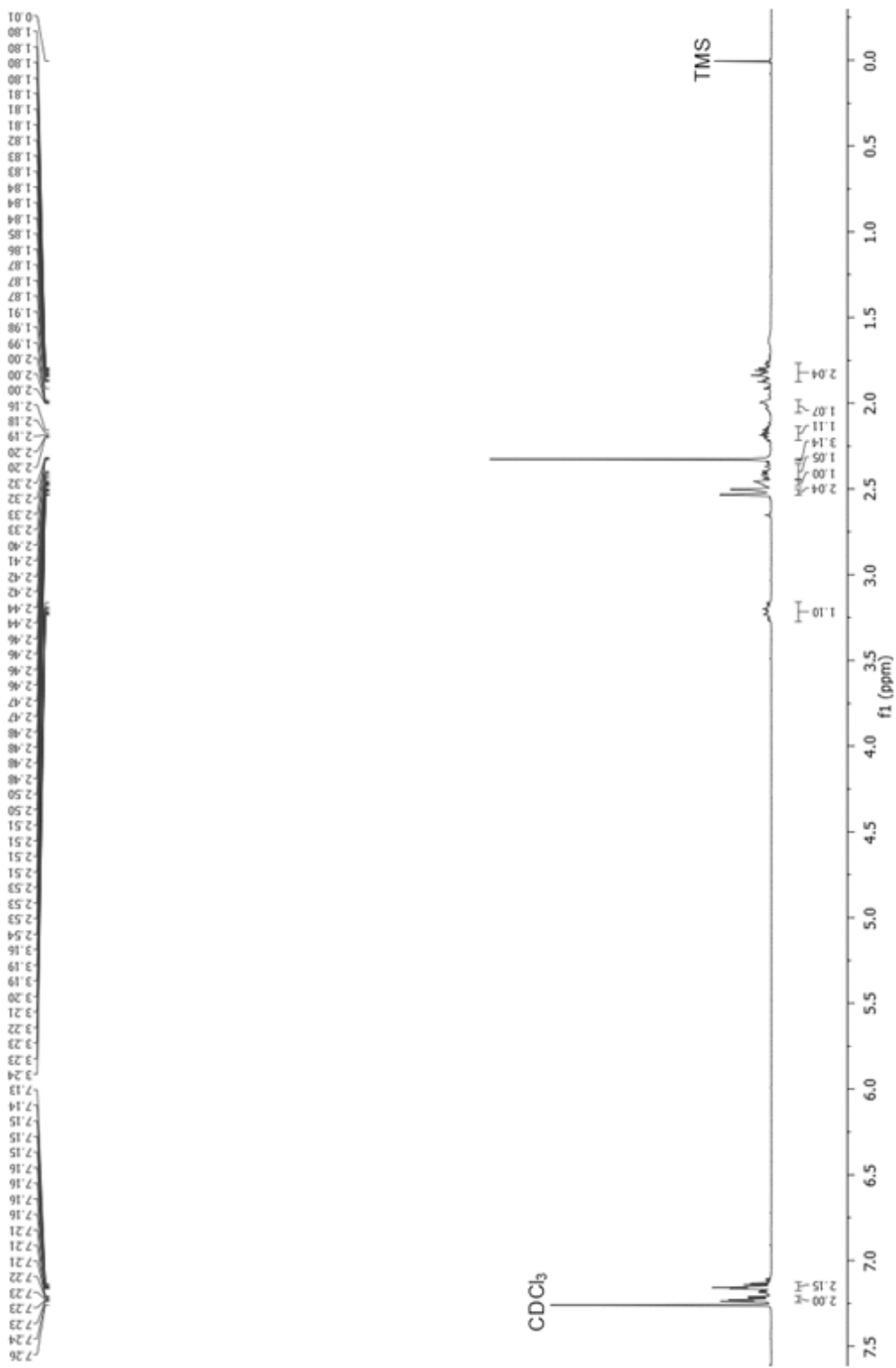


Figure A.19 ^1H NMR (300 MHz, CDCl_3) spectrum of isolated product (Table 3.3, Entry 2)

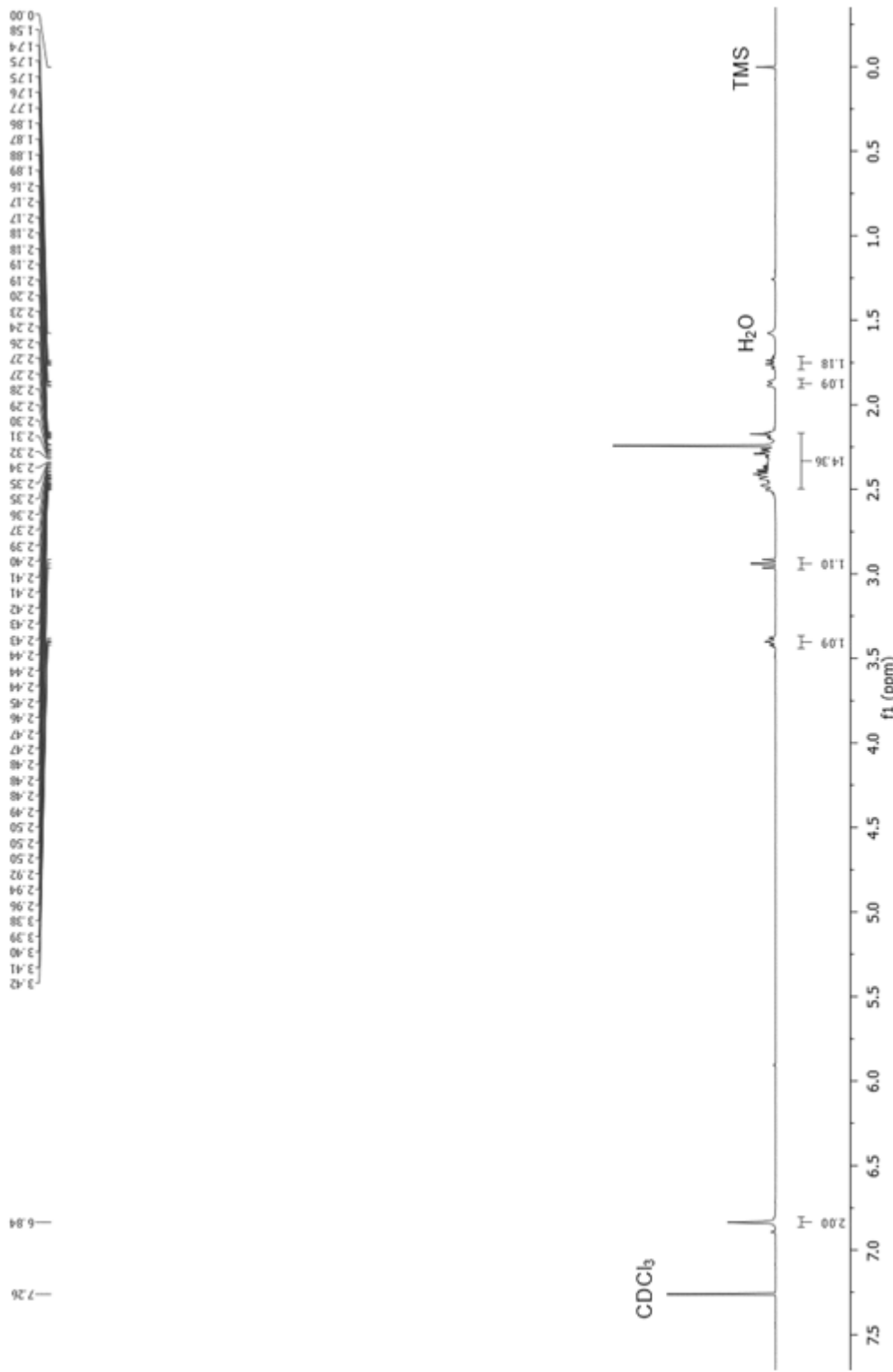


Figure A.20 ^1H NMR (600 MHz, CDCl_3) spectrum of isolated product (Table 3.3, Entry 3)

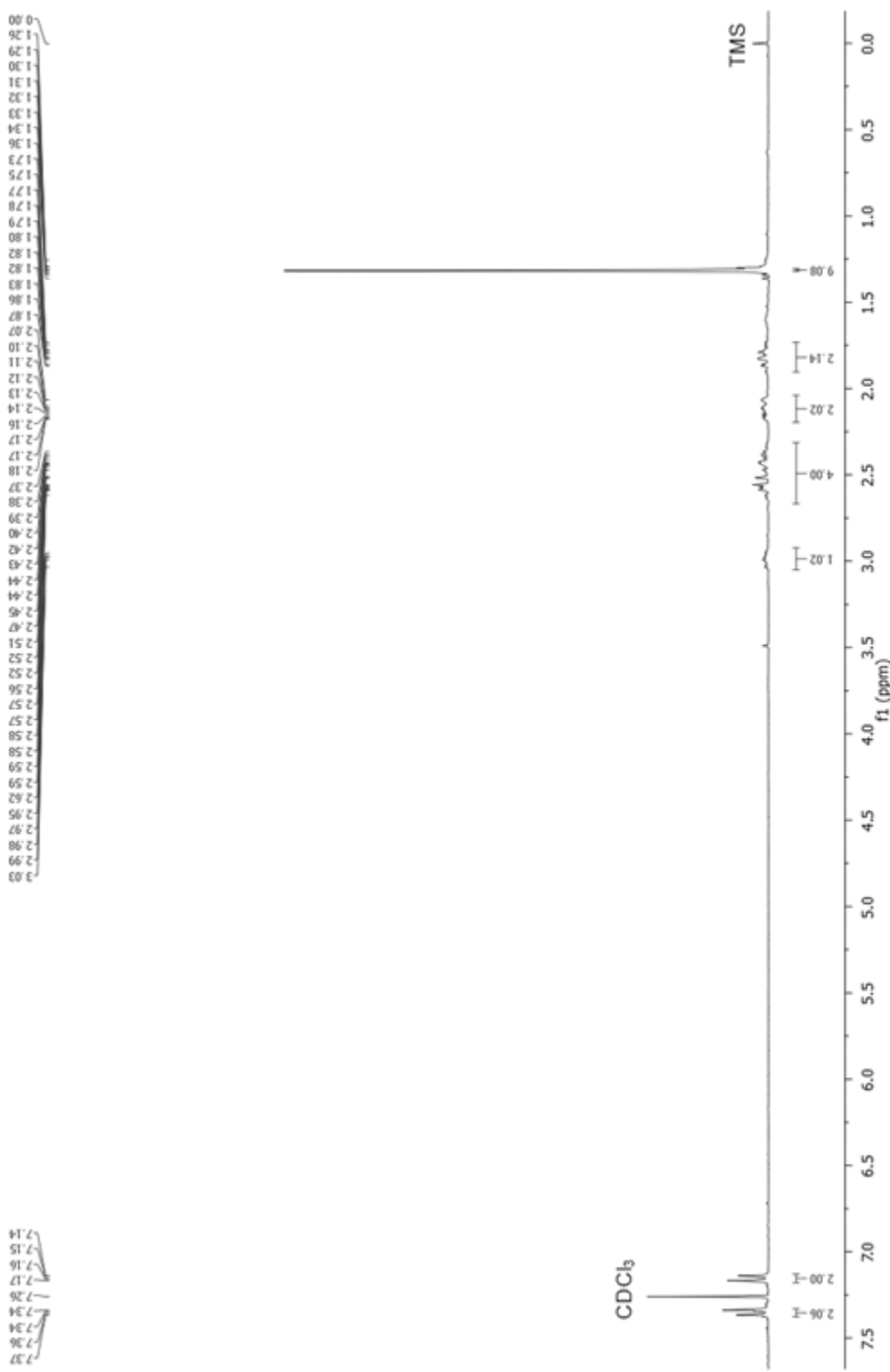


Figure A.21 ^1H NMR (600 MHz, CDCl_3) spectrum of isolated product (Table 3.3, Entry 4)

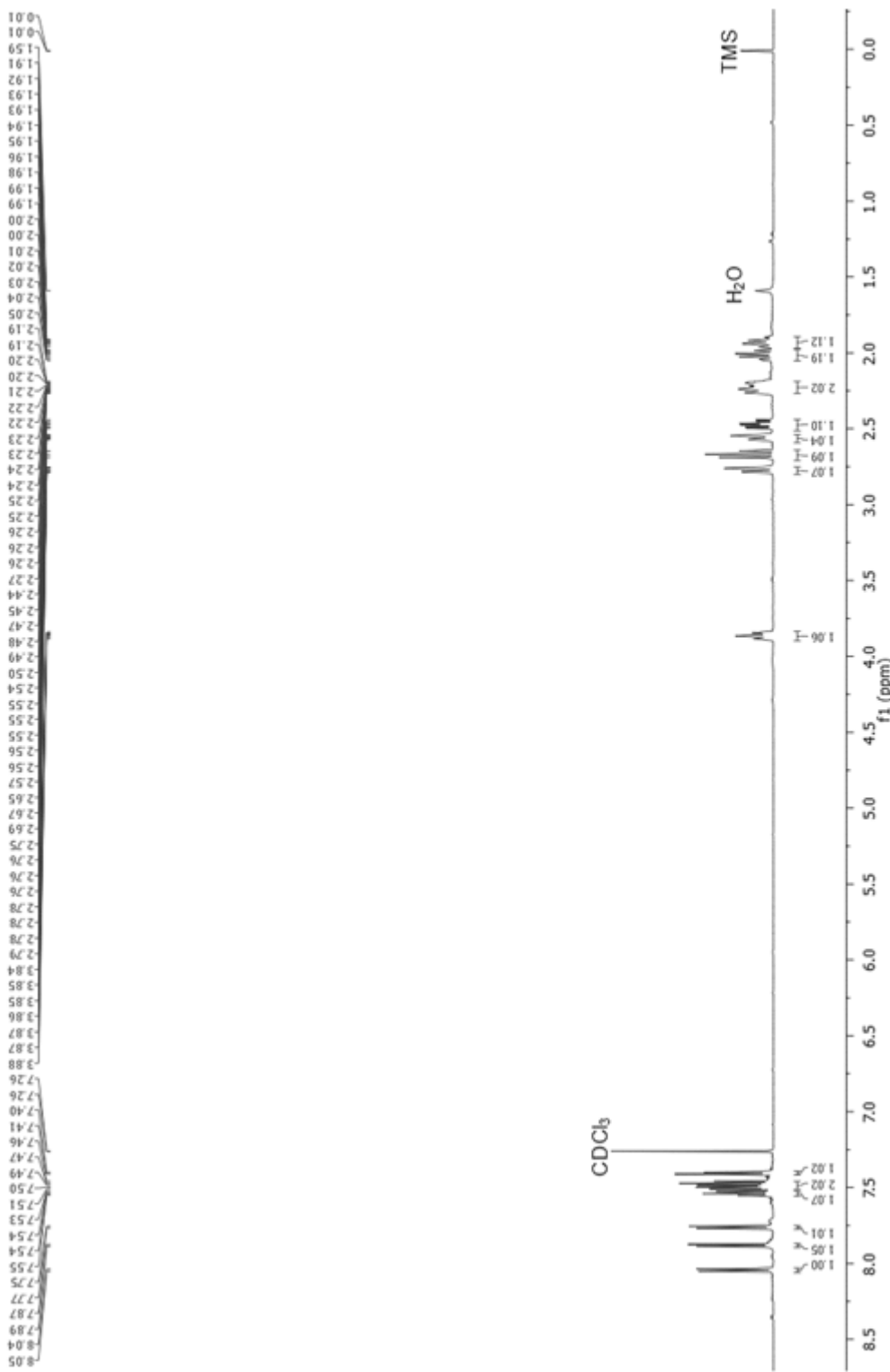


Figure A.22 ${}^1\text{H}$ NMR (600 MHz, CDCl₃) spectrum of isolated product (Table 3.3, Entry 5)

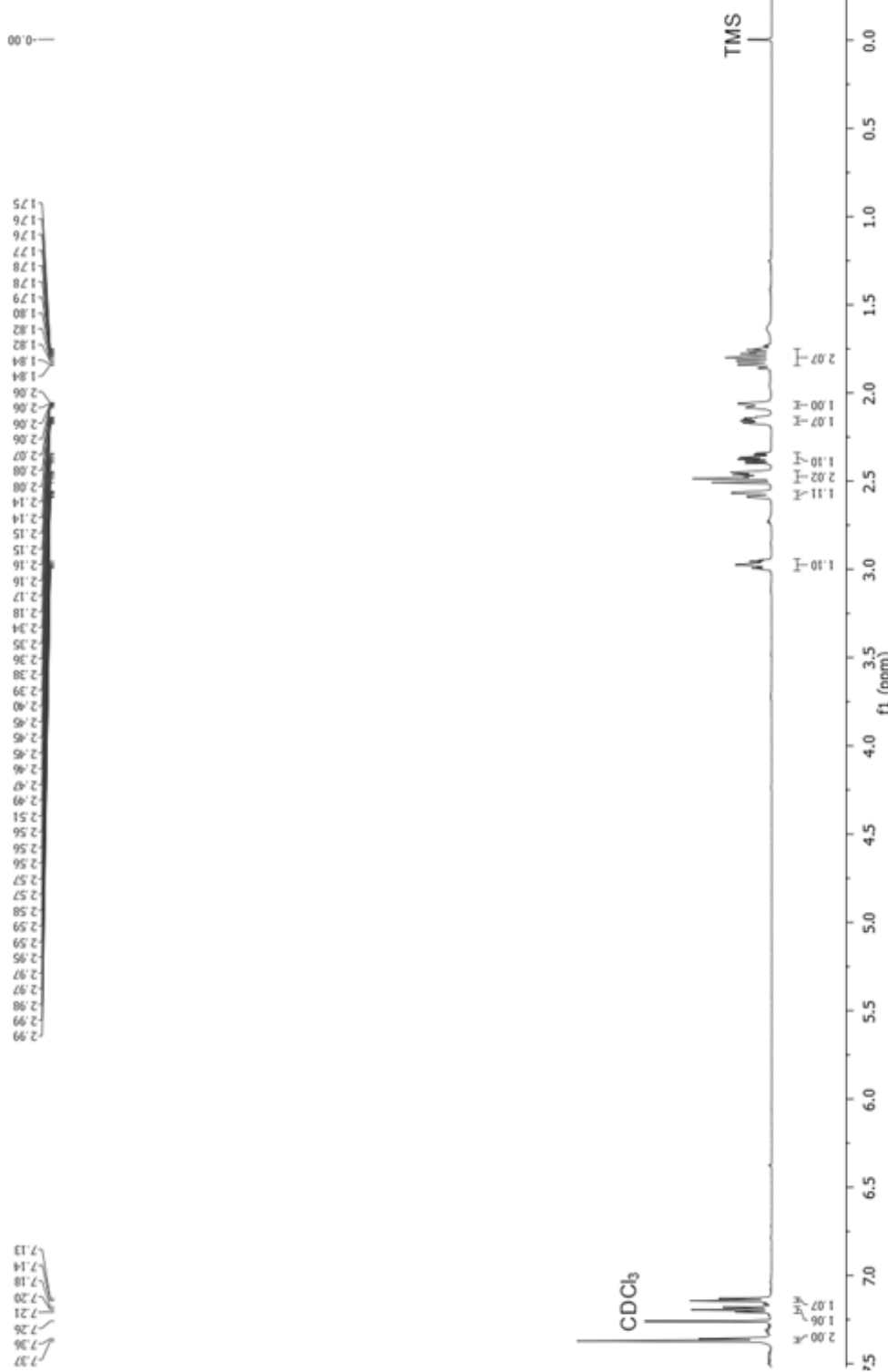


Figure A.23 ^1H NMR (600 MHz, CDCl_3) spectrum of isolated product (Table 3.3, Entry 6)

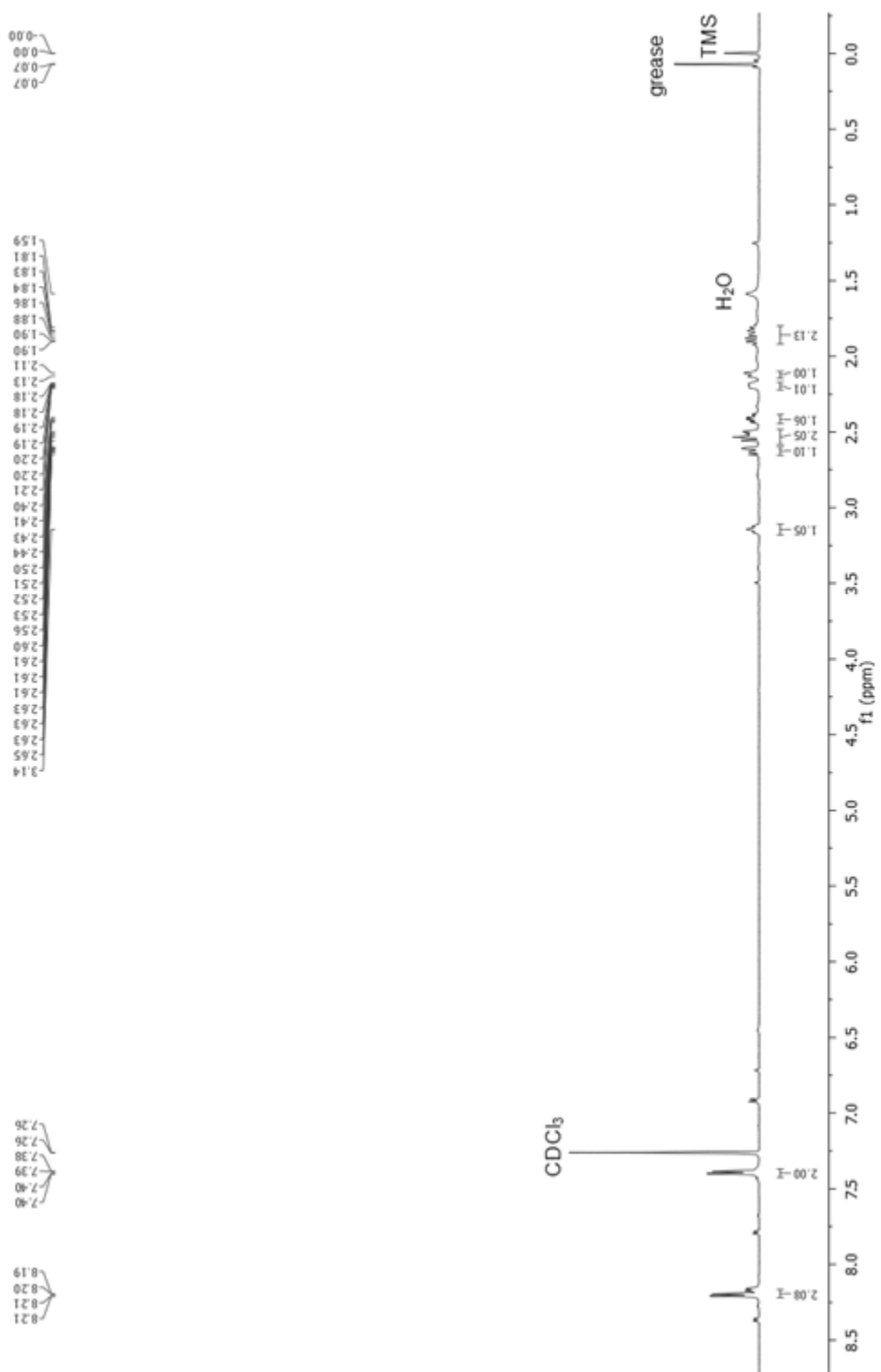


Figure A.24 ${}^1\text{H}$ NMR (600 MHz, CDCl_3) spectrum of isolated product (Table 3.3, Entry 8)

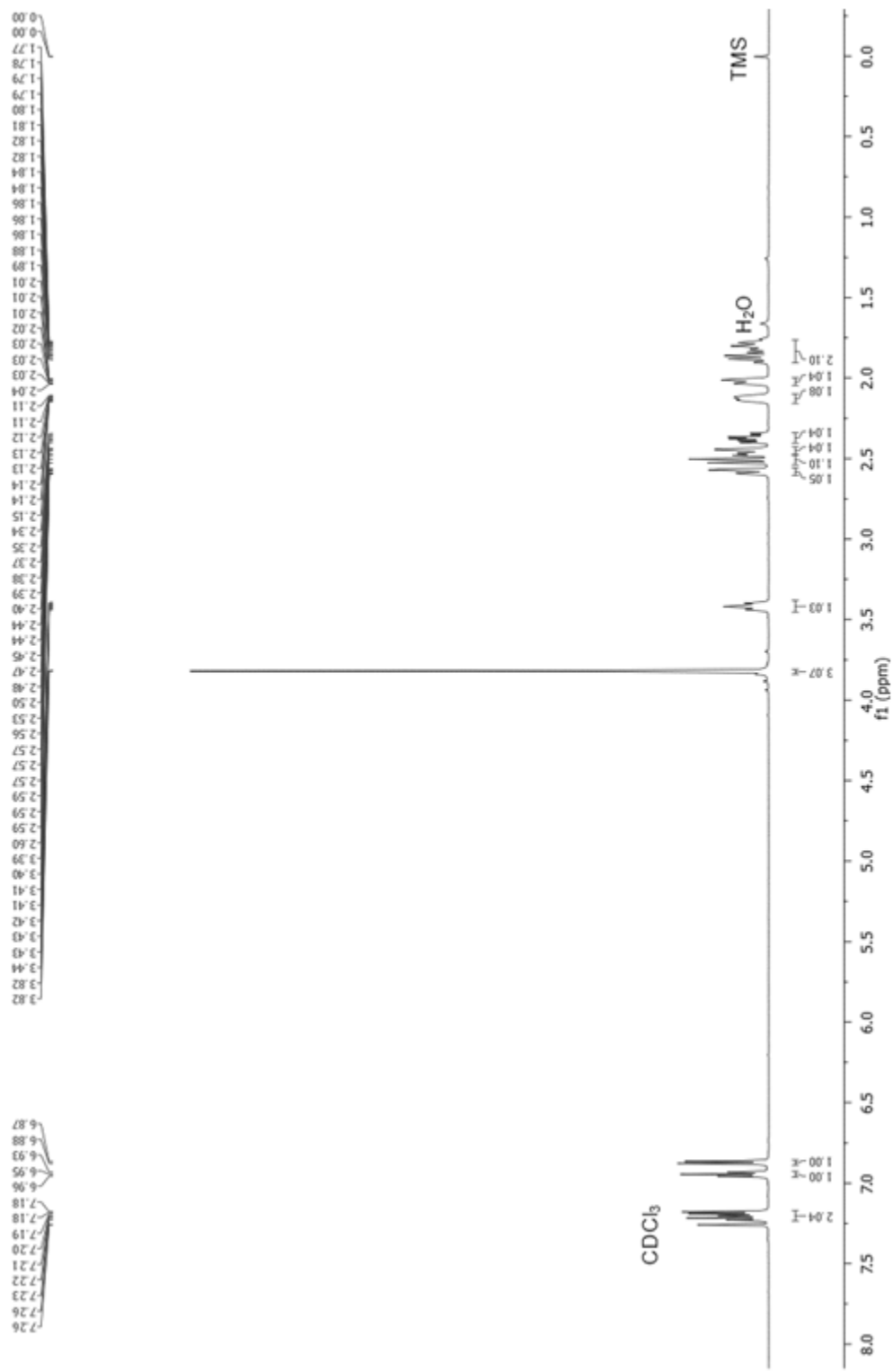


Figure A.25 ^1H NMR (600 MHz, CDCl_3) spectrum of isolated product (Table 3.3, Entry 9)

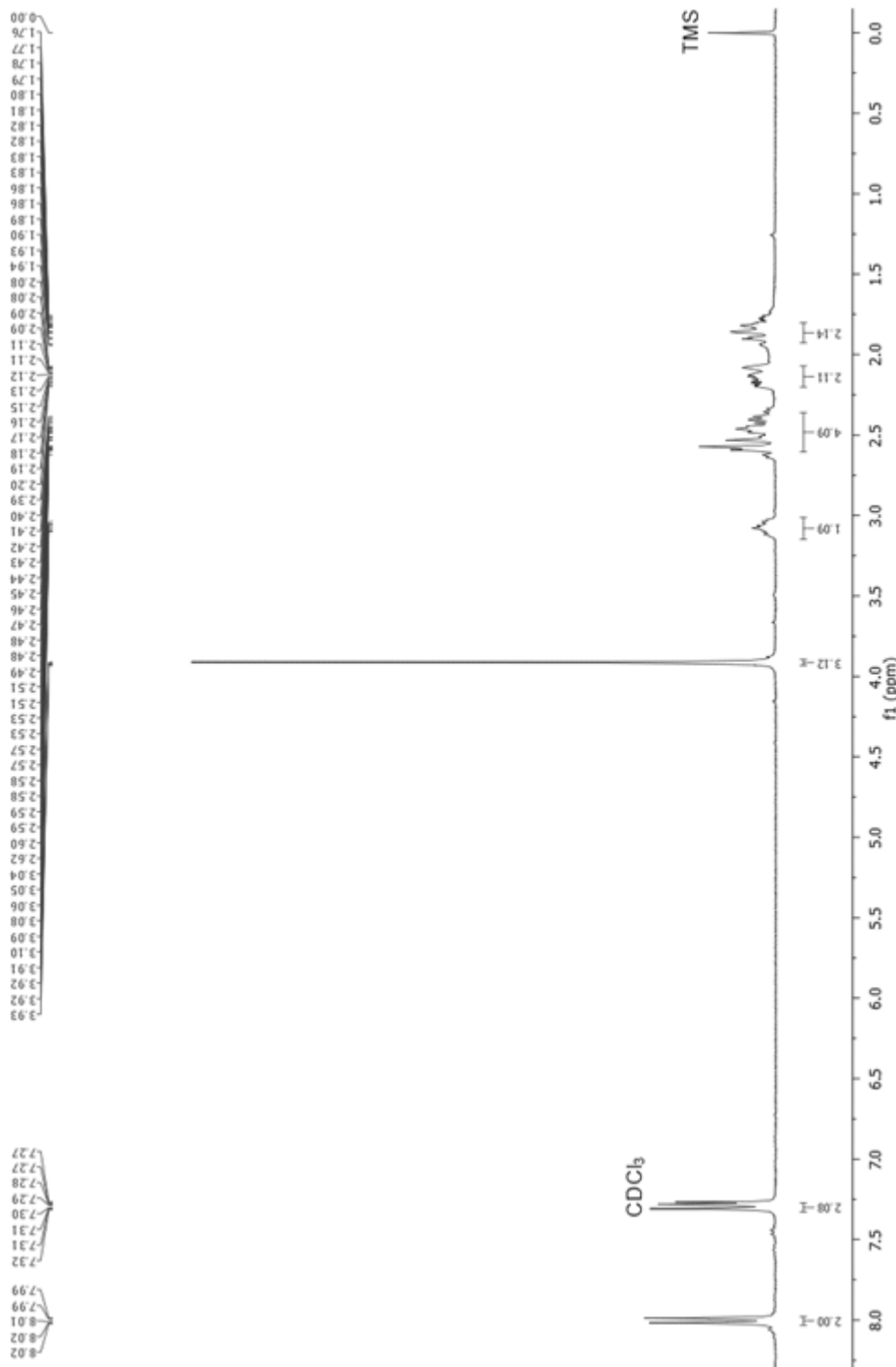


Figure A.26 ^1H NMR (300 MHz, CDCl_3) spectrum of isolated product (Table 3.3, Entry 10)

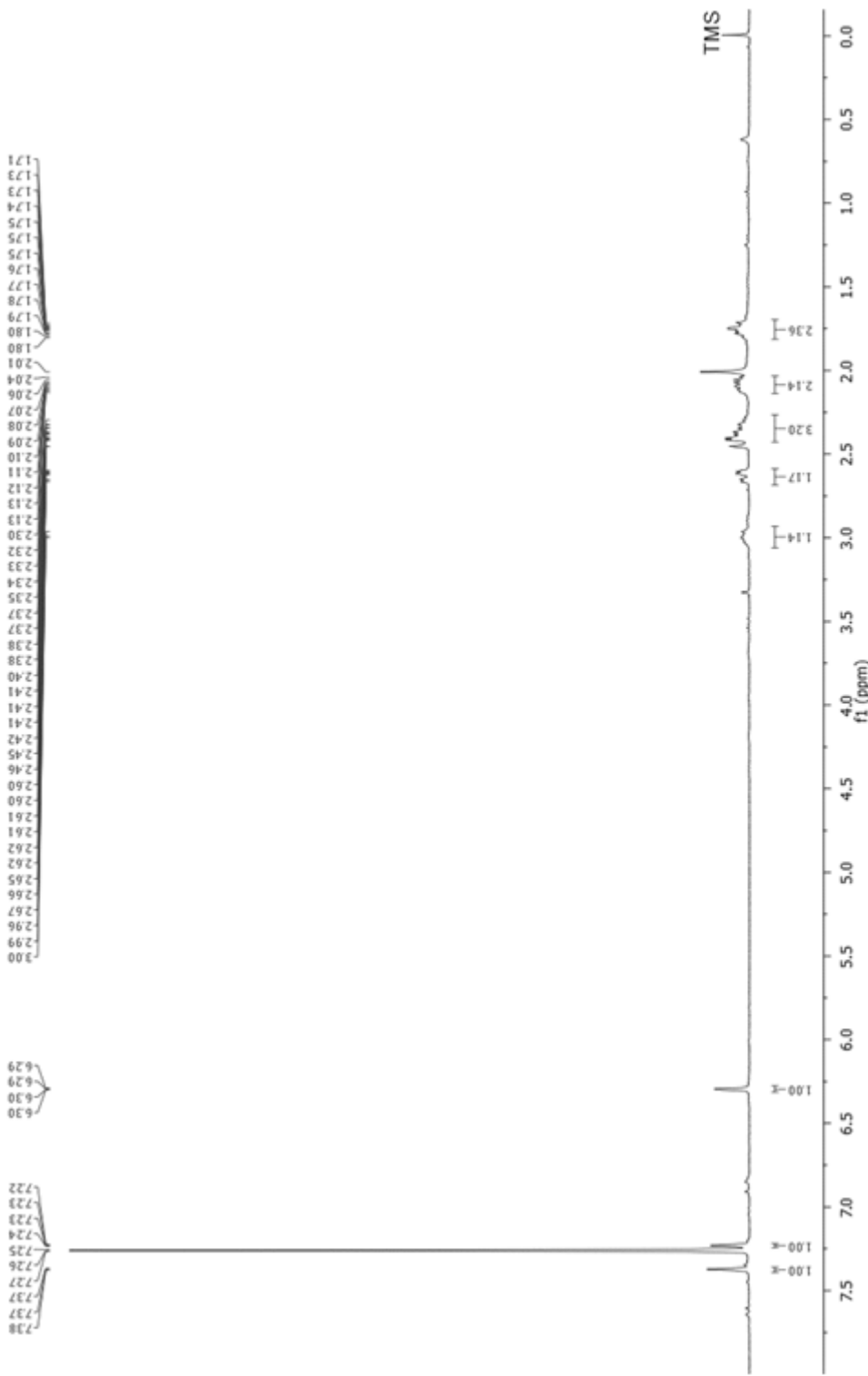


Figure A.27 ^1H NMR (300 MHz, CDCl_3) spectrum of isolated product (Table 3.4, Entry 1)

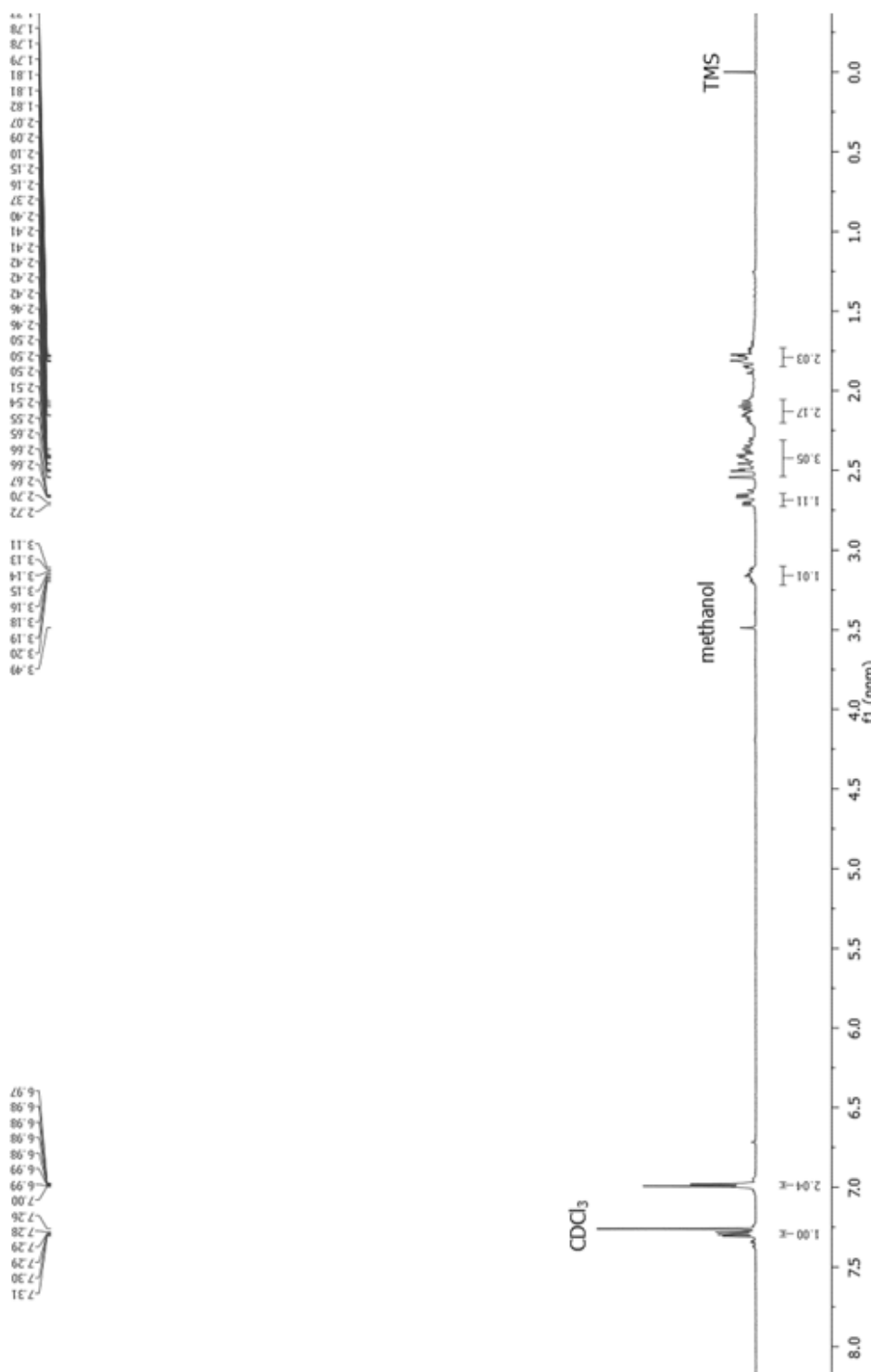


Figure A.28 ^1H NMR (300 MHz, CDCl_3) spectrum of isolated product (Table 3.4, Entry 2)

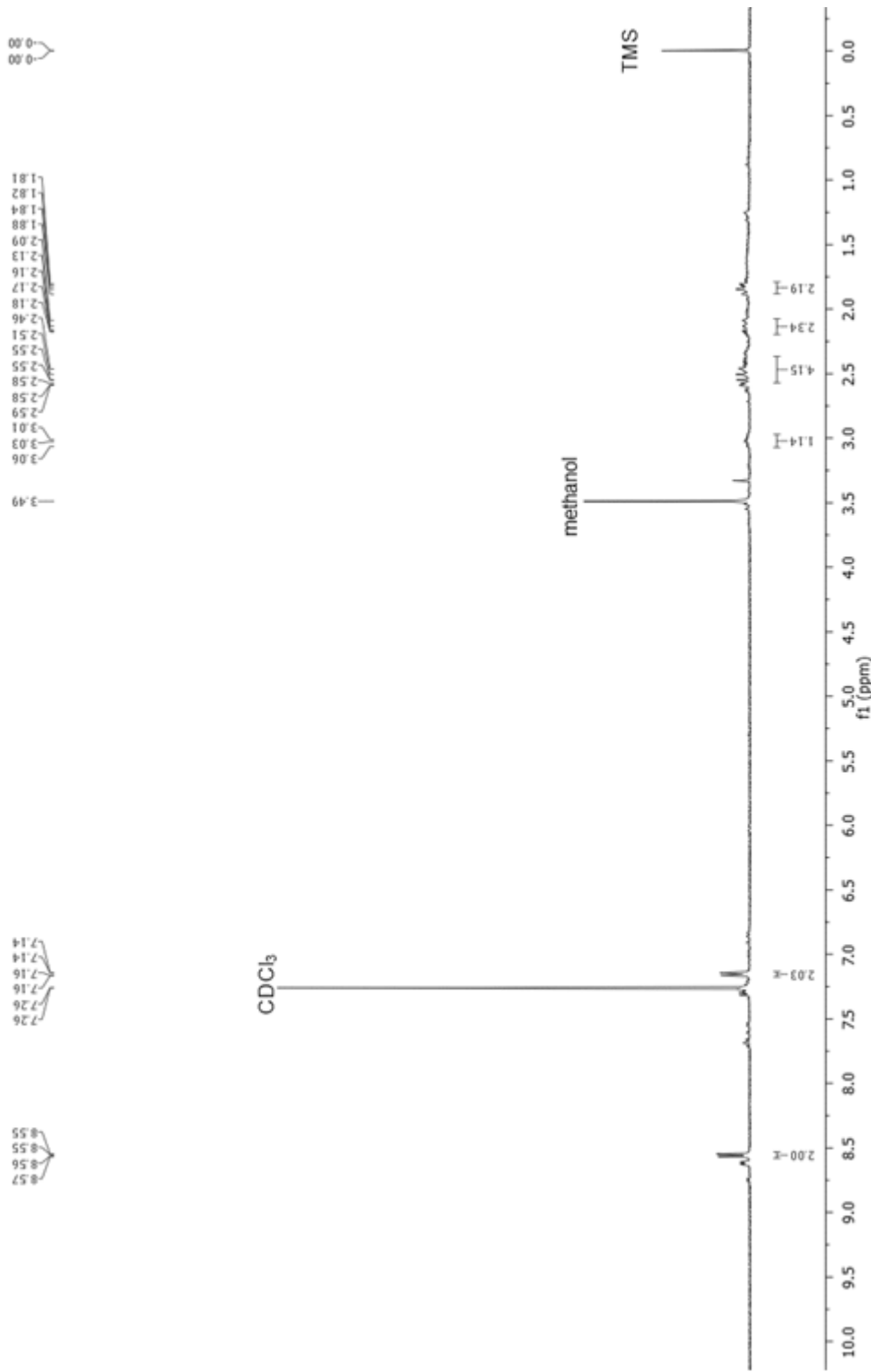


Figure A.29 ^1H NMR (300 MHz, CDCl_3) spectrum of isolated product (Table 3.4, Entry 5)

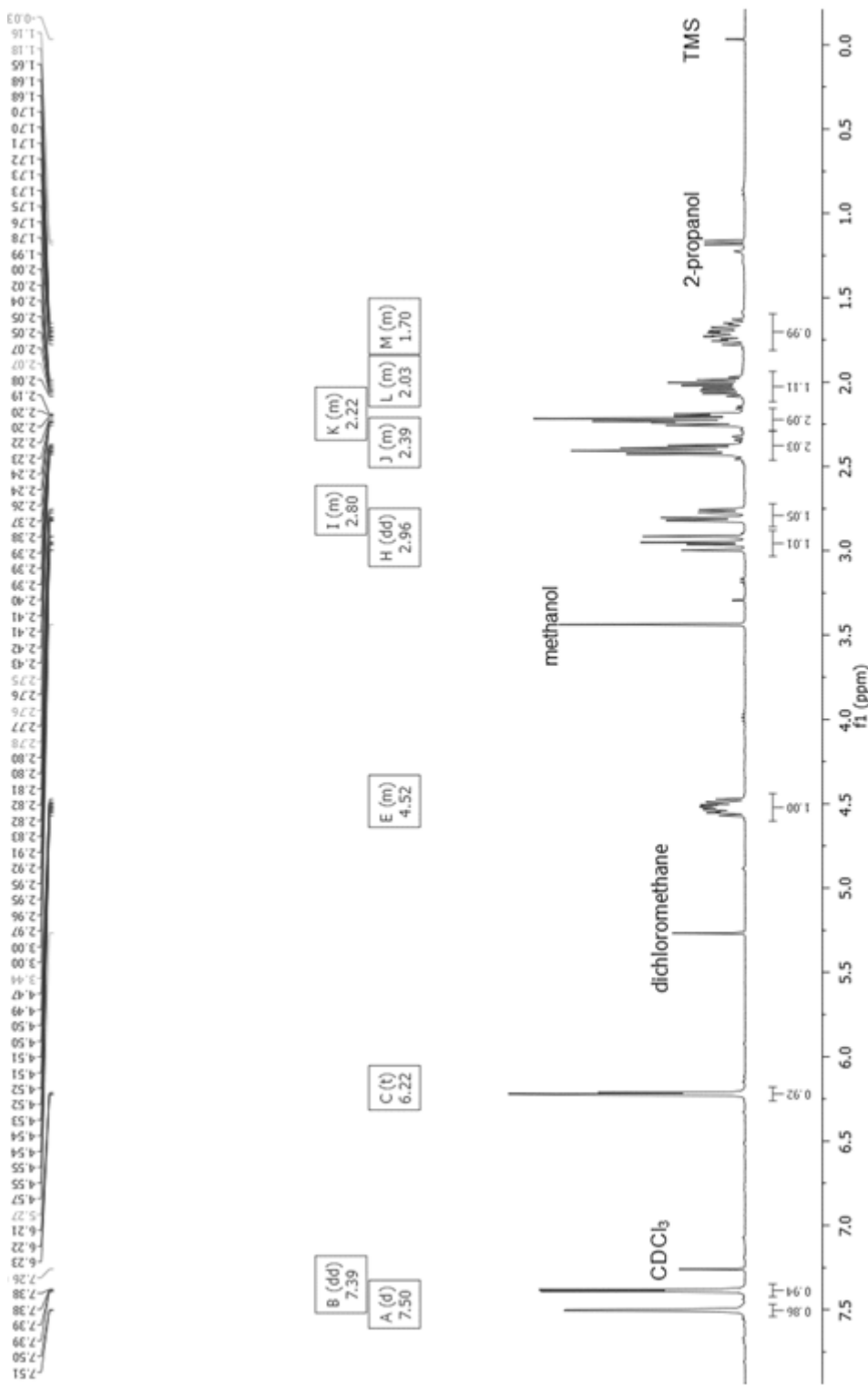


Figure A.30 ^1H NMR (300 MHz, CDCl_3) spectrum of isolated product (Table 3.4, Entry 4)

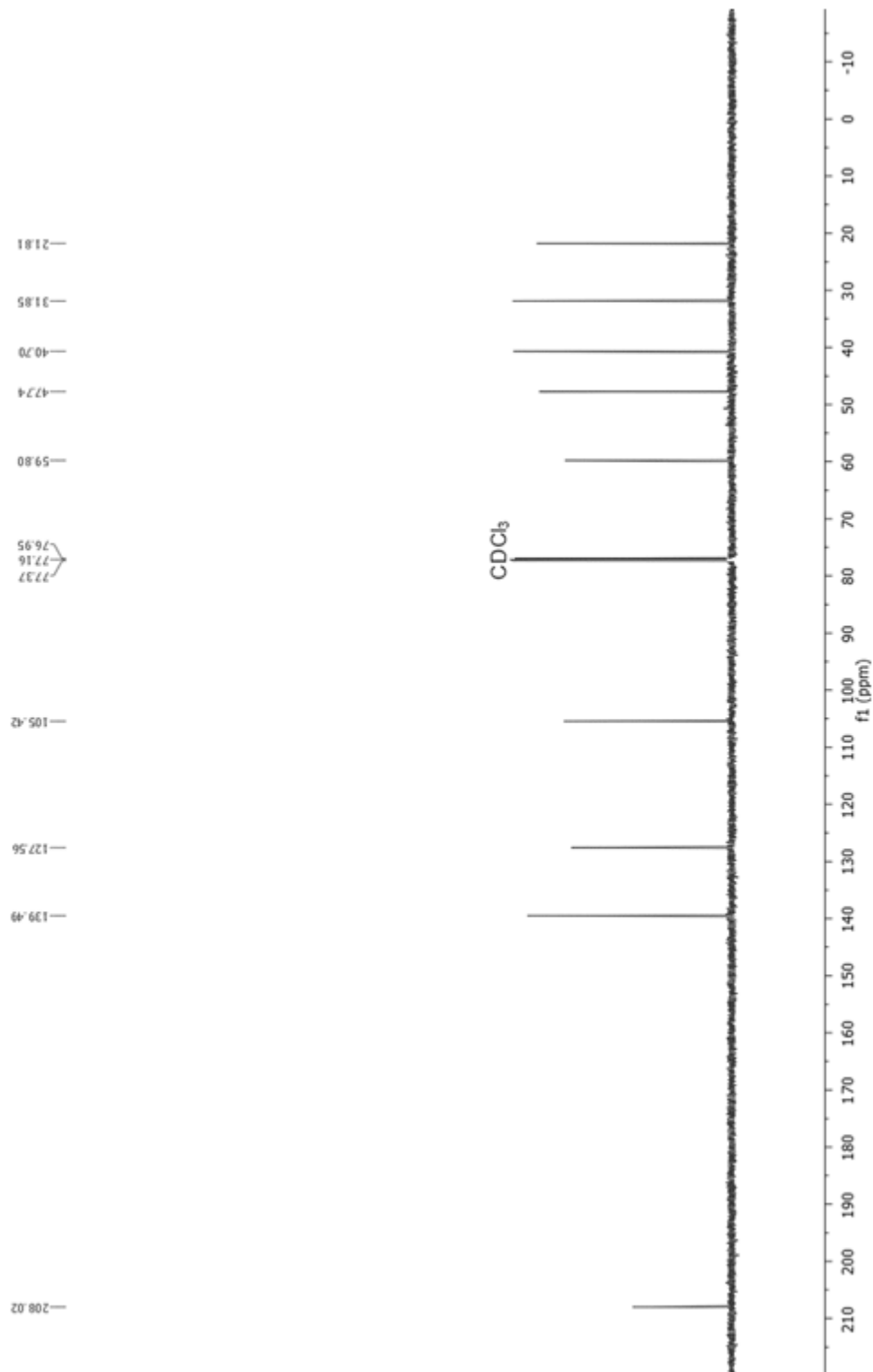


Figure A.31 ^{13}C NMR (150 MHz, CDCl_3) spectrum of isolated product (Table 3.4, Entry 4)

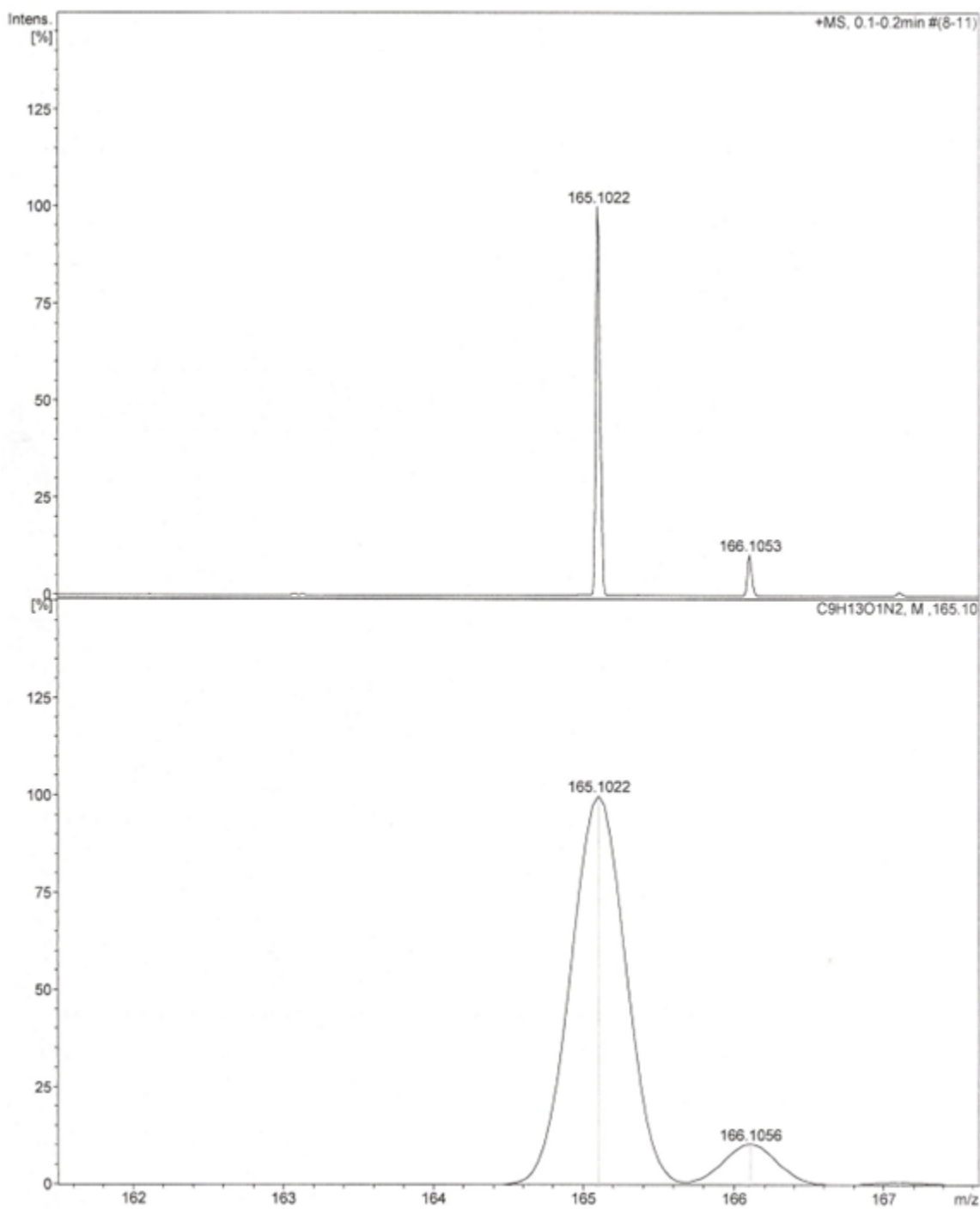


Figure A.32 HRMS of isolated product (Table 3.4, Entry 4)

HRMS-ESI (m/z): $[M+H]^+$ calcd (bottom) for $C_9H_{13}N_2O$, 165.1022, found (top)
165.1022

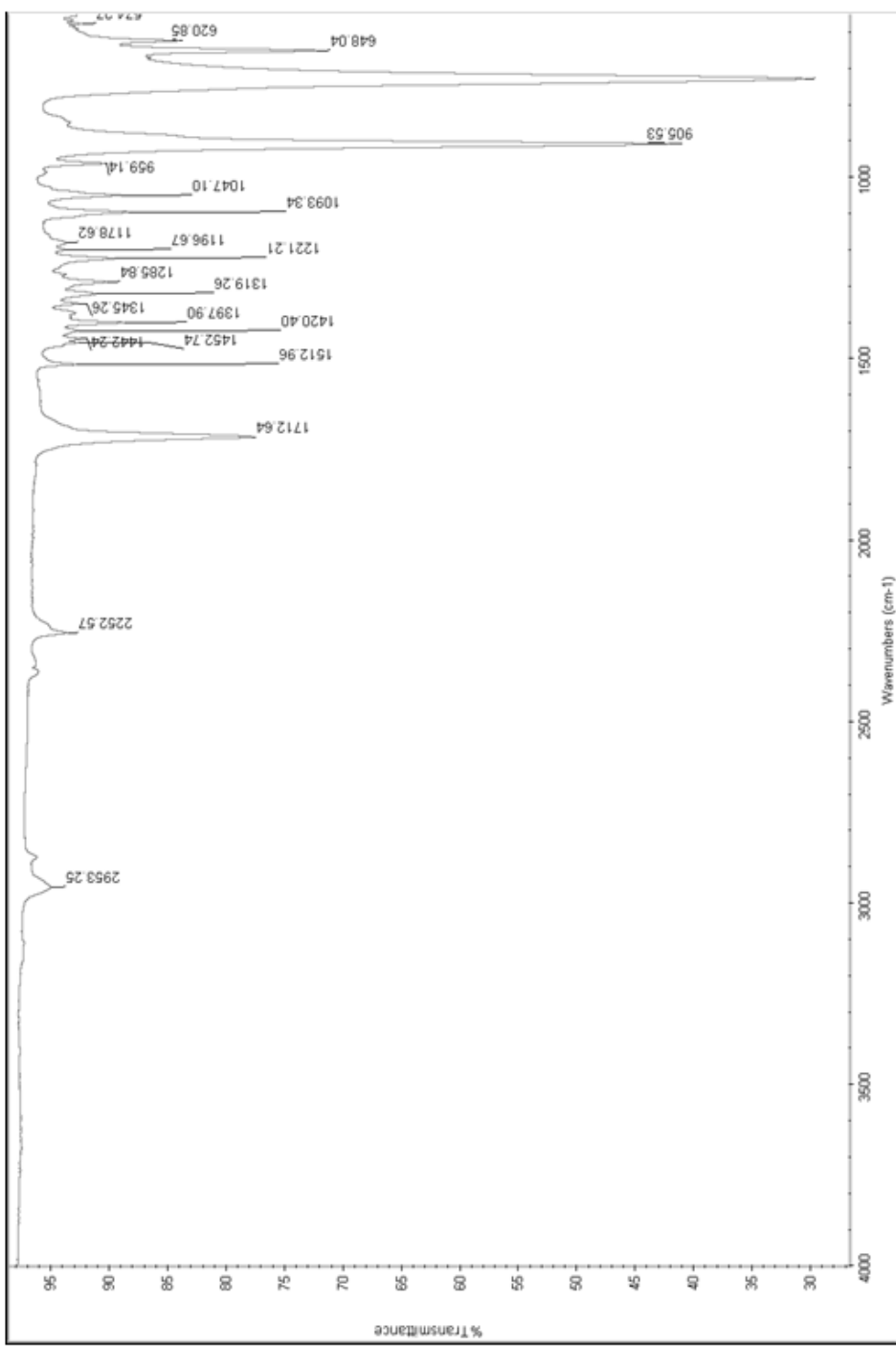


Figure A.33 IR spectrum of isolated product (Table 3.4, Entry 4)

A.3

Chapter IV Compounds

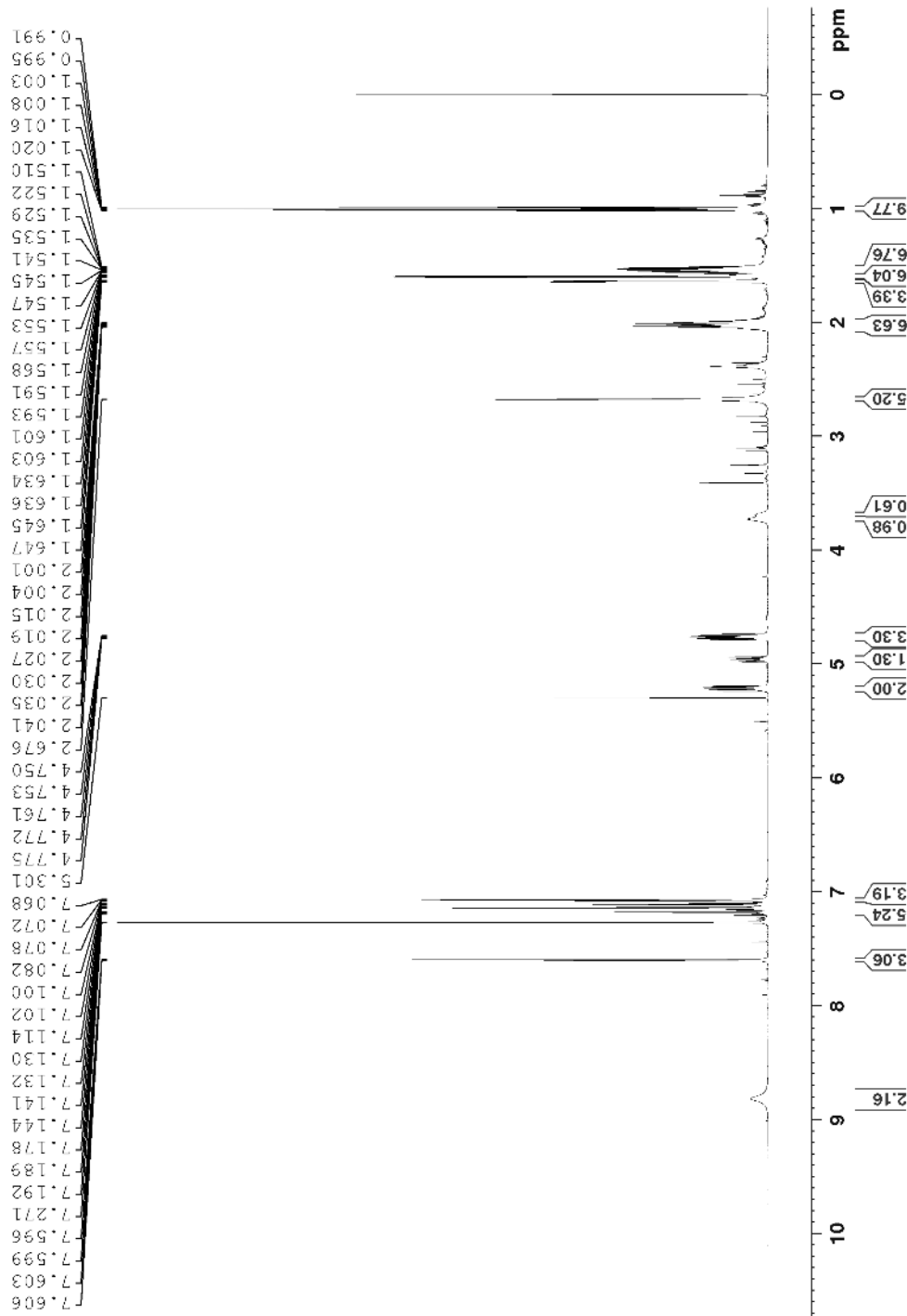


Figure A.34 ${}^1\text{H}$ NMR (600 MHz, CDCl_3) spectrum of 10

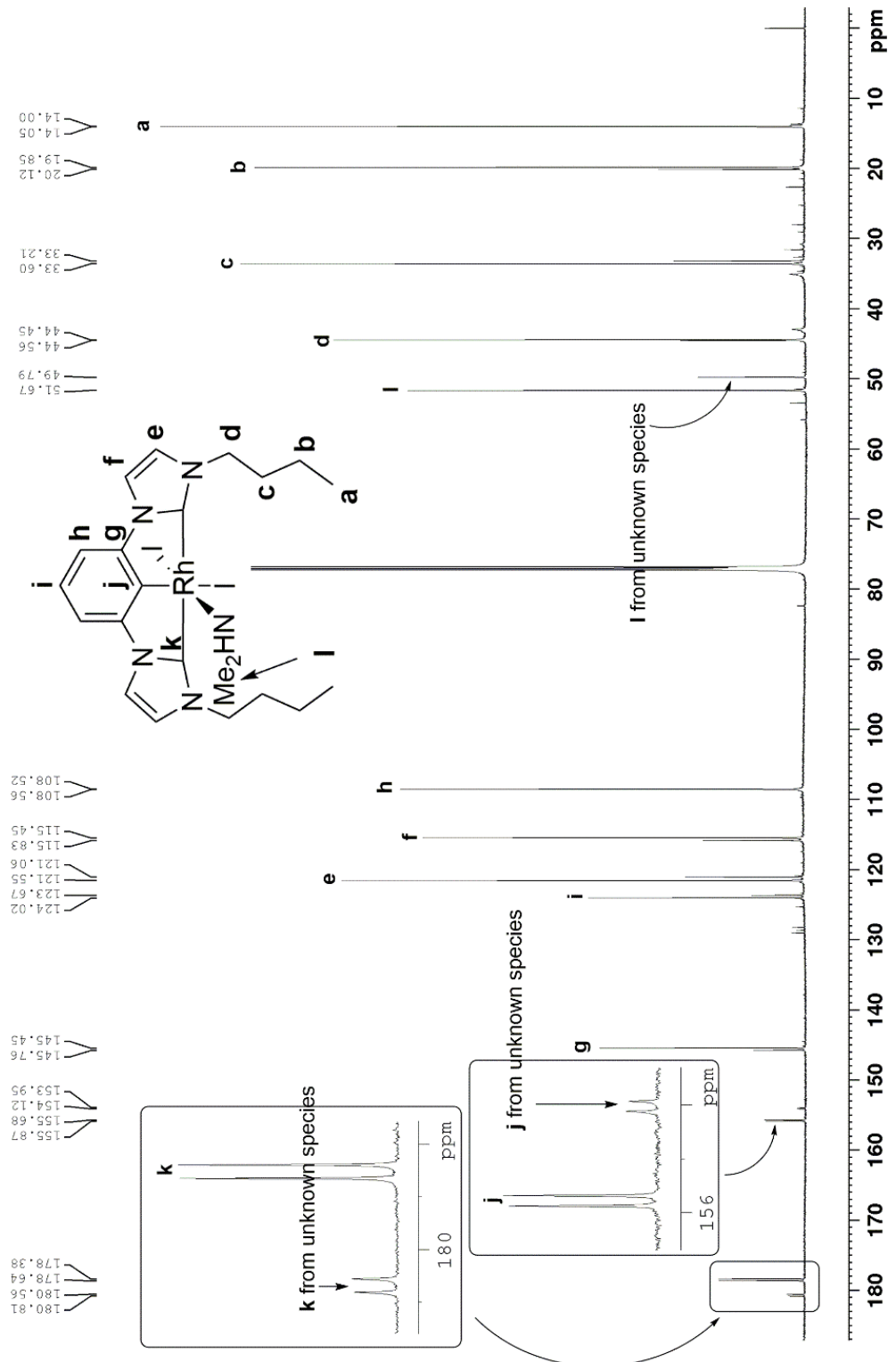


Figure A.35 ^{13}C NMR (150 MHz, CDCl_3) spectrum of **10**

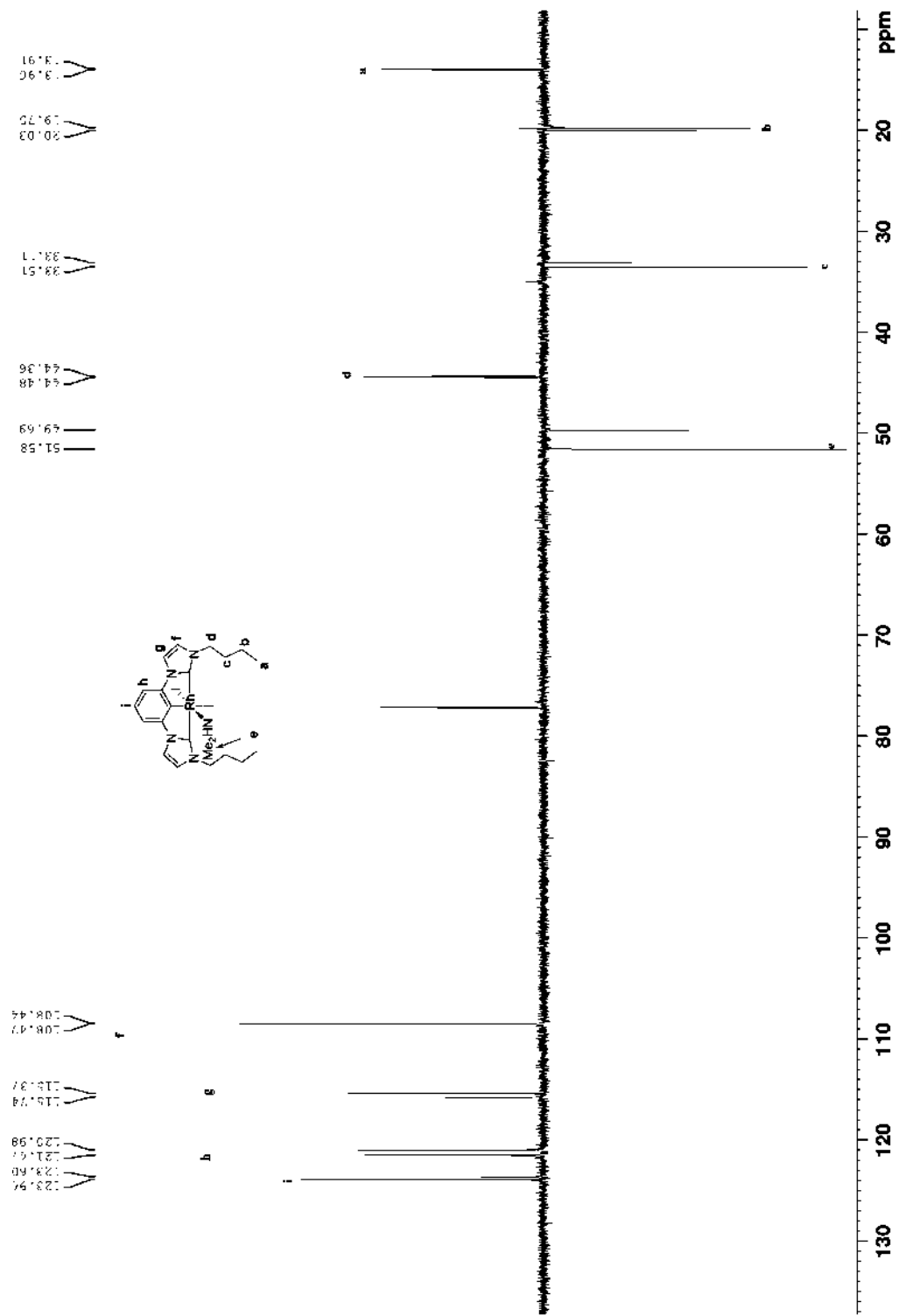


Figure A.36 ^{13}C DEPT 135 NMR (150 MHz, CDCl_3) spectrum of 10

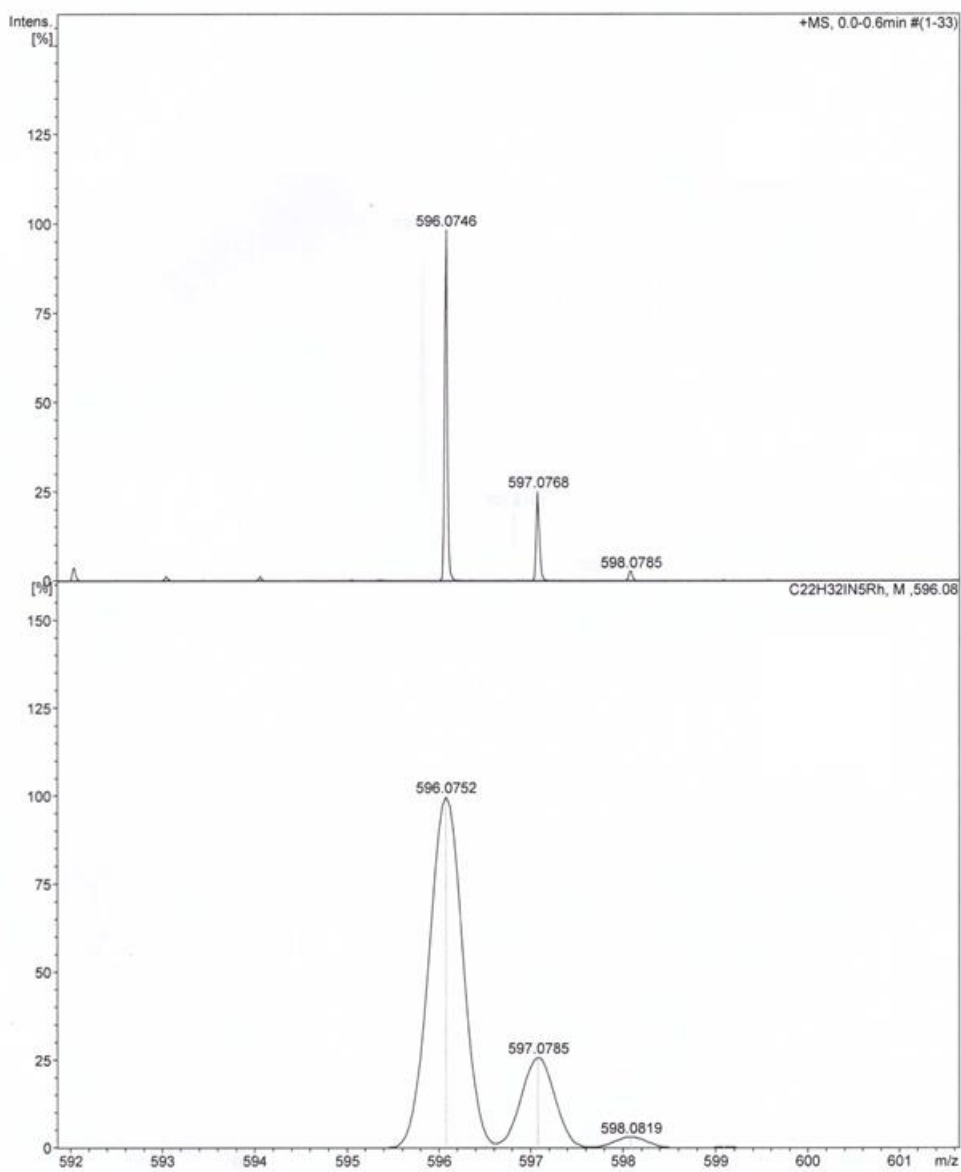


Figure A.37 HRMS of **10**

HRMS-ESI (m/z): $[M-I]^+$ calcd (bottom) for $C_{22}H_{32}IN_5Rh$, 596.0752; found (top), 596.0740

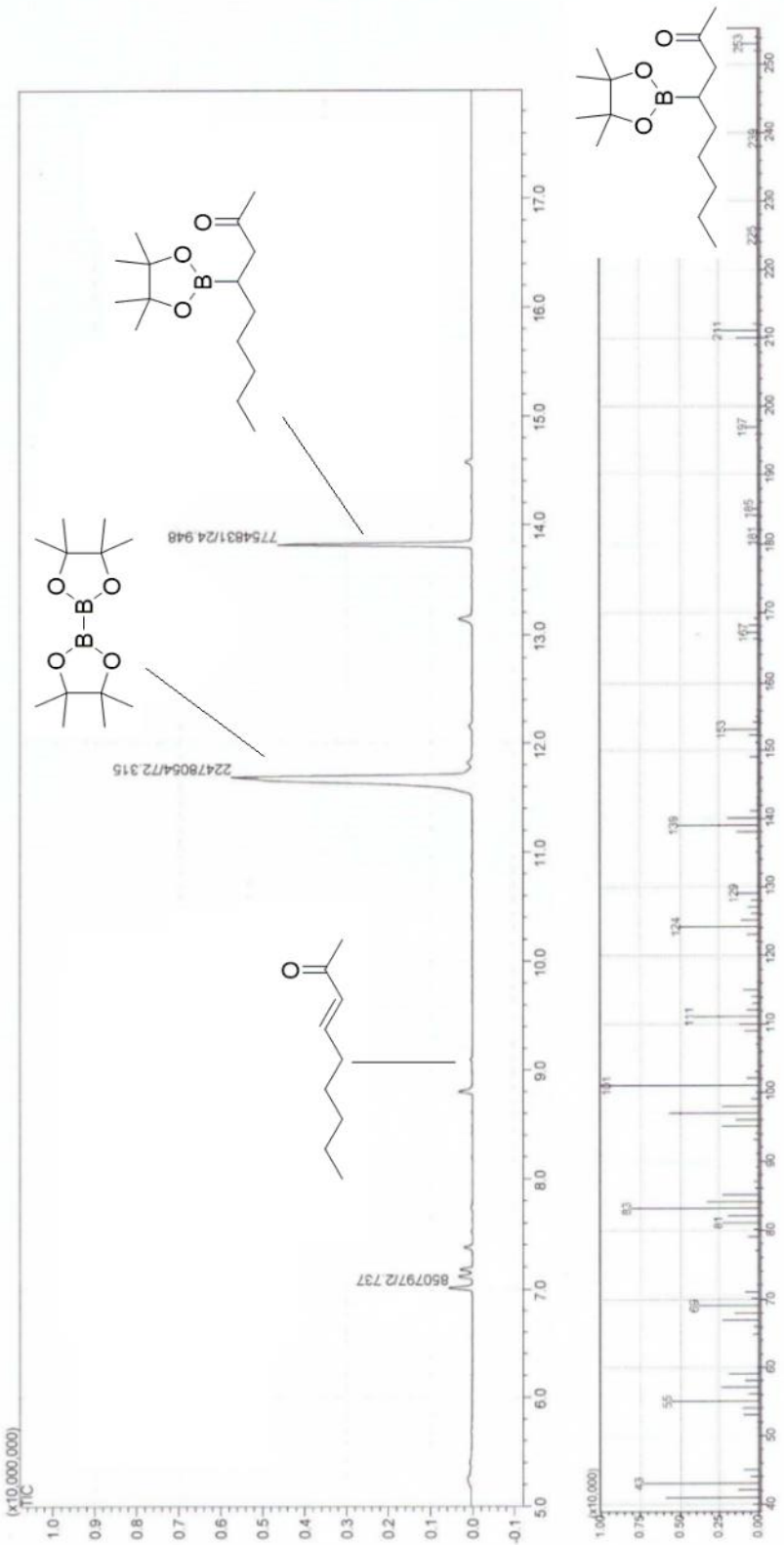


Figure A.38 GC-MS chromatogram spectrum of catalytic trial (Table 4.1, Entry 2)

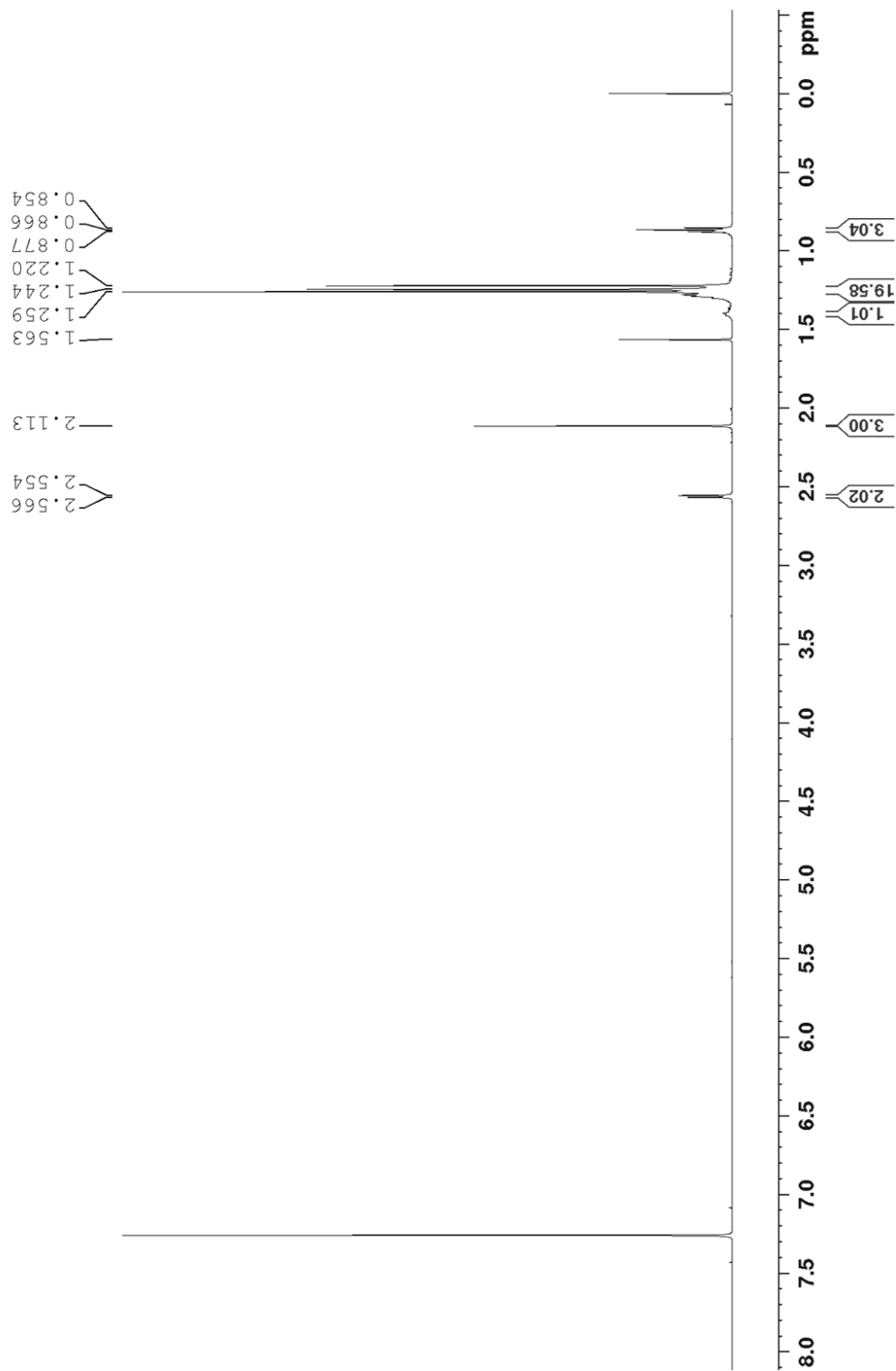


Figure A.39 ^1H NMR spectrum (600 MHz, CDCl_3) of isolated product (Table 4.1, Entry 2)

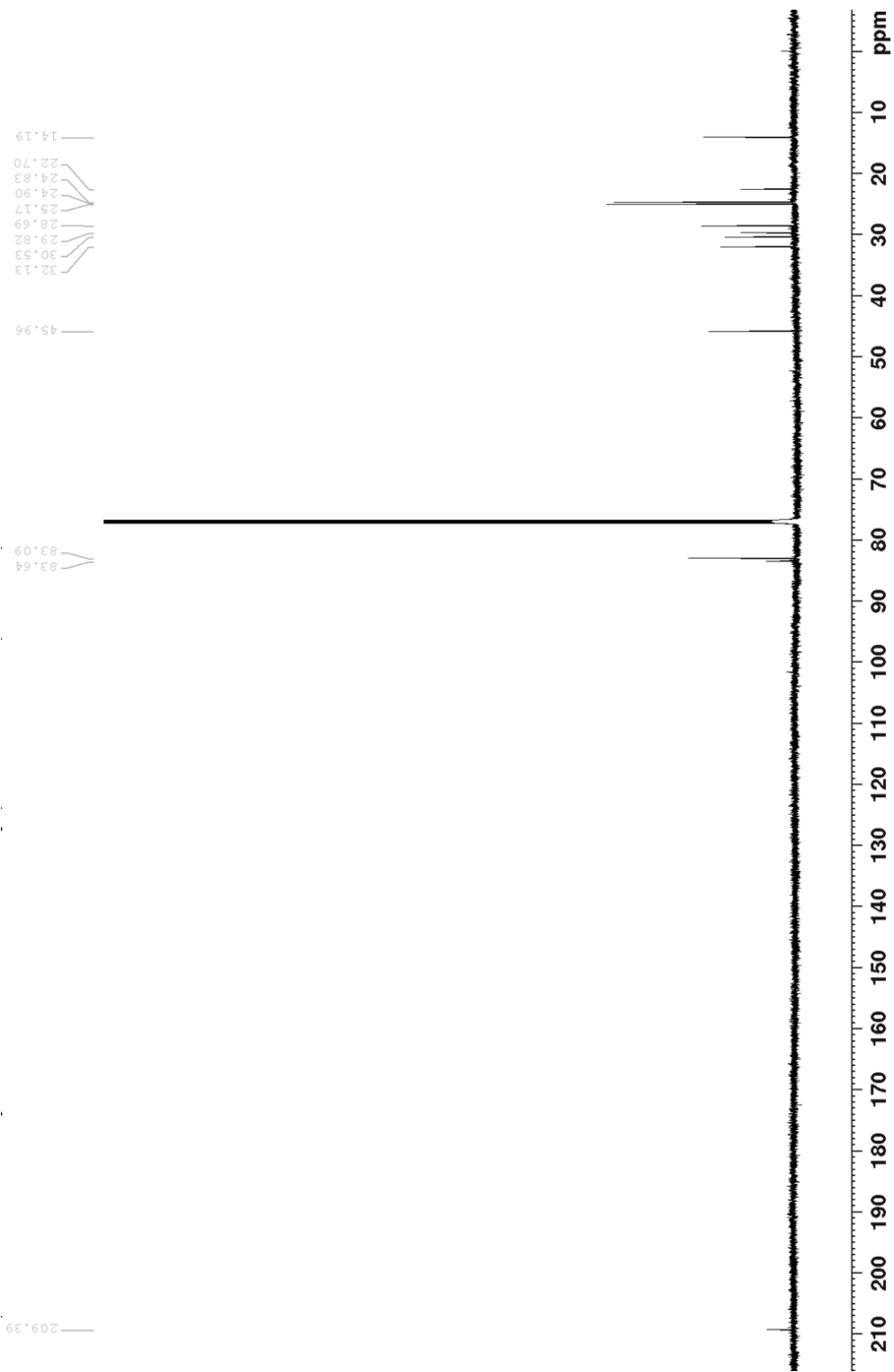


Figure A.40 ^{13}C NMR (150 MHz, CDCl_3) spectrum of isolated product (Table 4.1, Entry 2)

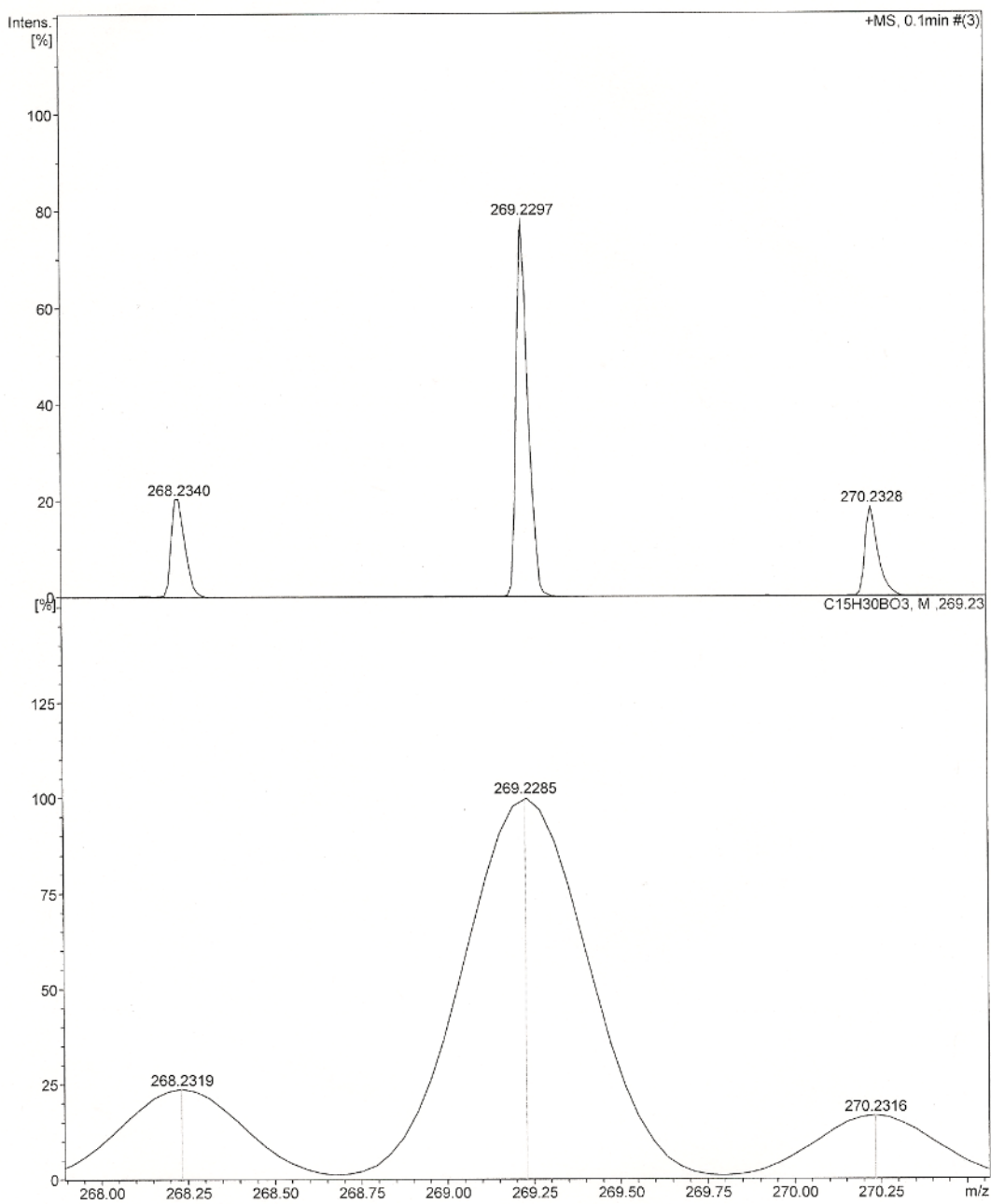


Figure A.41 HRMS of product (Table 4.1, Entry 2)

HRMS-ESI (m/z): $[\text{M}+\text{H}]^+$ calcd (bottom) for $\text{C}_{15}\text{H}_{30}\text{BO}_3$, 269.2285; found (top) 269.2297

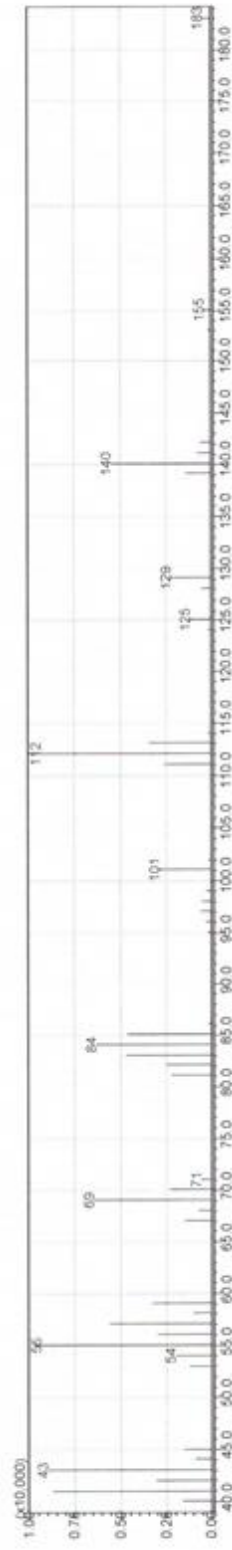
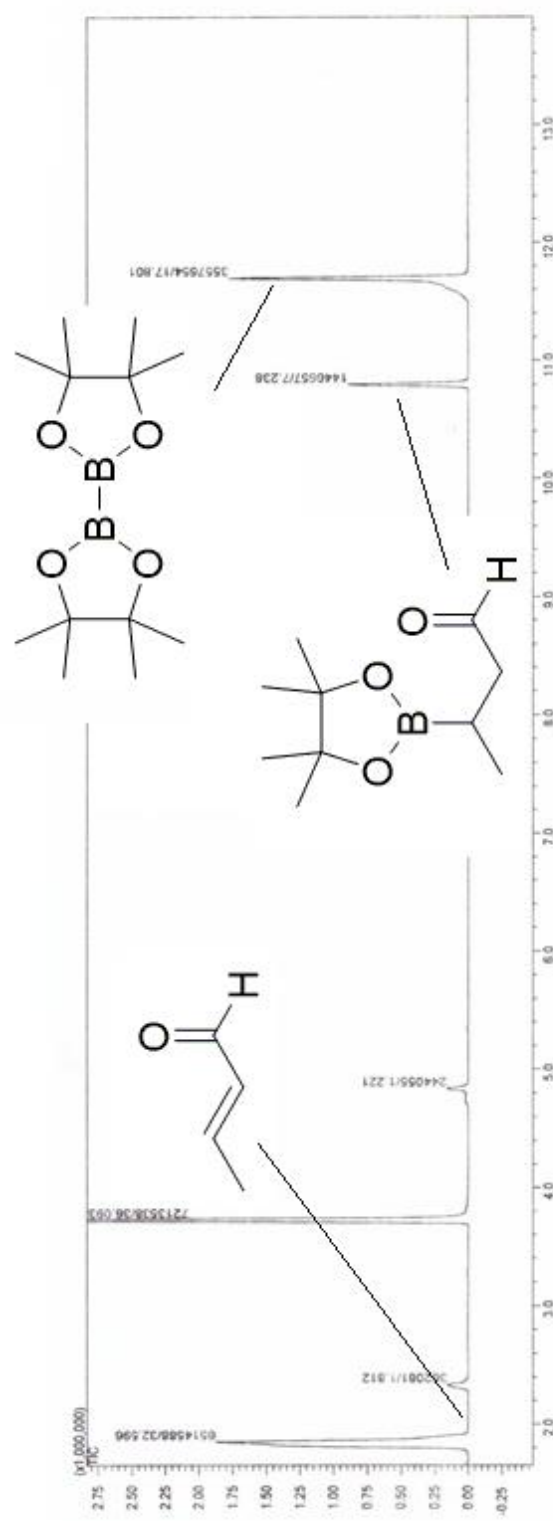


Figure A.42 GC-MS chromatogram spectrum of catalytic trial (Table 4.2, Entry 1)

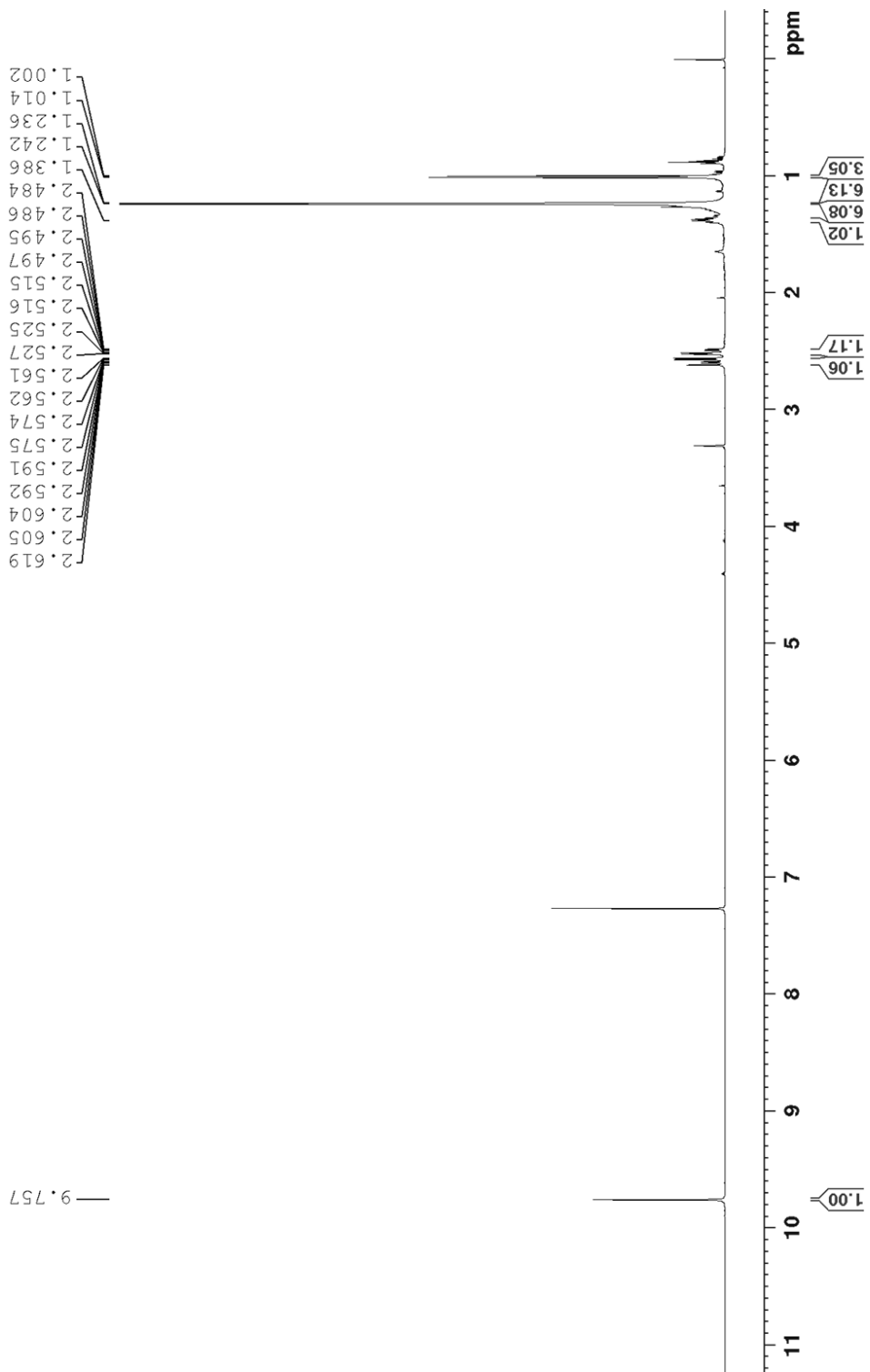


Figure A.43 ${}^1\text{H}$ NMR (600 MHz, CDCl_3) spectrum of isolated product (Table 4.2, Entry 1)

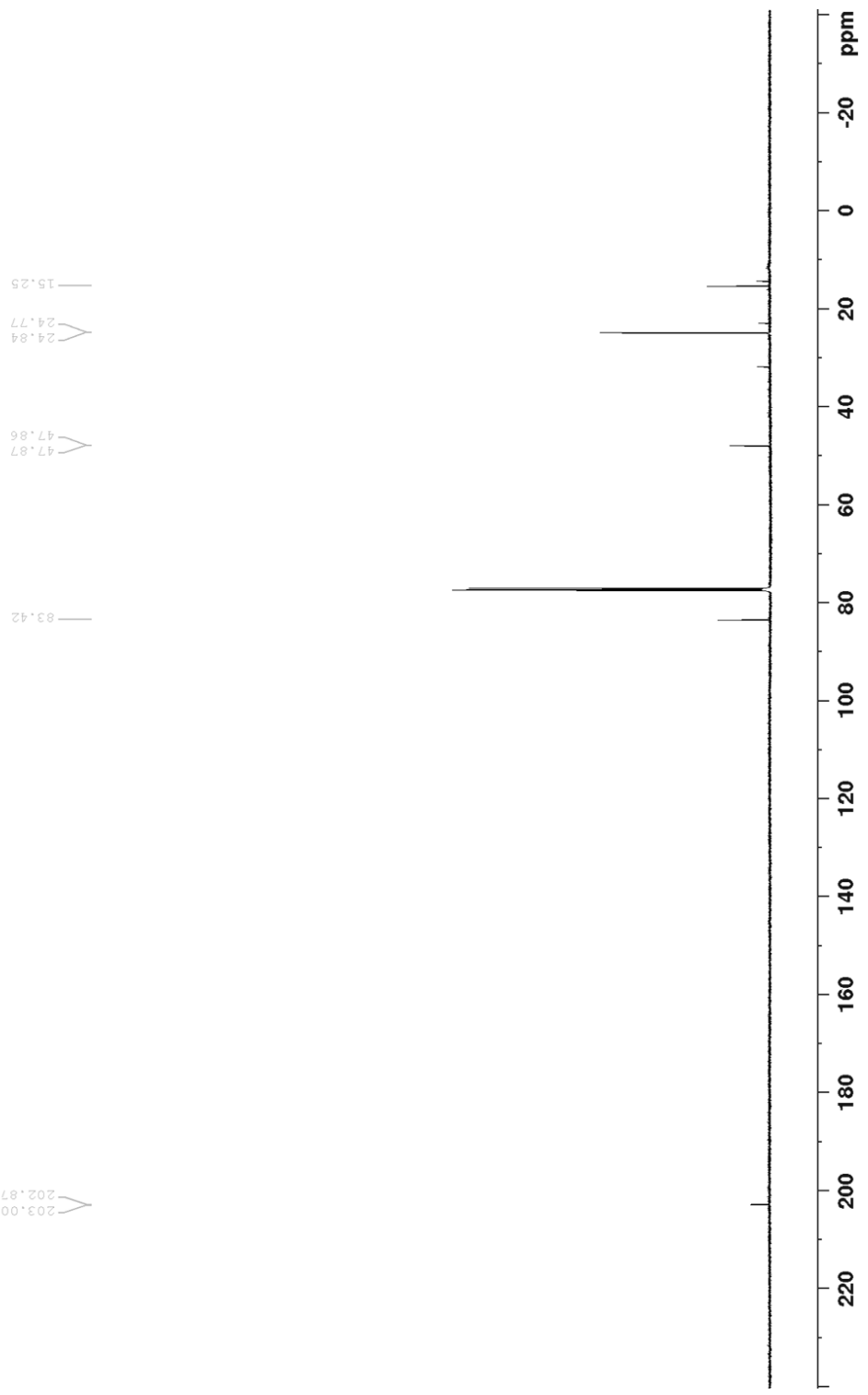


Figure A.44 ^{13}C NMR (150 MHz, CDCl_3) spectrum of isolated product (Table 4.2, Entry 1)

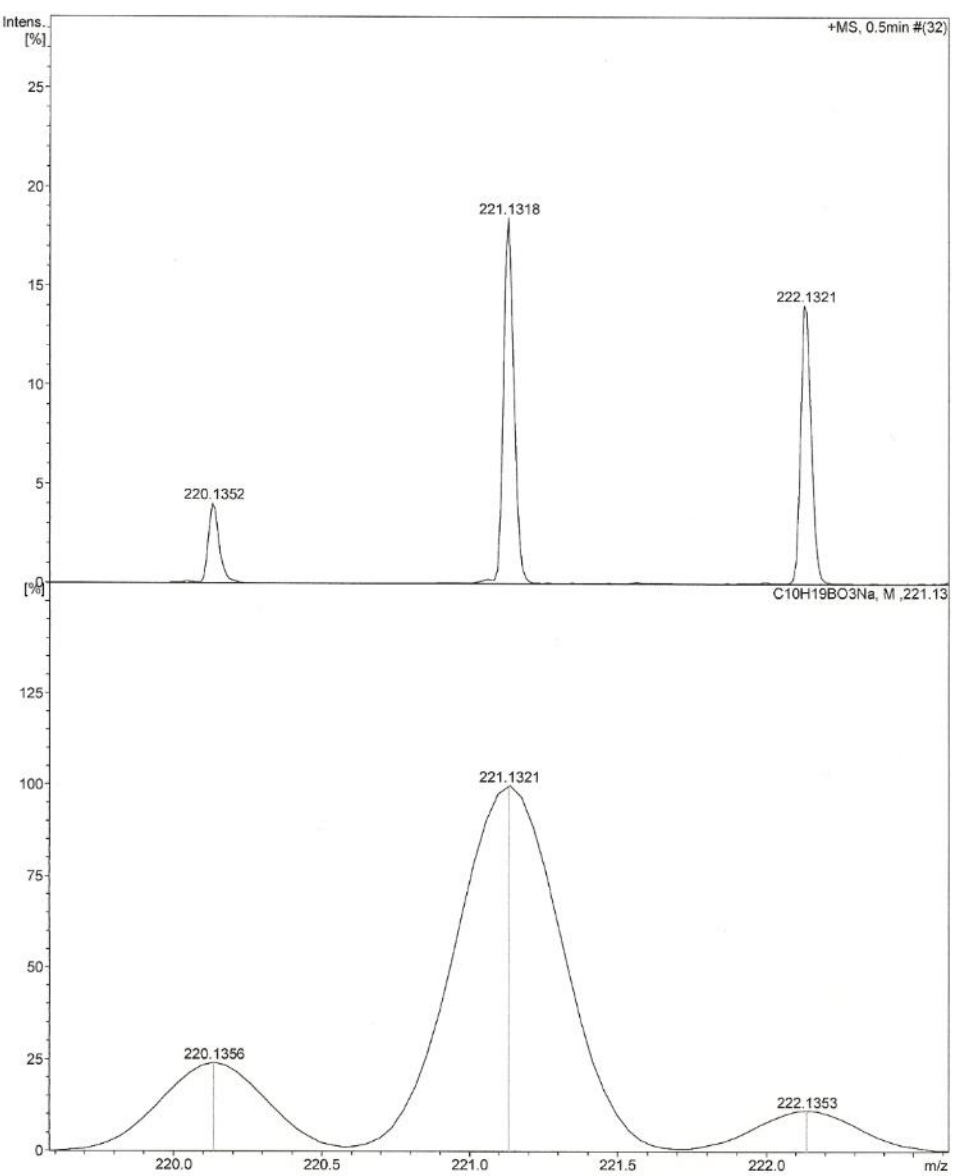


Figure A.45 HRMS of product (Table 4.2, Entry 1)

HRMS-ESI (m/z): $[M+H]^+$ calcd (B) for $C_{10}H_{19}BO_3$, 199.1502; found (A), 199.1506

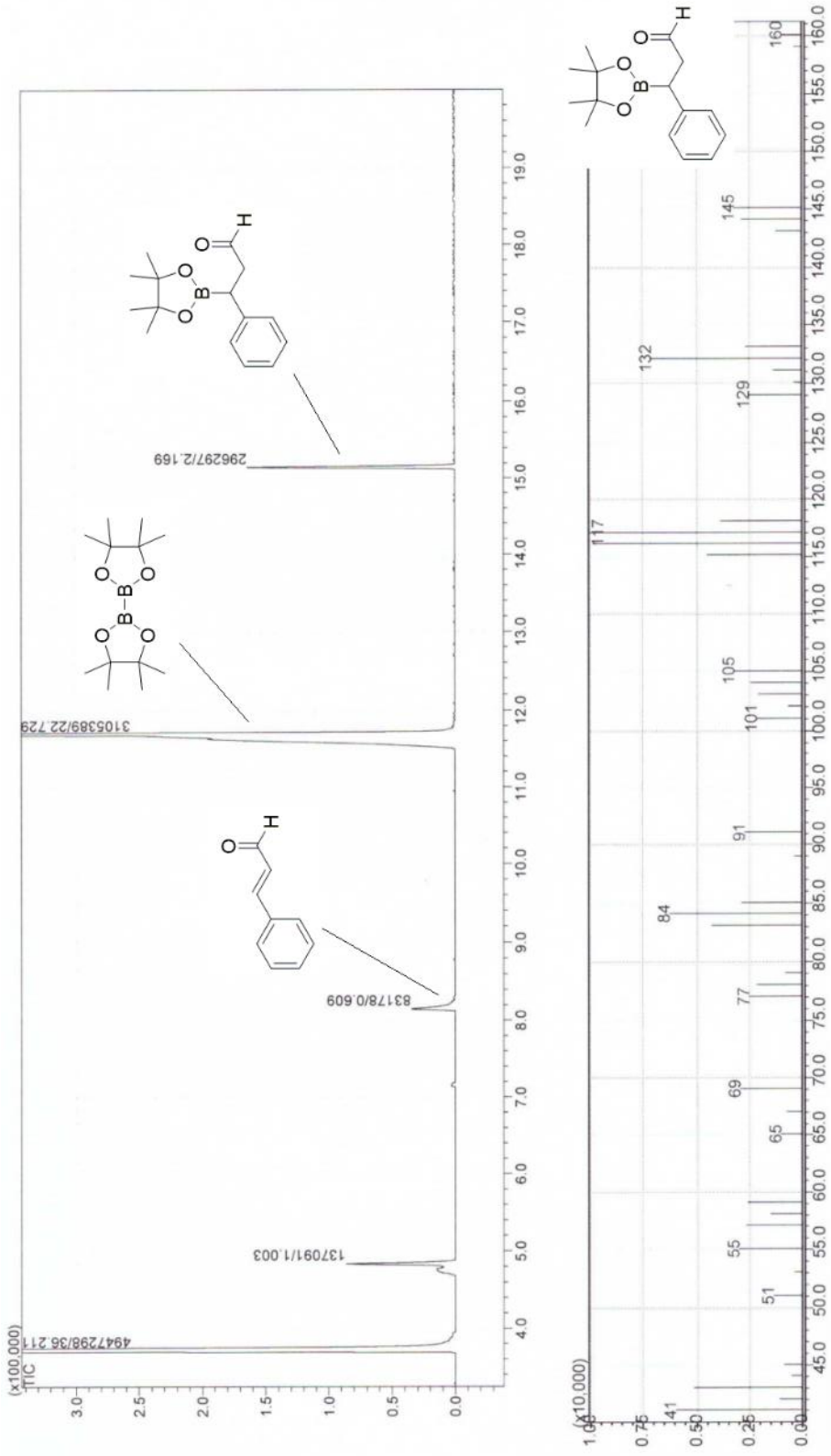


Figure A.46 GC-MS chromatogram spectrum of catalytic trial (Table 4.2, Entry 2)

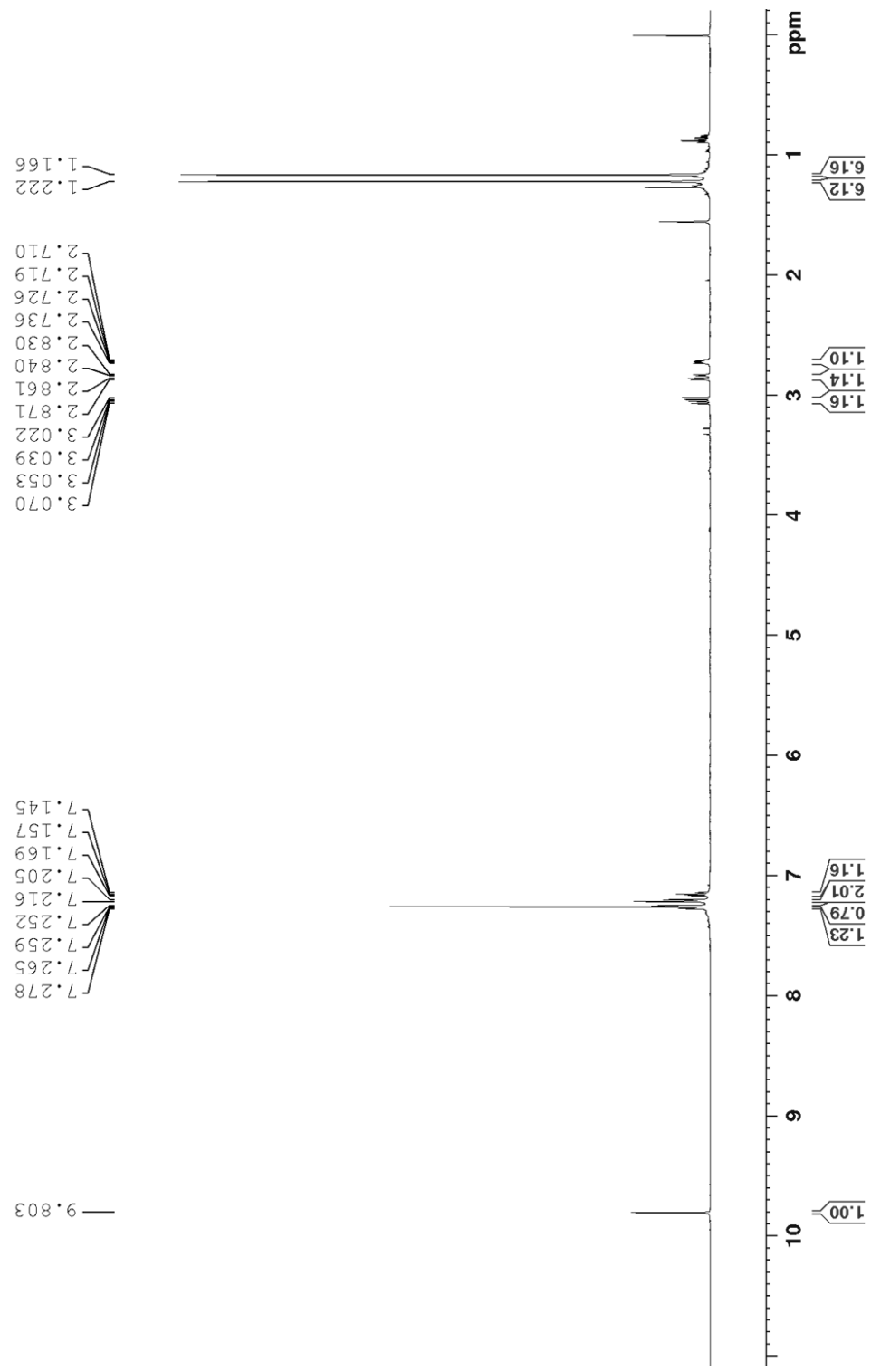


Figure A.47 ^1H NMR (600 MHz, CDCl_3) spectrum of isolated product (Table 4.2, Entry 2)

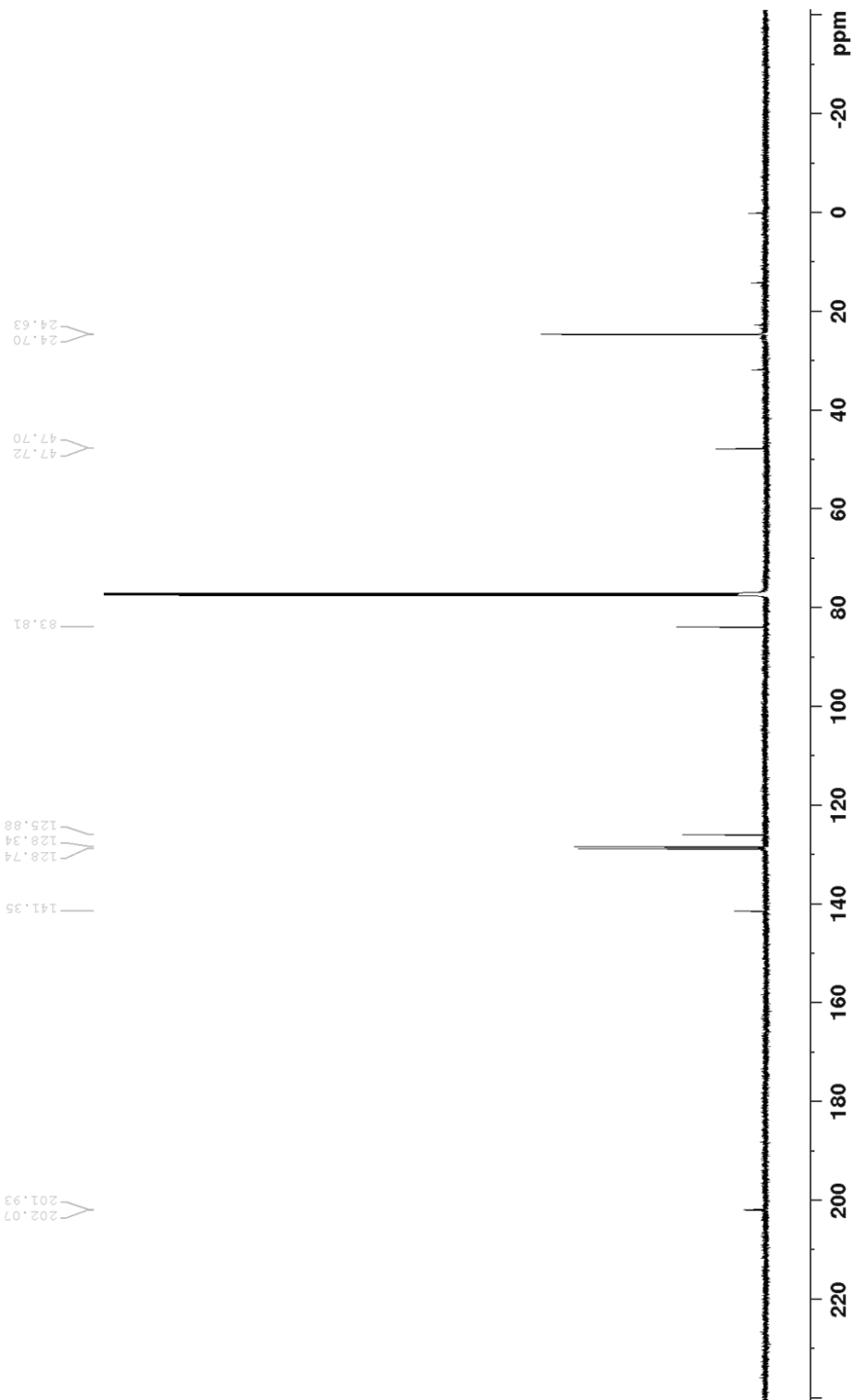


Figure A.48 ^{13}C NMR (150 MHz, CDCl_3) spectrum of isolated product (Table 4.2, Entry 2)

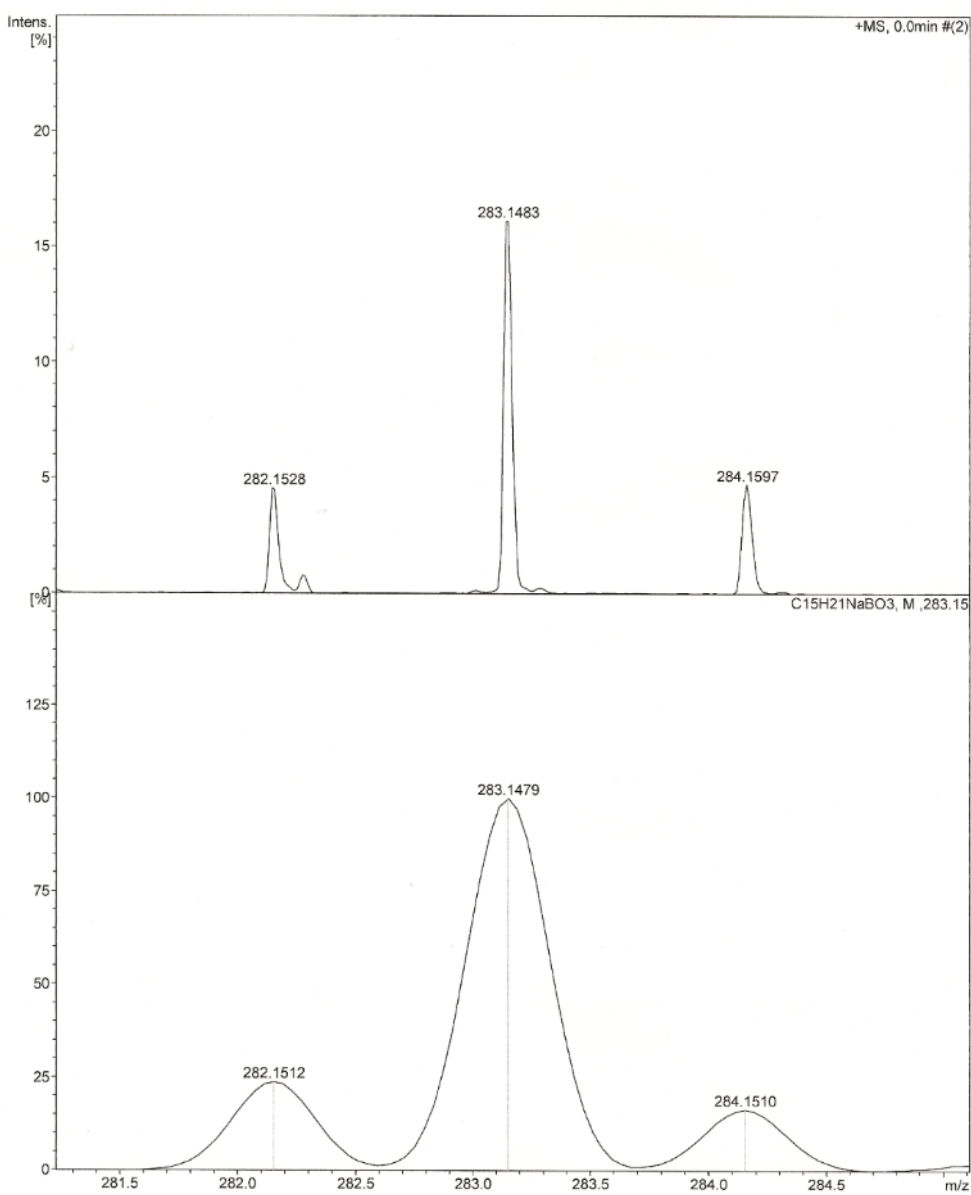


Figure A.49 HRMS of product (Table 4.2, Entry 2)

HRMS-ESI (m/z): [M-OH]⁺ calcd (bottom) for C₁₅H₂₀BO₂, 243.1554; found (top) 243.1559

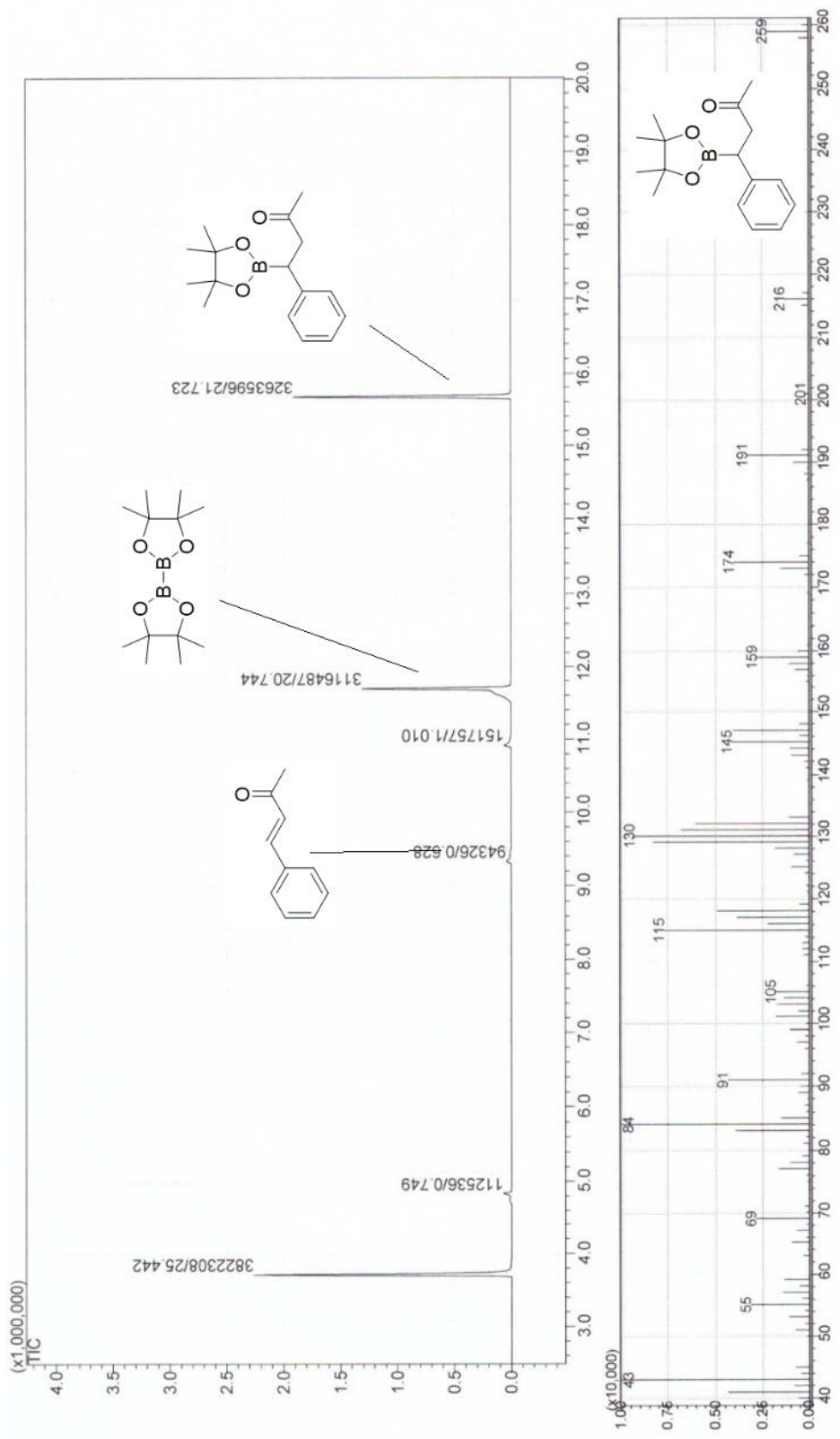


Figure A.50 GC-MS chromatogram spectrum of catalytic trial (Table 4.2, Entry 3)

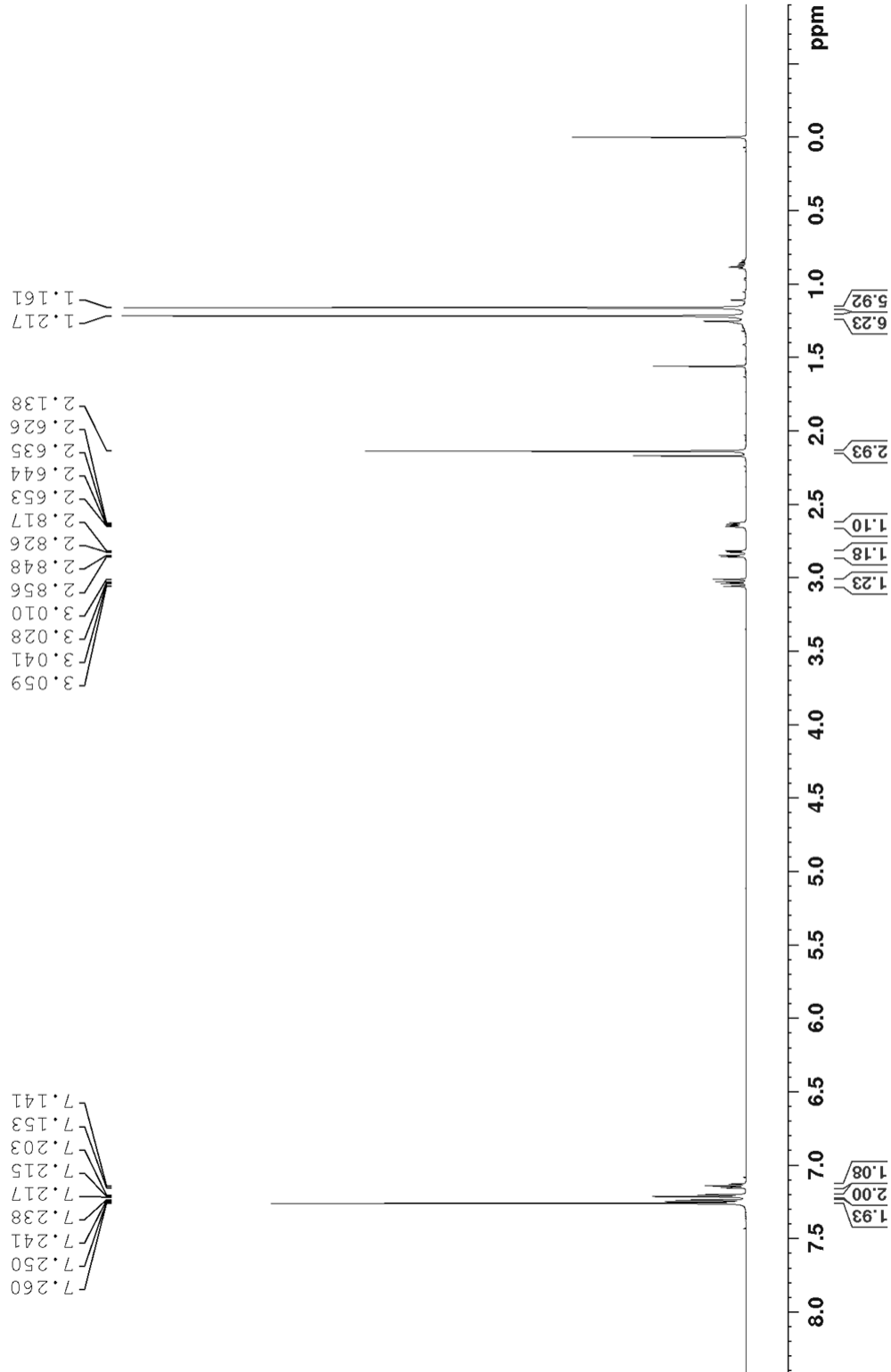


Figure A.51 ^1H NMR (600 MHz, CDCl_3) spectrum of isolated product (Table 4.2, Entry 3)

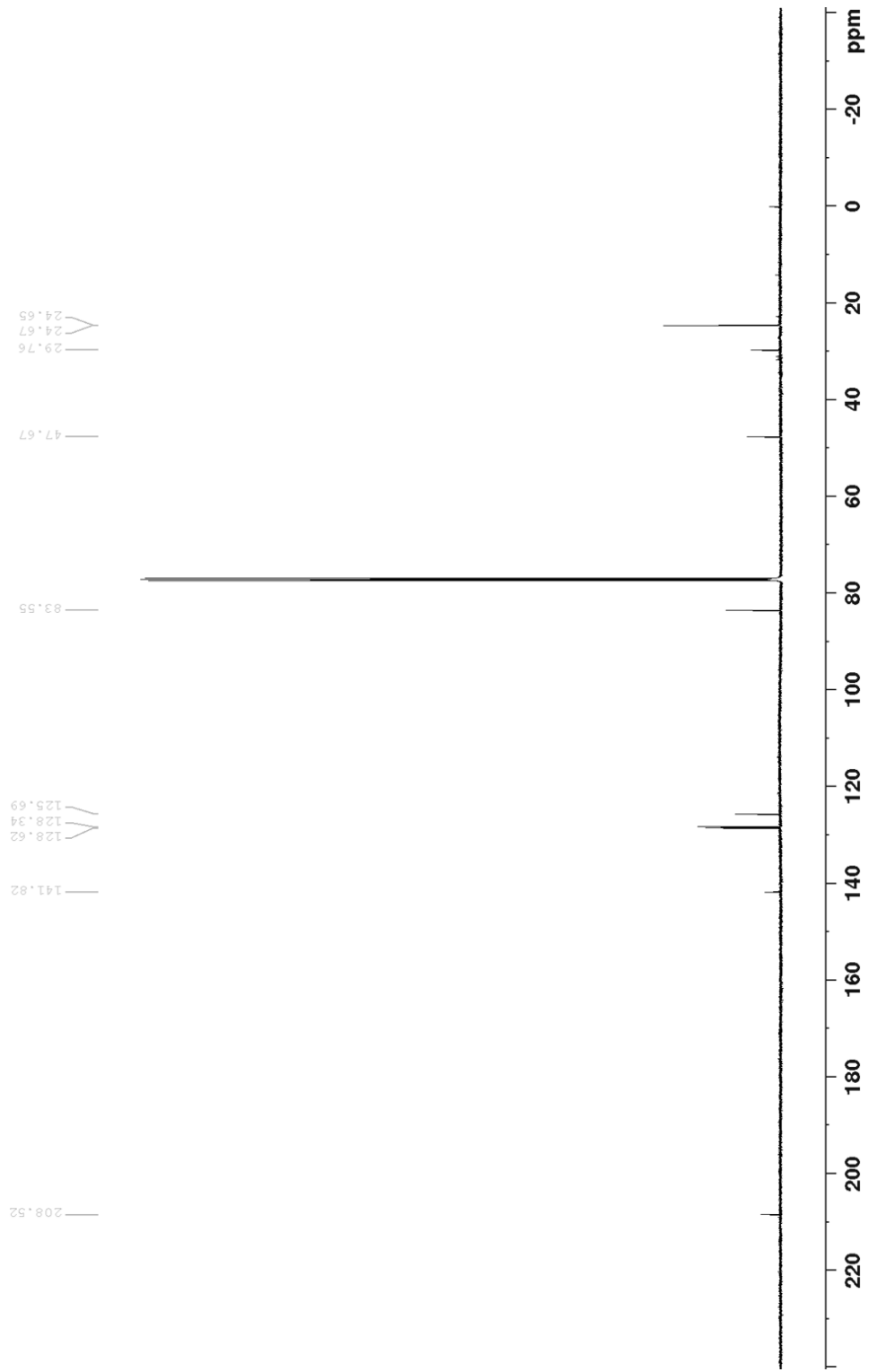


Figure A.52 ^{13}C NMR (150 MHz, CDCl_3) spectrum of isolated product (Table 4.2, Entry 3)

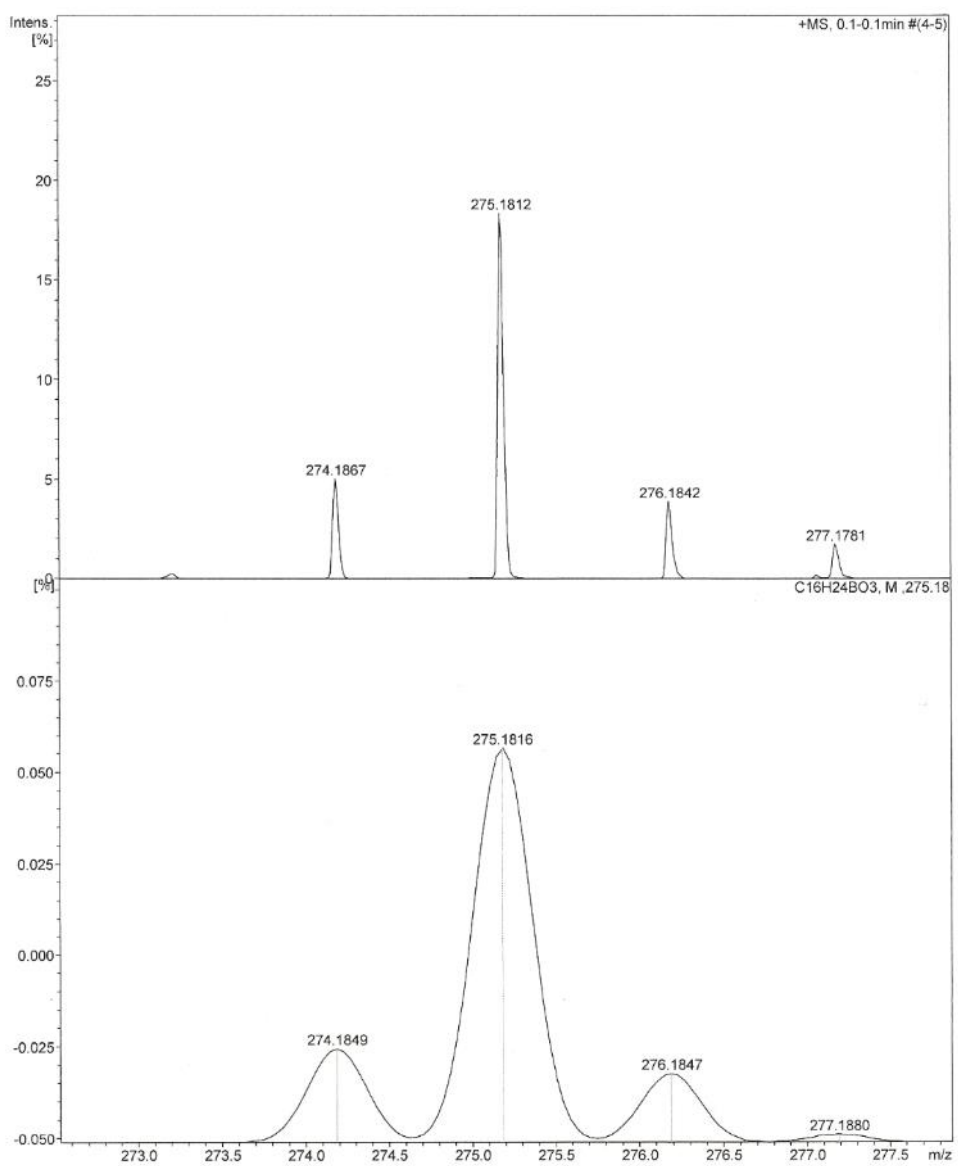


Figure A.53 HRMS of product (Table 4.2, Entry 3)

HRMS-ESI (m/z): $[M+H]^+$ calcd (bottom) for C₁₆H₂₄BO₃, 275.1816; found (top)
275.1812

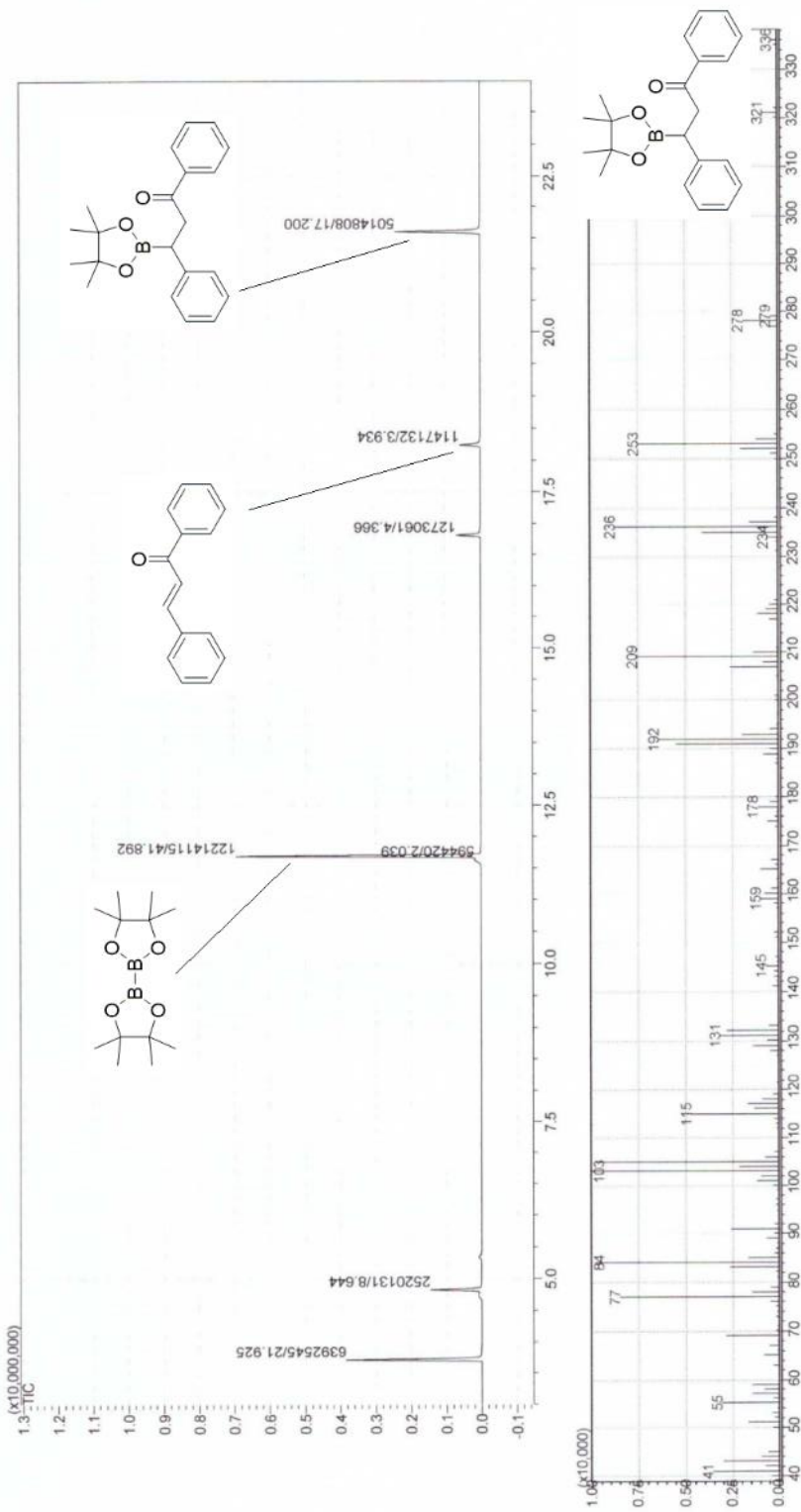


Figure A.54 GC-MS chromatogram spectrum of catalytic trial (Table 4.2, Entry 4)

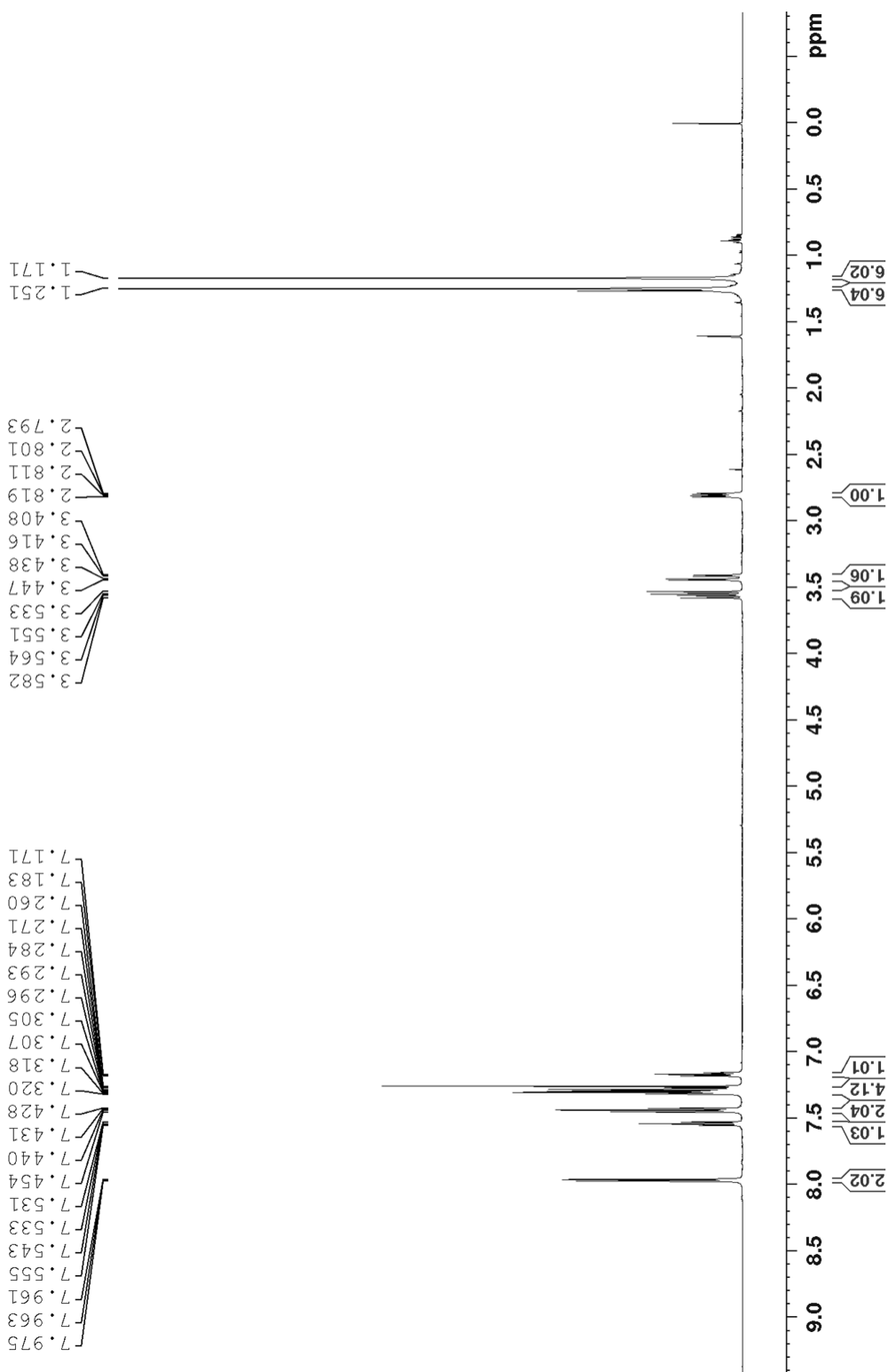


Figure A.55 ^1H NMR (600 MHz, CDCl_3) spectrum of isolated product (Table 4.2, Entry 4)

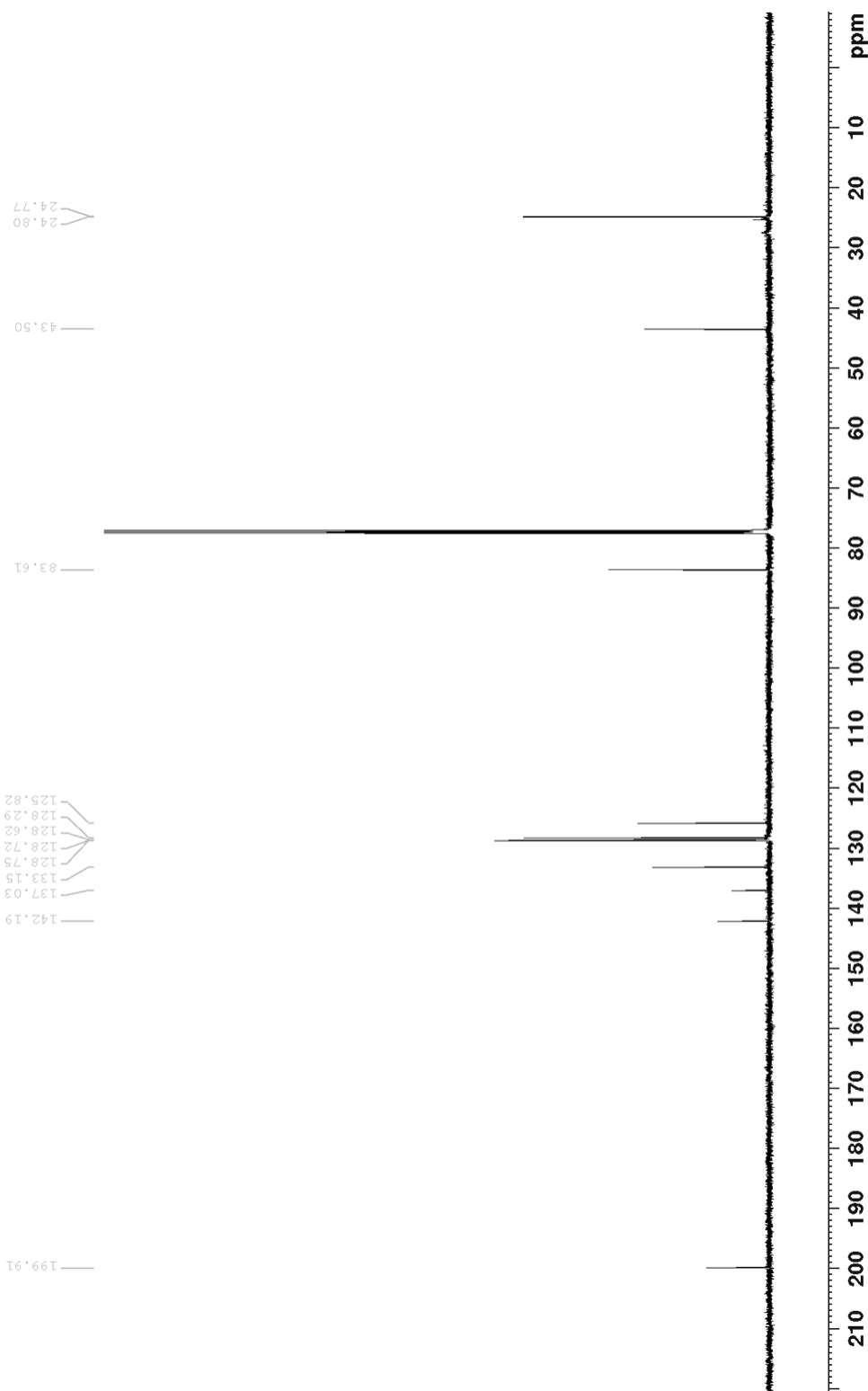


Figure A.56 ^{13}C NMR (150 MHz, CDCl_3) spectrum of isolated product (Table 4.2, Entry 4)

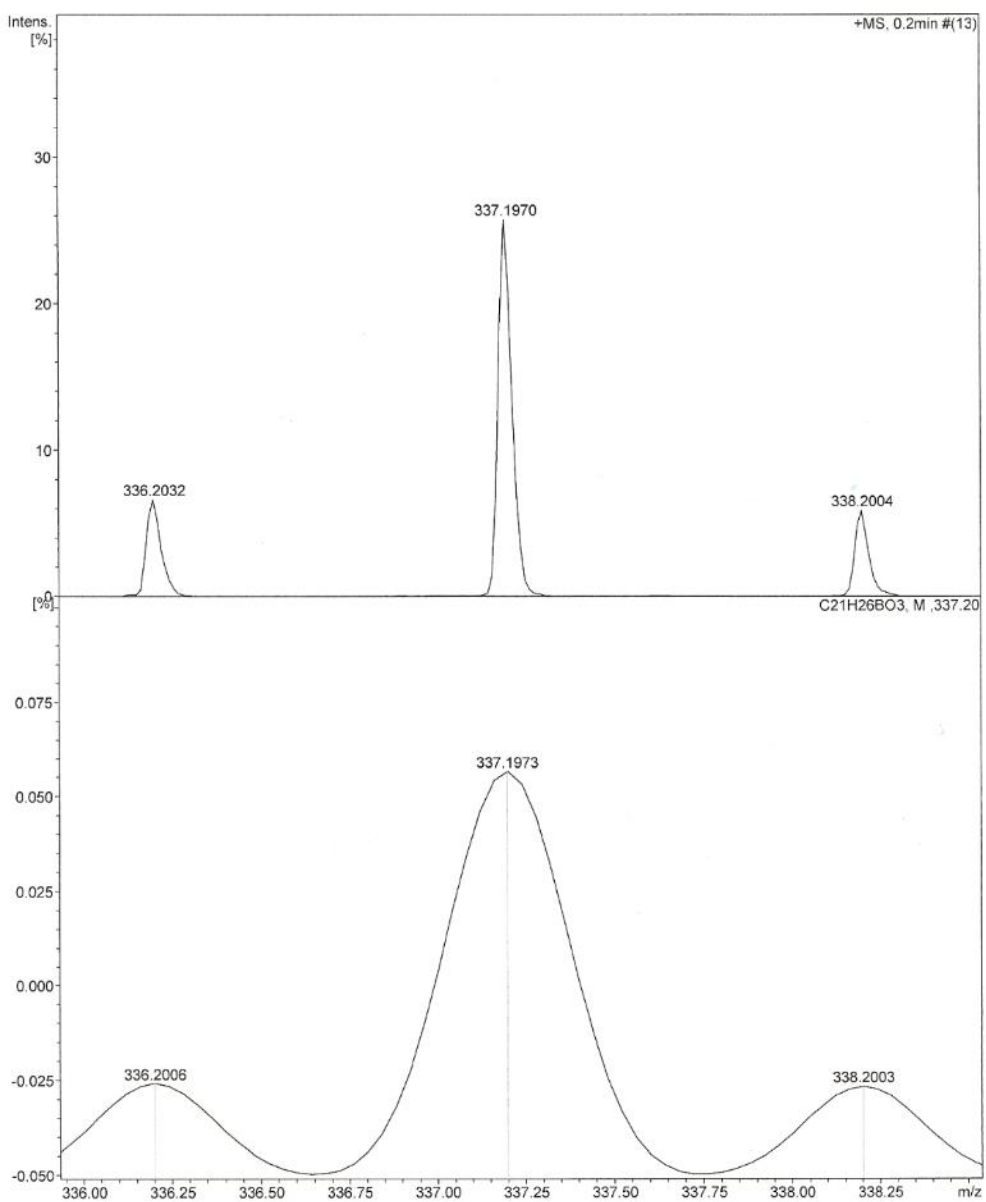


Figure A.57 HRMS of product (Table 4.2, Entry 4)

HRMS-ESI (m/z): $[M+H]^+$ calcd (bottom) for $C_{25}H_{26}BO_3$, 337.1970; found (top) 337.1973

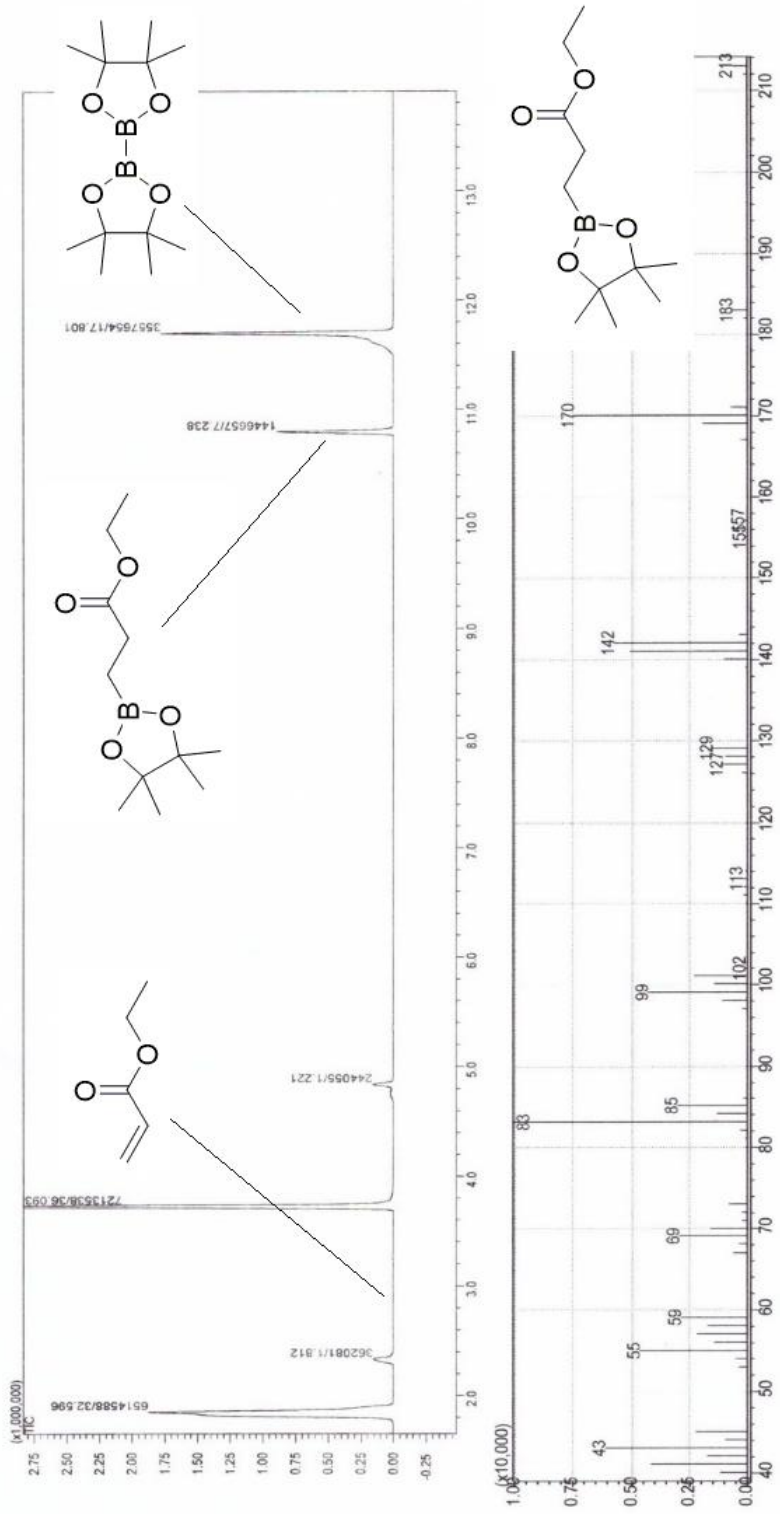


Figure A.58 GC-MS chromatogram spectrum of catalytic trial (Table 4.2, Entry 7)

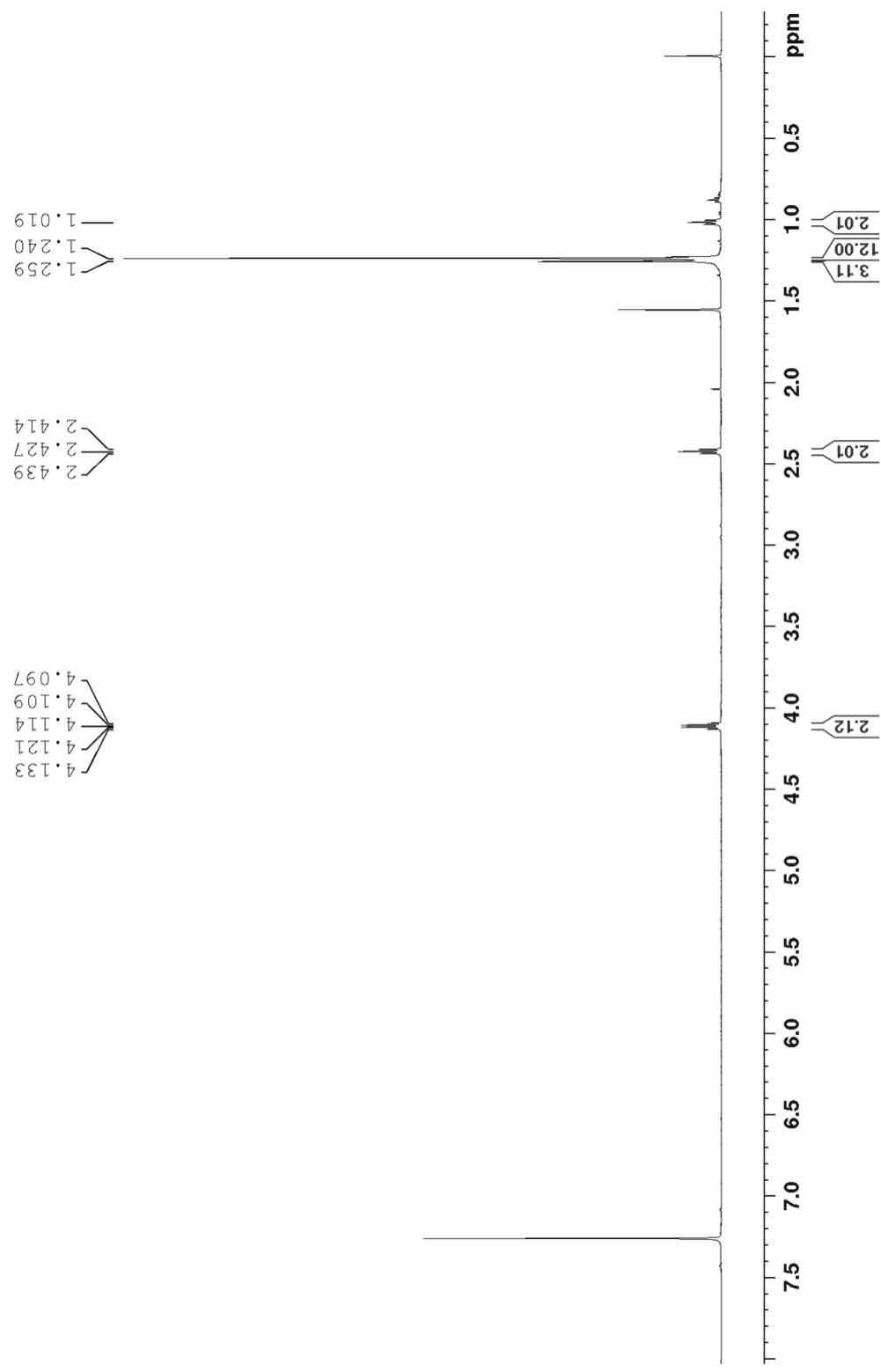


Figure A.59 ${}^1\text{H}$ NMR (600 MHz, CDCl_3) spectrum of isolated product (Table 4.2, Entry 7)

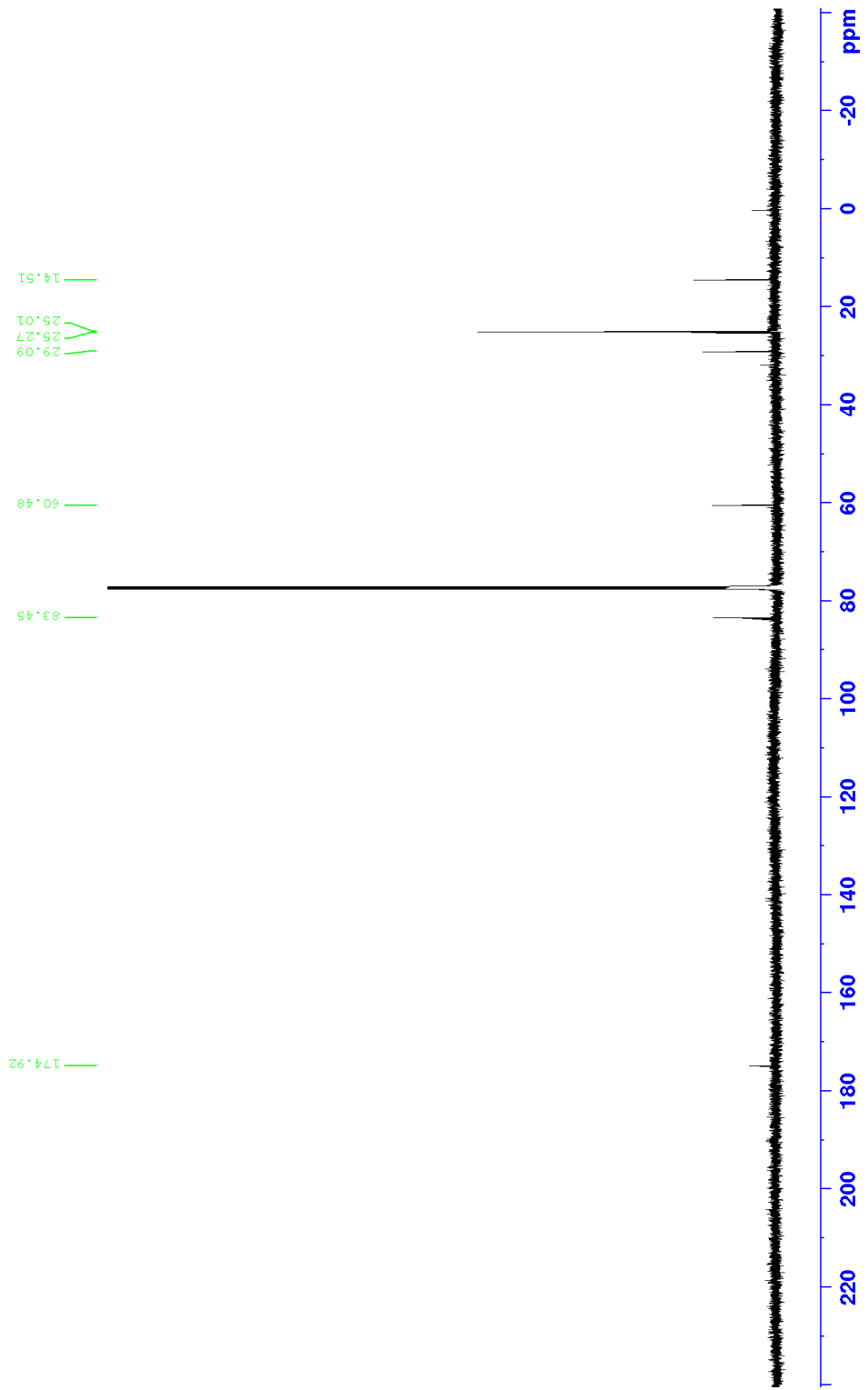


Figure A.60 ^{13}C NMR spectrum (150 MHz, CDCl_3) of isolated product (Table 4.2, Entry 7)

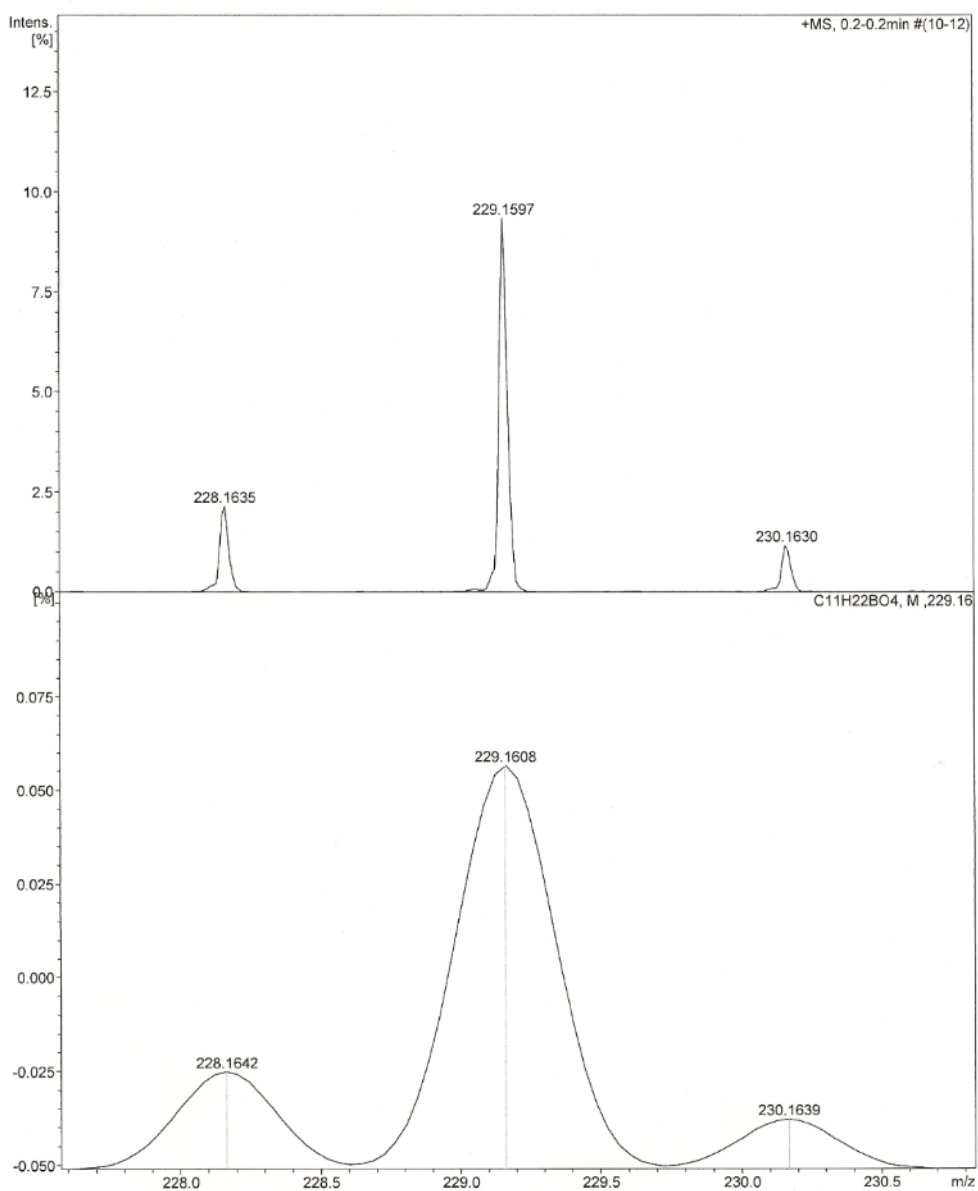


Figure A.61 HRMS of product (Table 4.2, Entry 7)

HRMS-ESI (m/z): $[M+H]^+$ calcd (bottom) for $C_{11}H_{22}BO_4$, 229.1608; found (top) 229.1597

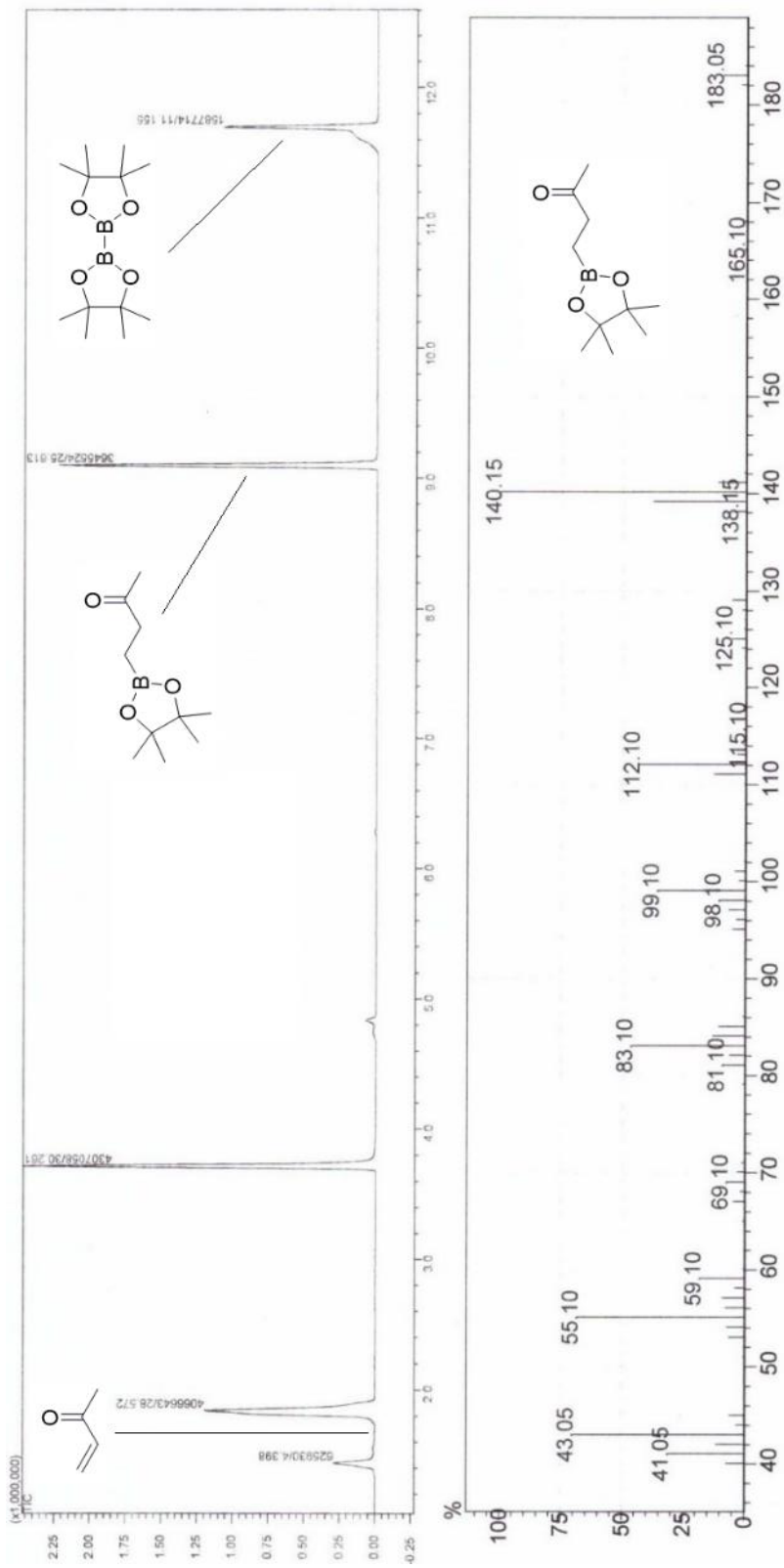


Figure A.62 GC-MS chromatogram spectrum of catalytic trial (Table 4.2, Entry 8)

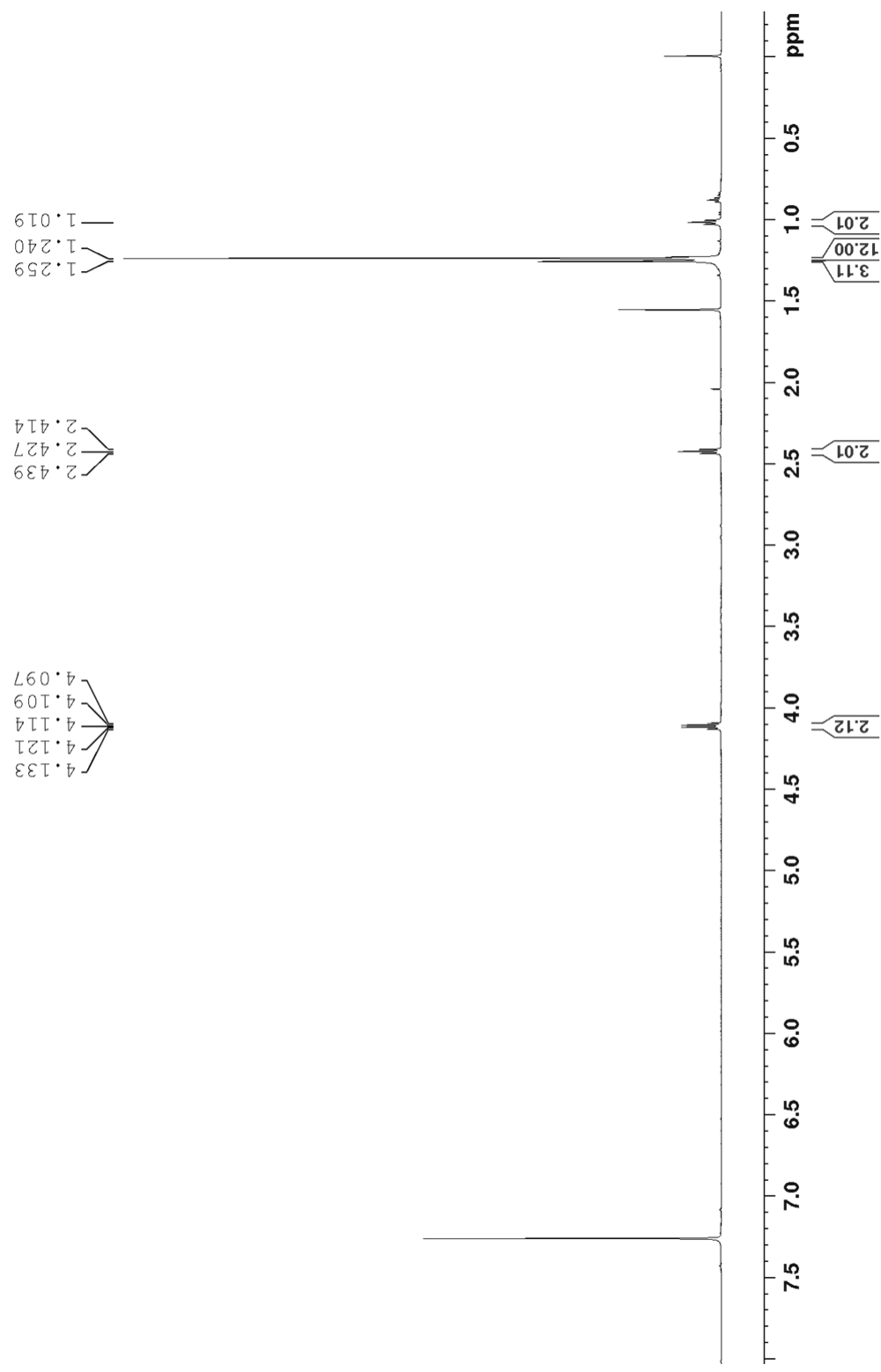


Figure A.63 ${}^1\text{H}$ NMR (600 MHz, CDCl_3) spectrum of isolated product (Table 4.2, Entry 8)

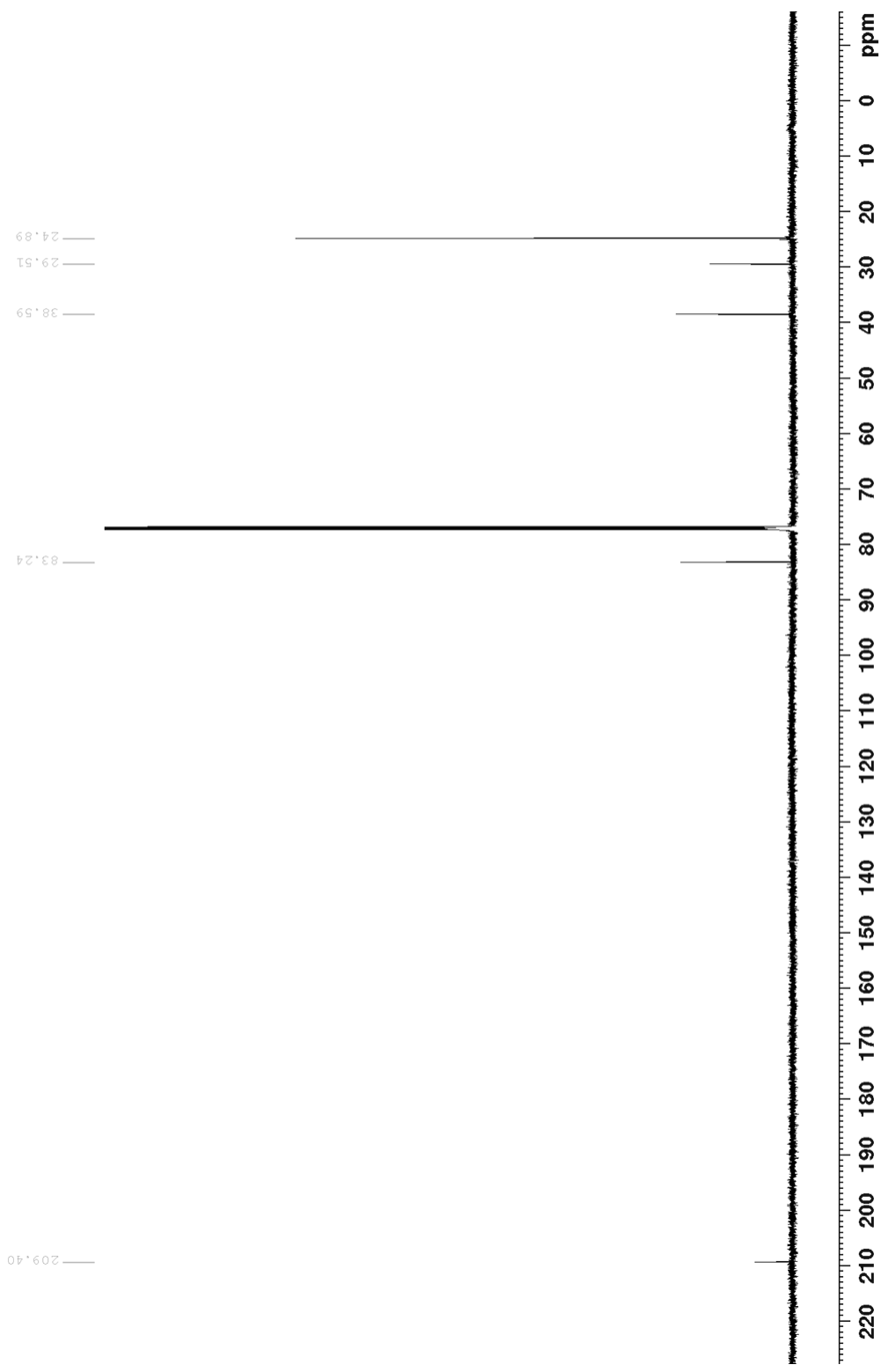


Figure A.64 ^{13}C NMR (150 MHz, CDCl_3) spectrum of isolated product (Table 4.2, Entry 8)

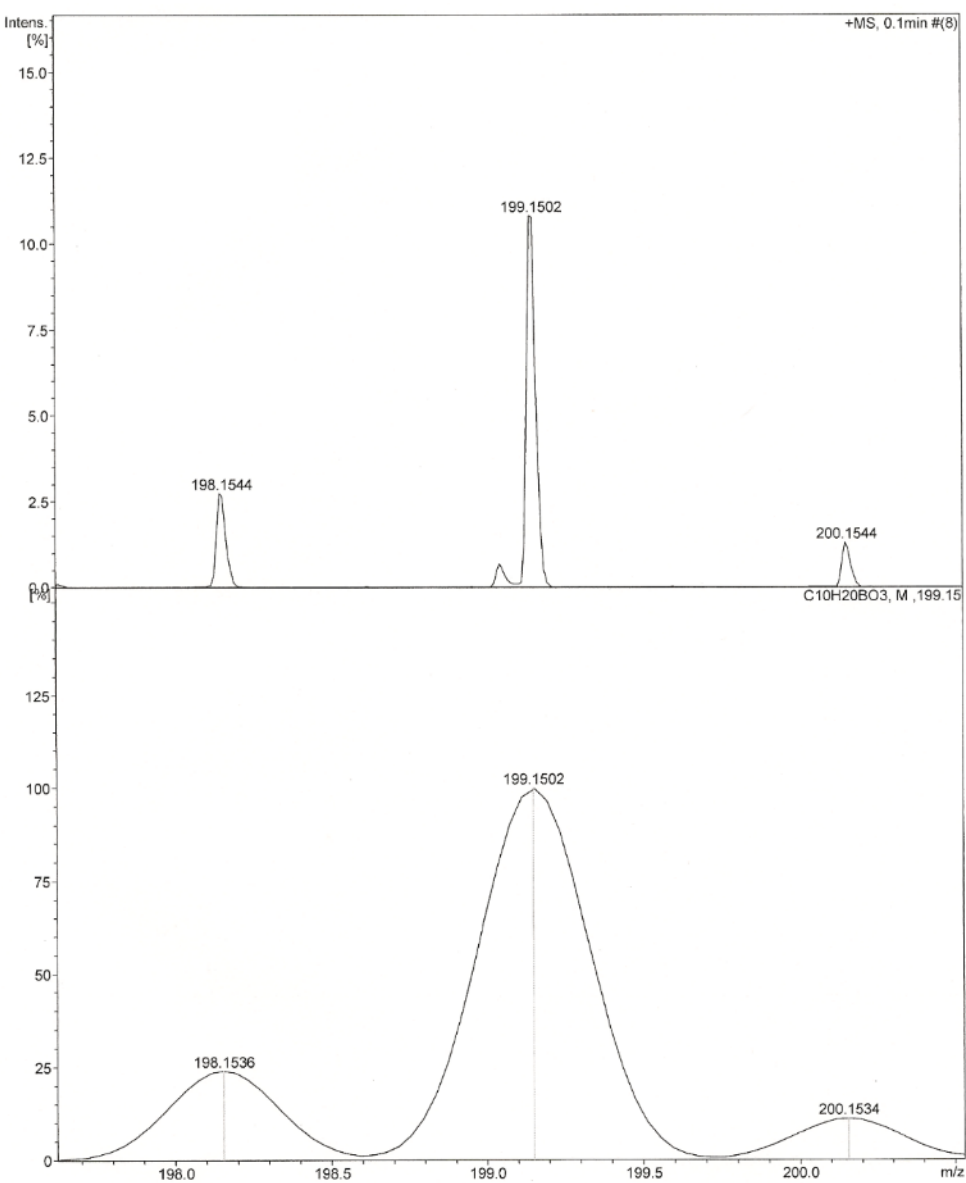


Figure A.65 HRMS of product (Table 4.2, Entry 8)

HRMS-ESI (m/z): $[M+H]^+$ calcd (bottom) for $C_{10}H_{20}BO_3$, 199.1502; found (top) 199.1502

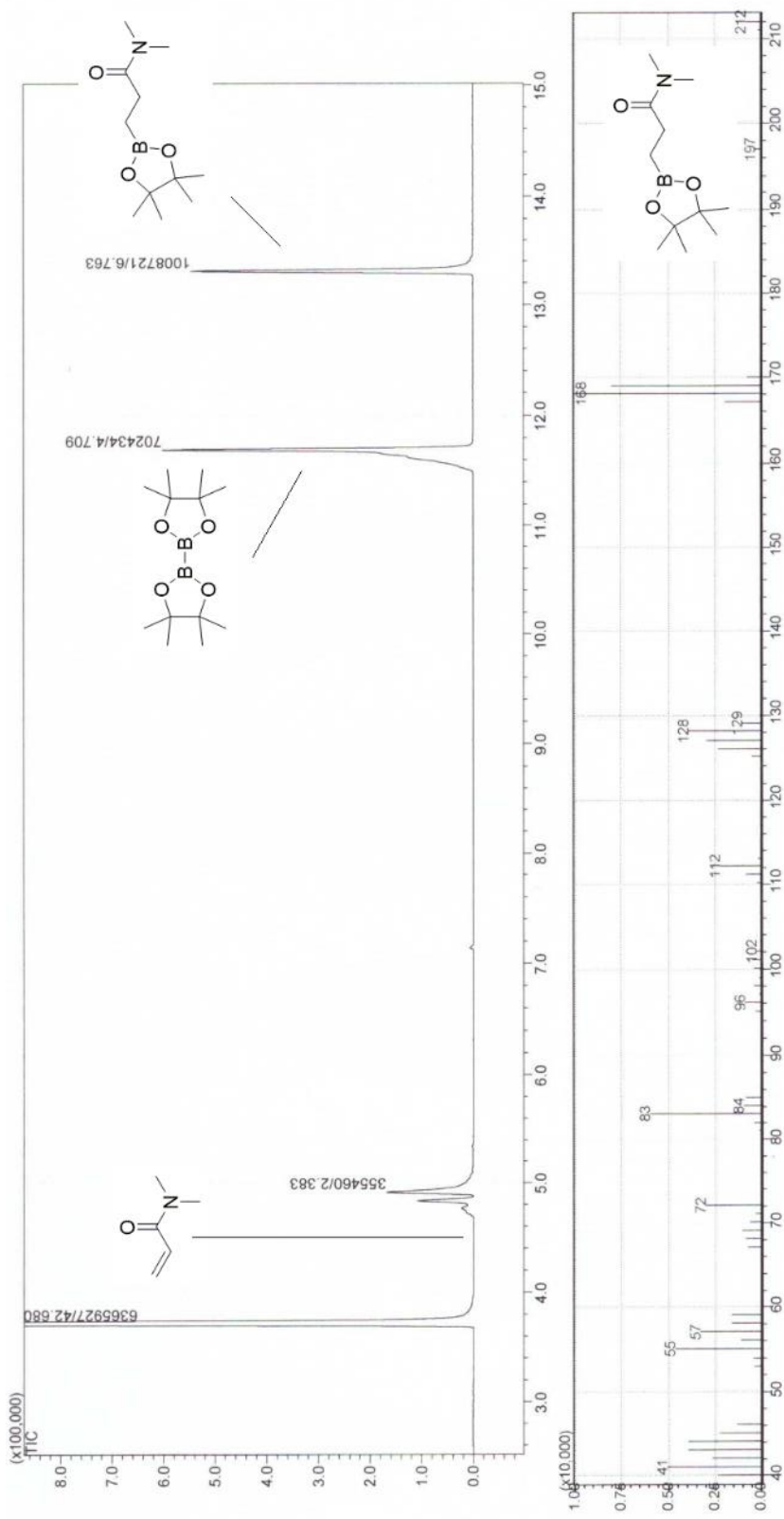


Figure A.66 GC-MS chromatogram spectrum of catalytic trial (Table 4.2, Entry 9)

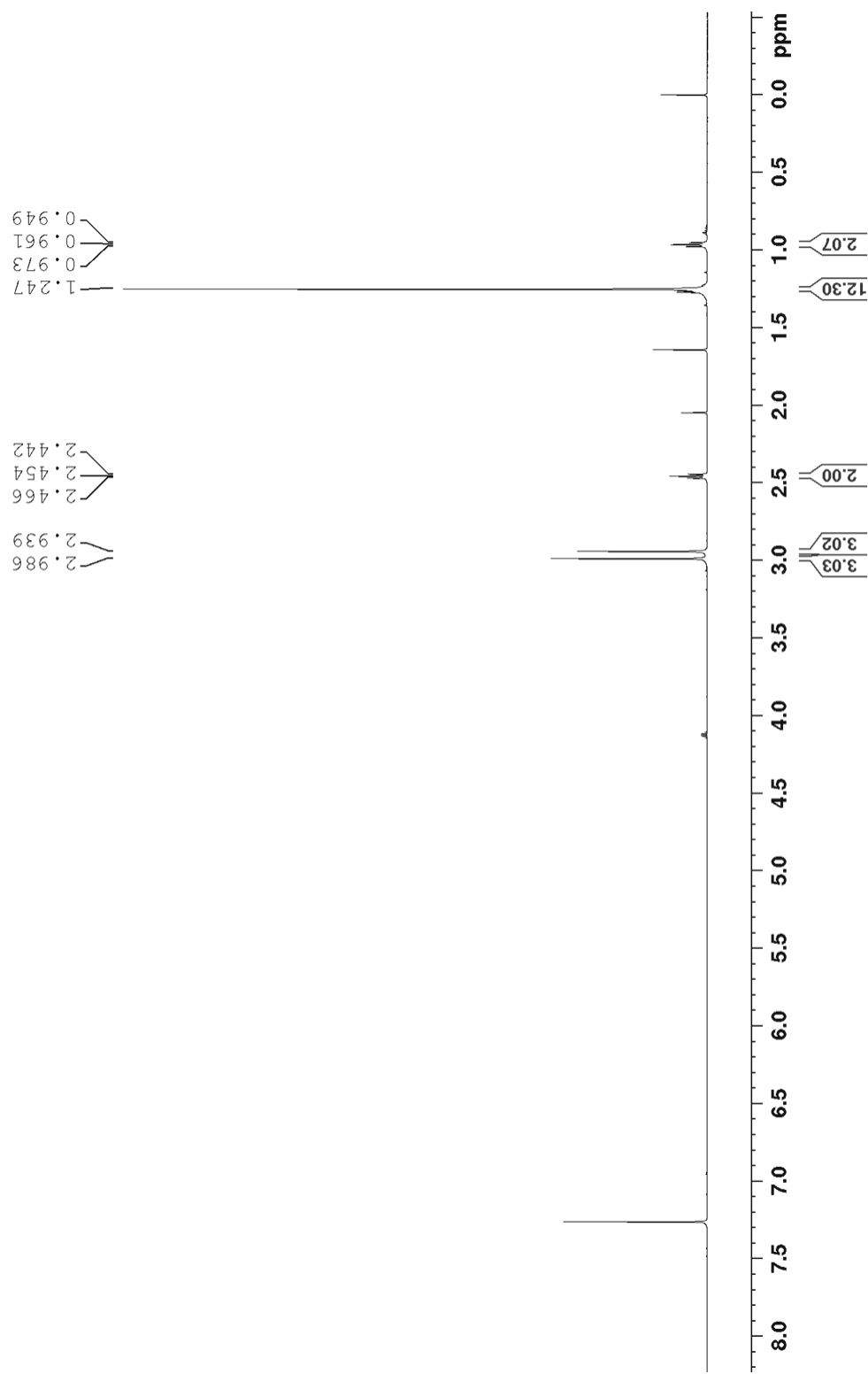


Figure A.67 ${}^1\text{H}$ NMR (600 MHz, CDCl_3) spectrum of isolated product (Table 4.2, Entry 10)

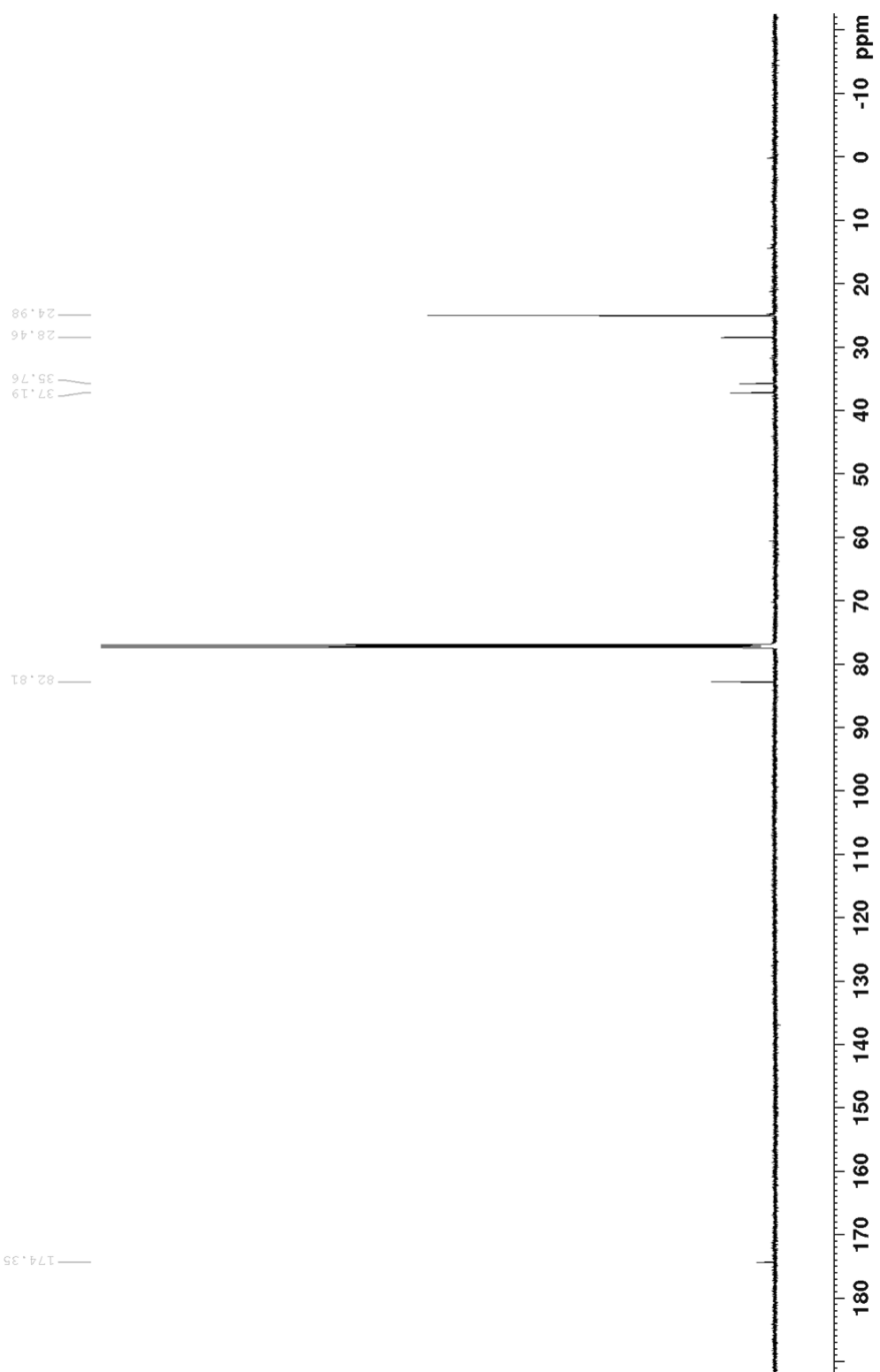


Figure A.68 ^{13}C NMR (150 MHz, CDCl_3) spectrum of isolated product (Table 4.2, Entry 10)

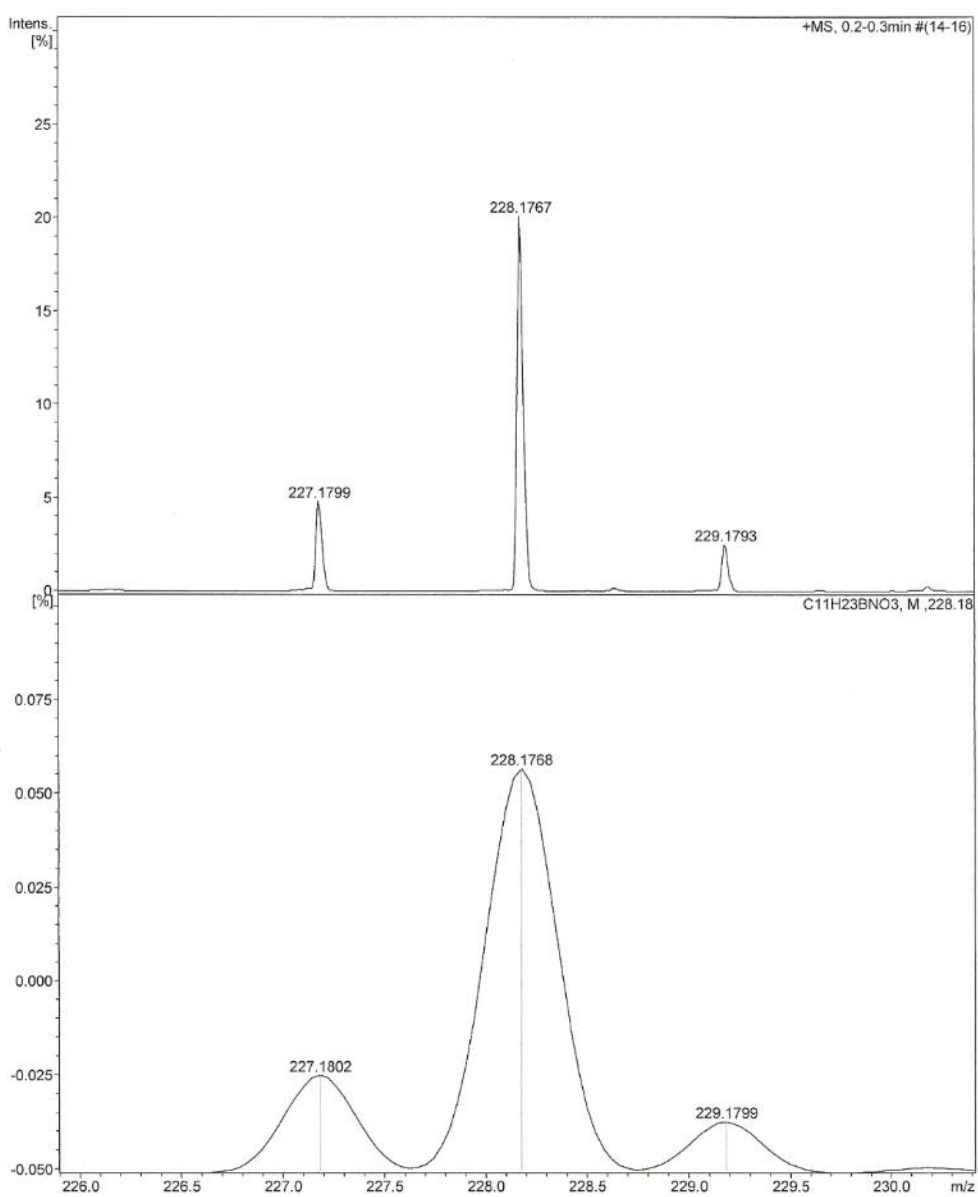


Figure A.69 HRMS of product (Table 4.2, Entry 10)

HRMS-ESI (m/z): $[M+H]^+$ calcd (bottom) for C₁₁H₂₃BNO₃, 228.1768; found (top) 228.1767

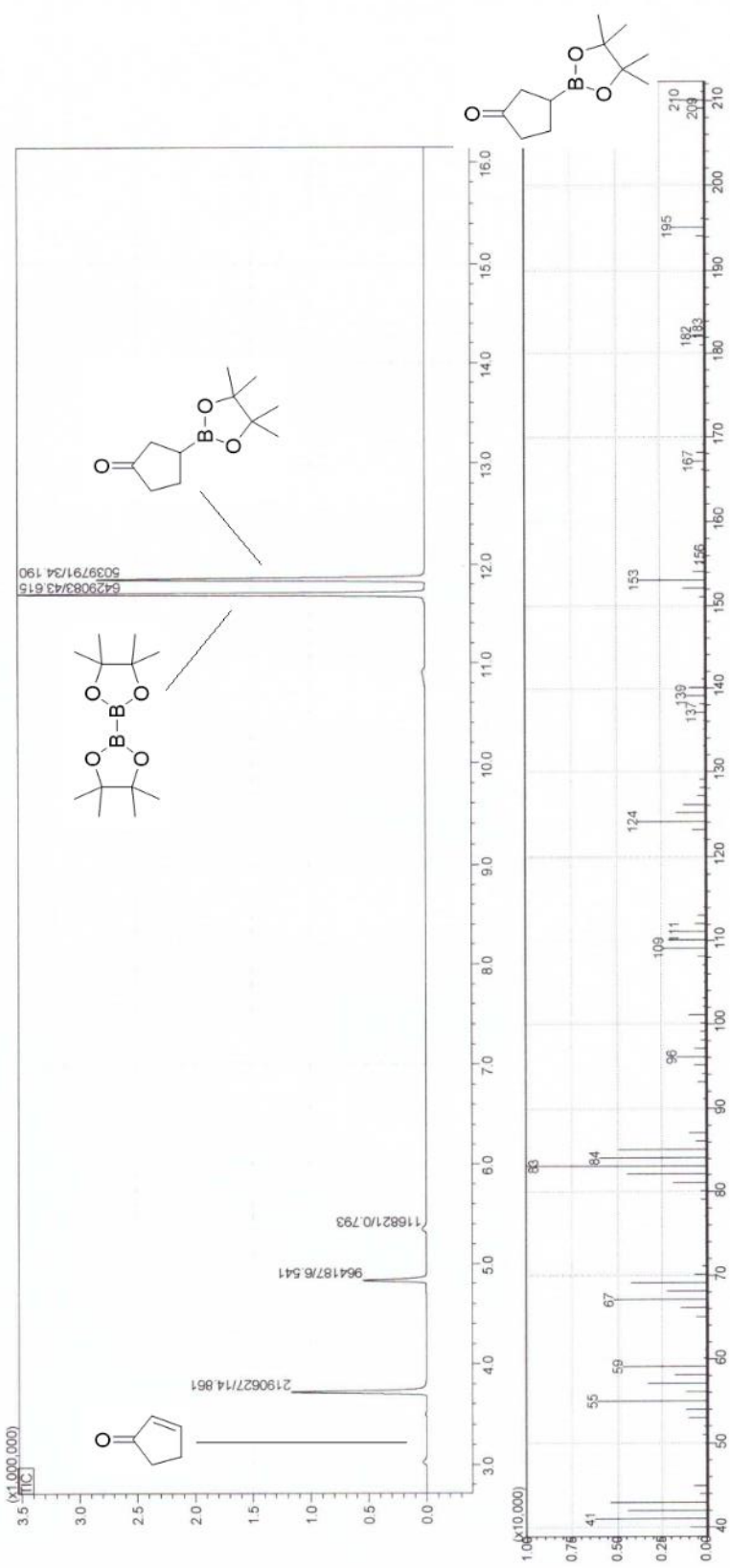


Figure A.70 GC-MS chromatogram spectrum of catalytic trial (Table 4.3, Entry 1)

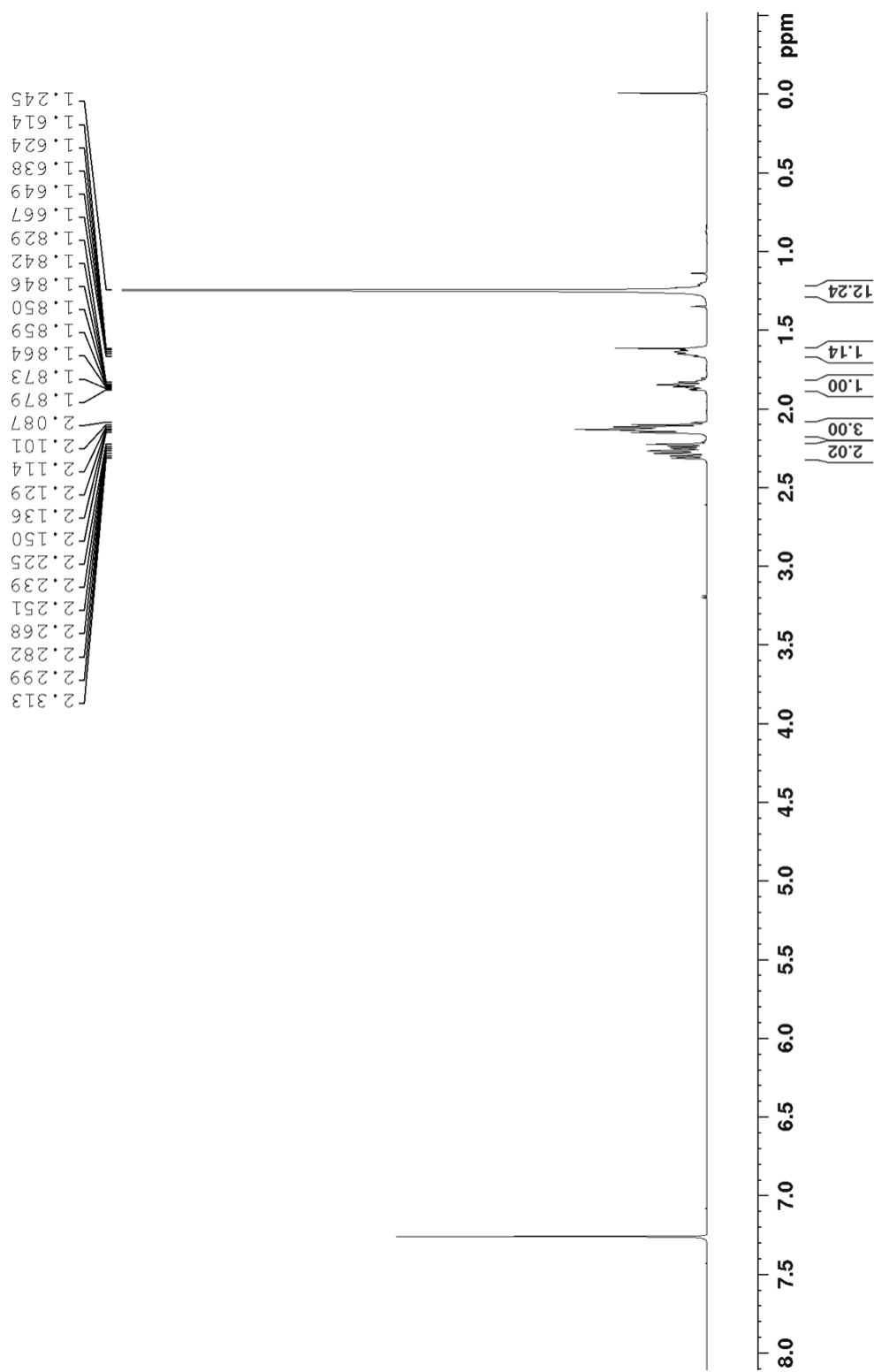


Figure A.71 ${}^1\text{H}$ NMR (600 MHz, CDCl_3) spectrum of isolated product (Table 4.3, Entry 1)

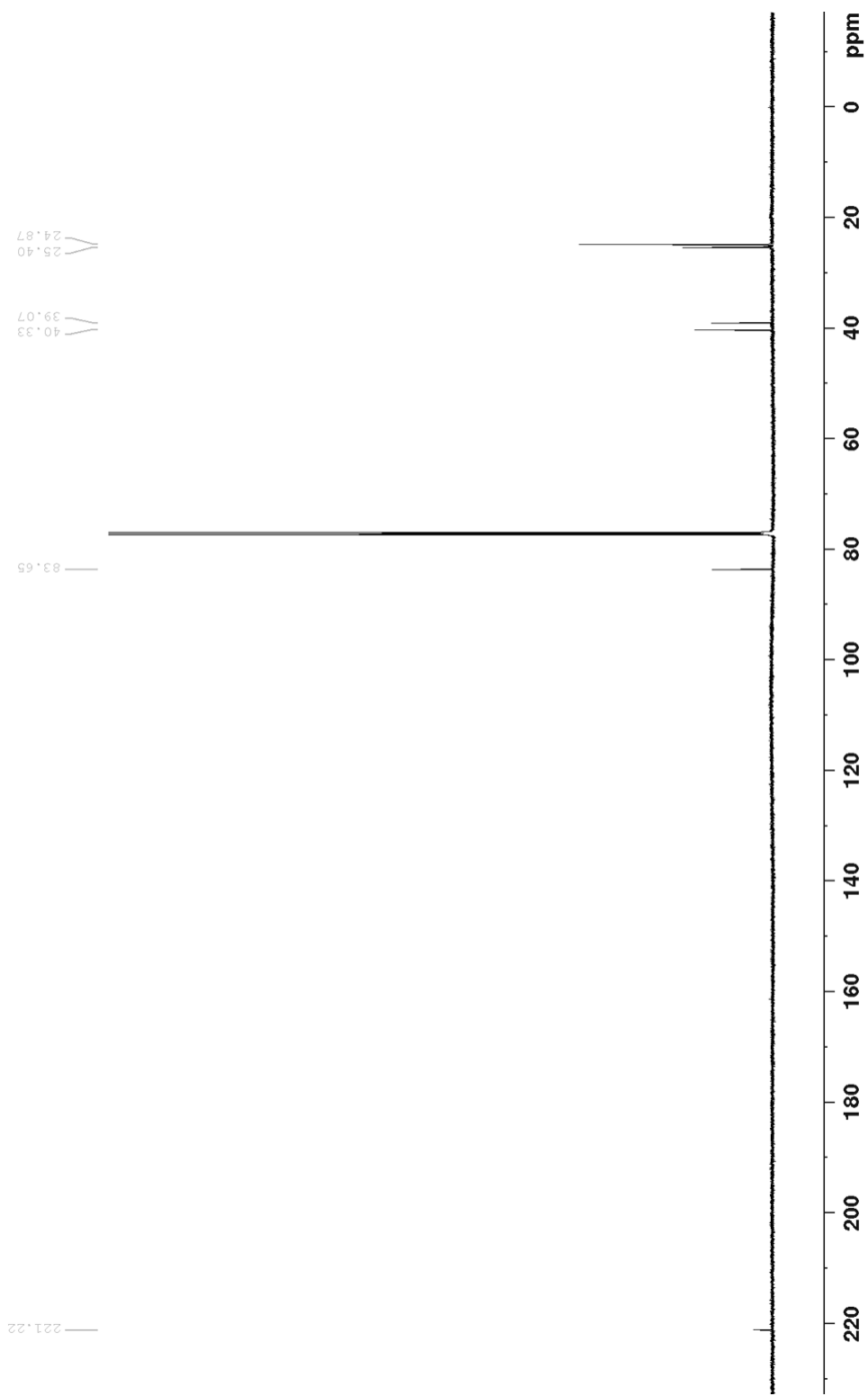


Figure A.72 ^{13}C NMR (150 MHz, CDCl_3) spectrum of isolated product (Table 4.3, Entry 1)

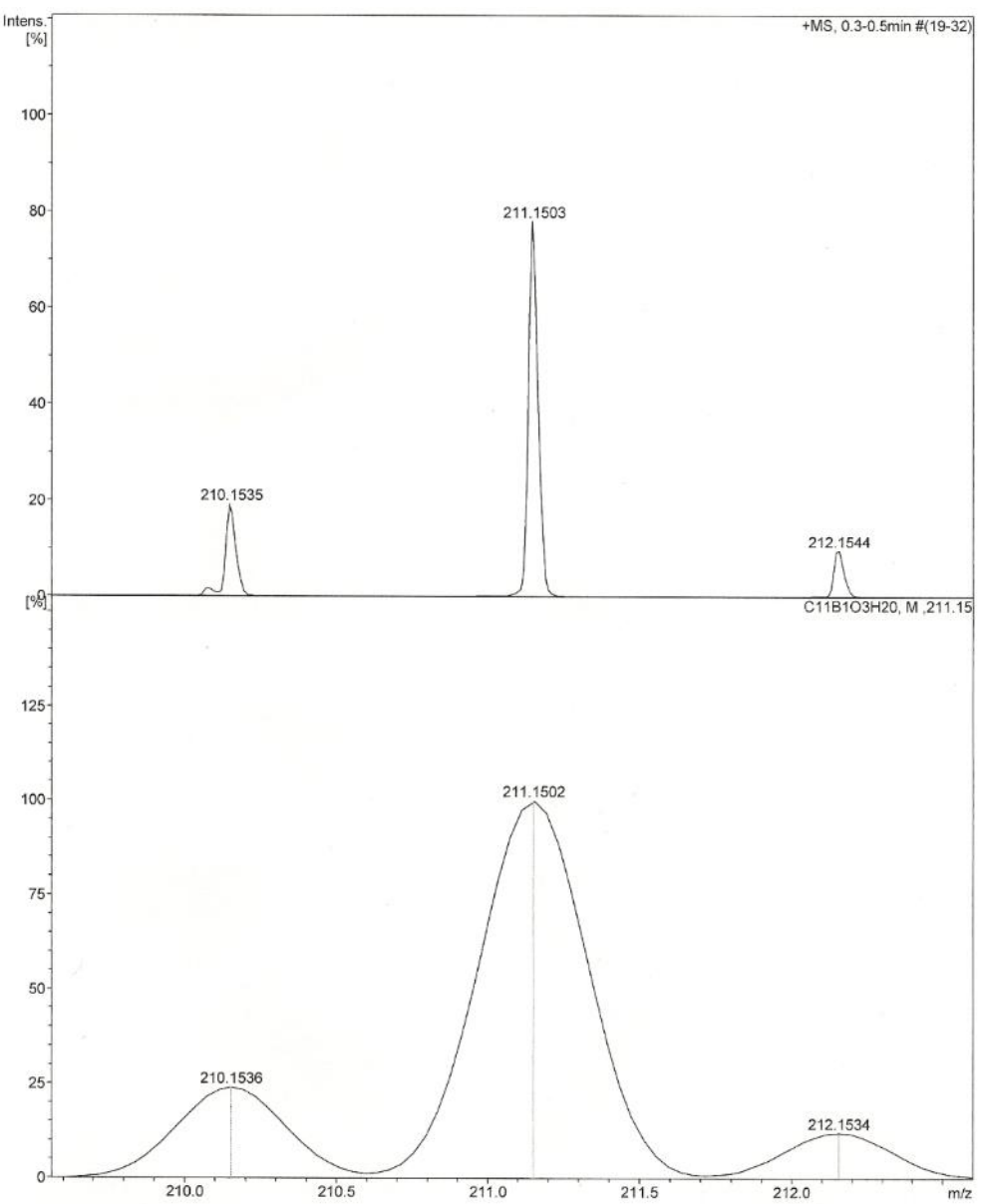


Figure A.73 HRMS of product (Table 4.3, Entry 1)

HRMS-ESI (m/z): $[M+H]^+$ calcd (bottom) for $C_{11}H_{20}BO_3$, 211.1502; found (top) 211.1503

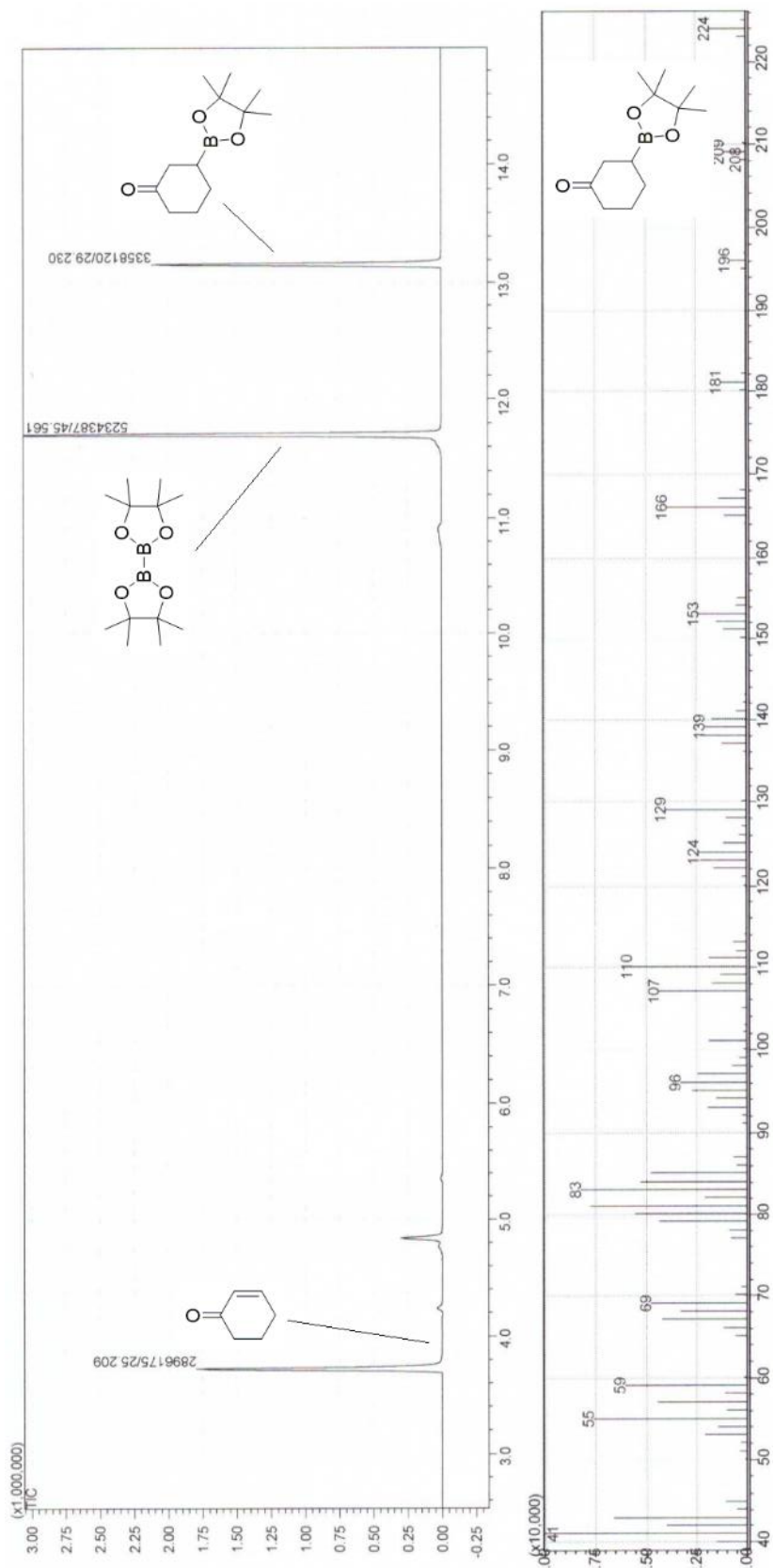


Figure A.74 GC-MS chromatogram spectrum of catalytic trial (Table 4.3, Entry 2)

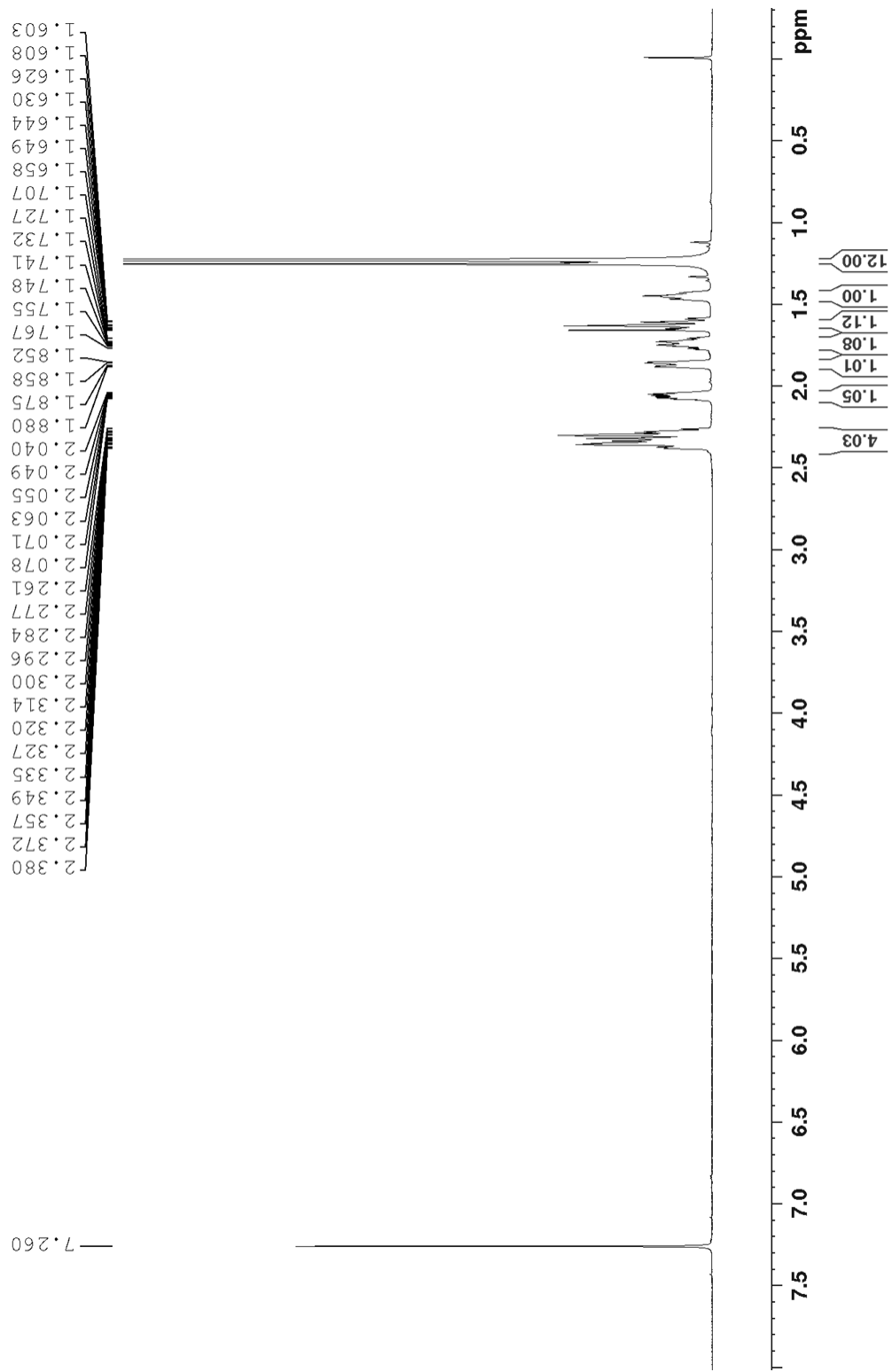


Figure A.75 ${}^1\text{H}$ NMR (600 MHz, CDCl_3) spectrum of isolated product (Table 4.3, Entry 2)

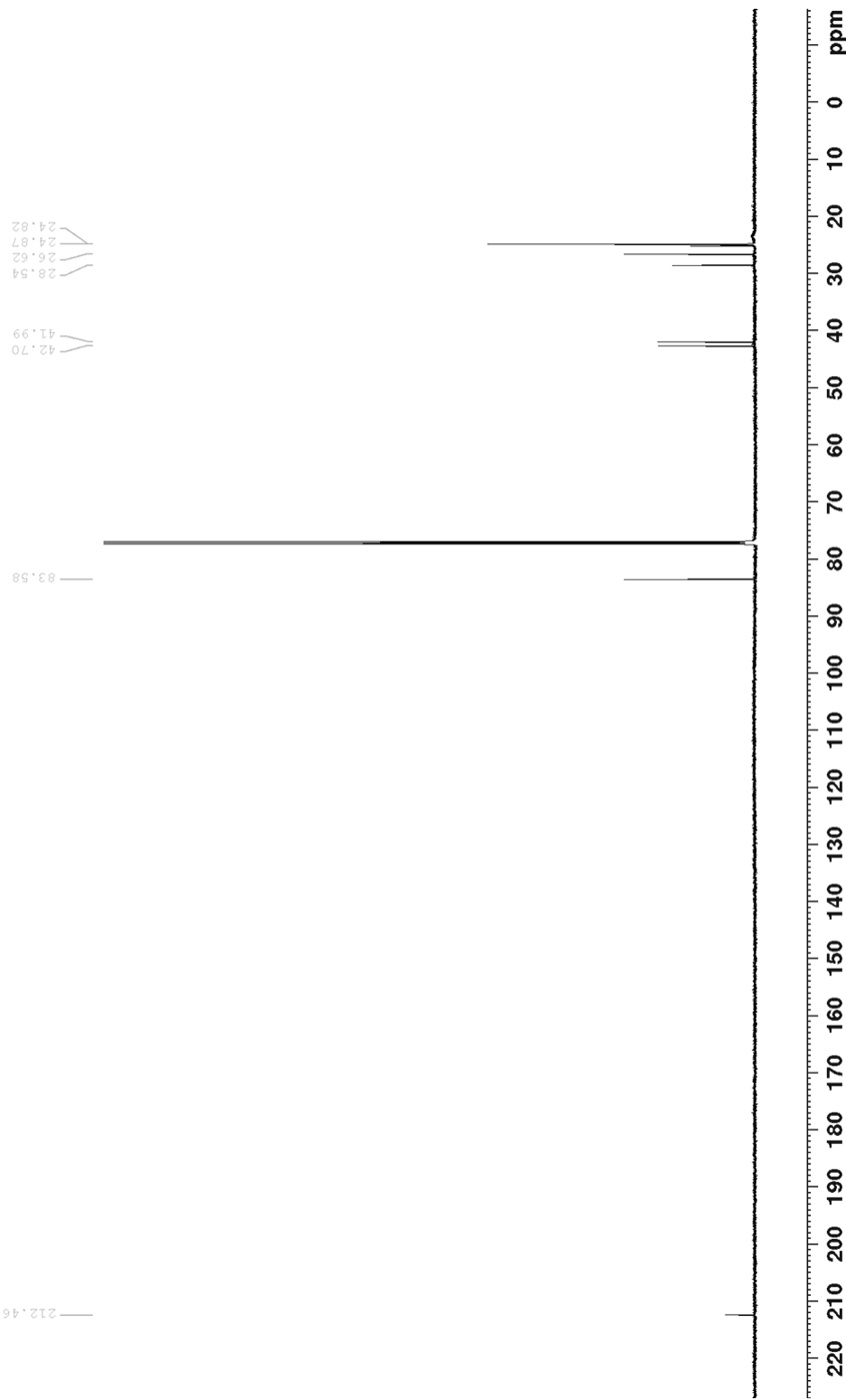


Figure A.76 ^{13}C NMR (150 MHz, CDCl_3) spectrum of isolated product (Table 4.3, Entry 2)

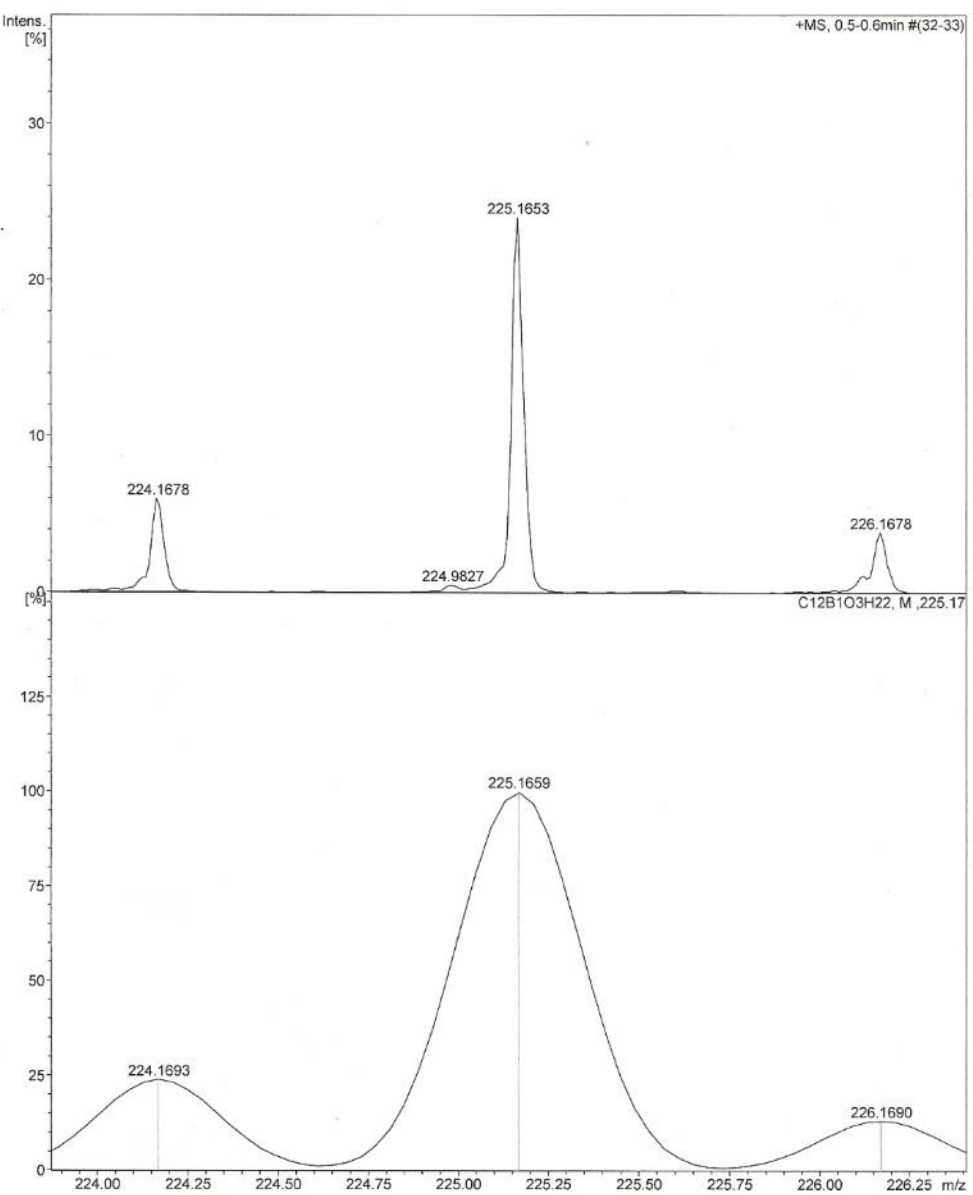


Figure A.77 HRMS of product (Table 4.3, Entry 2)

HRMS-ESI (m/z): $[M+H]^+$ calcd (bottom) for $C_{12}H_{22}BO_3$, 225.1659; found (top) 225.1653

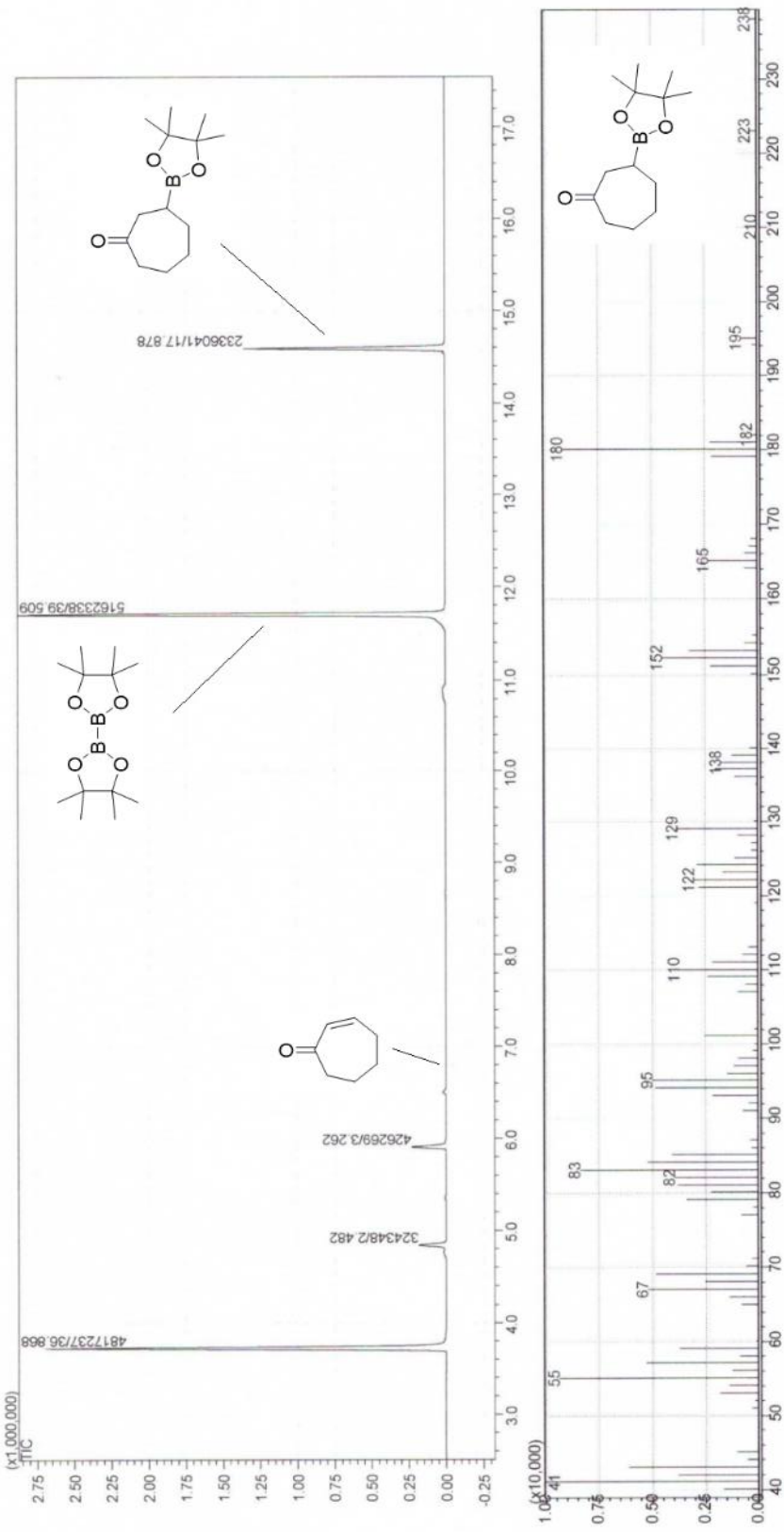


Figure A.78 GC-MS chromatogram spectrum of catalytic trial (Table 4.3, Entry 3)

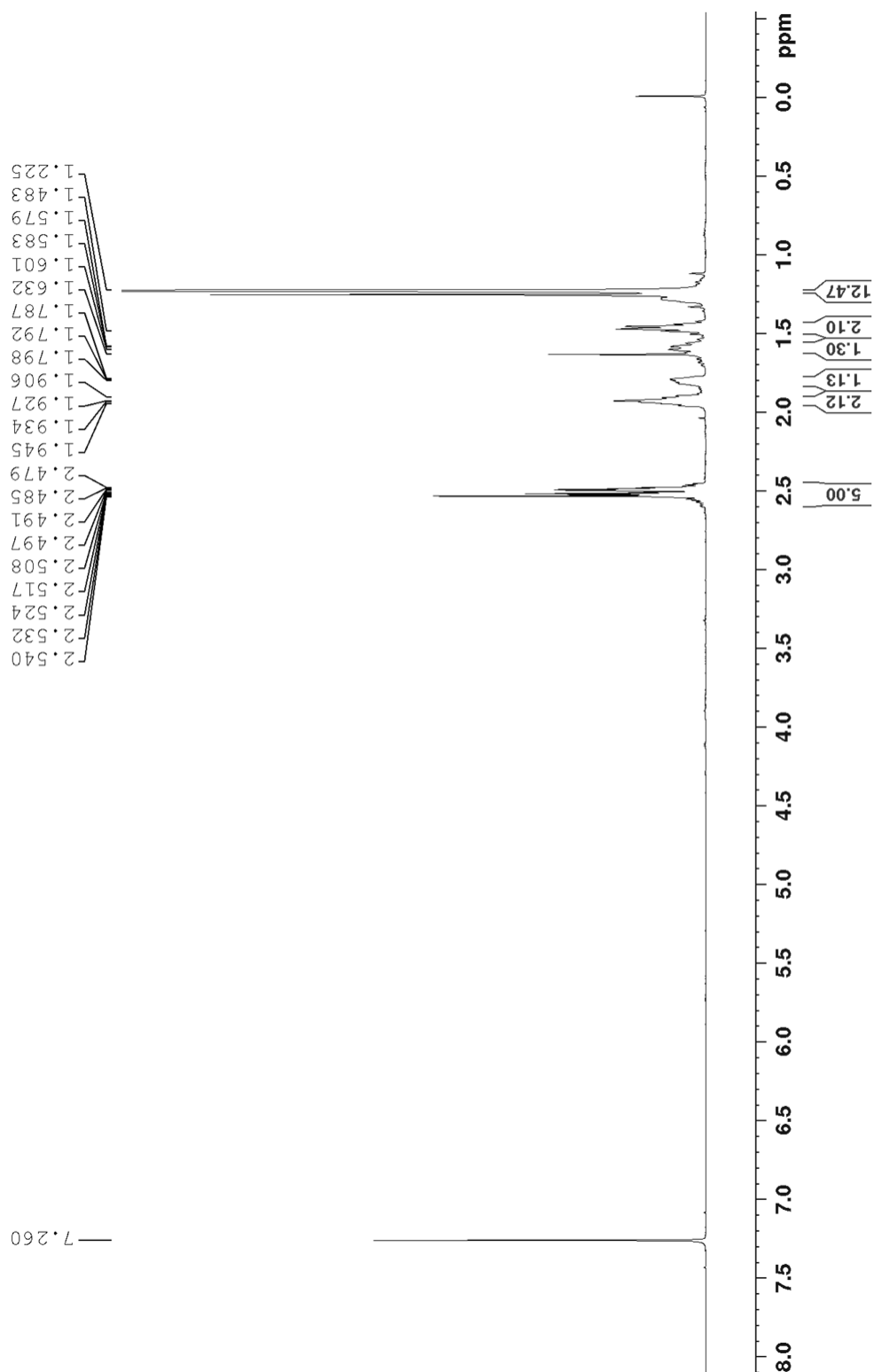


Figure A.79 ^1H NMR (600 MHz, CDCl_3) spectrum of isolated product (Table 4.3, Entry 3)

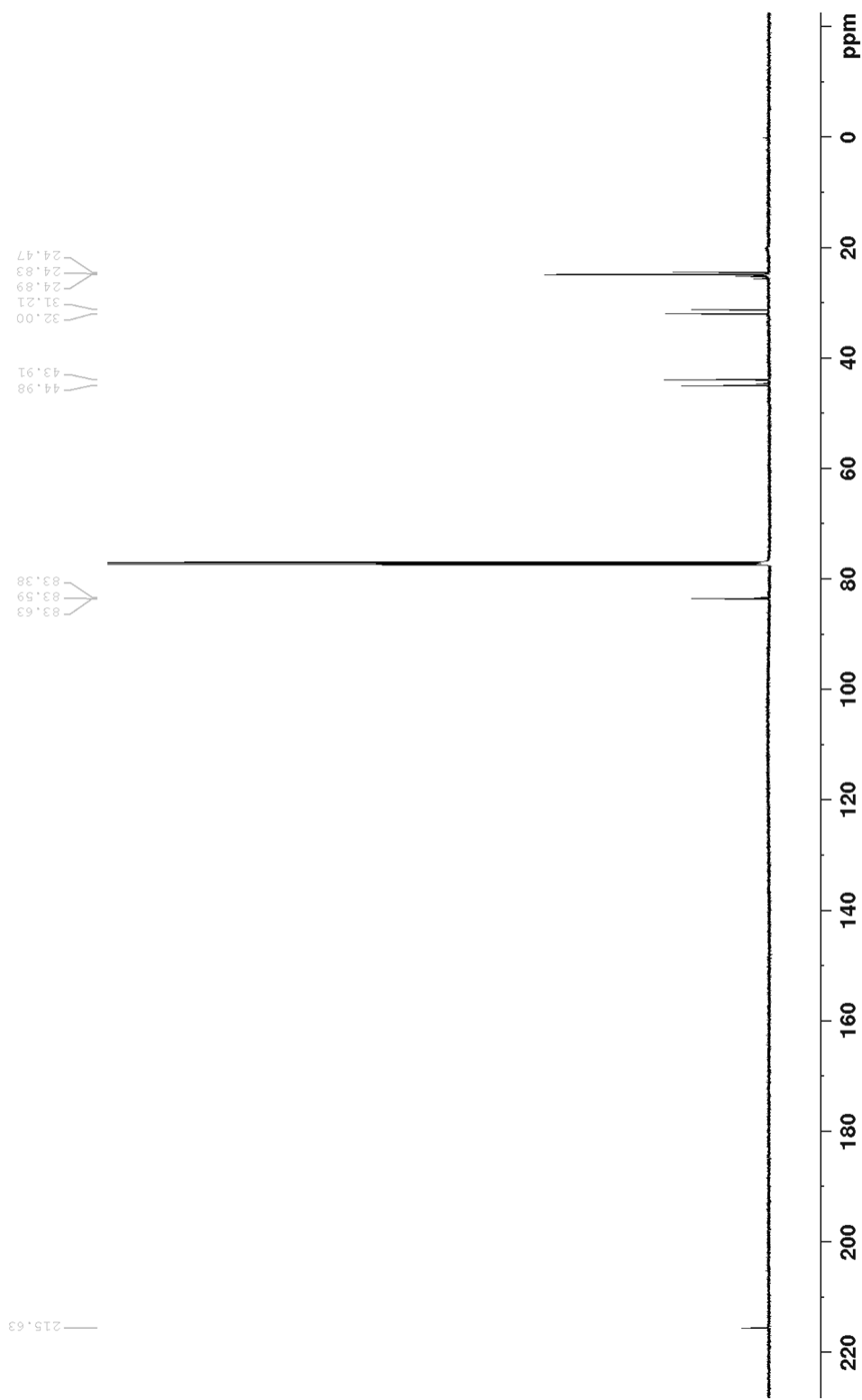


Figure A.80 ^{13}C NMR (150 MHz, CDCl_3) spectrum of isolated product (Table 4.3, Entry 3)

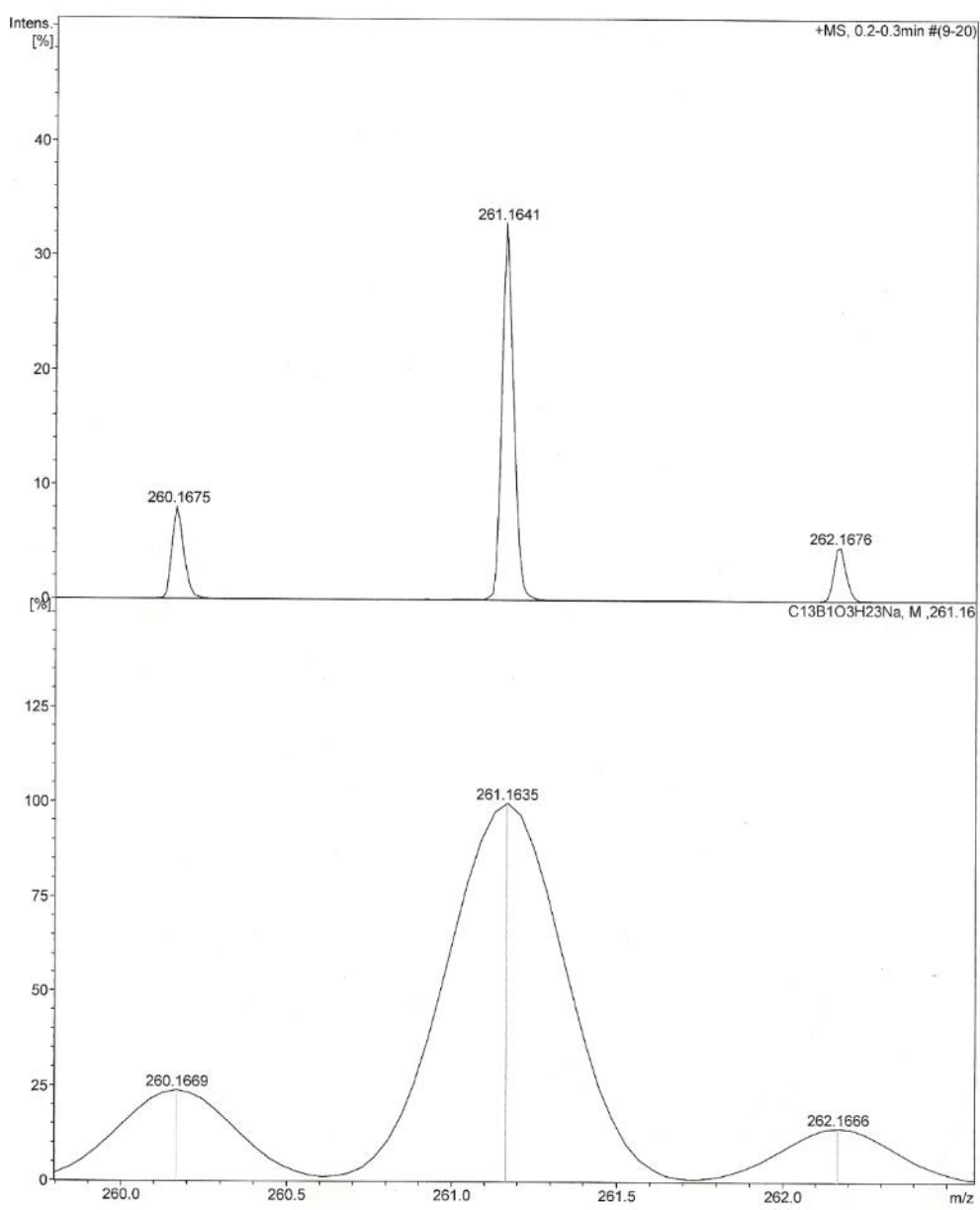
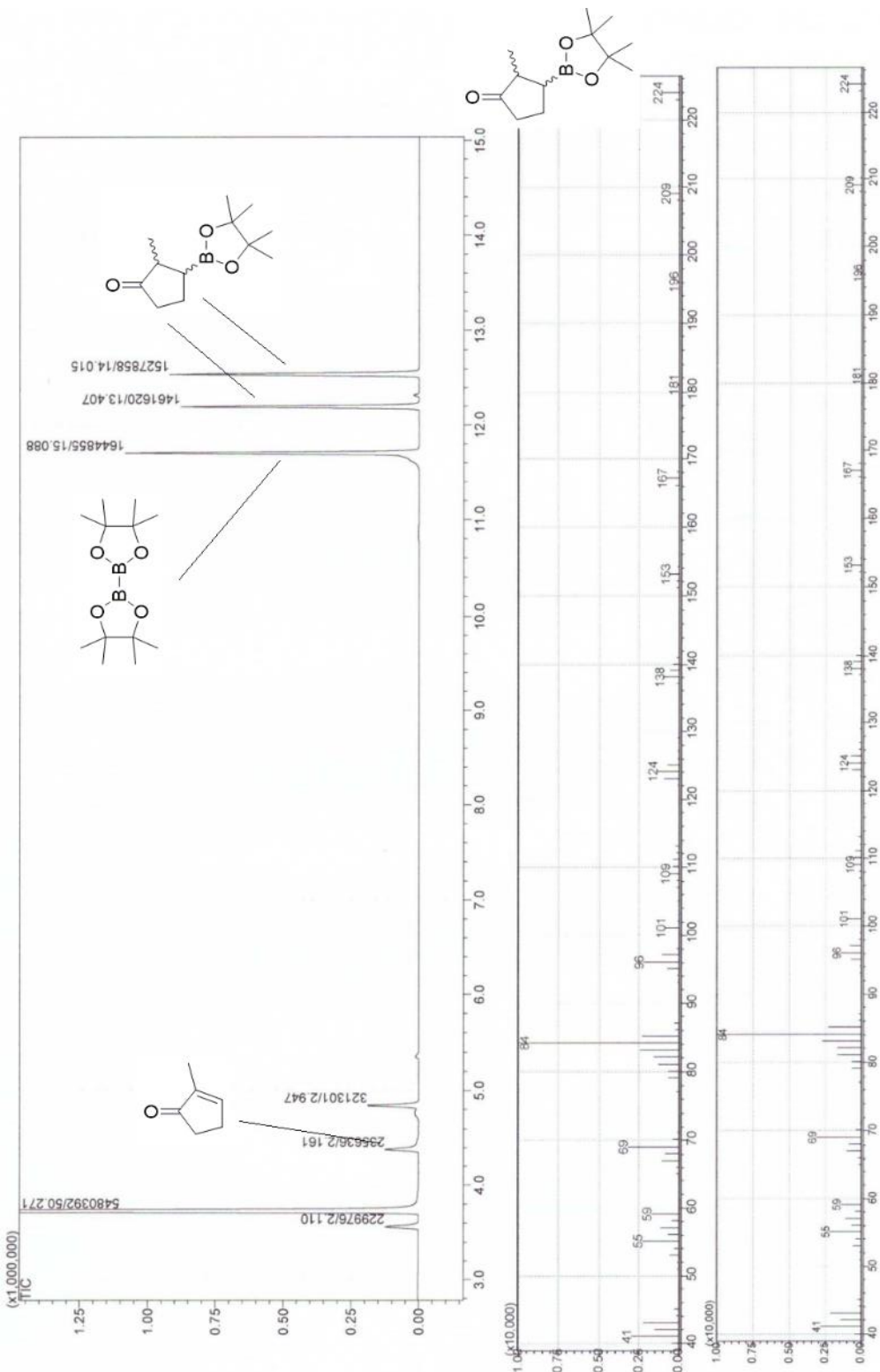


Figure A.81 HRMS of product (Table 4.3, Entry 3)

HRMS-ESI (m/z): [M+H]⁺ calcd (bottom) for C₃₂H₂₃BO₃, 239.1815; found (top) 239.1820



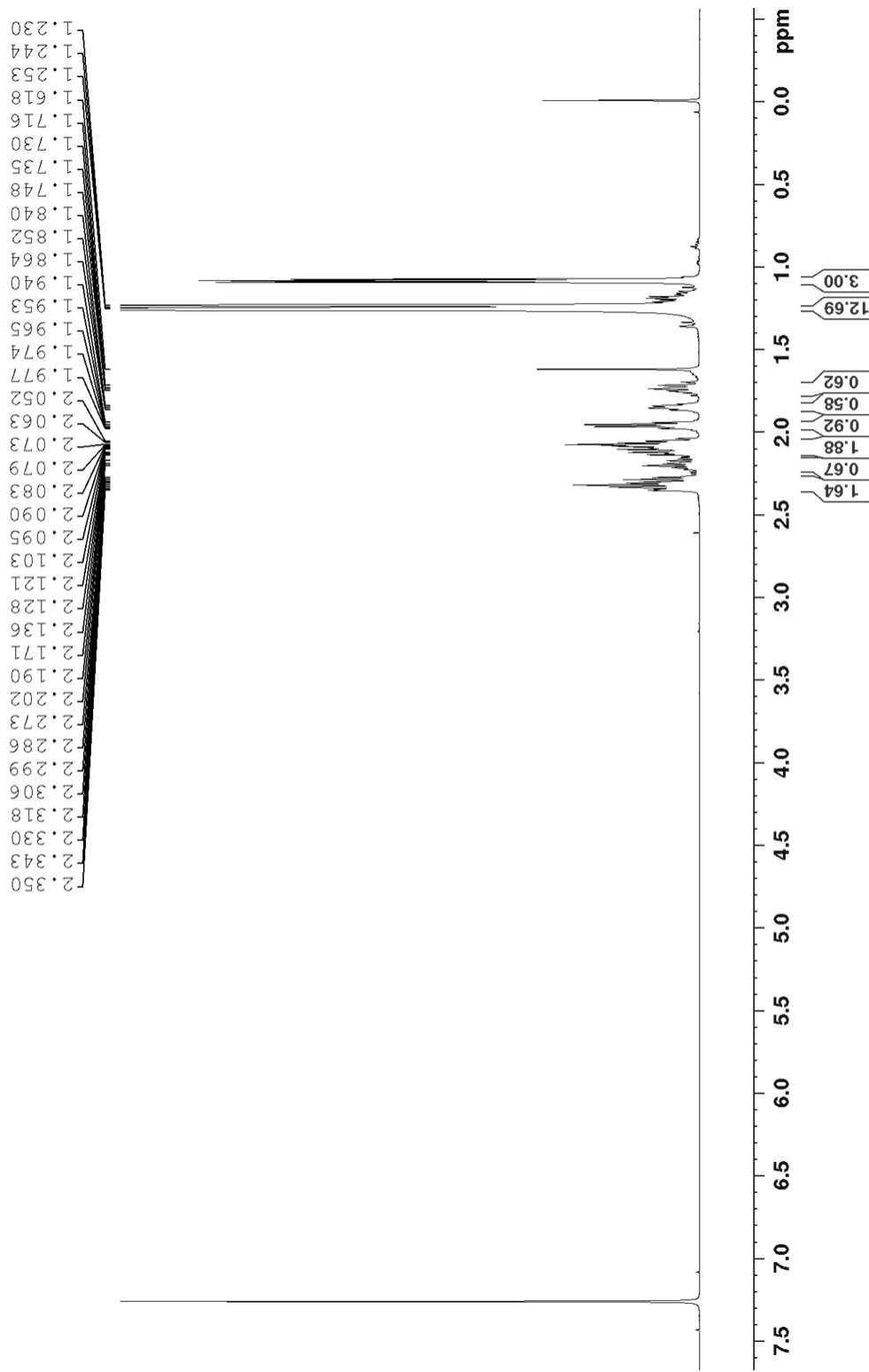


Figure A.83 ^1H NMR (600 MHz, CDCl_3) spectrum of isolated product (Table 4.3, Entry 4)

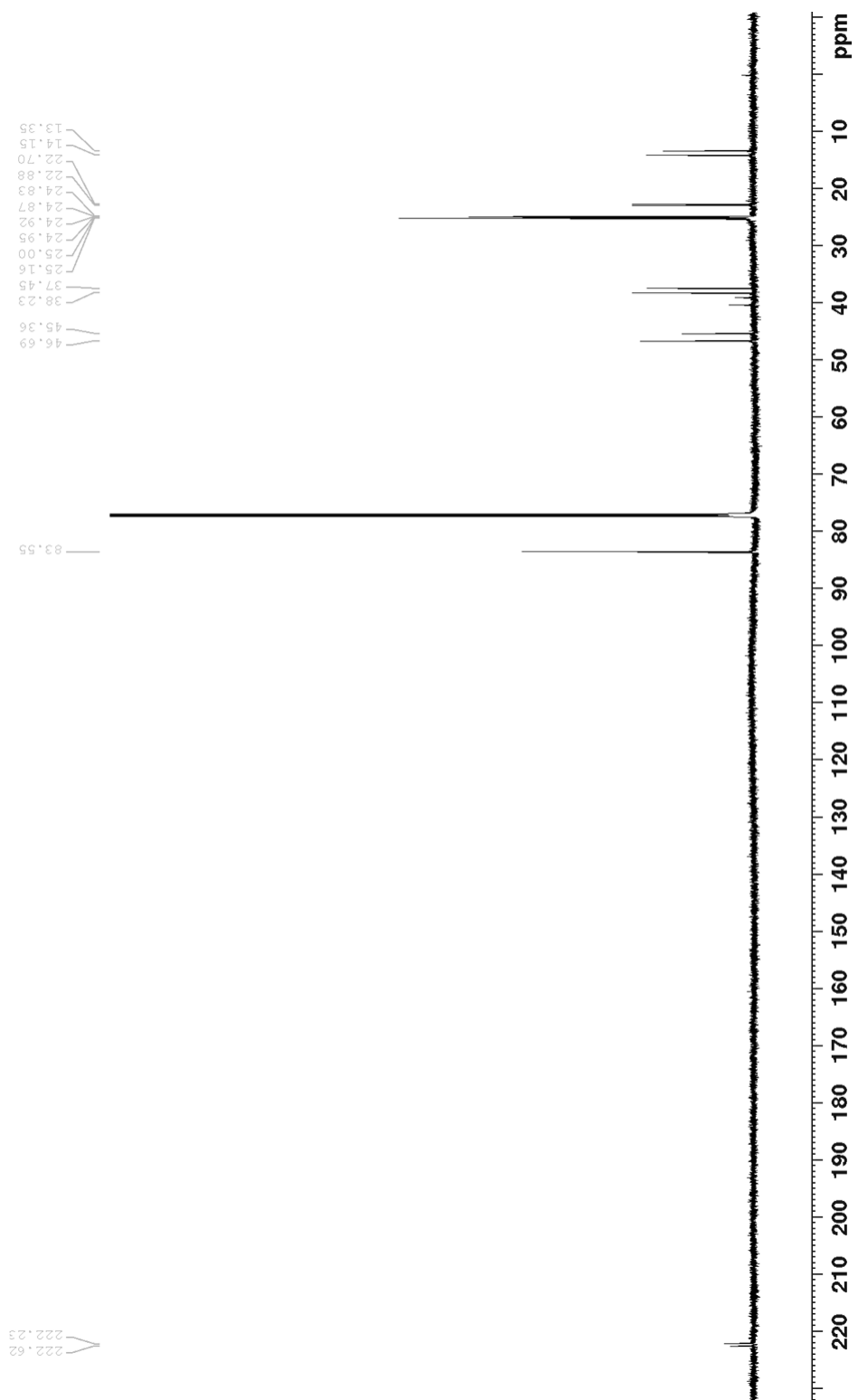


Figure A.84 ^{13}C NMR (150 MHz, CDCl_3) spectrum of isolated product (Table 4.3, Entry 4)

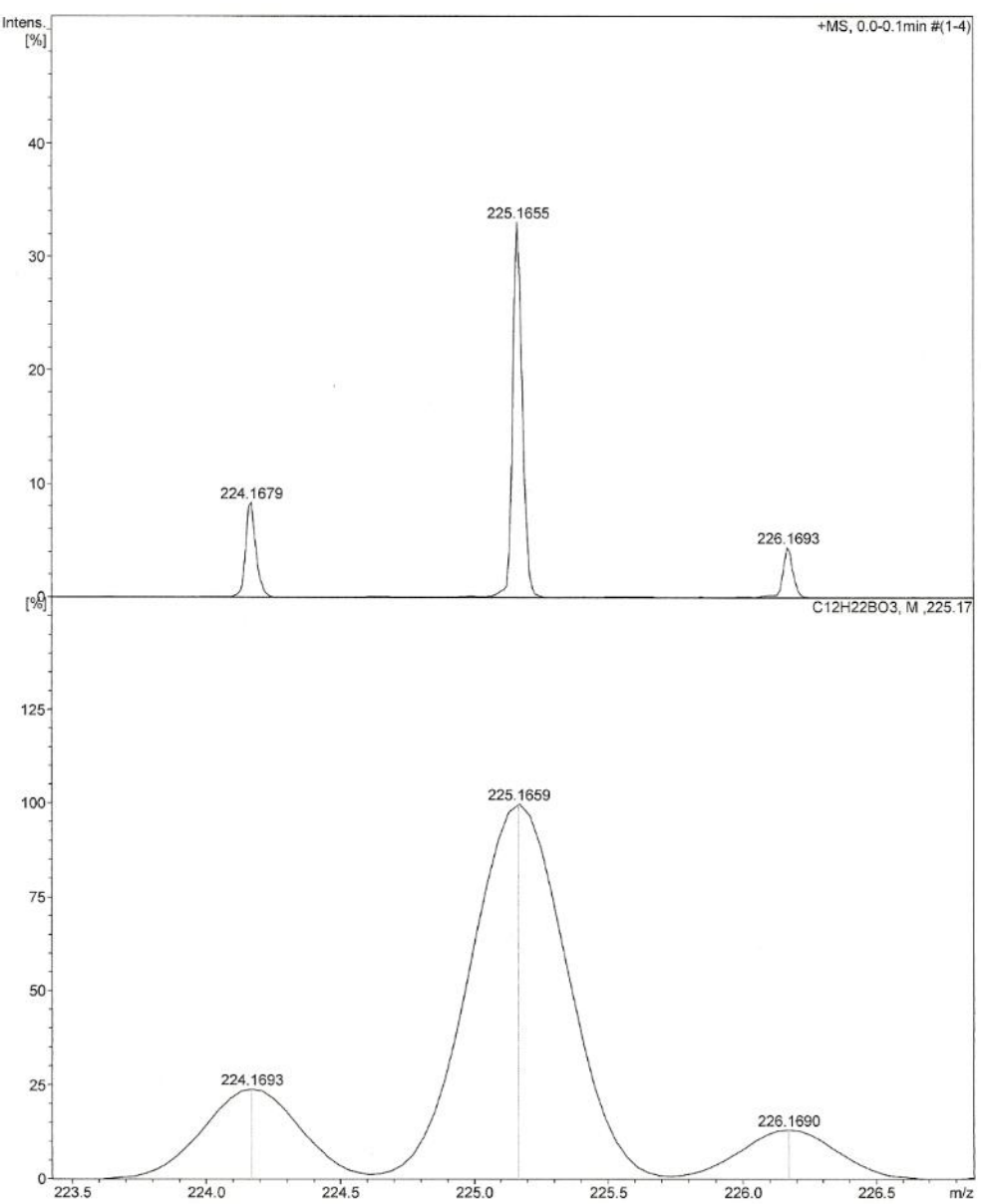


Figure A.85 HRMS of product (Table 4.3, Entry 4)

HRMS-ESI (m/z): $[M+H]^+$ calcd (bottom) for $C_{12}H_{22}BO_3$, 225.1659; found (top) 225.1655

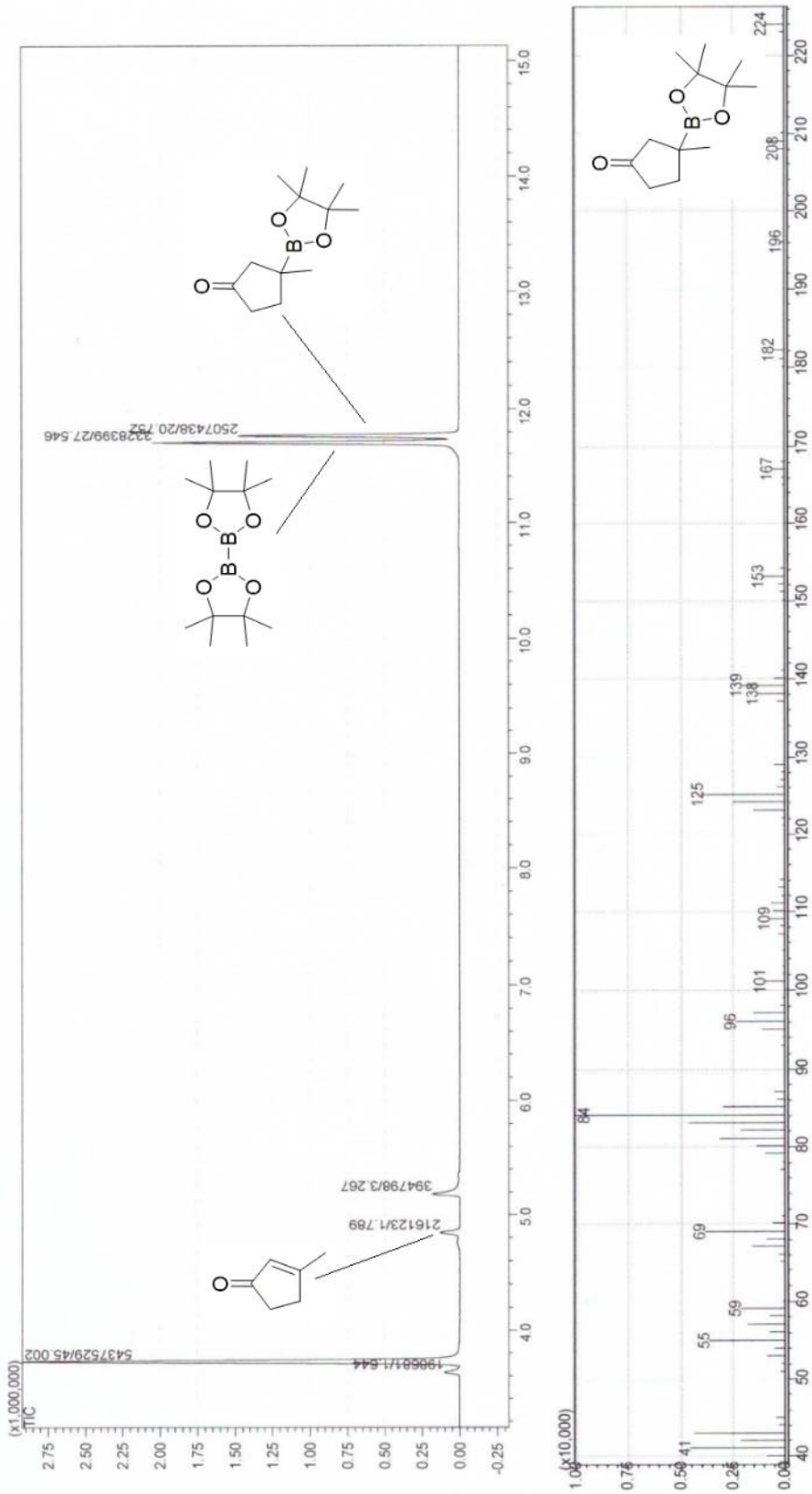


Figure A.86 GC-MS chromatogram spectrum of catalytic trial (Table 4.3, Entry 5)

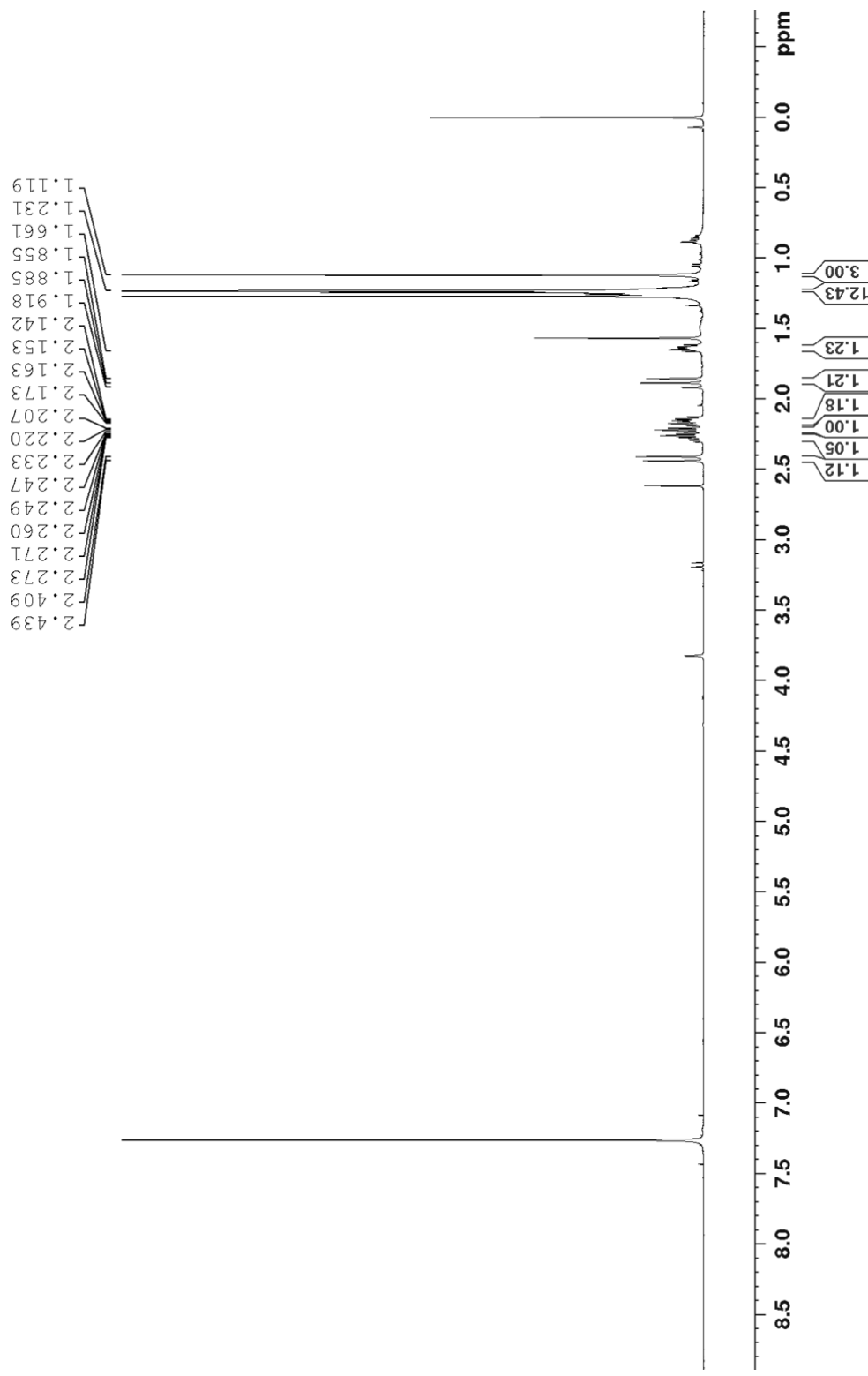


Figure A.87 ${}^1\text{H}$ NMR (600 MHz, CDCl_3) spectrum of isolated product (Table 4.3, Entry 5)

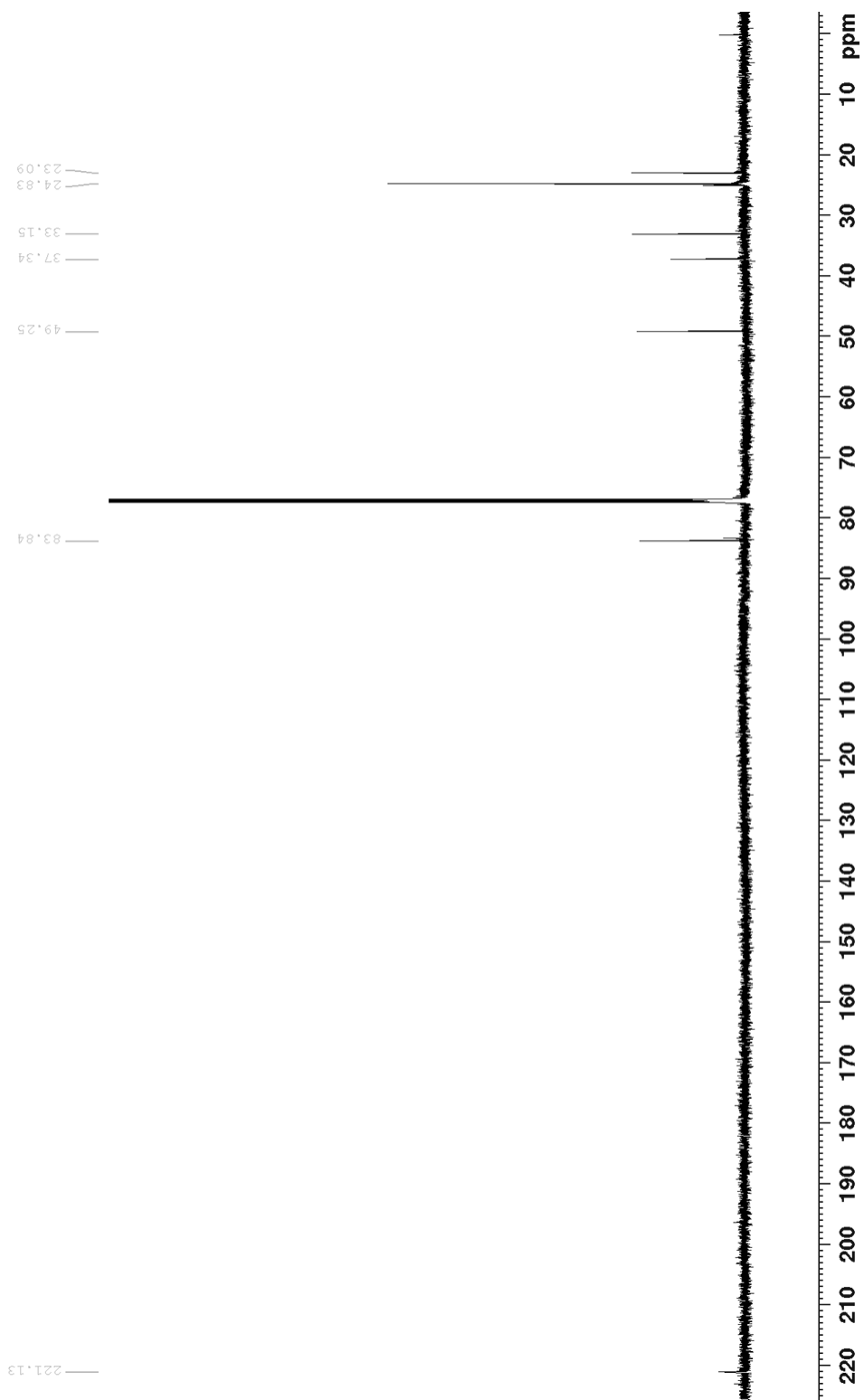


Figure A.88 ^{13}C NMR (150 MHz, CDCl_3) spectrum of isolated product (Table 4.3, Entry 5)

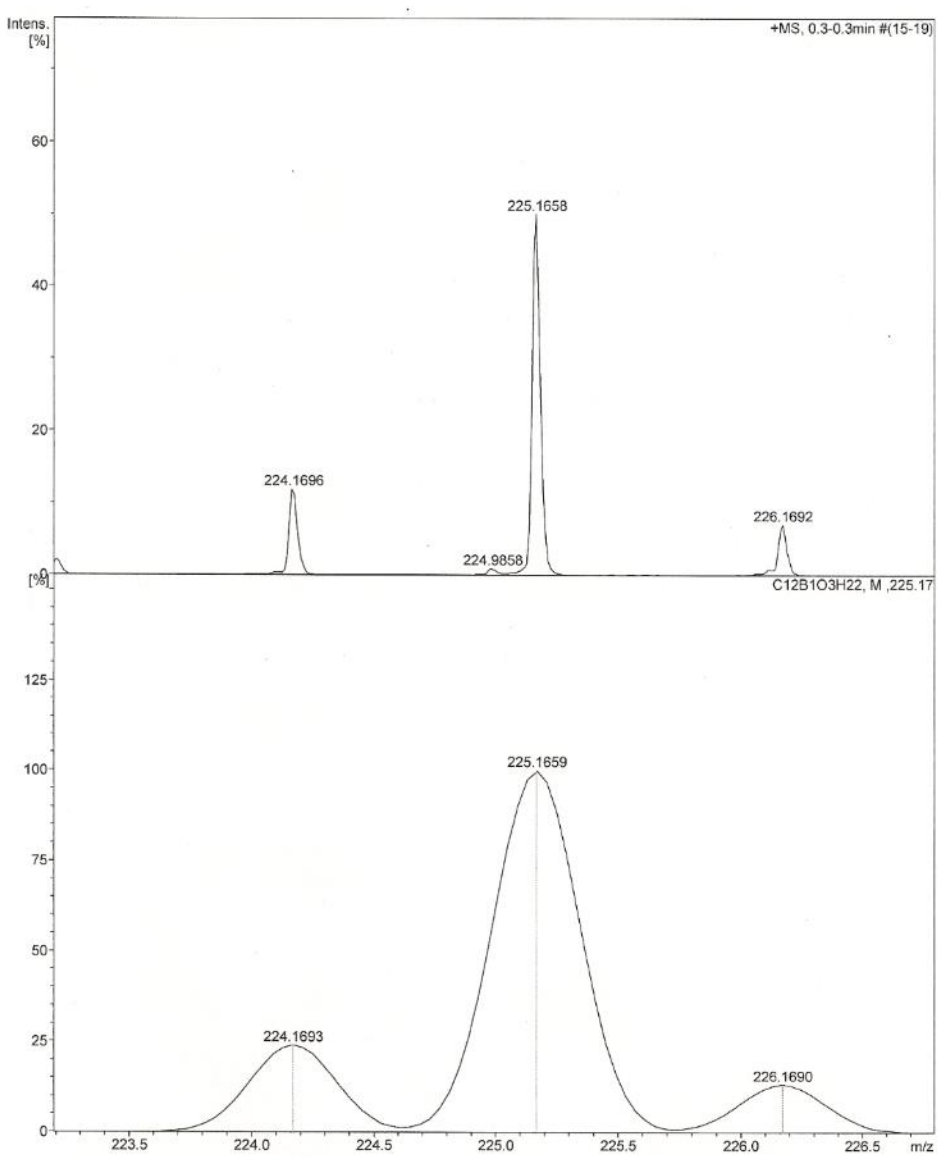


Figure A.89 HRMS of product (Table 4.3, Entry 5)

HRMS-ESI (m/z): $[\text{M}+\text{H}]^+$ calcd (bottom) for $\text{C}_{12}\text{H}_{22}\text{BO}_3$, 225.1659; found (top) 225.1658

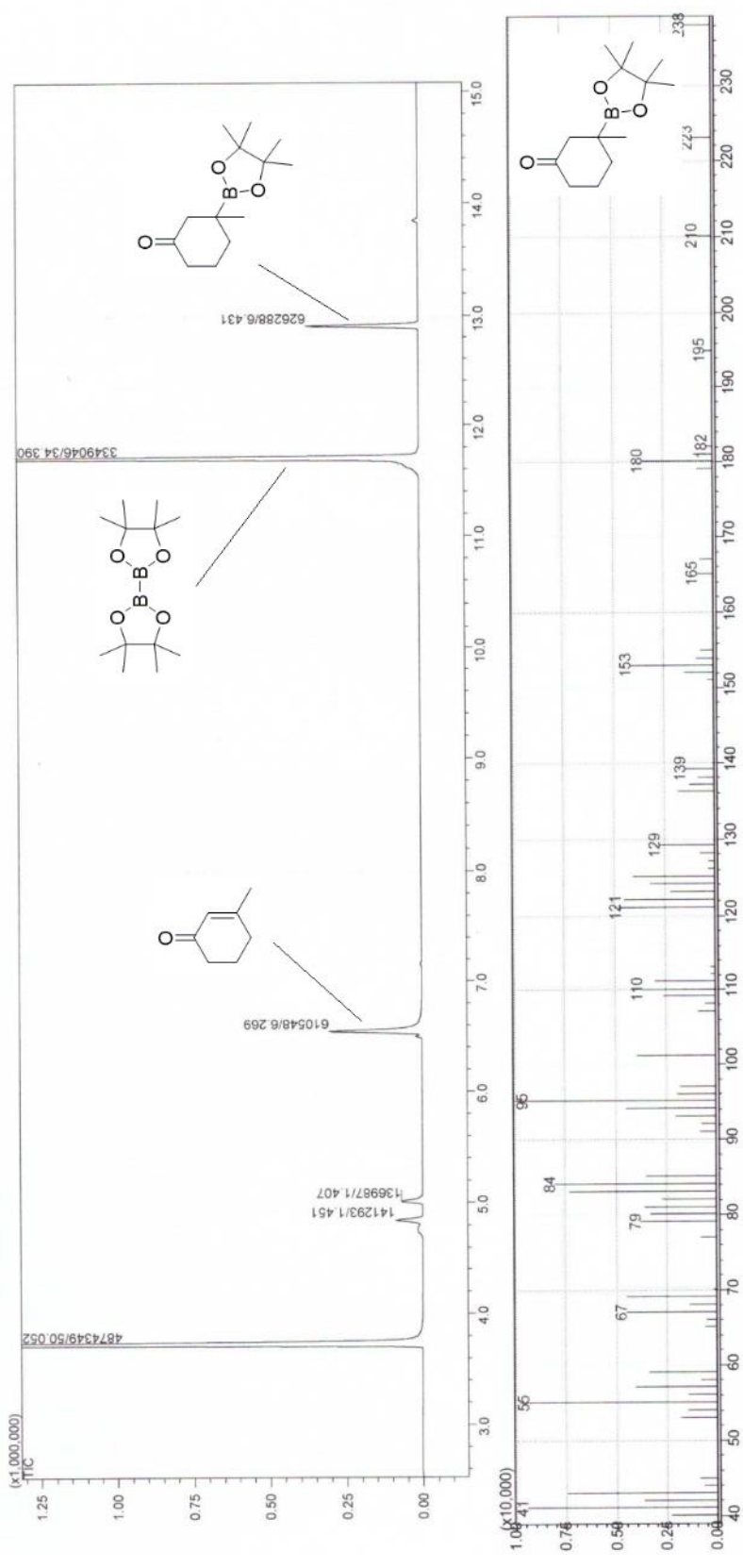


Figure A.90 GC-MS chromatogram spectrum of catalytic trial (Table 4.3, Entry 6)

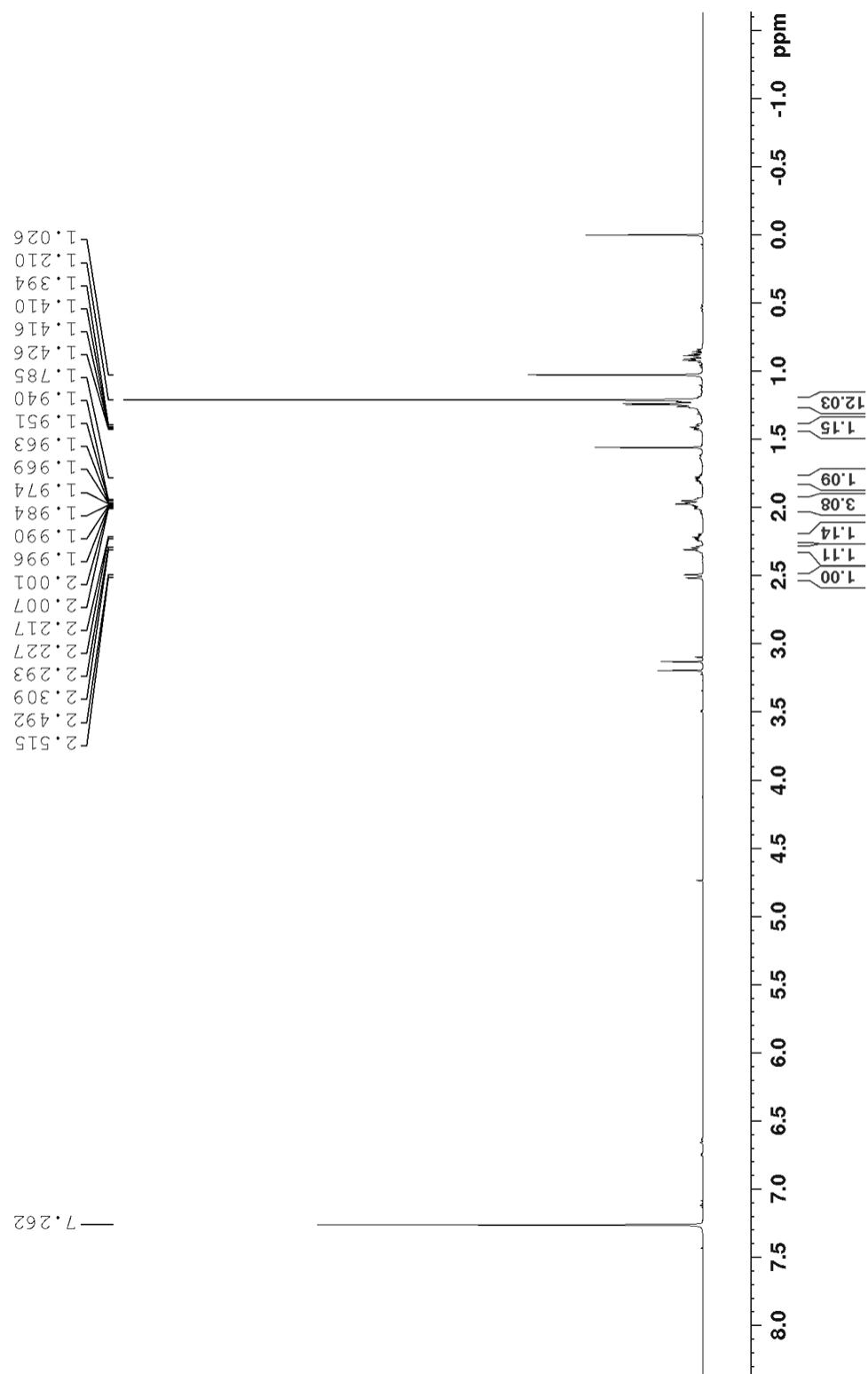


Figure A.91 ${}^1\text{H}$ NMR (600 MHz, CDCl_3) spectrum of isolated product (Table 4.3, Entry 6)

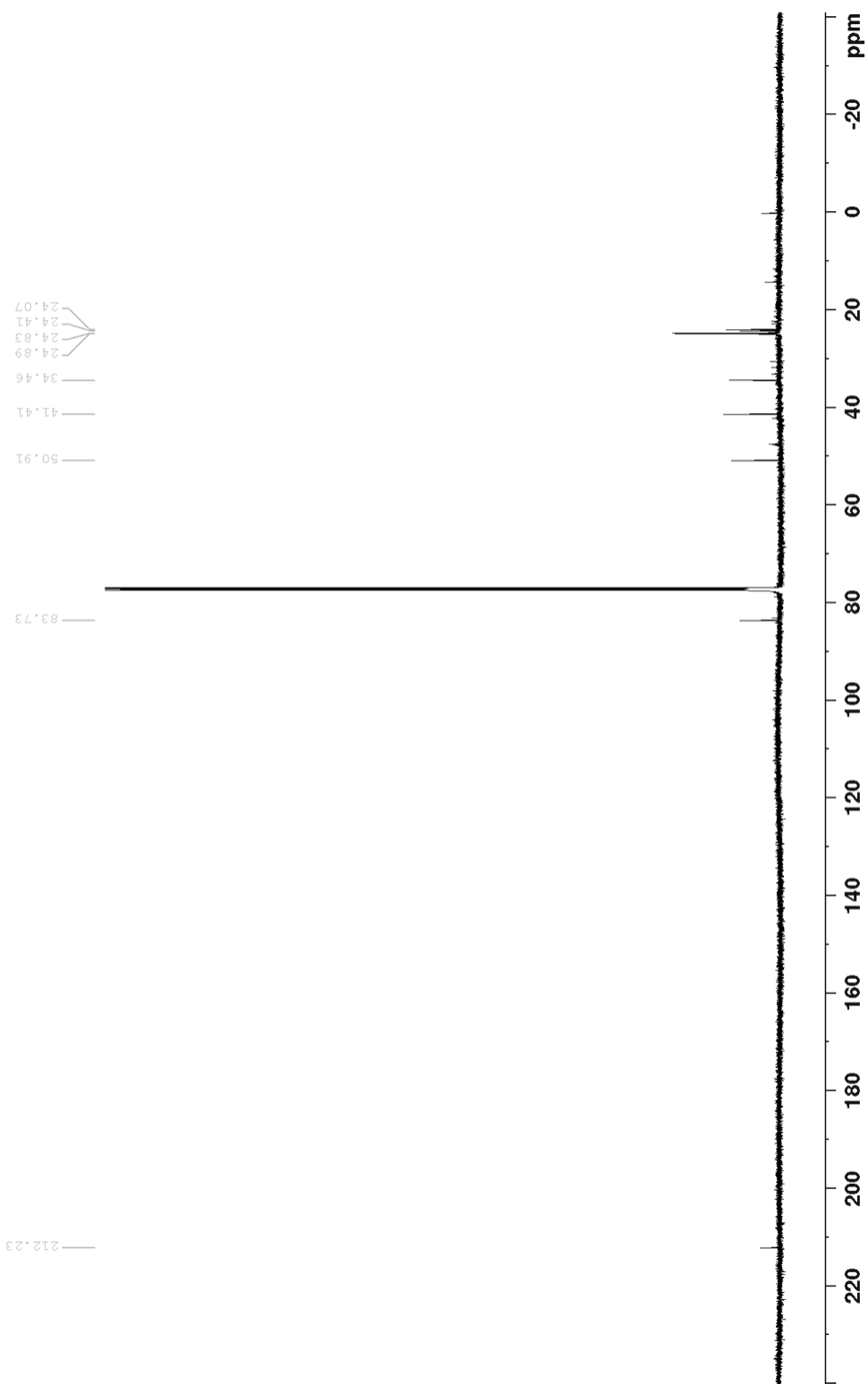


Figure A.92 ^{13}C NMR (150 MHz, CDCl_3) spectrum of isolated product (Table 4.3, Entry 6)

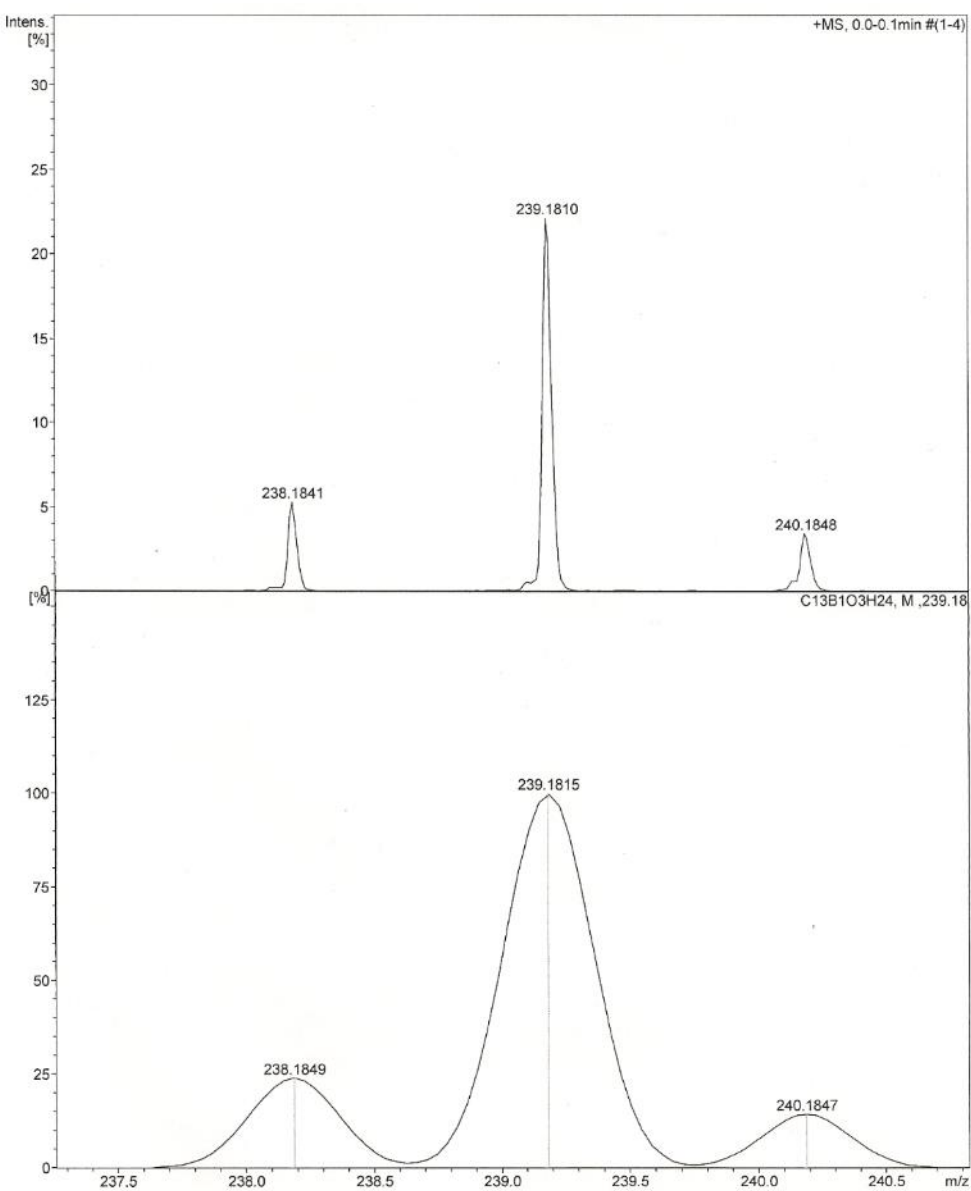


Figure A.93 HRMS of product (Table 4.3, Entry 6)

HRMS-ESI (m/z): $[\text{M}+\text{H}]^+$ calcd (bottom) for $\text{C}_{13}\text{H}_{24}\text{BO}_3$, 39.1815; found (top) 239.1810

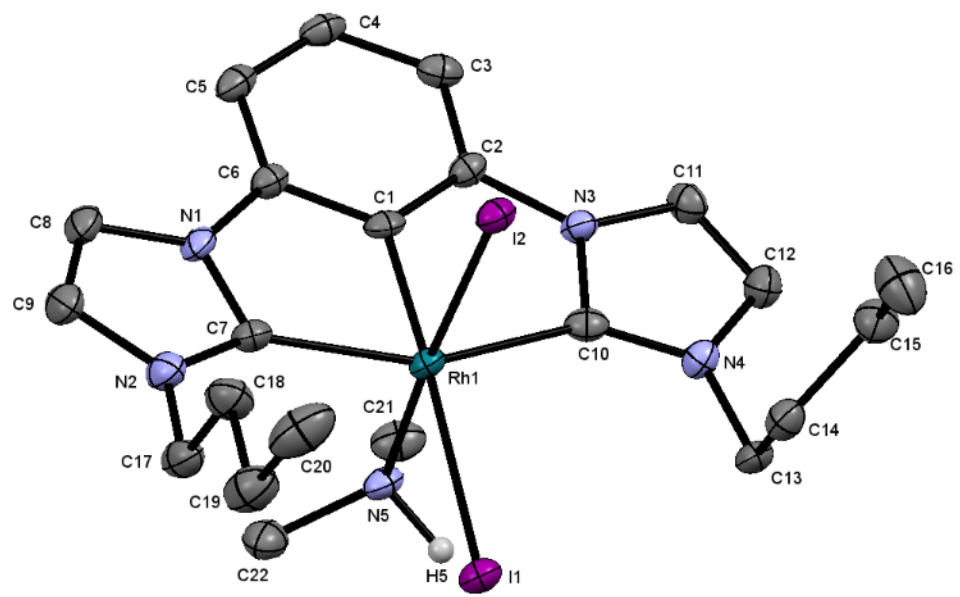


Figure A.94 X-ray molecular structure of 9

Table A.13 Crystal Data and Structure Refinement for **9**

Empirical formula	C ₂₂ H ₃₂ I ₂ N ₅ Rh		
Formula weight	723.23		
Temperature	100(2) K		
Wavelength	0.71073 Å		
Crystal system	Monoclinic		
Space group	P2 ₁ /c		
Unit cell dimensions	<i>a</i> = 15.6046(11) Å	<i>α</i> = 90°	
	<i>b</i> = 11.3102(8) Å	<i>β</i> = 108.373(4)°	
	<i>c</i> = 15.4899(11) Å	<i>γ</i> = 90°	
Volume	2594.5(3) Å ³		
Z	4		
Density (calculated)	1.852 g.cm ⁻³		
Absorption coefficient (μ)	3.056 mm ⁻¹		
F(000)	1400		
Crystal color, habit	?, ?		
Crystal size	0.20 × 0.20 × 0.20 mm ³		
θ range for data collection	1.375 to 27.984°		
Index ranges	-20 ≤ <i>h</i> ≤ 20, -14 ≤ <i>k</i> ≤ 14, -20 ≤ <i>l</i> ≤ 20		
Reflections collected	22210		
Independent reflections	6172 [R _{int} = 0.0346]		
Completeness to θ = 26.000°	99.8 %		
Refinement method	Full-matrix least-squares on F ²		
Data / restraints / parameters	6172 / 0 / 275		
Goodness-of-fit on F ²	1.051		
Final R indices [I>2σ(I)]	R ₁ = 0.0301, wR ₂ = 0.0657		
R indices (all data)	R ₁ = 0.0388, wR ₂ = 0.0704		
Extinction coefficient	n/a		
Largest diff. peak and hole	2.326 and -1.183 e ⁻ .Å ⁻³		

Table A.14 Atomic Coordinates and Equivalent Isotropic Displacement Parameters (\AA^2) for **9**

	x	y	z	U(eq)
Rh(1)	0.26891(2)	0.48238(2)	0.46866(2)	0.015(1)
I(1)	0.39244(2)	0.48305(2)	0.36634(2)	0.019(1)
I(2)	0.15535(2)	0.32681(2)	0.36317(2)	0.019(1)
N(1)	0.1201(2)	0.6461(3)	0.4476(2)	0.019(1)
N(2)	0.1581(2)	0.6895(3)	0.3299(2)	0.024(1)
N(3)	0.2682(2)	0.3325(3)	0.62030(19)	0.017(1)
N(4)	0.3776(2)	0.2575(3)	0.58261(19)	0.019(1)
N(5)	0.3652(2)	0.5986(3)	0.55695(19)	0.019(1)
C(1)	0.1884(2)	0.4918(3)	0.5423(2)	0.018(1)
C(2)	0.1971(2)	0.4138(3)	0.6123(2)	0.017(1)
C(3)	0.1410(3)	0.4185(3)	0.6665(2)	0.021(1)
C(4)	0.0751(3)	0.5073(3)	0.6468(2)	0.021(1)
C(5)	0.0646(2)	0.5883(3)	0.5771(2)	0.022(1)
C(6)	0.1223(2)	0.5783(3)	0.5248(2)	0.018(1)
C(7)	0.1817(2)	0.6174(3)	0.4035(2)	0.019(1)
C(8)	0.0609(3)	0.7330(3)	0.4012(3)	0.024(1)
C(9)	0.0846(3)	0.7583(4)	0.3268(3)	0.027(1)
C(10)	0.3161(2)	0.3447(3)	0.5597(2)	0.020(1)
C(11)	0.3014(3)	0.2398(3)	0.6797(2)	0.021(1)
C(12)	0.3697(3)	0.1933(3)	0.6555(3)	0.025(1)
C(13)	0.4421(2)	0.2295(3)	0.5338(2)	0.021(1)
C(14)	0.3979(3)	0.1586(3)	0.4479(2)	0.023(1)
C(15)	0.3620(3)	0.0389(3)	0.4636(3)	0.027(1)
C(16)	0.3162(4)	-0.0256(4)	0.3750(3)	0.039(1)
C(17)	0.1969(3)	0.6836(3)	0.2545(3)	0.026(1)
C(18)	0.1471(3)	0.5941(4)	0.1832(3)	0.030(1)
C(19)	0.1882(3)	0.5841(4)	0.1057(3)	0.035(1)
C(20)	0.1407(3)	0.4915(5)	0.0360(3)	0.044(1)
C(21)	0.3726(3)	0.5986(4)	0.6548(2)	0.027(1)
C(22)	0.3601(3)	0.7217(3)	0.5242(3)	0.026(1)
H(5)	0.4251	0.5693	0.5553	0.023
H(3)	0.1471	0.3639	0.7147	0.025

Table A.14 (Continued)

H(4)	0.0359	0.5123	0.6828	0.025
H(5A)	0.0198	0.6483	0.5654	0.026
H(8)	0.0132	0.7677	0.4183	0.029
H(9)	0.0558	0.8136	0.2806	0.032
H(11)	0.2803	0.2143	0.7278	0.026
H(12)	0.4060	0.1278	0.6835	0.029
H(13A)	0.4931	0.1837	0.5742	0.025
H(13B)	0.4667	0.3039	0.5174	0.025
H(14A)	0.3475	0.2055	0.4077	0.027
H(14B)	0.4427	0.1468	0.4153	0.027
H(15A)	0.3182	0.0496	0.4973	0.032
H(15B)	0.4125	-0.0099	0.5016	0.032
H(16A)	0.2694	0.0252	0.3350	0.059
H(16B)	0.2885	-0.0986	0.3878	0.059
H(16C)	0.3611	-0.0450	0.3449	0.059
H(17A)	0.2614	0.6613	0.2788	0.031
H(17B)	0.1932	0.7625	0.2259	0.031
H(18A)	0.0830	0.6178	0.1578	0.036
H(18B)	0.1493	0.5157	0.2123	0.036
H(19A)	0.1840	0.6618	0.0752	0.042
H(19B)	0.2529	0.5633	0.1313	0.042
H(20A)	0.1477	0.4136	0.0652	0.066
H(20B)	0.1673	0.4902	-0.0134	0.066
H(20C)	0.0763	0.5109	0.0113	0.066
H(21A)	0.3174	0.6316	0.6624	0.041
H(21B)	0.4245	0.6467	0.6888	0.041
H(21C)	0.3809	0.5173	0.6780	0.041
H(22A)	0.3620	0.7225	0.4616	0.040
H(22B)	0.4113	0.7668	0.5633	0.040
H(22C)	0.3035	0.7576	0.5260	0.040

U(eq) is defined as one third of the trace of the orthogonalized U_{ij} tensor.

Table A.15 Anisotropic Displacement Parameters (\AA^2) for **9**

	U₁₁	U₂₂	U₃₃	U₂₃	U₁₃	U₁₂
Rh(1)	0.0105(1)	0.0186(1)	0.0167(1)	0.0000(1)	0.0041(1)	0.0007(1)
I(1)	0.0140(1)	0.0253(1)	0.0190(1)	-0.0010(1)	0.0059(1)	0.0001(1)
I(2)	0.0141(1)	0.0223(1)	0.0209(1)	-0.0029(1)	0.0051(1)	-0.0009(1)
N(1)	0.0107(15)	0.0203(15)	0.0239(15)	0.0006(12)	0.0025(12)	0.0028(12)
N(2)	0.0168(16)	0.0273(17)	0.0278(16)	0.0073(13)	0.0058(13)	0.0025(14)
N(3)	0.0136(15)	0.0213(15)	0.0171(13)	0.0024(11)	0.0060(12)	0.0007(12)
N(4)	0.0175(16)	0.0210(15)	0.0181(14)	0.0005(11)	0.0047(12)	0.0028(13)
N(5)	0.0117(15)	0.0237(15)	0.0222(15)	-0.0033(12)	0.0052(12)	-0.0011(13)
C(1)	0.0108(17)	0.0220(17)	0.0214(16)	-0.0019(14)	0.0048(14)	-0.0042(14)
C(2)	0.0140(17)	0.0209(17)	0.0162(15)	-0.0023(13)	0.0038(13)	0.0003(14)
C(3)	0.020(2)	0.0233(18)	0.0200(17)	-0.0034(14)	0.0078(15)	-0.0065(16)
C(4)	0.0149(18)	0.0264(19)	0.0234(17)	-0.0102(14)	0.0089(15)	-0.0034(15)
C(5)	0.0137(18)	0.0227(18)	0.0273(18)	-0.0089(15)	0.0056(15)	-0.0005(15)
C(6)	0.0142(18)	0.0199(17)	0.0190(16)	-0.0027(13)	0.0052(14)	-0.0006(14)
C(7)	0.0136(18)	0.0216(18)	0.0223(17)	0.0002(14)	0.0072(14)	-0.0011(15)
C(8)	0.0150(19)	0.0227(19)	0.0309(19)	0.0012(15)	0.0032(16)	0.0033(16)
C(9)	0.018(2)	0.0257(19)	0.034(2)	0.0072(16)	0.0037(17)	0.0029(16)
C(10)	0.0164(18)	0.0239(18)	0.0175(16)	-0.0027(14)	0.0042(14)	-0.0049(15)
C(11)	0.023(2)	0.0224(18)	0.0176(16)	0.0054(14)	0.0042(15)	-0.0004(16)
C(12)	0.022(2)	0.0222(19)	0.0280(19)	0.0041(15)	0.0060(16)	0.0027(16)
C(13)	0.0137(18)	0.0221(18)	0.0292(18)	0.0034(15)	0.0100(15)	0.0021(15)
C(14)	0.020(2)	0.0263(19)	0.0224(17)	0.0011(15)	0.0080(15)	0.0041(16)
C(15)	0.026(2)	0.026(2)	0.0270(19)	-0.0021(16)	0.0062(17)	-0.0006(17)
C(16)	0.047(3)	0.030(2)	0.034(2)	0.0025(18)	0.002(2)	-0.004(2)
C(17)	0.020(2)	0.032(2)	0.0268(18)	0.0115(16)	0.0086(16)	0.0034(17)
C(18)	0.030(2)	0.033(2)	0.030(2)	0.0070(17)	0.0141(18)	-0.0006(19)
C(19)	0.028(2)	0.049(3)	0.029(2)	0.0083(19)	0.0106(18)	0.005(2)
C(20)	0.030(3)	0.070(4)	0.033(2)	-0.006(2)	0.011(2)	0.006(2)
C(21)	0.022(2)	0.038(2)	0.0207(18)	-0.0062(16)	0.0048(16)	-0.0057(18)
C(22)	0.021(2)	0.0247(19)	0.033(2)	-0.0039(16)	0.0071(17)	-0.0040(17)

$$-2\pi^2[h^2a^*{}^2U_{11} + \dots + 2hka*b^*U_{12}] \quad (\text{A.3})$$

Table A.16 Bond Lengths [Å] for **9**

atom-atom	distance	atom-atom	distance
Rh(1)-C(1)	1.948(4)	Rh(1)-C(10)	2.074(4)
Rh(1)-C(7)	2.083(4)	Rh(1)-N(5)	2.136(3)
Rh(1)-I(2)	2.6610(4)	Rh(1)-I(1)	2.8555(4)
N(1)-C(7)	1.382(4)	N(1)-C(8)	1.385(5)
N(1)-C(6)	1.411(4)	N(2)-C(7)	1.355(5)
N(2)-C(9)	1.374(5)	N(2)-C(17)	1.477(5)
N(3)-C(10)	1.379(4)	N(3)-C(11)	1.383(4)
N(3)-C(2)	1.416(4)	N(4)-C(10)	1.344(5)
N(4)-C(12)	1.380(5)	N(4)-C(13)	1.472(4)
N(5)-C(22)	1.475(5)	N(5)-C(21)	1.484(4)
N(5)-H(5)	1.0000	C(1)-C(2)	1.371(5)
C(1)-C(6)	1.385(5)	C(2)-C(3)	1.392(5)
C(3)-C(4)	1.401(5)	C(3)-H(3)	0.9500
C(4)-C(5)	1.386(5)	C(4)-H(4)	0.9500
C(5)-C(6)	1.393(5)	C(5)-H(5A)	0.9500
C(8)-C(9)	1.348(5)	C(8)-H(8)	0.9500
C(9)-H(9)	0.9500	C(11)-C(12)	1.344(5)
C(11)-H(11)	0.9500	C(12)-H(12)	0.9500
C(13)-C(14)	1.520(5)	C(13)-H(13A)	0.9900
C(13)-H(13B)	0.9900	C(14)-C(15)	1.514(5)
C(14)-H(14A)	0.9900	C(14)-H(14B)	0.9900
C(15)-C(16)	1.520(6)	C(15)-H(15A)	0.9900
C(15)-H(15B)	0.9900	C(16)-H(16A)	0.9800
C(16)-H(16B)	0.9800	C(16)-H(16C)	0.9800
C(17)-C(18)	1.519(6)	C(17)-H(17A)	0.9900
C(17)-H(17B)	0.9900	C(18)-C(19)	1.532(5)
C(18)-H(18A)	0.9900	C(18)-H(18B)	0.9900
C(19)-C(20)	1.519(7)	C(19)-H(19A)	0.9900
C(19)-H(19B)	0.9900	C(20)-H(20A)	0.9800
C(20)-H(20B)	0.9800	C(20)-H(20C)	0.9800
C(21)-H(21A)	0.9800	C(21)-H(21B)	0.9800
C(21)-H(21C)	0.9800	C(22)-H(22A)	0.9800
C(22)-H(22B)	0.9800	C(22)-H(22C)	0.9800

Symmetry transformations used to generate equivalent atoms.

Table A.17 Bond Angles [°] for **9**

atom-atom-atom	angle	atom-atom-atom	angle
C(1)-Rh(1)-C(10)	78.41(15)	C(1)-Rh(1)-C(7)	78.48(14)
C(10)-Rh(1)-C(7)	156.61(14)	C(1)-Rh(1)-N(5)	92.55(13)
C(10)-Rh(1)-N(5)	89.97(12)	C(7)-Rh(1)-N(5)	94.56(13)
C(1)-Rh(1)-I(2)	88.20(10)	C(10)-Rh(1)-I(2)	86.90(10)
C(7)-Rh(1)-I(2)	88.86(10)	N(5)-Rh(1)-I(2)	176.57(8)
C(1)-Rh(1)-I(1)	176.12(10)	C(10)-Rh(1)-I(1)	102.84(10)
C(7)-Rh(1)-I(1)	100.46(10)	N(5)-Rh(1)-I(1)	83.80(8)
I(2)-Rh(1)-I(1)	95.525(11)	C(7)-N(1)-C(8)	111.4(3)
C(7)-N(1)-C(6)	117.1(3)	C(8)-N(1)-C(6)	131.2(3)
C(7)-N(2)-C(9)	111.8(3)	C(7)-N(2)-C(17)	124.6(3)
C(9)-N(2)-C(17)	122.9(3)	C(10)-N(3)-C(11)	111.0(3)
C(10)-N(3)-C(2)	117.0(3)	C(11)-N(3)-C(2)	132.0(3)
C(10)-N(4)-C(12)	111.2(3)	C(10)-N(4)-C(13)	124.7(3)
C(12)-N(4)-C(13)	124.0(3)	C(22)-N(5)-C(21)	109.3(3)
C(22)-N(5)-Rh(1)	114.2(2)	C(21)-N(5)-Rh(1)	117.8(2)
C(22)-N(5)-H(5)	104.7	C(21)-N(5)-H(5)	104.7
Rh(1)-N(5)-H(5)	104.7	C(2)-C(1)-C(6)	119.5(3)
C(2)-C(1)-Rh(1)	120.4(3)	C(6)-C(1)-Rh(1)	120.1(3)
C(1)-C(2)-C(3)	121.9(3)	C(1)-C(2)-N(3)	111.5(3)
C(3)-C(2)-N(3)	126.6(3)	C(2)-C(3)-C(4)	117.0(3)
C(2)-C(3)-H(3)	121.5	C(4)-C(3)-H(3)	121.5
C(5)-C(4)-C(3)	122.8(3)	C(5)-C(4)-H(4)	118.6
C(3)-C(4)-H(4)	118.6	C(4)-C(5)-C(6)	117.4(3)
C(4)-C(5)-H(5A)	121.3	C(6)-C(5)-H(5A)	121.3
C(1)-C(6)-C(5)	121.4(3)	C(1)-C(6)-N(1)	111.6(3)
C(5)-C(6)-N(1)	126.9(3)	N(2)-C(7)-N(1)	103.2(3)
N(2)-C(7)-Rh(1)	144.2(3)	N(1)-C(7)-Rh(1)	112.5(2)
C(9)-C(8)-N(1)	106.0(3)	C(9)-C(8)-H(8)	127.0
N(1)-C(8)-H(8)	127.0	C(8)-C(9)-N(2)	107.5(3)
C(8)-C(9)-H(9)	126.2	N(2)-C(9)-H(9)	126.2
N(4)-C(10)-N(3)	104.0(3)	N(4)-C(10)-Rh(1)	143.3(3)
N(3)-C(10)-Rh(1)	112.7(3)	C(12)-C(11)-N(3)	106.0(3)

Table A.17 (Continued)

C(12)-C(11)-H(11)	127.0	N(3)-C(11)-H(11)	127.0
C(11)-C(12)-N(4)	107.8(3)	C(11)-C(12)-H(12)	126.1
N(4)-C(12)-H(12)	126.1	N(4)-C(13)-C(14)	111.6(3)
N(4)-C(13)-H(13A)	109.3	C(14)-C(13)-H(13A)	109.3
N(4)-C(13)-H(13B)	109.3	C(14)-C(13)-H(13B)	109.3
H(13A)-C(13)-H(13B)	108.0	C(15)-C(14)-C(13)	114.8(3)
C(15)-C(14)-H(14A)	108.6	C(13)-C(14)-H(14A)	108.6
C(15)-C(14)-H(14B)	108.6	C(13)-C(14)-H(14B)	108.6
H(14A)-C(14)-H(14B)	107.5	C(14)-C(15)-C(16)	112.1(3)
C(14)-C(15)-H(15A)	109.2	C(16)-C(15)-H(15A)	109.2
C(14)-C(15)-H(15B)	109.2	C(16)-C(15)-H(15B)	109.2
H(15A)-C(15)-H(15B)	107.9	C(15)-C(16)-H(16A)	109.5
C(15)-C(16)-H(16B)	109.5	H(16A)-C(16)-H(16B)	109.5
C(15)-C(16)-H(16C)	109.5	H(16A)-C(16)-H(16C)	109.5
H(16B)-C(16)-H(16C)	109.5	N(2)-C(17)-C(18)	111.2(3)
N(2)-C(17)-H(17A)	109.4	C(18)-C(17)-H(17A)	109.4
N(2)-C(17)-H(17B)	109.4	C(18)-C(17)-H(17B)	109.4
H(17A)-C(17)-H(17B)	108.0	C(17)-C(18)-C(19)	112.0(3)
C(17)-C(18)-H(18A)	109.2	C(19)-C(18)-H(18A)	109.2
C(17)-C(18)-H(18B)	109.2	C(19)-C(18)-H(18B)	109.2
H(18A)-C(18)-H(18B)	107.9	C(20)-C(19)-C(18)	112.1(4)
C(20)-C(19)-H(19A)	109.2	C(18)-C(19)-H(19A)	109.2
C(20)-C(19)-H(19B)	109.2	C(18)-C(19)-H(19B)	109.2
H(19A)-C(19)-H(19B)	107.9	C(19)-C(20)-H(20A)	109.5
C(19)-C(20)-H(20B)	109.5	H(20A)-C(20)-H(20B)	109.5
C(19)-C(20)-H(20C)	109.5	H(20A)-C(20)-H(20C)	109.5
H(20B)-C(20)-H(20C)	109.5	N(5)-C(21)-H(21A)	109.5
N(5)-C(21)-H(21B)	109.5	H(21A)-C(21)-H(21B)	109.5
N(5)-C(21)-H(21C)	109.5	H(21A)-C(21)-H(21C)	109.5
H(21B)-C(21)-H(21C)	109.5	N(5)-C(22)-H(22A)	109.5
N(5)-C(22)-H(22B)	109.5	H(22A)-C(22)-H(22B)	109.5
N(5)-C(22)-H(22C)	109.5	H(22A)-C(22)-H(22C)	109.5
H(22B)-C(22)-H(22C)	109.5		

Symmetry transformations used to generate equivalent atoms.

Table A.18 Torsion Angles [°] for **9**

atom-atom-atom-atom	angle	atom-atom-atom-atom	angle
C(6)-C(1)-C(2)-C(3)	0.3(5)	Rh(1)-C(1)-C(2)-C(3)	179.7(3)
C(6)-C(1)-C(2)-N(3)	-179.7(3)	Rh(1)-C(1)-C(2)-N(3)	-0.3(4)
C(10)-N(3)-C(2)-C(1)	0.7(4)	C(11)-N(3)-C(2)-C(1)	179.9(3)
C(10)-N(3)-C(2)-C(3)	-179.3(3)	C(11)-N(3)-C(2)-C(3)	-0.1(6)
C(1)-C(2)-C(3)-C(4)	-0.4(5)	N(3)-C(2)-C(3)-C(4)	179.6(3)
C(2)-C(3)-C(4)-C(5)	-0.1(5)	C(3)-C(4)-C(5)-C(6)	0.6(5)
C(2)-C(1)-C(6)-C(5)	0.3(5)	Rh(1)-C(1)-C(6)-C(5)	-179.1(3)
C(2)-C(1)-C(6)-N(1)	-176.8(3)	Rh(1)-C(1)-C(6)-N(1)	3.8(4)
C(4)-C(5)-C(6)-C(1)	-0.7(5)	C(4)-C(5)-C(6)-N(1)	175.9(3)
C(7)-N(1)-C(6)-C(1)	-0.2(4)	C(8)-N(1)-C(6)-C(1)	173.3(3)
C(7)-N(1)-C(6)-C(5)	-177.1(3)	C(8)-N(1)-C(6)-C(5)	-3.6(6)
C(9)-N(2)-C(7)-N(1)	-1.1(4)	C(17)-N(2)-C(7)-N(1)	-172.5(3)
C(9)-N(2)-C(7)-Rh(1)	175.9(4)	C(17)-N(2)-C(7)-Rh(1)	4.5(7)
C(8)-N(1)-C(7)-N(2)	0.3(4)	C(6)-N(1)-C(7)-N(2)	175.1(3)
C(8)-N(1)-C(7)-Rh(1)	-177.8(2)	C(6)-N(1)-C(7)-Rh(1)	-3.0(4)
C(7)-N(1)-C(8)-C(9)	0.6(4)	C(6)-N(1)-C(8)-C(9)	-173.2(4)
N(1)-C(8)-C(9)-N(2)	-1.3(4)	C(7)-N(2)-C(9)-C(8)	1.6(5)
C(17)-N(2)-C(9)-C(8)	173.1(3)	C(12)-N(4)-C(10)-N(3)	-0.6(4)
C(13)-N(4)-C(10)-N(3)	176.3(3)	C(12)-N(4)-C(10)-Rh(1)	-179.2(3)
C(13)-N(4)-C(10)-Rh(1)	-2.3(6)	C(11)-N(3)-C(10)-N(4)	0.8(4)
C(2)-N(3)-C(10)-N(4)	-179.9(3)	C(11)-N(3)-C(10)-Rh(1)	179.9(2)
C(2)-N(3)-C(10)-Rh(1)	-0.8(4)	C(10)-N(3)-C(11)-C(12)	-0.6(4)
C(2)-N(3)-C(11)-C(12)	-179.9(3)	N(3)-C(11)-C(12)-N(4)	0.2(4)
C(10)-N(4)-C(12)-C(11)	0.3(4)	C(13)-N(4)-C(12)-C(11)	-176.7(3)
C(10)-N(4)-C(13)-C(14)	-79.2(4)	C(12)-N(4)-C(13)-C(14)	97.4(4)
N(4)-C(13)-C(14)-C(15)	-62.2(4)	C(13)-C(14)-C(15)-C(16)	178.2(4)
C(7)-N(2)-C(17)-C(18)	85.9(4)	C(9)-N(2)-C(17)-C(18)	-84.5(4)
N(2)-C(17)-C(18)-C(19)	-178.4(3)	C(17)-C(18)-C(19)-C(20)	178.0(4)

Symmetry transformations used to generate equivalent atoms.

Table A.19 Hydrogen Bonds for **9**

D-H...A d(D-H) d(H...A) d(D...A) <(DHA)

A.3.1 Crystal Summary for **9**

X-Ray Intensity data were collected at 100 K on a Bruker AXS diffractometer using MoK α radiation ($\lambda = 0.71073 \text{ \AA}$) and an APEXII CCD area detector. Raw data frames were read by program SAINT¹ and integrated using 3D profiling algorithms. The resulting data were reduced to produce hkl reflections and their intensities and estimated standard deviations. The data were corrected using multi-scan absorption correction through the APEX2³⁰⁵ crystallographic software suite.

The structure was solved using ShelXS³⁰⁶ and refined using ShelXL³⁰⁷ full-matrix least-squares refinement. Molecular drawings and reports were generated using Olex2.³⁰⁸ The non-H atoms were refined with anisotropic thermal parameters and all of the H atoms were calculated in idealized positions and refined riding on their parent atoms. In the final cycle of refinement, 22210 reflections (of which 6172 are observed with $I > 2\sigma(I)$) were used to refine 275 parameters and the resulting R_1 , wR_2 and S (goodness of fit) were 3.01%, 6.50% respectively. The refinement was carried out by minimizing the wR_2 function using F^2 rather than F values. R_1 is calculated to provide a reference to the conventional R value but its function is not minimized.

The size of the crystal was 0.20 x 0.20 x 0.20 mm at the time of data collection. The structure presented shows the expected, complete molecule in the asymmetric unit as indicated by the chemist who grew the molecule. Bond distances should be treated as a close approximation until better data can be acquired.

The model was refined by full-matrix least-squares analysis of F^2 against all reflections. All non-hydrogen atoms were refined with anisotropic thermal displacement parameters. Unless otherwise noted, hydrogen atoms were included in calculated positions. Thermal parameters for the hydrogens were tied to the isotropic thermal parameter of the atom to which they are bonded (1.5 \times for methyl, 1.2 \times for all others).

A.4

Chapter V Compounds

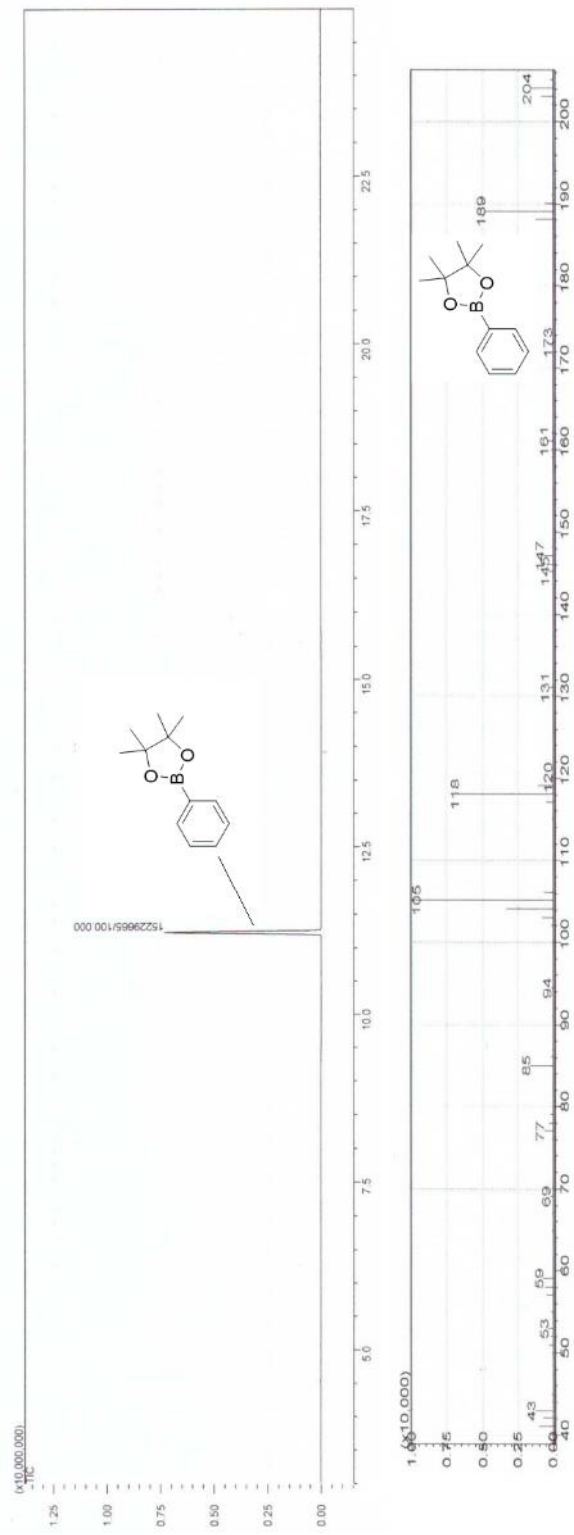


Figure A.95 GC-MS chromatogram spectrum of catalytic trial (Table 5.1, Entry 4)

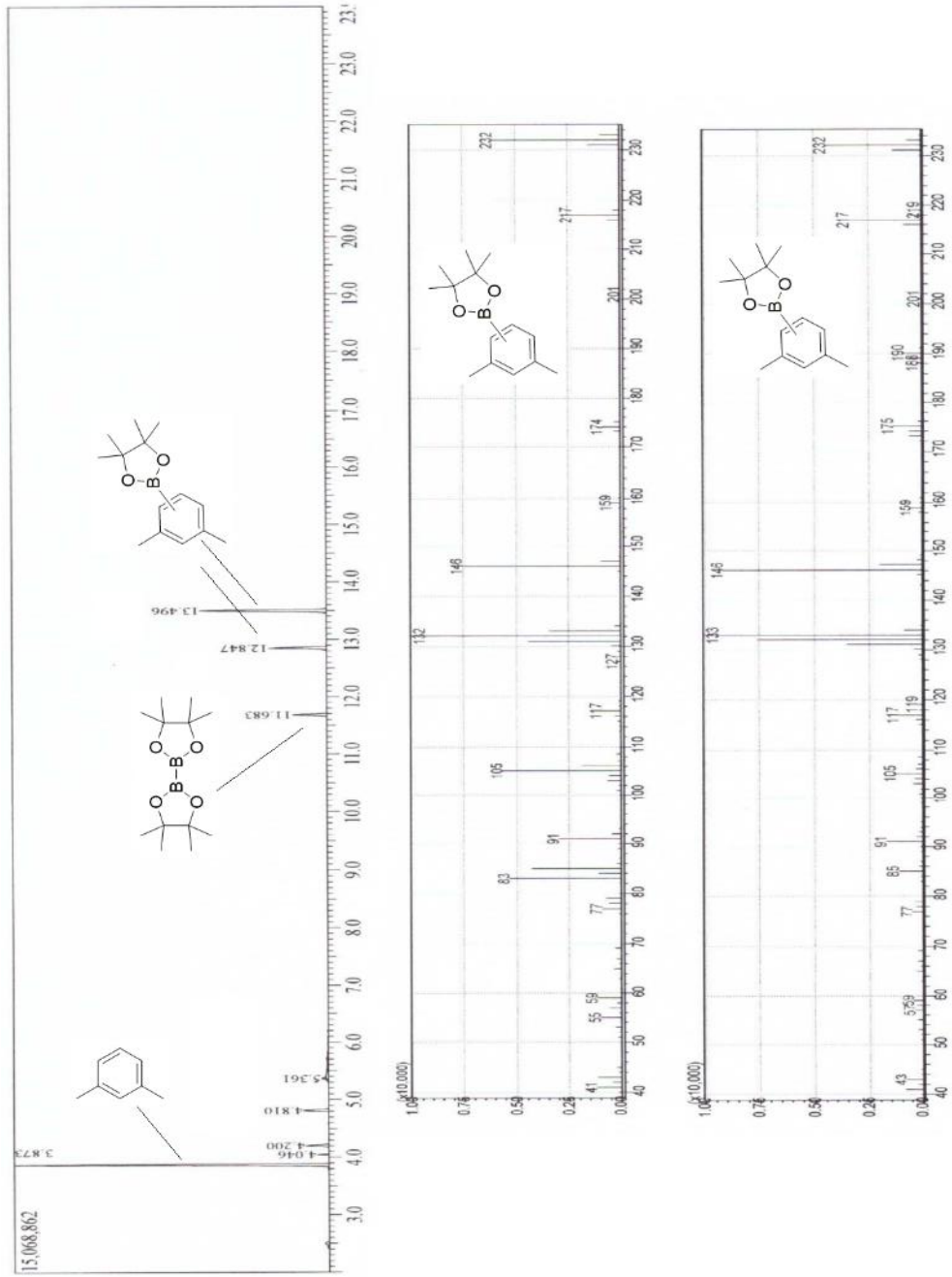


Figure A.96 GC-MS chromatogram spectrum of catalytic trial (Table 5.2, Entry 1)

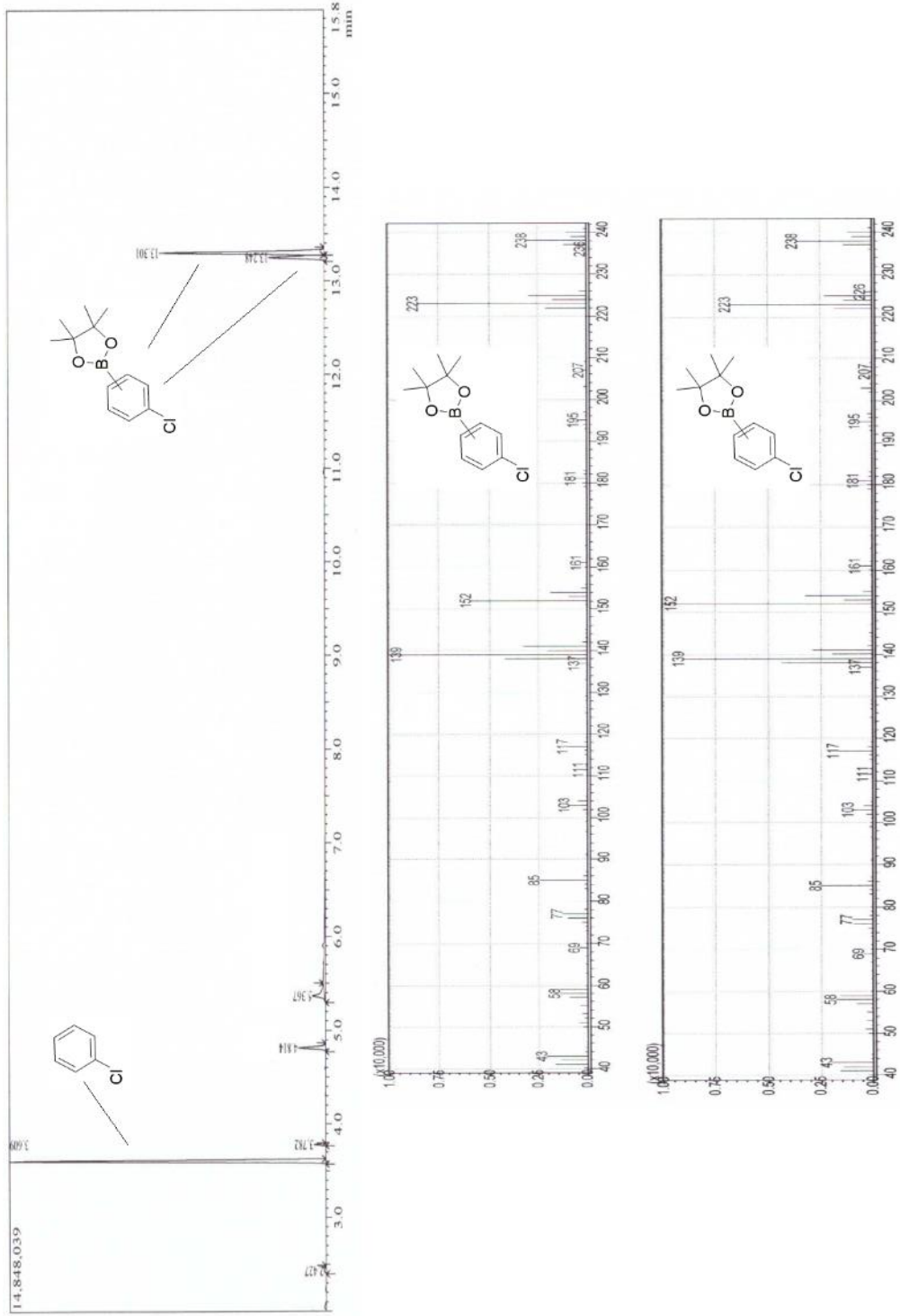


Figure A.97 GC-MS chromatogram spectrum of catalytic trial (Table 5.2, Entry 2)

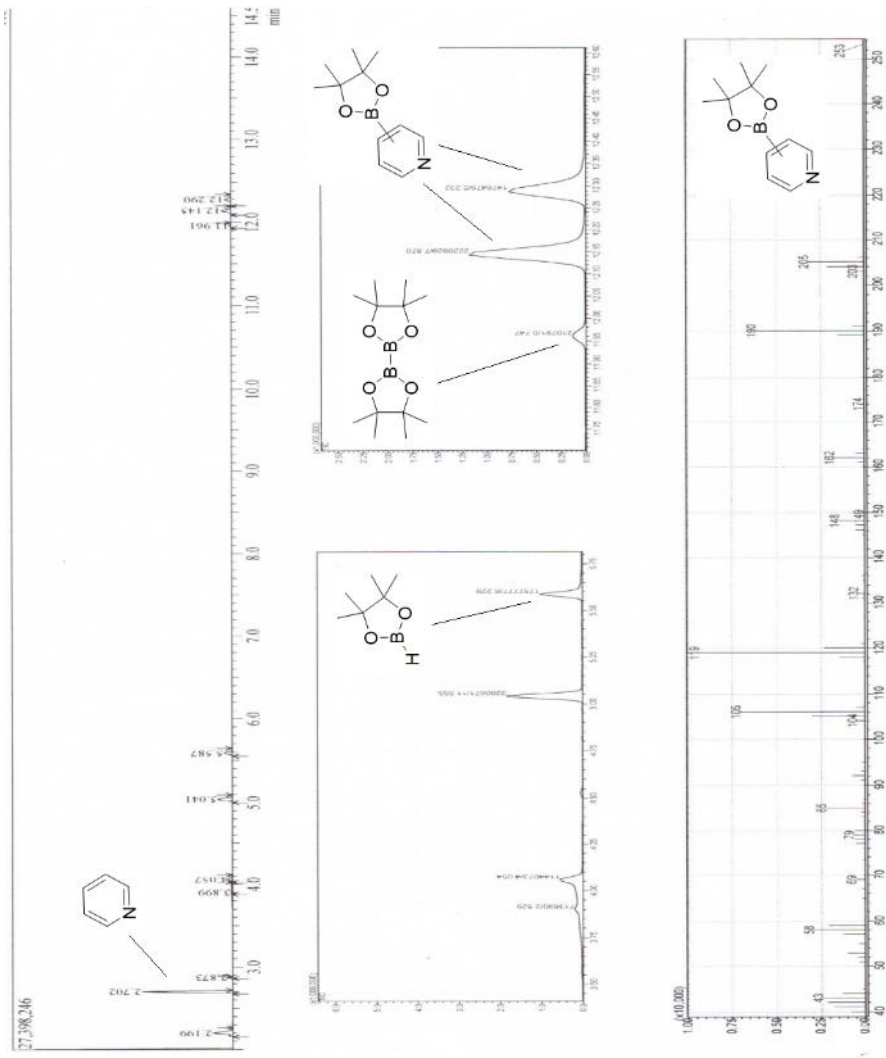


Figure A.98 GC-MS chromatogram spectrum of catalytic trial (Table 5.2, Entry 3)

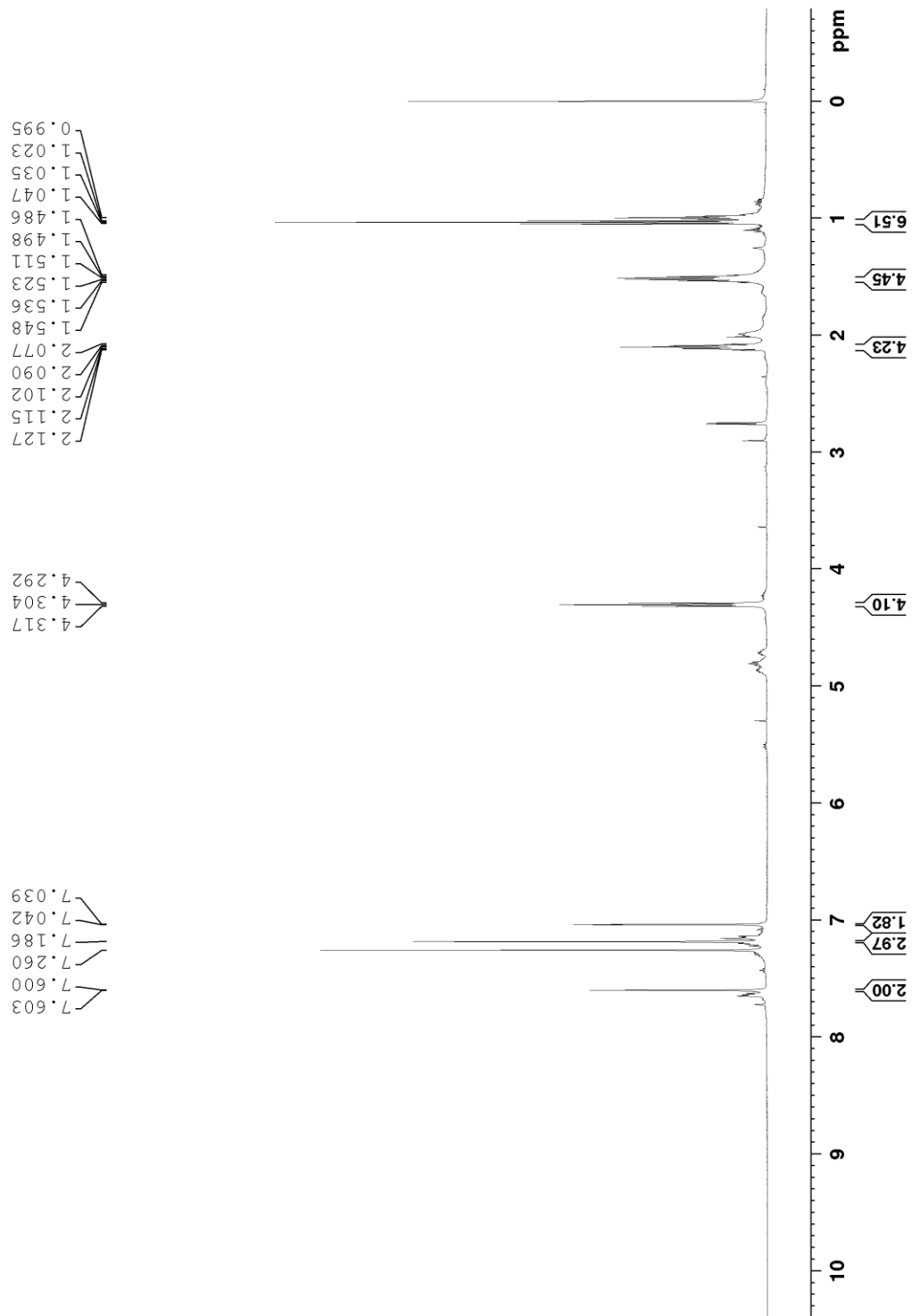


Figure A.99 ^1H NMR (600 MHz, CDCl_3) spectrum of **13**

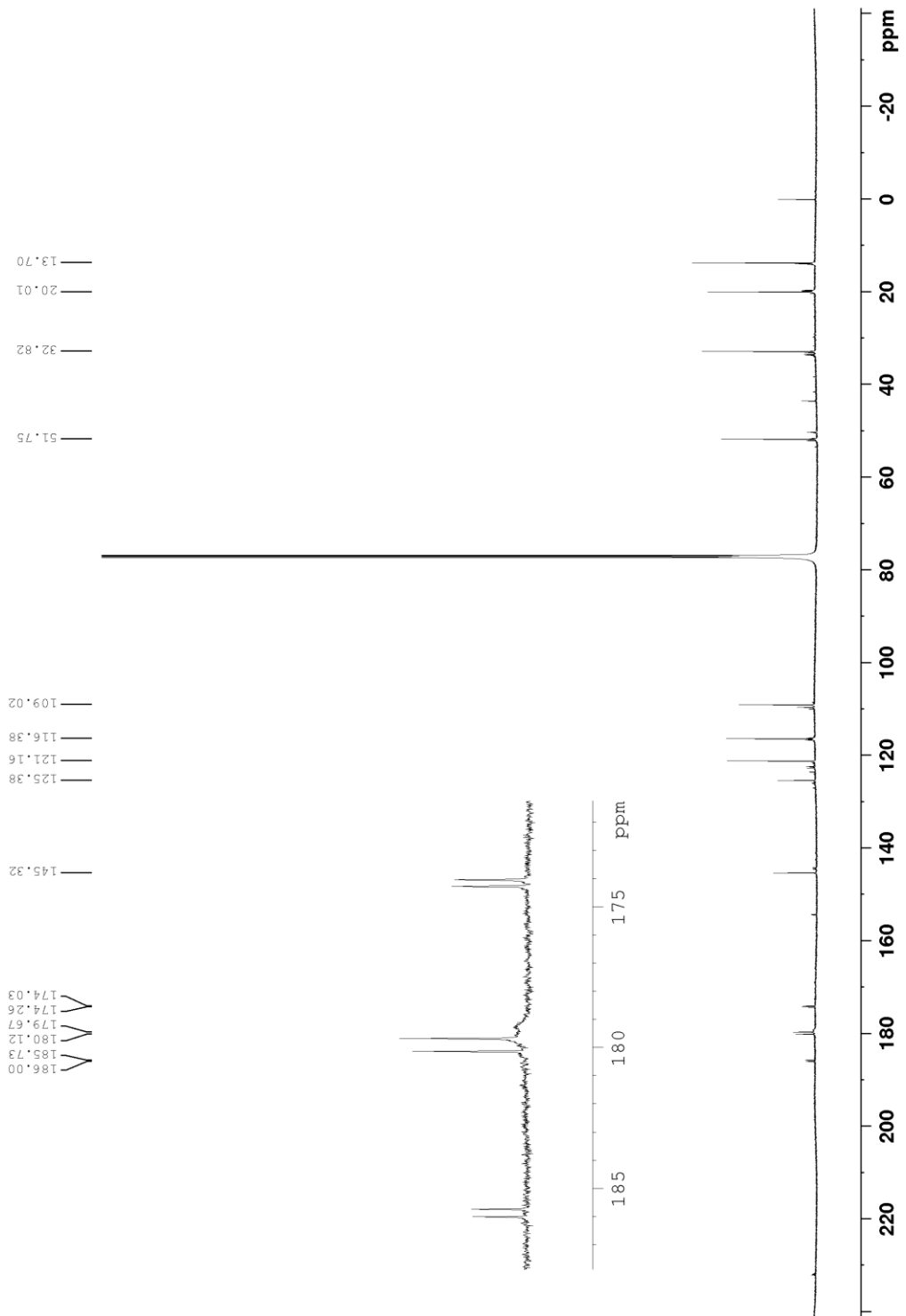


Figure A.100 ^{13}C NMR (150 MHz, CDCl_3) spectrum of **13**

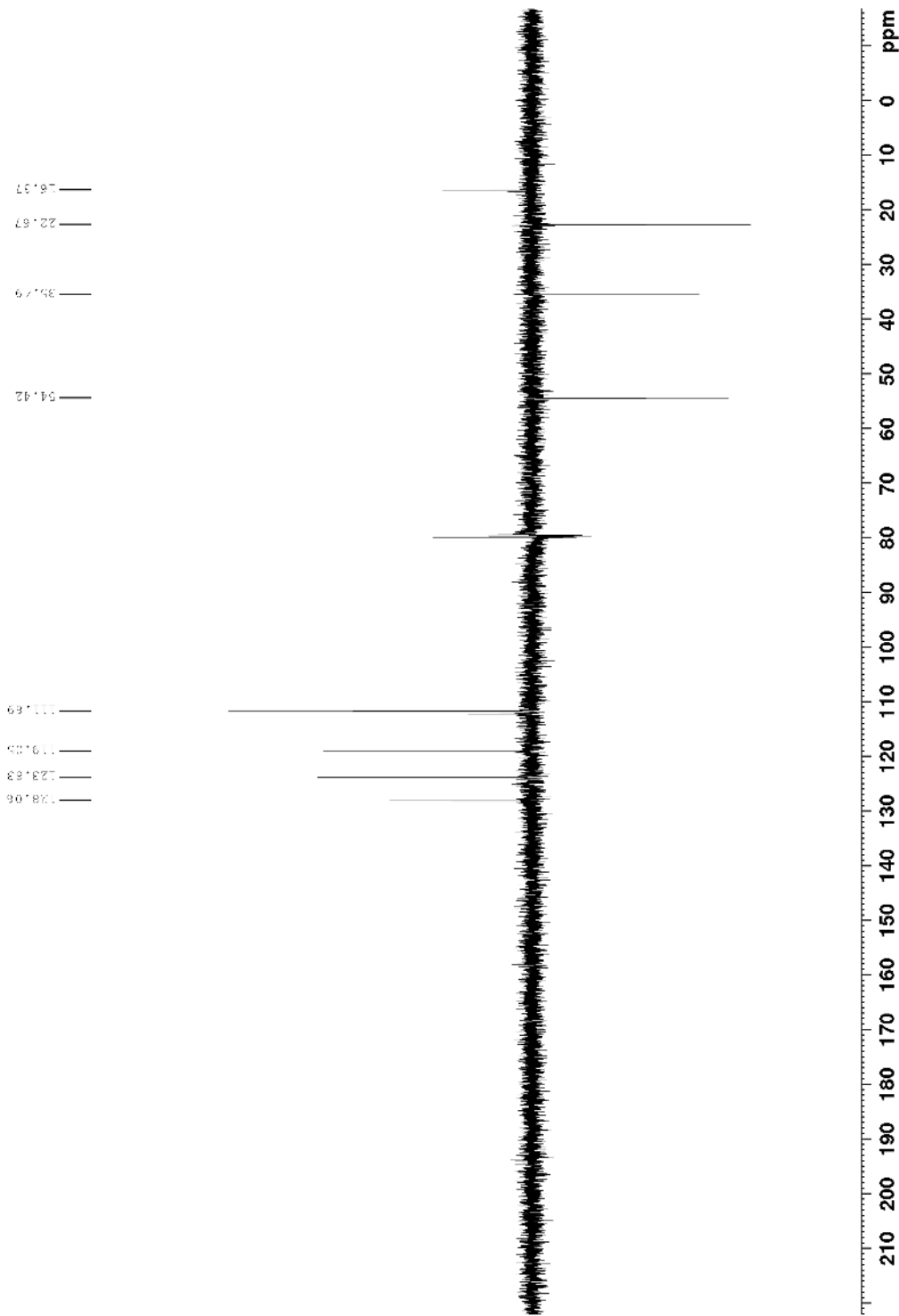


Figure A.101 ^{13}C DEPT 135 NMR (150 MHz, CDCl_3) spectrum of 13

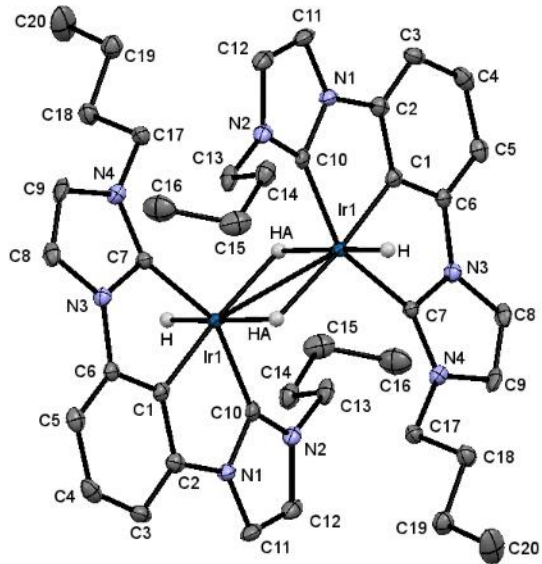


Figure A.102 X-ray molecular structure of **12**

Table A.20 Crystal Data and Structure Refinement for **12**

Empirical formula	$C_{20}H_{25}IrN_4$		
Formula weight	513.64		
Temperature	100(2) K		
Wavelength	0.71073 Å		
Crystal system	Monoclinic		
Space group	P2 ₁ /c		
Unit cell dimensions	$a = 10.9713(3)$ Å	$\alpha = 90^\circ$	
	$b = 16.1248(4)$ Å	$\beta = 113.3340(10)^\circ$	
	$c = 11.6392(3)$ Å	$\gamma = 90^\circ$	
Volume	$1890.68(9)$ Å ³		
Z	4		
Density (calculated)	1.804 g.cm ⁻³		
Absorption coefficient (μ)	7.071 mm ⁻¹		
F(000)	1000		
Crystal color, habit	Brown, Tablet		
Crystal size	$0.202 \times 0.150 \times 0.098$ mm ³		
θ range for data collection	2.022 to 27.984°		
Index ranges	$-14 \leq h \leq 14, -21 \leq k \leq 20, -15 \leq l \leq 15$		
Reflections collected	15540		
Independent reflections	4513 [$R_{int} = 0.0392$]		
Completeness to $\theta = 25.242^\circ$	99.8 %		
Absorption correction	Numerical		
Max. and min. transmission	0.5749 and 0.4294		
Refinement method	Full-matrix least-squares on F^2		
Data / restraints / parameters	4513 / 0 / 226		
Goodness-of-fit on F^2	1.042		
Final R indices [$I > 2\sigma(I)$]	$R_1 = 0.0213, wR_2 = 0.0530$		
R indices (all data)	$R_1 = 0.0251, wR_2 = 0.0552$		
Extinction coefficient	n/a		
Largest diff. peak and hole	0.878 and -1.201 e ⁻ .Å ⁻³		

Table A.21 Atomic Coordinates and Equivalent Isotropic Displacement Parameters (\AA^2) for **12**

	x	y	z	U(eq)
Ir(1)	0.52974(2)	0.55649(2)	0.59778(2)	0.010(1)
N(1)	0.7165(2)	0.68641(15)	0.6063(2)	0.014(1)
N(2)	0.5511(3)	0.70914(16)	0.4309(2)	0.015(1)
N(3)	0.6361(2)	0.48540(16)	0.8462(2)	0.013(1)
N(4)	0.4382(3)	0.43500(15)	0.7671(3)	0.014(1)
C(1)	0.6955(3)	0.58674(19)	0.7386(3)	0.013(1)
C(2)	0.7776(3)	0.64793(19)	0.7254(3)	0.014(1)
C(3)	0.8989(3)	0.6666(2)	0.8213(3)	0.018(1)
C(4)	0.9365(3)	0.6204(2)	0.9318(3)	0.019(1)
C(5)	0.8567(3)	0.55784(18)	0.9480(3)	0.017(1)
C(6)	0.7366(3)	0.54248(18)	0.8498(3)	0.013(1)
C(7)	0.5230(3)	0.48289(18)	0.7372(3)	0.011(1)
C(8)	0.6217(3)	0.43857(18)	0.9400(3)	0.016(1)
C(9)	0.4978(3)	0.4068(2)	0.8900(3)	0.018(1)
C(10)	0.5924(3)	0.65565(19)	0.5276(3)	0.015(1)
C(11)	0.7492(3)	0.7567(2)	0.5554(3)	0.019(1)
C(12)	0.6465(3)	0.7707(2)	0.4464(3)	0.020(1)
C(13)	0.4208(3)	0.7066(2)	0.3284(3)	0.018(1)
C(14)	0.3326(3)	0.7776(2)	0.3368(3)	0.021(1)
C(15)	0.1914(3)	0.7739(2)	0.2367(4)	0.026(1)
C(16)	0.1833(4)	0.7821(3)	0.1040(4)	0.032(1)
C(17)	0.3011(3)	0.4160(2)	0.6827(3)	0.015(1)
C(18)	0.1984(3)	0.4568(2)	0.7217(3)	0.018(1)
C(19)	0.0593(3)	0.4261(2)	0.6421(3)	0.019(1)
C(20)	-0.0494(4)	0.4673(3)	0.6722(4)	0.036(1)
H(3A)	0.9531	0.7084	0.8124	0.021
H(4A)	1.0177	0.6318	0.9968	0.023
H(5A)	0.8833	0.5277	1.0220	0.020
H(8A)	0.6846	0.4307	1.0210	0.020
H(9A)	0.4593	0.3722	0.9303	0.022
H(11A)	0.8267	0.7877	0.5900	0.023
H(12A)	0.6397	0.8138	0.3910	0.024

Table A.21 (Continued)

H(13A)	0.3784	0.6541	0.3303	0.021
H(13B)	0.4310	0.7101	0.2495	0.021
H(14A)	0.3288	0.7765	0.4186	0.025
H(14B)	0.3726	0.8298	0.3291	0.025
H(15A)	0.1516	0.7216	0.2443	0.032
H(15B)	0.1397	0.8180	0.2522	0.032
H(16A)	0.0921	0.7793	0.0462	0.048
H(16B)	0.2203	0.8344	0.0948	0.048
H(16C)	0.2323	0.7379	0.0869	0.048
H(17A)	0.2884	0.3564	0.6800	0.018
H(17B)	0.2867	0.4343	0.5989	0.018
H(18A)	0.2189	0.4445	0.8090	0.021
H(18B)	0.2020	0.5165	0.7131	0.021
H(19A)	0.0559	0.3667	0.6537	0.023
H(19B)	0.0417	0.4358	0.5547	0.023
H(20A)	-0.1341	0.4450	0.6187	0.053
H(20B)	-0.0342	0.4568	0.7580	0.053
H(20C)	-0.0484	0.5260	0.6589	0.053

U(eq) is defined as one third of the trace of the orthogonalized U_{ij} tensor.

Table A.22 Anisotropic Displacement Parameters (\AA^2) for **12**

	U₁₁	U₂₂	U₃₃	U₂₃	U₁₃	U₁₂
Ir(1)	0.0110(1)	0.0097(1)	0.0100(1)	0.0002(1)	0.0052(1)	-0.0003(1)
N(1)	0.0174(12)	0.0114(13)	0.0167(13)	-0.0023(10)	0.0104(11)	-0.0035(10)
N(2)	0.0224(13)	0.0108(13)	0.0172(13)	0.0007(10)	0.0121(11)	-0.0001(10)
N(3)	0.0153(12)	0.0122(13)	0.0126(13)	0.0001(10)	0.0063(10)	0.0006(10)
N(4)	0.0145(12)	0.0140(13)	0.0137(13)	0.0014(10)	0.0071(11)	0.0012(10)
C(1)	0.0155(14)	0.0106(14)	0.0161(15)	-0.0016(12)	0.0099(12)	0.0012(11)
C(2)	0.0134(13)	0.0134(15)	0.0181(16)	-0.0025(12)	0.0076(12)	0.0011(11)
C(3)	0.0154(14)	0.0161(16)	0.0235(17)	-0.0067(13)	0.0092(13)	-0.0046(12)
C(4)	0.0140(14)	0.0206(17)	0.0178(16)	-0.0058(13)	0.0022(13)	0.0015(12)
C(5)	0.0194(15)	0.0144(16)	0.0174(17)	-0.0019(12)	0.0079(14)	0.0045(12)
C(6)	0.0150(14)	0.0127(14)	0.0137(15)	-0.0029(11)	0.0082(13)	0.0005(11)
C(7)	0.0112(13)	0.0109(14)	0.0101(14)	-0.0002(11)	0.0040(11)	0.0001(11)
C(8)	0.0240(16)	0.0144(16)	0.0105(15)	0.0026(11)	0.0065(13)	0.0026(12)
C(9)	0.0287(16)	0.0189(17)	0.0119(15)	0.0041(12)	0.0127(14)	0.0011(13)
C(10)	0.0198(14)	0.0136(15)	0.0144(15)	-0.0022(12)	0.0107(13)	0.0003(12)
C(11)	0.0263(16)	0.0134(16)	0.0266(18)	-0.0019(13)	0.0192(15)	-0.0055(13)
C(12)	0.0298(17)	0.0116(15)	0.0273(18)	-0.0025(13)	0.0202(15)	-0.0027(13)
C(13)	0.0255(16)	0.0164(16)	0.0129(15)	0.0037(12)	0.0097(13)	0.0051(13)
C(14)	0.0269(17)	0.0184(17)	0.0220(17)	-0.0007(14)	0.0147(15)	0.0033(14)
C(15)	0.0227(17)	0.0182(18)	0.042(2)	0.0022(16)	0.0161(16)	0.0033(14)
C(16)	0.0228(17)	0.034(2)	0.034(2)	0.0024(17)	0.0044(16)	-0.0019(16)
C(17)	0.0155(14)	0.0151(15)	0.0155(15)	-0.0039(12)	0.0075(12)	-0.0023(12)
C(18)	0.0178(15)	0.0192(16)	0.0176(17)	-0.0049(13)	0.0081(14)	-0.0010(12)
C(19)	0.0179(15)	0.0228(17)	0.0188(17)	-0.0011(14)	0.0085(14)	0.0014(13)
C(20)	0.0191(17)	0.057(3)	0.032(2)	-0.011(2)	0.0116(17)	0.0087(18)

$$-2\pi^2[h^2a^{*2}U_{11} + \dots + 2hka^*b^*U_{12}] \quad (\text{A.4})$$

Table A.23 Bond Lengths [Å] for **12**

atom-atom	distance	atom-atom	distance
Ir(1)-C(1)	1.967(3)	Ir(1)-C(7)	2.035(3)
Ir(1)-C(10)	2.035(3)	Ir(1)-Ir(1)#1	2.7837(2)
N(1)-C(11)	1.390(4)	N(1)-C(10)	1.397(4)
N(1)-C(2)	1.421(4)	N(2)-C(10)	1.346(4)
N(2)-C(12)	1.401(4)	N(2)-C(13)	1.455(4)
N(3)-C(7)	1.379(4)	N(3)-C(8)	1.387(4)
N(3)-C(6)	1.425(4)	N(4)-C(7)	1.357(4)
N(4)-C(9)	1.393(4)	N(4)-C(17)	1.466(4)
C(1)-C(2)	1.385(4)	C(1)-C(6)	1.388(4)
C(2)-C(3)	1.390(4)	C(3)-C(4)	1.400(5)
C(4)-C(5)	1.397(4)	C(5)-C(6)	1.382(5)
C(8)-C(9)	1.350(5)	C(11)-C(12)	1.341(5)
C(13)-C(14)	1.527(4)	C(14)-C(15)	1.526(5)
C(15)-C(16)	1.518(5)	C(17)-C(18)	1.521(4)
C(18)-C(19)	1.521(4)	C(19)-C(20)	1.522(4)

Table A.24 Bond Angles [°] for **12**

atom-atom-atom	angle	atom-atom-atom	angle
C(1)-Ir(1)-C(7)	78.10(12)	C(1)-Ir(1)-C(10)	77.99(12)
C(7)-Ir(1)-C(10)	154.55(12)	C(1)-Ir(1)-Ir(1)#1	133.10(8)
C(7)-Ir(1)-Ir(1)#1	101.52(8)	C(10)-Ir(1)-Ir(1)#1	101.12(8)
C(11)-N(1)-C(10)	111.1(3)	C(11)-N(1)-C(2)	132.0(3)
C(10)-N(1)-C(2)	116.4(2)	C(10)-N(2)-C(12)	111.1(3)
C(10)-N(2)-C(13)	124.3(3)	C(12)-N(2)-C(13)	124.5(3)
C(7)-N(3)-C(8)	111.5(2)	C(7)-N(3)-C(6)	116.7(2)
C(8)-N(3)-C(6)	131.1(3)	C(7)-N(4)-C(9)	111.0(3)
C(7)-N(4)-C(17)	125.0(3)	C(9)-N(4)-C(17)	124.0(3)
C(2)-C(1)-C(6)	119.0(3)	C(2)-C(1)-Ir(1)	120.8(2)
C(6)-C(1)-Ir(1)	120.1(2)	C(3)-C(2)-C(1)	121.6(3)
C(3)-C(2)-N(1)	128.3(3)	C(1)-C(2)-N(1)	110.1(3)
C(2)-C(3)-C(4)	117.5(3)	C(5)-C(4)-C(3)	122.4(3)
C(6)-C(5)-C(4)	117.5(3)	C(5)-C(6)-C(1)	122.0(3)
C(5)-C(6)-N(3)	127.8(3)	C(1)-C(6)-N(3)	110.1(3)
N(4)-C(7)-N(3)	103.9(2)	N(4)-C(7)-Ir(1)	141.4(2)
N(3)-C(7)-Ir(1)	114.40(19)	C(9)-C(8)-N(3)	106.0(3)
C(8)-C(9)-N(4)	107.6(3)	N(2)-C(10)-N(1)	103.8(2)
N(2)-C(10)-Ir(1)	141.6(2)	N(1)-C(10)-Ir(1)	114.3(2)
C(12)-C(11)-N(1)	106.2(3)	C(11)-C(12)-N(2)	107.9(3)
N(2)-C(13)-C(14)	111.6(3)	C(15)-C(14)-C(13)	113.6(3)
C(16)-C(15)-C(14)	113.9(3)	N(4)-C(17)-C(18)	113.2(2)
C(19)-C(18)-C(17)	111.1(3)	C(18)-C(19)-C(20)	113.9(3)

Table A.25 Torsion Angles [°] for **12**

atom-atom-atom-atom	angle	atom-atom-atom-atom	angle
C(6)-C(1)-C(2)-C(3)	-0.9(4)	Ir(1)-C(1)-C(2)-C(3)	-176.0(2)
C(6)-C(1)-C(2)-N(1)	-179.0(2)	Ir(1)-C(1)-C(2)-N(1)	5.8(3)
C(11)-N(1)-C(2)-C(3)	-7.8(5)	C(10)-N(1)-C(2)-C(3)	-179.2(3)
C(11)-N(1)-C(2)-C(1)	170.2(3)	C(10)-N(1)-C(2)-C(1)	-1.2(3)
C(1)-C(2)-C(3)-C(4)	1.0(4)	N(1)-C(2)-C(3)-C(4)	178.8(3)
C(2)-C(3)-C(4)-C(5)	-0.5(4)	C(3)-C(4)-C(5)-C(6)	-0.1(4)
C(4)-C(5)-C(6)-C(1)	0.2(4)	C(4)-C(5)-C(6)-N(3)	-176.5(3)
C(2)-C(1)-C(6)-C(5)	0.3(4)	Ir(1)-C(1)-C(6)-C(5)	175.5(2)
C(2)-C(1)-C(6)-N(3)	177.5(2)	Ir(1)-C(1)-C(6)-N(3)	-7.3(3)
C(7)-N(3)-C(6)-C(5)	178.6(3)	C(8)-N(3)-C(6)-C(5)	9.1(5)
C(7)-N(3)-C(6)-C(1)	1.6(3)	C(8)-N(3)-C(6)-C(1)	-168.0(3)
C(9)-N(4)-C(7)-N(3)	-1.5(3)	C(17)-N(4)-C(7)-N(3)	177.6(3)
C(9)-N(4)-C(7)-Ir(1)	-173.6(3)	C(17)-N(4)-C(7)-Ir(1)	5.6(5)
C(8)-N(3)-C(7)-N(4)	1.3(3)	C(6)-N(3)-C(7)-N(4)	-170.3(2)
C(8)-N(3)-C(7)-Ir(1)	175.83(19)	C(6)-N(3)-C(7)-Ir(1)	4.3(3)
C(7)-N(3)-C(8)-C(9)	-0.5(3)	C(6)-N(3)-C(8)-C(9)	169.4(3)
N(3)-C(8)-C(9)-N(4)	-0.4(3)	C(7)-N(4)-C(9)-C(8)	1.3(3)
C(17)-N(4)-C(9)-C(8)	-177.9(3)	C(12)-N(2)-C(10)-N(1)	1.0(3)
C(13)-N(2)-C(10)-N(1)	-174.9(2)	C(12)-N(2)-C(10)-Ir(1)	174.6(3)
C(13)-N(2)-C(10)-Ir(1)	-1.3(5)	C(11)-N(1)-C(10)-N(2)	-1.0(3)
C(2)-N(1)-C(10)-N(2)	172.2(2)	C(11)-N(1)-C(10)-Ir(1)	-176.60(19)
C(2)-N(1)-C(10)-Ir(1)	-3.4(3)	C(10)-N(1)-C(11)-C(12)	0.6(3)
C(2)-N(1)-C(11)-C(12)	-171.2(3)	N(1)-C(11)-C(12)-N(2)	0.1(3)
C(10)-N(2)-C(12)-C(11)	-0.7(3)	C(13)-N(2)-C(12)-C(11)	175.2(3)
C(10)-N(2)-C(13)-C(14)	107.5(3)	C(12)-N(2)-C(13)-C(14)	-67.8(3)
N(2)-C(13)-C(14)-C(15)	-175.7(3)	C(13)-C(14)-C(15)-C(16)	-63.1(4)
C(7)-N(4)-C(17)-C(18)	-110.9(3)	C(9)-N(4)-C(17)-C(18)	68.1(4)
N(4)-C(17)-C(18)-C(19)	-172.3(3)	C(17)-C(18)-C(19)-C(20)	-177.4(3)

A.4.1 Crystal Summary for 12

Crystal data for C₂₀H₂₇IrN₄; M_r = 513.64; Monoclinic; space group P2₁/c; a = 10.9713(3) Å; b = 16.1248(4) Å; c = 11.6392(3) Å; α = 90°; β = 113.3340(10)°; γ = 90°; V = 1890.68(9) Å³; Z = 4; T = 100(2) K; λ (Mo-Kα) = 0.71073 Å; μ (Mo-Kα) = 7.071 mm⁻¹; d_{calc} = 1.804 g.cm⁻³; 15540 reflections collected; 4513 unique (R_{int} = 0.0392); giving R_1 = 0.0213, wR₂ = 0.0530 for 4050 data with [$I > 2\sigma(I)$] and R_1 = 0.0251, wR₂ = 0.0552 for all 4513 data. Residual electron density (e⁻.Å⁻³) max/min: 0.878/-1.201.

An arbitrary sphere of data were collected on a Brown Tablet-like crystal, having approximate dimensions of 0.202 × 0.150 × 0.098 mm, on a Bruker APEX-II diffractometer using a combination of ω - and φ -scans of 0.5°.³⁰³ Data were corrected for absorption and polarization effects and analyzed for space group determination. The structure was solved by vecmap methods and expanded routinely.³⁰⁴ The model was refined by full-matrix least-squares analysis of F² against all reflections. All non-hydrogen atoms were refined with anisotropic thermal displacement parameters. Unless otherwise noted, hydrogen atoms were included in calculated positions. Thermal parameters for the hydrogens were tied to the isotropic thermal parameter of the atom to which they are bonded (1.5 × for methyl, 1.2 × for all others).

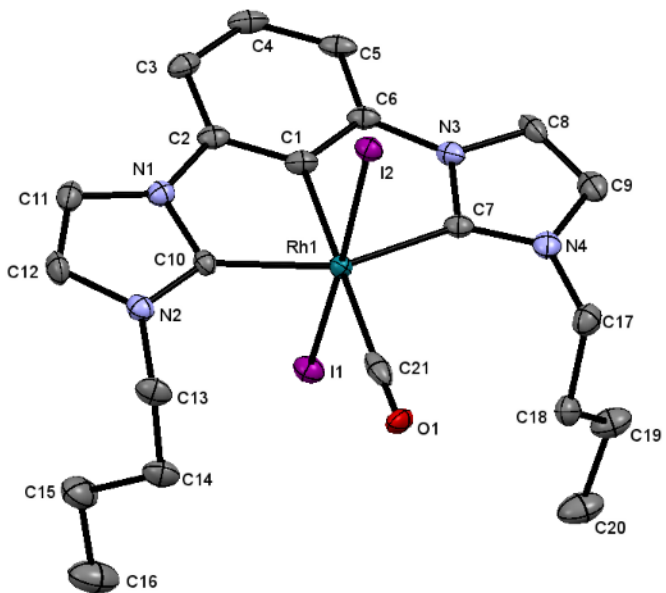


Figure A.103 X-ray molecular structure of **13**

Table A.26 Crystal Data and Structure Refinement for **13**

Empirical formula	$C_{21}H_{25}I_2N_4ORh$		
Formula weight	706.16		
Temperature	99.99 K		
Wavelength	0.71073 Å		
Crystal system	Triclinic		
Space group	P-1		
Unit cell dimensions	$a = 8.2638(2)$ Å	$\alpha = 88.0310(10)^\circ$	
	$b = 8.4439(2)$ Å	$\beta = 84.8720(10)^\circ$	
	$c = 16.8412(3)$ Å	$\gamma = 83.4470(10)^\circ$	
Volume	$1162.46(4)$ Å ³		
Z	2		
Density (calculated)	2.017 g.cm ⁻³		
Absorption coefficient (μ)	3.410 mm ⁻¹		
F(000)	676		
Crystal color, habit	Orange, Plates		
Crystal size	$0.32 \times 0.261 \times 0.257$ mm ³		
θ range for data collection	1.214 to 27.877°		
Index ranges	$-10 \leq h \leq 10, -11 \leq k \leq 11, -22 \leq l \leq 22$		
Reflections collected	19052		
Independent reflections	5399 [$R_{int} = 0.0236$]		
Completeness to $\theta = 26.000^\circ$	98.7 %		
Absorption correction	Semi-empirical from equivalents		
Max. and min. transmission	0.7844 and 0.5599		
Refinement method	Full-matrix least-squares on F^2		
Data / restraints / parameters	5399 / 0 / 265		
Goodness-of-fit on F^2	1.147		
Final R indices [$I > 2\sigma(I)$]	$R_1 = 0.0227, wR_2 = 0.0556$		
R indices (all data)	$R_1 = 0.0244, wR_2 = 0.0643$		
Extinction coefficient	0.00035(14)		
Largest diff. peak and hole	1.081 and -1.133 e ⁻ .Å ⁻³		

Table A.27 Atomic Coordinates and Equivalent Isotropic Displacement Parameters (\AA^2) for **13**

	x	y	z	U(eq)
I(1)	0.58445(3)	0.17770(3)	0.66374(2)	0.020(1)
I(2)	0.24862(2)	0.42658(2)	0.92496(2)	0.016(1)
Rh(1)	0.40734(3)	0.31112(3)	0.78936(2)	0.013(1)
O(1)	0.1627(3)	0.5047(3)	0.69051(14)	0.021(1)
N(1)	0.7061(3)	0.4096(3)	0.84159(16)	0.016(1)
N(2)	0.6217(3)	0.6069(3)	0.76610(16)	0.017(1)
N(3)	0.3920(3)	-0.0082(3)	0.85819(16)	0.016(1)
N(4)	0.1708(3)	0.0324(3)	0.79806(16)	0.019(1)
C(1)	0.5661(4)	0.1880(4)	0.85714(19)	0.017(1)
C(2)	0.7008(4)	0.2541(4)	0.87652(19)	0.016(1)
C(3)	0.8150(4)	0.1704(4)	0.92297(19)	0.020(1)
C(4)	0.7860(4)	0.0151(4)	0.94787(19)	0.022(1)
C(5)	0.6505(4)	-0.0547(4)	0.92935(19)	0.020(1)
C(6)	0.5394(4)	0.0351(4)	0.88336(19)	0.017(1)
C(7)	0.3042(4)	0.1019(4)	0.81198(18)	0.016(1)
C(8)	0.3126(4)	-0.1440(4)	0.8727(2)	0.020(1)
C(9)	0.1757(5)	-0.1179(4)	0.8346(2)	0.023(1)
C(10)	0.5825(4)	0.4646(4)	0.79491(18)	0.014(1)
C(11)	0.8208(4)	0.5179(4)	0.8413(2)	0.021(1)
C(12)	0.7669(4)	0.6402(4)	0.7938(2)	0.021(1)
C(13)	0.5309(5)	0.7080(4)	0.7085(2)	0.022(1)
C(14)	0.5662(5)	0.6520(4)	0.6235(2)	0.024(1)
C(15)	0.7432(5)	0.6495(6)	0.5900(2)	0.034(1)
C(16)	0.7654(6)	0.5933(6)	0.5039(3)	0.043(1)
C(17)	0.0431(4)	0.1046(4)	0.7485(2)	0.022(1)
C(18)	0.0984(4)	0.1005(4)	0.6596(2)	0.021(1)
C(19)	0.1293(5)	-0.0658(5)	0.6266(2)	0.030(1)
C(20)	0.2061(6)	-0.0675(6)	0.5410(2)	0.036(1)
C(21)	0.2474(5)	0.4390(4)	0.7235(2)	0.024(1)
H(3)	0.9079	0.2163	0.9371	0.024
H(4)	0.8629	-0.0452	0.9789	0.026
H(5)	0.6338	-0.1599	0.9474	0.024

Table A.27 (Continued)

H(8)	0.3479	-0.2362	0.9031	0.025
H(9)	0.0958	-0.1899	0.8330	0.027
H(11)	0.9170	0.5076	0.8688	0.025
H(12)	0.8193	0.7335	0.7814	0.026
H(13A)	0.5592	0.8184	0.7109	0.026
H(13B)	0.4123	0.7097	0.7241	0.026
H(14A)	0.4971	0.7226	0.5888	0.029
H(14B)	0.5337	0.5431	0.6211	0.029
H(15A)	0.8136	0.5770	0.6233	0.040
H(15B)	0.7775	0.7578	0.5919	0.040
H(16A)	0.6900	0.6605	0.4718	0.064
H(16B)	0.7422	0.4822	0.5028	0.064
H(16C)	0.8782	0.6014	0.4820	0.064
H(17A)	0.0117	0.2167	0.7640	0.026
H(17B)	-0.0547	0.0469	0.7588	0.026
H(18A)	0.0137	0.1633	0.6299	0.026
H(18B)	0.2001	0.1526	0.6501	0.026
H(19A)	0.0244	-0.1126	0.6289	0.036
H(19B)	0.2026	-0.1333	0.6606	0.036
H(20A)	0.1345	-0.0002	0.5071	0.054
H(20B)	0.2206	-0.1770	0.5219	0.054
H(20C)	0.3127	-0.0264	0.5388	0.054

U(eq) is defined as one third of the trace of the orthogonalized U_{ij} tensor.

Table A.28 Anisotropic Displacement Parameters (\AA^2) for **13**

	U₁₁	U₂₂	U₃₃	U₂₃	U₁₃	U₁₂
I(1)	0.0220(1)	0.0206(1)	0.0170(1)	-0.0006(1)	0.0016(1)	-0.0015(1)
I(2)	0.0178(1)	0.0161(1)	0.0144(1)	-0.0006(1)	0.0004(1)	-0.0010(1)
Rh(1)	0.0128(1)	0.0126(1)	0.0121(1)	0.0008(1)	-0.0006(1)	-0.0014(1)
O(1)	0.0121(10)	0.0369(14)	0.0147(11)	0.0010(10)	-0.0035(9)	-0.0039(10)
N(1)	0.0157(12)	0.0169(13)	0.0145(13)	-0.0018(10)	-0.0007(10)	-0.0004(10)
N(2)	0.0199(13)	0.0164(13)	0.0157(13)	-0.0011(10)	0.0011(11)	-0.0029(11)
N(3)	0.0229(14)	0.0136(12)	0.0128(12)	0.0001(10)	-0.0008(11)	-0.0020(11)
N(4)	0.0193(13)	0.0215(14)	0.0145(13)	-0.0038(11)	0.0015(11)	-0.0035(11)
C(1)	0.0190(15)	0.0181(15)	0.0129(14)	-0.0003(12)	-0.0016(12)	0.0034(12)
C(2)	0.0186(15)	0.0180(15)	0.0119(14)	-0.0027(11)	-0.0001(12)	0.0026(12)
C(3)	0.0178(15)	0.0271(17)	0.0138(15)	-0.0037(13)	-0.0025(12)	0.0025(13)
C(4)	0.0241(16)	0.0253(17)	0.0126(15)	-0.0007(13)	-0.0027(13)	0.0098(14)
C(5)	0.0302(18)	0.0165(15)	0.0112(14)	-0.0006(12)	0.0001(13)	0.0055(13)
C(6)	0.0223(16)	0.0153(14)	0.0125(14)	-0.0008(11)	-0.0010(12)	0.0030(12)
C(7)	0.0195(15)	0.0173(15)	0.0116(14)	-0.0016(11)	-0.0002(12)	0.0001(12)
C(8)	0.0287(18)	0.0155(15)	0.0171(15)	-0.0006(12)	0.0060(13)	-0.0087(13)
C(9)	0.0291(18)	0.0211(16)	0.0186(16)	-0.0050(13)	0.0033(14)	-0.0077(14)
C(10)	0.0149(14)	0.0141(14)	0.0129(14)	-0.0010(11)	0.0018(11)	-0.0034(11)
C(11)	0.0174(15)	0.0264(17)	0.0193(16)	-0.0052(13)	0.0002(13)	-0.0062(13)
C(12)	0.0209(16)	0.0197(16)	0.0248(17)	-0.0017(13)	0.0014(13)	-0.0105(13)
C(13)	0.0265(17)	0.0163(15)	0.0212(17)	0.0039(13)	-0.0013(14)	0.0038(13)
C(14)	0.0291(18)	0.0229(17)	0.0201(17)	0.0048(13)	-0.0030(14)	0.0011(15)
C(15)	0.0263(19)	0.049(3)	0.0246(19)	0.0051(17)	0.0031(15)	-0.0051(18)
C(16)	0.041(2)	0.058(3)	0.025(2)	0.006(2)	0.0049(18)	0.008(2)
C(17)	0.0171(15)	0.0261(17)	0.0230(17)	-0.0040(14)	-0.0015(13)	-0.0024(13)
C(18)	0.0159(15)	0.0274(18)	0.0212(17)	0.0008(13)	-0.0014(13)	-0.0047(13)
C(19)	0.035(2)	0.033(2)	0.0214(18)	-0.0057(15)	-0.0065(16)	0.0022(17)
C(20)	0.039(2)	0.045(2)	0.0215(19)	-0.0084(17)	-0.0055(17)	0.0064(19)
C(21)	0.0295(19)	0.0212(17)	0.0200(17)	-0.0057(14)	0.0124(15)	-0.0112(15)

$$-2\pi^2[h^2a^*{}^2U_{11} + \dots + 2hka*b^*U_{12}] \quad (\text{A.5})$$

Table A.29 Bond Lengths [Å] for **13**

atom-atom	distance	atom-atom	distance
I(1)-Rh(1)	2.6685(3)	I(2)-Rh(1)	2.6854(3)
Rh(1)-C(1)	1.995(3)	Rh(1)-C(7)	2.057(3)
Rh(1)-C(10)	2.061(3)	Rh(1)-C(21)	1.999(4)
O(1)-C(21)	1.032(5)	N(1)-C(2)	1.424(4)
N(1)-C(10)	1.374(4)	N(1)-C(11)	1.389(4)
N(2)-C(10)	1.343(4)	N(2)-C(12)	1.387(4)
N(2)-C(13)	1.469(4)	N(3)-C(6)	1.415(4)
N(3)-C(7)	1.376(4)	N(3)-C(8)	1.388(4)
N(4)-C(7)	1.349(4)	N(4)-C(9)	1.389(5)
N(4)-C(17)	1.468(4)	C(1)-C(2)	1.370(5)
C(1)-C(6)	1.386(5)	C(2)-C(3)	1.394(4)
C(3)-H(3)	0.9500	C(3)-C(4)	1.403(5)
C(4)-H(4)	0.9500	C(4)-C(5)	1.387(5)
C(5)-H(5)	0.9500	C(5)-C(6)	1.394(4)
C(8)-H(8)	0.9500	C(8)-C(9)	1.343(5)
C(9)-H(9)	0.9500	C(11)-H(11)	0.9500
C(11)-C(12)	1.343(5)	C(12)-H(12)	0.9500
C(13)-H(13A)	0.9900	C(13)-H(13B)	0.9900
C(13)-C(14)	1.517(5)	C(14)-H(14A)	0.9900
C(14)-H(14B)	0.9900	C(14)-C(15)	1.518(5)
C(15)-H(15A)	0.9900	C(15)-H(15B)	0.9900
C(15)-C(16)	1.530(6)	C(16)-H(16A)	0.9800
C(16)-H(16B)	0.9800	C(16)-H(16C)	0.9800
C(17)-H(17A)	0.9900	C(17)-H(17B)	0.9900
C(17)-C(18)	1.527(5)	C(18)-H(18A)	0.9900
C(18)-H(18B)	0.9900	C(18)-C(19)	1.514(5)
C(19)-H(19A)	0.9900	C(19)-H(19B)	0.9900
C(19)-C(20)	1.523(5)	C(20)-H(20A)	0.9800
C(20)-H(20B)	0.9800	C(20)-H(20C)	0.9800

Symmetry transformations used to generate equivalent atoms.

Table A.30 Bond Angles [°] for **13**

atom-atom-atom	angle	atom-atom-atom	angle
I(1)-Rh(1)-I(2)	174.272(12)	C(1)-Rh(1)-I(1)	87.12(9)
C(1)-Rh(1)-I(2)	87.17(9)	C(1)-Rh(1)-C(7)	77.84(14)
C(1)-Rh(1)-C(10)	77.54(14)	C(1)-Rh(1)-C(21)	178.53(13)
C(7)-Rh(1)-I(1)	89.21(9)	C(7)-Rh(1)-I(2)	89.06(9)
C(7)-Rh(1)-C(10)	155.36(13)	C(10)-Rh(1)-I(1)	88.63(8)
C(10)-Rh(1)-I(2)	90.68(8)	C(21)-Rh(1)-I(1)	94.12(10)
C(21)-Rh(1)-I(2)	91.59(10)	C(21)-Rh(1)-C(7)	102.94(14)
C(21)-Rh(1)-C(10)	101.70(13)	C(10)-N(1)-C(2)	116.8(3)
C(10)-N(1)-C(11)	111.1(3)	C(11)-N(1)-C(2)	132.0(3)
C(10)-N(2)-C(12)	110.4(3)	C(10)-N(2)-C(13)	125.0(3)
C(12)-N(2)-C(13)	124.4(3)	C(7)-N(3)-C(6)	117.0(3)
C(7)-N(3)-C(8)	111.1(3)	C(8)-N(3)-C(6)	132.0(3)
C(7)-N(4)-C(9)	110.3(3)	C(7)-N(4)-C(17)	124.1(3)
C(9)-N(4)-C(17)	125.6(3)	C(2)-C(1)-Rh(1)	120.0(2)
C(2)-C(1)-C(6)	120.7(3)	C(6)-C(1)-Rh(1)	119.3(3)
C(1)-C(2)-N(1)	111.2(3)	C(1)-C(2)-C(3)	121.3(3)
C(3)-C(2)-N(1)	127.4(3)	C(2)-C(3)-H(3)	121.6
C(2)-C(3)-C(4)	116.8(3)	C(4)-C(3)-H(3)	121.6
C(3)-C(4)-H(4)	118.4	C(5)-C(4)-C(3)	123.1(3)
C(5)-C(4)-H(4)	118.4	C(4)-C(5)-H(5)	121.2
C(4)-C(5)-C(6)	117.7(3)	C(6)-C(5)-H(5)	121.2
C(1)-C(6)-N(3)	111.4(3)	C(1)-C(6)-C(5)	120.4(3)
C(5)-C(6)-N(3)	128.2(3)	N(3)-C(7)-Rh(1)	114.5(2)
N(4)-C(7)-Rh(1)	140.9(2)	N(4)-C(7)-N(3)	104.6(3)
N(3)-C(8)-H(8)	127.1	C(9)-C(8)-N(3)	105.7(3)
C(9)-C(8)-H(8)	127.1	N(4)-C(9)-H(9)	125.8
C(8)-C(9)-N(4)	108.3(3)	C(8)-C(9)-H(9)	125.8
N(1)-C(10)-Rh(1)	114.4(2)	N(2)-C(10)-Rh(1)	140.9(2)
N(2)-C(10)-N(1)	104.7(3)	N(1)-C(11)-H(11)	127.2
C(12)-C(11)-N(1)	105.5(3)	C(12)-C(11)-H(11)	127.2
N(2)-C(12)-H(12)	125.8	C(11)-C(12)-N(2)	108.3(3)
C(11)-C(12)-H(12)	125.8	N(2)-C(13)-H(13A)	108.9

Table A.30 (Continued)

N(2)-C(13)-H(13B)	108.9	N(2)-C(13)-C(14)	113.2(3)
H(13A)-C(13)-H(13B)	107.7	C(14)-C(13)-H(13A)	108.9
C(14)-C(13)-H(13B)	108.9	C(13)-C(14)-H(14A)	108.5
C(13)-C(14)-H(14B)	108.5	C(13)-C(14)-C(15)	115.0(3)
H(14A)-C(14)-H(14B)	107.5	C(15)-C(14)-H(14A)	108.5
C(15)-C(14)-H(14B)	108.5	C(14)-C(15)-H(15A)	109.5
C(14)-C(15)-H(15B)	109.5	C(14)-C(15)-C(16)	110.8(4)
H(15A)-C(15)-H(15B)	108.1	C(16)-C(15)-H(15A)	109.5
C(16)-C(15)-H(15B)	109.5	C(15)-C(16)-H(16A)	109.5
C(15)-C(16)-H(16B)	109.5	C(15)-C(16)-H(16C)	109.5
H(16A)-C(16)-H(16B)	109.5	H(16A)-C(16)-H(16C)	109.5
H(16B)-C(16)-H(16C)	109.5	N(4)-C(17)-H(17A)	109.1
N(4)-C(17)-H(17B)	109.1	N(4)-C(17)-C(18)	112.6(3)
H(17A)-C(17)-H(17B)	107.8	C(18)-C(17)-H(17A)	109.1
C(18)-C(17)-H(17B)	109.1	C(17)-C(18)-H(18A)	108.8
C(17)-C(18)-H(18B)	108.8	H(18A)-C(18)-H(18B)	107.7
C(19)-C(18)-C(17)	113.9(3)	C(19)-C(18)-H(18A)	108.8
C(19)-C(18)-H(18B)	108.8	C(18)-C(19)-H(19A)	109.1
C(18)-C(19)-H(19B)	109.1	C(18)-C(19)-C(20)	112.6(4)
H(19A)-C(19)-H(19B)	107.8	C(20)-C(19)-H(19A)	109.1
C(20)-C(19)-H(19B)	109.1	C(19)-C(20)-H(20A)	109.5
C(19)-C(20)-H(20B)	109.5	C(19)-C(20)-H(20C)	109.5
H(20A)-C(20)-H(20B)	109.5	H(20A)-C(20)-H(20C)	109.5
H(20B)-C(20)-H(20C)	109.5	O(1)-C(21)-Rh(1)	178.6(3)

Symmetry transformations used to generate equivalent atoms.

Table A.31 Torsion Angles [°] for **13**

atom-atom-atom-atom	angle	atom-atom-atom-atom	angle
Rh(1)-C(1)-C(2)-N(1)	-0.9(4)	Rh(1)-C(1)-C(2)-C(3)	-179.2(2)
Rh(1)-C(1)-C(6)-N(3)	-2.1(4)	Rh(1)-C(1)-C(6)-C(5)	178.6(2)
N(1)-C(2)-C(3)-C(4)	-177.3(3)	N(1)-C(11)-C(12)-N(2)	0.2(4)
N(2)-C(13)-C(14)-C(15)	-60.9(4)	N(3)-C(8)-C(9)-N(4)	-0.5(4)
N(4)-C(17)-C(18)-C(19)	66.1(4)	C(1)-C(2)-C(3)-C(4)	0.8(5)
C(2)-N(1)-C(10)-Rh(1)	2.6(3)	C(2)-N(1)-C(10)-N(2)	-176.4(3)
C(2)-N(1)-C(11)-C(12)	175.5(3)	C(2)-C(1)-C(6)-N(3)	178.7(3)
C(2)-C(1)-C(6)-C(5)	-0.6(5)	C(2)-C(3)-C(4)-C(5)	-1.0(5)
C(3)-C(4)-C(5)-C(6)	0.4(5)	C(4)-C(5)-C(6)-N(3)	-178.8(3)
C(4)-C(5)-C(6)-C(1)	0.4(5)	C(6)-N(3)-C(7)-Rh(1)	-0.4(3)
C(6)-N(3)-C(7)-N(4)	-178.9(3)	C(6)-N(3)-C(8)-C(9)	178.9(3)
C(6)-C(1)-C(2)-N(1)	178.4(3)	C(6)-C(1)-C(2)-C(3)	0.0(5)
C(7)-N(3)-C(6)-C(1)	1.5(4)	C(7)-N(3)-C(6)-C(5)	-179.3(3)
C(7)-N(3)-C(8)-C(9)	0.5(4)	C(7)-N(4)-C(9)-C(8)	0.5(4)
C(7)-N(4)-C(17)-C(18)	74.0(4)	C(8)-N(3)-C(6)-C(1)	-176.8(3)
C(8)-N(3)-C(6)-C(5)	2.4(6)	C(8)-N(3)-C(7)-Rh(1)	178.3(2)
C(8)-N(3)-C(7)-N(4)	-0.2(3)	C(9)-N(4)-C(7)-Rh(1)	-178.0(3)
C(9)-N(4)-C(7)-N(3)	-0.2(3)	C(9)-N(4)-C(17)-C(18)	-103.4(4)
C(10)-N(1)-C(2)-C(1)	-1.2(4)	C(10)-N(1)-C(2)-C(3)	177.1(3)
C(10)-N(1)-C(11)-C(12)	-0.1(4)	C(10)-N(2)-C(12)-C(11)	-0.3(4)
C(10)-N(2)-C(13)-C(14)	-77.9(4)	C(11)-N(1)-C(2)-C(1)	-176.6(3)
C(11)-N(1)-C(2)-C(3)	1.6(5)	C(11)-N(1)-C(10)-Rh(1)	178.9(2)
C(11)-N(1)-C(10)-N(2)	-0.1(3)	C(12)-N(2)-C(10)-Rh(1)	-178.3(3)
C(12)-N(2)-C(10)-N(1)	0.2(3)	C(12)-N(2)-C(13)-C(14)	97.2(4)
C(13)-N(2)-C(10)-Rh(1)	-2.6(5)	C(13)-N(2)-C(10)-N(1)	175.9(3)
C(13)-N(2)-C(12)-C(11)	-176.0(3)	C(13)-C(14)-C(15)-C(16)	-179.3(3)
C(17)-N(4)-C(7)-Rh(1)	4.2(5)	C(17)-N(4)-C(7)-N(3)	-177.9(3)
C(17)-N(4)-C(9)-C(8)	178.2(3)	C(17)-C(18)-C(19)-C(20)	-172.2(3)

Symmetry transformations used to generate equivalent atoms.

A.4.2 Crystal Summary for 13

Crystal data for C₂₁H₂₅I₂N₄ORh; M_r = 706.16; Triclinic; space group P-1; $a = 8.2638(2)$ Å; $b = 8.4439(2)$ Å; $c = 16.8412(3)$ Å; $\alpha = 88.0310(10)^\circ$; $\beta = 84.8720(10)^\circ$; $\gamma = 83.4470(10)^\circ$; V = 1162.46(4) Å³; Z = 2; T = 99.99 K; $\lambda(\text{Mo-K}\alpha) = 0.71073$ Å; $\mu(\text{Mo-K}\alpha) = 3.410$ mm⁻¹; $d_{\text{calc}} = 2.017$ g·cm⁻³; 19052 reflections collected; 5399 unique ($R_{\text{int}} = 0.0236$); giving $R_1 = 0.0227$, $wR_2 = 0.0556$ for 5152 data with [$I > 2\sigma(I)$] and $R_1 = 0.0244$, $wR_2 = 0.0643$ for all 5399 data. Residual electron density (e⁻·Å⁻³) max/min: 1.081/-1.133.

An arbitrary sphere of data were collected on a orange plate-like crystal, having approximate dimensions of 0.32 × 0.261 × 0.257 mm, on a Bruker APEX-II diffractometer using a combination of ω - and φ -scans of 0.5°.³⁰³ Data were corrected for absorption and polarization effects and analyzed for space group determination. The structure was solved by direct methods and expanded routinely.³⁰⁴ The model was refined by full-matrix least-squares analysis of F² against all reflections. All non-hydrogen atoms were refined with anisotropic thermal displacement parameters. Unless otherwise noted, hydrogen atoms were included in calculated positions. Thermal parameters for the hydrogens were tied to the isotropic thermal parameter of the atom to which they are bonded (1.5 × for methyl, 1.2 × for all others).

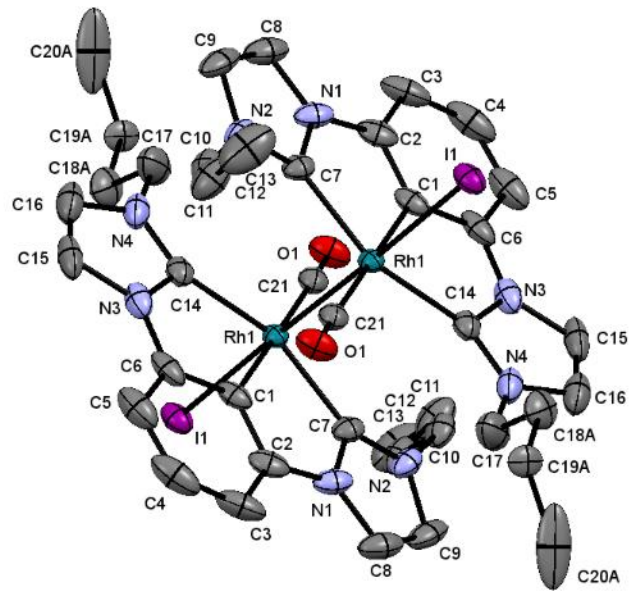


Figure A.104 X-ray molecular structure of **14**

Table A.32 Crystal Data and Structure Refinement **14**

Empirical formula	$C_{21.62}H_{26.24}ClN_4ORh$		
Formula weight	623.44		
Temperature	100.0 K		
Wavelength	0.71073 Å		
Crystal system	Monoclinic		
Space group	P 1 21/n 1		
Unit cell dimensions	$a = 13.0363(3)$ Å	$\alpha = 90^\circ$	
	$b = 10.3210(3)$ Å	$\beta = 108.0290(10)^\circ$	
	$c = 18.0439(5)$ Å	$\gamma = 90^\circ$	
Volume	$2308.56(11)$ Å ³		
Z	4		
Density (calculated)	1.794 g.cm ⁻³		
Absorption coefficient (μ)	2.213 mm ⁻¹		
F(000)	1228		
Crystal color, habit	red, Tablet		
Crystal size	$0.315 \times 0.256 \times 0.17$ mm ³		
θ range for data collection	2.303 to 27.883°		
Index ranges	$-17 \leq h \leq 14, -13 \leq k \leq 13, -23 \leq l \leq 23$		
Reflections collected	21056		
Independent reflections	5503 [R _{int} = 0.0348]		
Completeness to $\theta = 26.000^\circ$	99.9 %		
Absorption correction	Semi-empirical from equivalents		
Max. and min. transmission	0.9484 and 0.8248		
Refinement method	Full-matrix least-squares on F ²		
Data / restraints / parameters	5503 / 0 / 311		
Goodness-of-fit on F ²	1.074		
Final R indices [I>2σ(I)]	$R_1 = 0.0357, wR_2 = 0.0936$		
R indices (all data)	$R_1 = 0.0456, wR_2 = 0.1002$		
Extinction coefficient	n/a		
Largest diff. peak and hole	1.384 and -1.406 e ⁻ .Å ⁻³		

Table A.33 Atomic Coordinates and Equivalent Isotropic Displacement Parameters (\AA^2) for **14**

	x	y	z	U(eq)
I(1)	0.24316(2)	0.23880(2)	0.43723(2)	0.030(1)
Rh(1)	0.41129(2)	0.41532(2)	0.48194(2)	0.020(1)
O(1)	0.2846(2)	0.5389(3)	0.58230(18)	0.037(1)
N(1)	0.3869(3)	0.4654(4)	0.3191(2)	0.032(1)
N(2)	0.2753(3)	0.5990(3)	0.3434(2)	0.030(1)
N(3)	0.5550(3)	0.1927(3)	0.5218(2)	0.034(1)
N(4)	0.5090(3)	0.2206(3)	0.6253(2)	0.037(1)
C(1)	0.4834(3)	0.3254(4)	0.4144(2)	0.028(1)
C(2)	0.4628(3)	0.3618(4)	0.3380(2)	0.034(1)
C(3)	0.5136(4)	0.2989(5)	0.2901(3)	0.045(1)
C(4)	0.5845(4)	0.1969(6)	0.3235(4)	0.053(2)
C(5)	0.6030(3)	0.1547(5)	0.3990(3)	0.045(1)
C(6)	0.5508(3)	0.2204(4)	0.4441(3)	0.035(1)
C(7)	0.3500(3)	0.5093(4)	0.3783(2)	0.027(1)
C(8)	0.3356(4)	0.5270(5)	0.2498(3)	0.042(1)
C(9)	0.2660(4)	0.6115(5)	0.2646(3)	0.044(1)
C(10)	0.2096(3)	0.6690(4)	0.3827(3)	0.034(1)
C(11)	0.1062(3)	0.5995(4)	0.3794(3)	0.036(1)
C(12)	0.0422(4)	0.6758(5)	0.4228(3)	0.049(1)
C(13)	-0.0670(4)	0.6142(7)	0.4146(4)	0.069(2)
C(14)	0.4972(3)	0.2731(4)	0.5548(2)	0.028(1)
C(15)	0.6004(3)	0.0911(4)	0.5735(3)	0.044(1)
C(16)	0.5717(4)	0.1096(4)	0.6364(3)	0.046(1)
C(17)	0.4545(5)	0.2661(5)	0.6796(3)	0.053(1)
C(18A)	0.3626(7)	0.1873(9)	0.6792(6)	0.042(2)
C(19A)	0.3092(9)	0.2320(12)	0.7401(7)	0.027(2)
C(20A)	0.3749(18)	0.2078(18)	0.8262(19)	0.092(10)
C(18B)	0.4568(9)	0.2071(12)	0.7517(8)	0.032(3)
C(19B)	0.3859(16)	0.2626(18)	0.8011(13)	0.057(5)
C(20B)	0.4154(17)	0.429(3)	0.8285(12)	0.107(11)
C(21)	0.3360(3)	0.4995(4)	0.5468(2)	0.027(1)
Cl(1)	0.3241(4)	0.5621(4)	0.8487(4)	0.106(2)

Table A.33 (Continued)

Cl(2)	0.5304(5)	0.4629(6)	0.9526(5)	0.161(3)
C(22)	0.3946(13)	0.5138(16)	0.9557(10)	0.064(6)
H(3)	0.5007	0.3240	0.2373	0.053
H(4)	0.6215	0.1549	0.2924	0.063
H(5)	0.6495	0.0837	0.4193	0.054
H(8)	0.3471	0.5125	0.2010	0.050
H(9)	0.2193	0.6689	0.2283	0.052
H(10A)	0.1917	0.7554	0.3584	0.041
H(10B)	0.2525	0.6821	0.4380	0.041
H(11A)	0.1233	0.5125	0.4030	0.043
H(11B)	0.0618	0.5883	0.3243	0.043
H(12A)	0.0845	0.6806	0.4787	0.059
H(12B)	0.0311	0.7654	0.4022	0.059
H(13A)	-0.1032	0.6626	0.4461	0.104
H(13B)	-0.0565	0.5242	0.4327	0.104
H(13C)	-0.1116	0.6161	0.3598	0.104
H(15)	0.6436	0.0223	0.5646	0.052
H(16)	0.5906	0.0562	0.6815	0.055
H(17A)	0.5065	0.2665	0.7329	0.064
H(17B)	0.4301	0.3563	0.6661	0.064
H(17C)	0.4798	0.3561	0.6928	0.064
H(17D)	0.3772	0.2725	0.6489	0.064
H(18A)	0.3862	0.0961	0.6899	0.051
H(18B)	0.3087	0.1907	0.6267	0.051
H(19A)	0.2389	0.1873	0.7293	0.032
H(19B)	0.2943	0.3261	0.7330	0.032
H(20A)	0.3396	0.2512	0.8601	0.138
H(20B)	0.4479	0.2425	0.8364	0.138
H(20C)	0.3788	0.1145	0.8367	0.138
H(18C)	0.5328	0.2081	0.7857	0.039
H(18D)	0.4364	0.1151	0.7406	0.039
H(19C)	0.3982	0.2096	0.8488	0.068
H(19D)	0.3088	0.2548	0.7704	0.068

Table A.33 (Continued)

H(20D)	0.4337	0.4368	0.8852	0.161
H(20E)	0.3521	0.4821	0.8032	0.161
H(20F)	0.4765	0.4575	0.8119	0.161
H(22A)	0.3997	0.5882	0.9914	0.077
H(22B)	0.3565	0.4416	0.9721	0.077

U_{eq} is defined as one third of the trace of the orthogonalized U_{ij} tensor.

Table A.34 Anisotropic Displacement Parameters (\AA^2) for **14**

	U₁₁	U₂₂	U₃₃	U₂₃	U₁₃	U₁₂
I(1)	0.0210(1)	0.0297(1)	0.0373(2)	-0.0094(1)	0.0043(1)	-0.0015(1)
Rh(1)	0.0167(1)	0.0207(1)	0.0205(2)	-0.0023(1)	0.0020(1)	0.0016(1)
O(1)	0.0281(14)	0.0496(18)	0.0364(17)	-0.0138(14)	0.0158(12)	-0.0045(13)
N(1)	0.0226(16)	0.050(2)	0.0223(17)	-0.0013(15)	0.0031(12)	-0.0081(14)
N(2)	0.0212(15)	0.0357(17)	0.0278(18)	0.0084(14)	0.0009(12)	-0.0026(13)
N(3)	0.0219(16)	0.0235(15)	0.049(2)	-0.0042(15)	0.0004(14)	0.0032(13)
N(4)	0.0322(18)	0.0226(15)	0.046(2)	0.0065(15)	-0.0009(15)	-0.0028(13)
C(1)	0.0168(16)	0.0337(19)	0.033(2)	-0.0143(16)	0.0050(14)	-0.0043(14)
C(2)	0.0199(18)	0.049(2)	0.032(2)	-0.0146(19)	0.0058(15)	-0.0107(17)
C(3)	0.030(2)	0.069(3)	0.036(3)	-0.028(2)	0.0143(18)	-0.017(2)
C(4)	0.031(2)	0.064(3)	0.067(4)	-0.039(3)	0.022(2)	-0.013(2)
C(5)	0.025(2)	0.042(2)	0.068(4)	-0.026(2)	0.013(2)	-0.0023(18)
C(6)	0.0208(18)	0.0312(19)	0.049(3)	-0.0198(19)	0.0055(17)	-0.0041(15)
C(7)	0.0197(17)	0.0344(19)	0.0238(19)	0.0003(15)	0.0013(14)	-0.0032(14)
C(8)	0.031(2)	0.067(3)	0.024(2)	0.002(2)	0.0028(16)	-0.016(2)
C(9)	0.032(2)	0.060(3)	0.028(2)	0.016(2)	-0.0072(17)	-0.016(2)
C(10)	0.0234(19)	0.032(2)	0.042(3)	0.0099(18)	0.0006(16)	0.0025(15)
C(11)	0.0232(19)	0.039(2)	0.042(3)	0.0150(19)	0.0038(17)	0.0031(16)
C(12)	0.035(2)	0.060(3)	0.053(3)	0.021(3)	0.014(2)	0.013(2)
C(13)	0.034(3)	0.109(5)	0.068(4)	0.031(4)	0.020(3)	0.011(3)
C(14)	0.0224(18)	0.0230(17)	0.034(2)	-0.0022(15)	0.0003(15)	-0.0029(14)
C(15)	0.027(2)	0.0185(18)	0.075(4)	0.002(2)	0.000(2)	0.0020(15)
C(16)	0.036(2)	0.027(2)	0.063(4)	0.013(2)	0.000(2)	-0.0007(18)
C(17)	0.080(4)	0.038(2)	0.043(3)	0.001(2)	0.023(3)	-0.018(2)
C(18A)	0.039(5)	0.038(5)	0.050(6)	0.003(4)	0.015(4)	-0.017(4)
C(19A)	0.019(5)	0.039(6)	0.029(6)	0.002(5)	0.015(4)	-0.011(4)
C(20A)	0.071(13)	0.043(10)	0.21(3)	0.034(14)	0.114(18)	0.015(9)
C(18B)	0.025(6)	0.031(6)	0.037(7)	0.014(5)	0.003(5)	0.000(5)
C(19B)	0.052(11)	0.053(11)	0.078(14)	0.024(9)	0.038(9)	0.019(9)
C(20B)	0.069(13)	0.22(3)	0.050(11)	0.039(15)	0.050(10)	0.078(17)
C(21)	0.0237(18)	0.0259(17)	0.027(2)	-0.0017(15)	0.0021(14)	-0.0034(14)
Cl(1)	0.093(3)	0.069(2)	0.173(5)	-0.002(3)	0.068(3)	-0.004(2)
Cl(2)	0.155(5)	0.126(4)	0.259(8)	0.094(5)	0.147(6)	0.092(4)
C(22)	0.056(9)	0.056(9)	0.061(11)	-0.017(8)	-0.010(8)	0.054(8)

$$-2\pi^2[h^2a^*{}^2U_{11} + \dots + 2hka^*b^*U_{12}] \quad (\text{A.6})$$

Table A.35 Bond Lengths [Å] for **14**

atom-atom	distance	atom-atom	distance
I(1)-Rh(1)	2.7711(3)	Rh(1)-Rh(1)#1	2.8102(5)
Rh(1)-C(1)	1.984(4)	Rh(1)-C(7)	2.037(4)
Rh(1)-C(14)	2.056(4)	Rh(1)-C(21)	1.949(4)
O(1)-C(21)	1.136(5)	N(1)-C(2)	1.425(6)
N(1)-C(7)	1.377(5)	N(1)-C(8)	1.377(6)
N(2)-C(7)	1.350(5)	N(2)-C(9)	1.396(6)
N(2)-C(10)	1.461(6)	N(3)-C(6)	1.415(6)
N(3)-C(14)	1.375(6)	N(3)-C(15)	1.406(5)
N(4)-C(14)	1.347(6)	N(4)-C(16)	1.385(6)
N(4)-C(17)	1.455(7)	C(1)-C(2)	1.373(6)
C(1)-C(6)	1.394(6)	C(2)-C(3)	1.401(6)
C(3)-H(3)	0.9500	C(3)-C(4)	1.408(8)
C(4)-H(4)	0.9500	C(4)-C(5)	1.378(8)
C(5)-H(5)	0.9500	C(5)-C(6)	1.388(6)
C(8)-H(8)	0.9500	C(8)-C(9)	1.343(8)
C(9)-H(9)	0.9500	C(10)-H(10A)	0.9900
C(10)-H(10B)	0.9900	C(10)-C(11)	1.512(6)
C(11)-H(11A)	0.9900	C(11)-H(11B)	0.9900
C(11)-C(12)	1.528(7)	C(12)-H(12A)	0.9900
C(12)-H(12B)	0.9900	C(12)-C(13)	1.525(7)
C(13)-H(13A)	0.9800	C(13)-H(13B)	0.9800
C(13)-H(13C)	0.9800	C(15)-H(15)	0.9500
C(15)-C(16)	1.315(8)	C(16)-H(16)	0.9500
C(17)-H(17A)	0.9900	C(17)-H(17B)	0.9900
C(17)-H(17C)	0.9900	C(17)-H(17D)	0.9900
C(17)-C(18A)	1.446(10)	C(17)-C(18B)	1.428(13)
C(18A)-H(18A)	0.9900	C(18A)-H(18B)	0.9900
C(18A)-C(19A)	1.543(15)	C(19A)-H(19A)	0.9900
C(19A)-H(19B)	0.9900	C(19A)-C(20A)	1.54(3)
C(20A)-H(20A)	0.9800	C(20A)-H(20B)	0.9800
C(20A)-H(20C)	0.9800	C(18B)-H(18C)	0.9900
C(18B)-H(18D)	0.9900	C(18B)-C(19B)	1.58(2)
C(19B)-H(19C)	0.9900	C(19B)-H(19D)	0.9900
C(19B)-C(20B)	1.79(3)	C(20B)-H(20D)	1.0543
C(20B)-H(20E)	1.0537	C(20B)-H(20F)	1.0556
Cl(1)-C(22)	1.930(18)	Cl(2)-C(22)	1.865(16)
C(22)-H(22A)	0.9900	C(22)-H(22B)	0.9900

Table A.36 Bond Angles [°] for **14**

atom-atom-atom	angle	atom-atom-atom	angle
I(1)-Rh(1)-Rh(1)#1	175.211(18)	C(1)-Rh(1)-I(1)	89.77(10)
C(1)-Rh(1)-Rh(1)#1	85.47(10)	C(1)-Rh(1)-C(7)	77.58(17)
C(1)-Rh(1)-C(14)	77.92(18)	C(7)-Rh(1)-I(1)	89.75(10)
C(7)-Rh(1)-Rh(1)#1	88.71(10)	C(7)-Rh(1)-C(14)	155.25(17)
C(14)-Rh(1)-I(1)	86.68(10)	C(14)-Rh(1)-Rh(1)#1	92.83(10)
C(21)-Rh(1)-I(1)	88.15(11)	C(21)-Rh(1)-Rh(1)#1	96.60(11)
C(21)-Rh(1)-C(1)	177.91(14)	C(21)-Rh(1)-C(7)	102.21(16)
C(21)-Rh(1)-C(14)	102.14(17)	C(7)-N(1)-C(2)	116.4(3)
C(8)-N(1)-C(2)	132.1(4)	C(8)-N(1)-C(7)	111.3(4)
C(7)-N(2)-C(9)	111.2(4)	C(7)-N(2)-C(10)	124.0(3)
C(9)-N(2)-C(10)	124.7(4)	C(14)-N(3)-C(6)	116.7(3)
C(14)-N(3)-C(15)	109.7(4)	C(15)-N(3)-C(6)	133.4(4)
C(14)-N(4)-C(16)	111.0(4)	C(14)-N(4)-C(17)	124.7(4)
C(16)-N(4)-C(17)	124.0(4)	C(2)-C(1)-Rh(1)	120.4(3)
C(2)-C(1)-C(6)	120.1(4)	C(6)-C(1)-Rh(1)	119.4(3)
C(1)-C(2)-N(1)	110.5(4)	C(1)-C(2)-C(3)	120.7(4)
C(3)-C(2)-N(1)	128.7(4)	C(2)-C(3)-H(3)	121.5
C(2)-C(3)-C(4)	117.1(5)	C(4)-C(3)-H(3)	121.5
C(3)-C(4)-H(4)	118.3	C(5)-C(4)-C(3)	123.4(5)
C(5)-C(4)-H(4)	118.3	C(4)-C(5)-H(5)	121.4
C(4)-C(5)-C(6)	117.3(5)	C(6)-C(5)-H(5)	121.4
C(1)-C(6)-N(3)	111.3(4)	C(5)-C(6)-N(3)	127.4(4)
C(5)-C(6)-C(1)	121.3(5)	N(1)-C(7)-Rh(1)	115.1(3)
N(2)-C(7)-Rh(1)	140.9(3)	N(2)-C(7)-N(1)	103.8(3)
N(1)-C(8)-H(8)	126.6	C(9)-C(8)-N(1)	106.8(4)
C(9)-C(8)-H(8)	126.6	N(2)-C(9)-H(9)	126.5
C(8)-C(9)-N(2)	106.9(4)	C(8)-C(9)-H(9)	126.6
N(2)-C(10)-H(10A)	108.9	N(2)-C(10)-H(10B)	108.9
N(2)-C(10)-C(11)	113.3(4)	H(10A)-C(10)-H(10B)	107.7
C(11)-C(10)-H(10A)	108.9	C(11)-C(10)-H(10B)	108.9
C(10)-C(11)-H(11A)	109.5	C(10)-C(11)-H(11B)	109.5
C(10)-C(11)-C(12)	110.9(4)	H(11A)-C(11)-H(11B)	108.0

Table A.36 (Continued)

C(12)-C(11)-H(11A)	109.5	C(12)-C(11)-H(11B)	109.5
C(11)-C(12)-H(12A)	109.2	C(11)-C(12)-H(12B)	109.2
H(12A)-C(12)-H(12B)	107.9	C(13)-C(12)-C(11)	112.1(5)
C(13)-C(12)-H(12A)	109.2	C(13)-C(12)-H(12B)	109.2
C(12)-C(13)-H(13A)	109.5	C(12)-C(13)-H(13B)	109.5
C(12)-C(13)-H(13C)	109.5	H(13A)-C(13)-H(13B)	109.5
H(13A)-C(13)-H(13C)	109.5	H(13B)-C(13)-H(13C)	109.5
N(3)-C(14)-Rh(1)	114.7(3)	N(4)-C(14)-Rh(1)	140.5(3)
N(4)-C(14)-N(3)	104.4(3)	N(3)-C(15)-H(15)	126.5
C(16)-C(15)-N(3)	106.9(4)	C(16)-C(15)-H(15)	126.6
N(4)-C(16)-H(16)	126.0	C(15)-C(16)-N(4)	107.9(4)
C(15)-C(16)-H(16)	126.0	N(4)-C(17)-H(17A)	109.0
N(4)-C(17)-H(17B)	109.0	N(4)-C(17)-H(17C)	105.6
N(4)-C(17)-H(17D)	105.6	H(17A)-C(17)-H(17B)	107.8
H(17C)-C(17)-H(17D)	106.1	C(18A)-C(17)-N(4)	113.0(6)
C(18A)-C(17)-H(17A)	109.0	C(18A)-C(17)-H(17B)	109.0
C(18B)-C(17)-N(4)	126.8(7)	C(18B)-C(17)-H(17C)	105.6
C(18B)-C(17)-H(17D)	105.6	C(17)-C(18A)-H(18A)	109.1
C(17)-C(18A)-H(18B)	109.1	C(17)-C(18A)-C(19A)	112.6(8)
H(18A)-C(18A)-H(18B)	107.8	C(19A)-C(18A)-H(18A)	109.1
C(19A)-C(18A)-H(18B)	109.1	C(18A)-C(19A)-H(19A)	108.3
C(18A)-C(19A)-H(19B)	108.3	C(18A)-C(19A)-C(20A)	115.9(11)
H(19A)-C(19A)-H(19B)	107.4	C(20A)-C(19A)-H(19A)	108.3
C(20A)-C(19A)-H(19B)	108.3	C(19A)-C(20A)-H(20A)	109.5
C(19A)-C(20A)-H(20B)	109.5	C(19A)-C(20A)-H(20C)	109.5
H(20A)-C(20A)-H(20B)	109.5	H(20A)-C(20A)-H(20C)	109.5
H(20B)-C(20A)-H(20C)	109.5	C(17)-C(18B)-H(18C)	107.2
C(17)-C(18B)-H(18D)	107.2	C(17)-C(18B)-C(19B)	120.6(11)
H(18C)-C(18B)-H(18D)	106.8	C(19B)-C(18B)-H(18C)	107.2
C(19B)-C(18B)-H(18D)	107.2	C(18B)-C(19B)-H(19C)	109.0
C(18B)-C(19B)-H(19D)	109.0	C(18B)-C(19B)-C(20B)	112.9(13)
H(19C)-C(19B)-H(19D)	107.8	C(20B)-C(19B)-H(19C)	108.9
C(20B)-C(19B)-H(19D)	109.1	C(19B)-C(20B)-H(20D)	115.4

Table A.36 (Continued)

C(19B)-C(20B)-H(20E)	115.4	C(19B)-C(20B)-H(20F)	115.7
H(20D)-C(20B)-H(20E)	102.9	H(20D)-C(20B)-H(20F)	102.8
H(20E)-C(20B)-H(20F)	102.8	O(1)-C(21)-Rh(1)	173.1(3)
Cl(1)-C(22)-H(22A)	111.4	Cl(1)-C(22)-H(22B)	111.4
Cl(2)-C(22)-Cl(1)	101.8(10)	Cl(2)-C(22)-H(22A)	111.4
Cl(2)-C(22)-H(22B)	111.4	H(22A)-C(22)-H(22B)	109.3

Table A.37 Torsion Angles [°] for **14**

atom-atom-atom-atom	angle	atom-atom-atom-atom	angle
Rh(1)-C(1)-C(2)-N(1)	-0.3(4)	Rh(1)-C(1)-C(2)-C(3)	179.9(3)
Rh(1)-C(1)-C(6)-N(3)	1.2(4)	Rh(1)-C(1)-C(6)-C(5)	-179.9(3)
N(1)-C(2)-C(3)-C(4)	-178.9(4)	N(1)-C(8)-C(9)-N(2)	-0.6(5)
N(2)-C(10)-C(11)-C(12)	178.8(3)	N(3)-C(15)-C(16)-N(4)	0.1(5)
N(4)-C(17)-C(18A)-C(19A)	176.9(7)	N(4)-C(17)-C(18B)-C(19B)	-175.2(11)
C(1)-C(2)-C(3)-C(4)	0.9(6)	C(2)-N(1)-C(7)-Rh(1)	-0.4(4)
C(2)-N(1)-C(7)-N(2)	-175.9(3)	C(2)-N(1)-C(8)-C(9)	175.3(4)
C(2)-C(1)-C(6)-N(3)	-175.5(3)	C(2)-C(1)-C(6)-C(5)	3.4(6)
C(2)-C(3)-C(4)-C(5)	2.0(7)	C(3)-C(4)-C(5)-C(6)	-2.1(7)
C(4)-C(5)-C(6)-N(3)	178.1(4)	C(4)-C(5)-C(6)-C(1)	-0.6(6)
C(6)-N(3)-C(14)-Rh(1)	2.0(4)	C(6)-N(3)-C(14)-N(4)	175.9(3)
C(6)-N(3)-C(15)-C(16)	-174.7(4)	C(6)-C(1)-C(2)-N(1)	176.3(3)
C(6)-C(1)-C(2)-C(3)	-3.5(6)	C(7)-N(1)-C(2)-C(1)	0.4(5)
C(7)-N(1)-C(2)-C(3)	-179.8(4)	C(7)-N(1)-C(8)-C(9)	0.5(5)
C(7)-N(2)-C(9)-C(8)	0.6(5)	C(7)-N(2)-C(10)-C(11)	-88.3(4)
C(8)-N(1)-C(2)-C(1)	-174.2(4)	C(8)-N(1)-C(2)-C(3)	5.6(7)
C(8)-N(1)-C(7)-Rh(1)	175.3(3)	C(8)-N(1)-C(7)-N(2)	-0.2(4)
C(9)-N(2)-C(7)-Rh(1)	-173.8(4)	C(9)-N(2)-C(7)-N(1)	-0.3(4)
C(9)-N(2)-C(10)-C(11)	88.6(5)	C(10)-N(2)-C(7)-Rh(1)	3.5(6)
C(10)-N(2)-C(7)-N(1)	177.1(3)	C(10)-N(2)-C(9)-C(8)	-176.7(4)
C(10)-C(11)-C(12)-C(13)	175.1(4)	C(14)-N(3)-C(6)-C(1)	-2.0(5)
C(14)-N(3)-C(6)-C(5)	179.1(4)	C(14)-N(3)-C(15)-C(16)	-0.4(5)
C(14)-N(4)-C(16)-C(15)	0.2(5)	C(14)-N(4)-C(17)-C(18A)	101.2(6)
C(14)-N(4)-C(17)-C(18B)	174.1(7)	C(15)-N(3)-C(6)-C(1)	172.0(4)
C(15)-N(3)-C(6)-C(5)	-6.8(7)	C(15)-N(3)-C(14)-Rh(1)	-173.4(3)
C(15)-N(3)-C(14)-N(4)	0.5(4)	C(16)-N(4)-C(14)-Rh(1)	170.8(3)
C(16)-N(4)-C(14)-N(3)	-0.4(4)	C(16)-N(4)-C(17)-C(18A)	-72.3(7)
C(16)-N(4)-C(17)-C(18B)	0.6(10)	C(17)-N(4)-C(14)-Rh(1)	-3.4(7)
C(17)-N(4)-C(14)-N(3)	-174.7(4)	C(17)-N(4)-C(16)-C(15)	174.5(4)
C(17)-C(18A)-C(19A)-C(20A)	-70.2(14)	C(17)-C(18B)-C(19B)-C(20B)	-58.6(18)

A.4.3 Crystal Summary for 14

Crystal data for C₂₁H₂₆ClIN₄ORh; M_r = 623.44; Monoclinic; space group P 1 21/n 1; $a = 13.0363(3)$ Å; $b = 10.3210(3)$ Å; $c = 18.0439(5)$ Å; $\alpha = 90^\circ$; $\beta = 108.0290(10)^\circ$; $\gamma = 90^\circ$; $V = 2308.56(11)$ Å³; Z = 4; T = 100.0 K; $\lambda(\text{Mo-K}\alpha) = 0.71073$ Å; $\mu(\text{Mo-K}\alpha) = 2.213$ mm⁻¹; $d_{\text{calc}} = 1.794$ g.cm⁻³; 21056 reflections collected; 5503 unique ($R_{\text{int}} = 0.0348$); giving $R_1 = 0.0357$, $wR_2 = 0.0936$ for 4663 data with [$I > 2\sigma(I)$] and $R_1 = 0.0456$, $wR_2 = 0.1002$ for all 5503 data. Residual electron density (e⁻.Å⁻³) max/min: 1.384/-1.406.

An arbitrary sphere of data were collected on a red Tablet-like crystal, having approximate dimensions of 0.315 × 0.256 × 0.17 mm, on a Bruker APEX-II CCD diffractometer using a combination of ω - and φ -scans of 0.5°.³⁰³ Data were corrected for absorption and polarization effects and analyzed for space group determination. The structure was solved by methods and expanded routinely.³⁰⁴ The model was refined by full-matrix least-squares analysis of F² against all reflections. All non-hydrogen atoms were refined with anisotropic thermal displacement parameters. Unless otherwise noted, hydrogen atoms were included in calculated positions. Thermal parameters for the hydrogens were tied to the isotropic thermal parameter of the atom to which they are bonded (1.5 × for methyl, 1.2 × for all others).